

A Neotropical complex of *Ripersiella* species (Hemiptera, Coccoomorpha, Rhizoecidae) collected from the nests of *Acropyga* ants (Hymenoptera, Formicidae)

Scott A. Schneider¹, John S. LaPolla²

1 United States Department of Agriculture, Agricultural Research Service, Henry A. Wallace Beltsville Agricultural Research Center, Systematic Entomology Laboratory, 10300 Baltimore Avenue, Beltsville, MD, 20705, USA **2** Department of Biological Sciences, Towson University, 8000 York Road, Towson, MD, 21252, USA

Corresponding author: Scott A. Schneider (scott.schneider3@usda.gov)

Academic editor: Takumasa Kondo | Received 8 July 2022 | Accepted 7 September 2022 | Published 29 September 2022

<https://zoobank.org/B80C686A-001C-4A72-9E8A-7DED3FEE9515>

Citation: Schneider SA, LaPolla JS (2022) A Neotropical complex of *Ripersiella* species (Hemiptera, Coccoomorpha, Rhizoecidae) collected from the nests of *Acropyga* ants (Hymenoptera, Formicidae). ZooKeys 1123: 1–30. <https://doi.org/10.3897/zookeys.1123.90141>

Abstract

We describe five new Neotropical species of *Ripersiella* living in association with *Acropyga* ants: *R. campensis* **sp. nov.**, *R. illicians* **sp. nov.**, *R. montanae* **sp. nov.**, *R. pediandensis* **sp. nov.**, and *R. telalia* **sp. nov.** We also redescribe *R. andensis* and *R. colombiensis* based on type specimens and other collections. Together, these seven species form a morphologically similar group that we informally refer to as the *andensis*-complex of *Ripersiella*. All members of the *andensis*-complex are confirmed or are speculated to be mutualists of *Acropyga* ants. We discuss the implications of these associations and provide an identification key to the Neotropical species of *Ripersiella* that are lacking bitubular cerores, including the new species.

Keywords

Coccoidea, mutualism, root mealybug, taxonomy, trophobiosis

Introduction

Acropyga Roger ants (Hymenoptera, Formicidae) are obligatory mutualists of scale insects. They primarily associate with root mealybugs from the family Xenococcidae Tang (Hemiptera, Coccoomorpha), who are likewise obligate mutualists of *Acropyga* (Williams 1998; LaPolla 2004; Williams 2004; Schneider and LaPolla 2011). The

ancient relationship (Blaimer et al. 2016) between *Acropyga* and Xenococcidae has been reinforced through the vertical transmission of associated lineages over generations (LaPolla et al. 2002; LaPolla 2005). However, partner fidelity among *Acropyga* species and their trophobionts has been imperfect and a small proportion of colonies associate with scale species belonging to other groups; most often this involves root mealybugs from the family Rhizoecidae Williams (Williams 1998; Johnson et al. 2001; Tanaka 2016; Caballero et al. 2019; Schneider and LaPolla 2020). These secondary relationships are presumed to be the result of horizontal transmission events (see Page 2003) from an ancestral xenococcid partner to a more recently acquired rhizoecid (or other scale) partner (Schneider and LaPolla 2020).

Some species of root mealybugs from the genus *Ripersiella* Tinsley (Hemiptera, Rhizoecidae) have previously been reported as mutualists of *Acropyga* ants, including *R. andensis* (Hambleton) (Caballero et al. 2019) and *R. colombiensis* (Hambleton) (Smith et al. 2007). In recent years, we have discovered several cryptic species of *Ripersiella* collected from nests of *Acropyga* ants in the Neotropical region. Each of the cryptic species is similar in appearance to *R. andensis* or *R. colombiensis* and they each key out as one of these two species using the best available identification tools (i.e., Williams and Granara de Willink 1992; Kozár and Konczné Benedicty 2007; Szita et al. 2020). It is intriguing to discover a complex of similar-looking *Ripersiella* species all associated with *Acropyga* ants. If this complex forms a monophyletic clade, such a result would offer the first evidence that a species radiation of rhizoecid trophobionts has taken place, independent from the radiation of Xenococcidae. Conversely, if they are non-monophyletic, this may suggest that living with *Acropyga* results in phenotypic convergence among trophobiotic root mealybugs that are somewhat distant relatives. Phylogenetic analysis and further testing of these competing hypotheses is underway.

In this article, we describe five new species of *Ripersiella* from Peru and the Dominican Republic. In combination with *R. andensis* and *R. colombiensis*, these seven species form a complex that we refer to informally here as the *andensis*-complex. Furthermore, we provide a key to the Neotropical species of *Ripersiella* which lack bitubular cereres to aid in the identification of species in the *andensis*-complex. A thorough treatment of the *Ripersiella* species from the Neotropical region was recently provided by Szita et al. (2020) and is therefore not repeated here. However, we do include descriptions and re-illustrations of *R. andensis* and *R. colombiensis* along with comments on their affiliation with *Acropyga*.

Many reports on the trophobiosis between *Acropyga* ants and scale lineages falling outside of Xenococcidae require verification to confirm that the ant and scale species were in fact directly associated (see Schneider and LaPolla 2020; Schneider et al. 2022). When excavating *Acropyga* nests we sometimes find free-living hypogeic scale insects neighboring the colony, but the ants show no interest in these individuals and workers do not collect honeydew from them. Some published reports, which included explicit documentation verifying direct species-to-species association, are unequivocal (Smith et al. 2007; LaPolla et al. 2008; Tanaka 2016; Schneider and LaPolla 2020). Here, we detail the evidence and methods that were used to confirm direct association between scale insect species and *Acropyga* ants or state when such evidence is lacking.

Methods

Specimens were preserved in 95–100% ethanol and stored at -80°C prior to preparation. Examined specimens were prepared either by slide mounting directly or by first extracting DNA prior to mounting their cuticle. Extractions were performed using the QIAamp DNA Mini Kit (Qiagen, Valencia, California) following the standard protocol; specimen cuticles were removed from the extraction buffer after the initial lysing step and subsequently mounted. DNA-extracted specimens were assigned a unique six-digit alphanumeric identifier beginning with “S” followed by four numbers used to identify the collection event and ending with a sequentially assigned letter to identify the individual specimen (e.g., S0439A). Their DNA extractions, preserved at -80°C , are housed at the USDA ARS Beltsville Agricultural Research Center, Beltsville, Maryland, USA. Individuals that were slide-mounted directly are identified with a sequentially assigned letter appended to the end of the collector number (e.g., JSL090804-05A). All specimens were slide-mounted following the protocol described in Normark et al. (2019).

The terminology used in this paper follows Hambleton (1946), Kozár and Konczné Benedicty (2007), and Williams and Granara de Willink (1992). Measurements were made on a Zeiss Axio Imager.M2 (Carl Zeiss Microscopy, LLC, White Plains, NY, USA) microscope with the aid of an AxioCam and AxioVision software. Slide-mounted specimens were examined under phase contrast and differential interference contrast. Cryo-SEM was carried out at the US Department of Agriculture, Electron and Confocal Microscopy Unit (Beltsville, MD, USA), using a Hitachi SU-7000 + Quorum PP3010 Cryo Prep System + Oxford X-Max EDS field emission scanning electron microscope (Hitachi High Technologies America, Pleasanton, CA, USA). Images were captured and processed using the techniques described in Bolton et al. (2014).

Identification of associated *Acropyga* ants was performed using the key to species provided by LaPolla (2004).

Type depositories are abbreviated as follows:

- MNHNSD** Museo Nacional de Historia Natural Prof. Eugenio de Jesús Marciano, Santo Domingo, Dominican Republic;
- UNAB** Museo Entomológico Facultad de Agronomía, Universidad Nacional de Colombia, Bogotá, Colombia;
- UKNMH** Natural History Museum, London, United Kingdom;
- UNMSM** Museo de Historia Natural, Universidad Nacional Mayor de San Marcos, Lima, Peru;
- USNM** Smithsonian National Museum of Natural History, Coccoomorpha collection at USDA Agricultural Research Service, Beltsville, Maryland, USA.

For our collections from Peru, we confirmed direct trophobiotic association between root mealybugs and *Acropyga* ants through careful observation of interacting partners using a nest-box, following the protocol described by Schneider et al. (2022). For collections from the Dominican Republic, we confirmed direct association through observa-

tions in the field; their association is further evidenced through repeated collection of the same species pairs from nests at multiple sites. One new species described here was collected from Peru by T.R. Schultz. Exercising an abundance of caution, we consider this association as likely but needing confirmation, since specimens were collected from a single nest and the field notes lacked details on how direct association was confirmed.

Taxonomy

Genus *Ripersiella* Tinsley, 1899

Ripersiella Tinsley in Cockerell, 1899: 278. Type species: *Ripersia rumicis* Maskell, 1892.

Rhizoecus (*Pararhizoecus*) Goux, 1941: 197. Type species: *Rhizoecus petiti* Goux, 1941. *Pararhizoecus* Goux, 1941; Goux 1943: 41.

Remark. The new species described below are placed in *Ripersiella* based on the following diagnosis, which is a condensed version of the comprehensive descriptions provided by Kozár and Konczné Benedicty (2007) and Szita et al. (2020). For further details on the genus and a broader treatment of species, refer to these references.

Diagnosis. Tritubular cerores (also referred to as tritubular pores or ducts) absent; bitubular cerores (bitubular pores/ducts) typically present, absent in some species; anal ring with or without elongate cells, lacking protuberances, and situated dorsally; body setae all flagellate, anal lobes usually poorly developed, bearing a set of 3 distinct long setae or with several short setae; trilocular pores present but never arranged in tight clusters on the venter; body oval to spherical and membranous; antennae geniculate with 5 or 6 segments.

Comments. In Kozár and Konczné Benedicty (2007) and Szita et al. (2020), species that lack bitubular cerores but are otherwise morphologically similar to the generic type species, *R. rumicis* (Maskell), have been tentatively placed in *Ripersiella*. We maintain the established precedent here. However, it is important to note that Choi and Lee (2022), in their phylogenetic analysis of mealybug clades, failed to recover a monophyletic *Ripersiella*, and our own preliminary phylogenomic analyses (unpublished data) show similar results. It is therefore likely that some or all of the new species described here will eventually require a change of combination corresponding with a revision of Rhizoecidae that is informed through both their morphology and molecular phylogenetic analysis.

Ripersiella andensis (Hambleton)

Fig. 1

Neorhizoecus andensis Hambleton, 1946: 41.

Rhizoecus andensis (Hambleton); Hambleton 1977: 369.

?*Ripersiella andensis* (Hambleton); Kozár and Konczné Benedicty 2003: 235.

Material examined. Lectotype. COLOMBIA • 1 adult ♀; Bogota; 22.ii.1935; L.M. Murillo; on roots of *Coffea arabica* L.; USNM. **Paralectotypes.** COLOMBIA • 2 adult ♀♀; same slide as lectotype; USNM • 3 adult ♀♀; same data as lectotype; USNM. **Other material.** COLOMBIA • 4 adult ♀♀; locality (?); 1955; D. Rios Castana; on coffee; USNM • 3 adult ♀♀; locality (?); iv.1956; S.G. Flanders; on coffee; USNM • 22 adult ♀♀; Chinchina Cald.; 18.xii.1975; R. Cardenas; USNM.

Description. Adult female ($N = 6$). Appearance in life not recorded, extent of wax production unknown.

General. Mounted on microscope slide, body broadly oval and membranous, 0.78–1.06 (0.98) mm long, widest near abdominal segments II–III, 0.41–0.58 (0.52) mm wide. Abdomen smoothly tapering toward apex; abdominal segment VIII 170–213 (180) μm wide at base. Anal lobes poorly developed with several flagellate setae on venter and dorsum, ranging from 15–33 μm long. Body setae flagellate, 10–22 μm on head, 9–15 μm on thorax, 11–17 μm on abdominal segments. Trilocular pores abundant and distributed among body setae; bitubular cereres absent; oral collar tubular ducts absent. Microtrichia present on abdominal segments. Eyes absent.

Venter. Cephalic plate absent. Labium with 3 segments; 70 μm long and 46 μm at widest point. Antennae geniculate, 5-segmented, closely situated near midline on ventral submargin of head; overall length 126–134 (132) μm ; length of segment I: 27–38 (34) μm ; segment II: 14–17 (16) μm ; segment III: 14–16 (15) μm ; segment IV: 13–18 (14) μm ; segment V: 52–53 (53) μm ; apical antennal segment with 1 spine-like and 4 falcate stout sensory setae; few flagellate setae on each antennal segment, 14–35 μm long; sensorium present on second antennal segment. Legs well developed; overall length of hind leg 235–241 (238) μm ; length of hind coxa 28–34 (34) μm ; hind trochanter + femur 91–95 (91) μm ; hind tibia + tarsus 88–91 (91) μm ; hind claw 22–25 (22) μm ; each claw with short setose digitule 2–3 μm long; flagellate setae present on each segment, around 19 μm long. Circulus absent. Multilocular disc pores in irregular rows or groups on segments VI–VIII, pores with 6–8 loculi in the outer ring.

Dorsum. Anal ring on dorsal surface near posterior margin, 48–52 μm in diameter; with oval cells, some cells bearing spicules; with three pairs of setae 33–39 μm long. Posterior pair of dorsal ostioles present, diameter of orifice measured along longitudinal axis approximately 45 μm ; anterior pair present but much smaller than posterior pair and poorly developed, diameter of orifice approximately 10 μm . Multilocular disc pores absent.

Diagnosis. The following newly described species are similar in appearance to *R. andensis*: *R. campensis*, *R. montanae*, and *R. pediandensis*. Consult the respective diagnosis sections under each species below for a discussion on how to distinguish them from *R. andensis*. Another new species, *R. telalia*, can easily be distinguished by the presence of well-developed anterior ostioles, which are present in *R. andensis* but are strongly reduced and may appear to be absent.

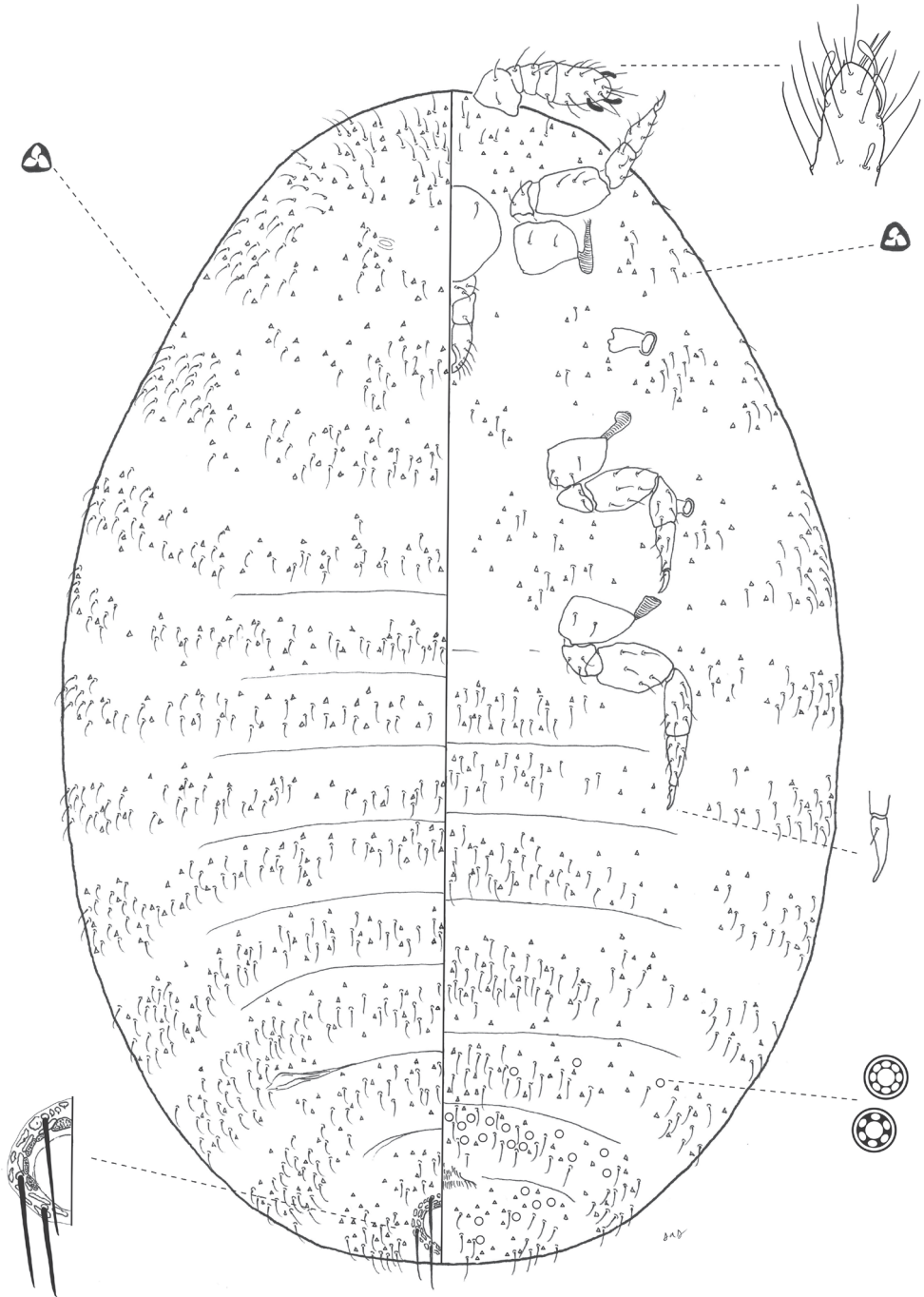


Figure 1. *Ripersiella andensis* (Hambleton). Adult female, full body view, re-illustrated by SAS from Williams and Granara de Willink (1992) and Kozár and Konczné Benedicty (2007).

Comments. *Ripersiella andensis* may associate with *Acropyga exsanguis* and *A. smithii* (Caballero et al. 2019); however, confirmation of their direct association is lacking, and Schneider and LaPolla (2020) considered their reported trophobiosis to be speculative. Given that there is a complex of species resembling *R. andensis* living in association with *Acropyga*, it seems likely that they do associate, and this simply requires confirmation. It would be useful to clearly establish whether there are both free-living and ant-associated populations as well.

***Ripersiella campensis* Schneider & LaPolla, sp. nov.**

<https://zoobank.org/5FACC224-2788-4034-A03B-83D0C95F321D>

Figures 2, 3

Material examined. Holotype. DOMINICAN REPUBLIC • 1 adult ♀; Loma Novillero (Fonestal Reserva) near Villa Altigracia; 18.7032, -70.1931, elev. 187 m; 4.viii.2009; JS LaPolla, SA Schneider leg.; associated with *Acropyga dubitata*, nest in 2° forest at base of tree root; USNM (nest DR8: prep JSL090804-05A). **Paratypes.** DOMINICAN REPUBLIC • 1 adult ♀; same data as holotype; USNM (nest DR8: prep S0439A) • 1 adult ♀; same data as holotype; UNAB (nest DR8: prep JSL090804-05B) • 1 adult ♀; Rancho Capote near Hato Mayor, 18.7971, -69.4194, elev. 112 m; 3.viii.2009; JS LaPolla, SA Schneider leg.; associated with *Acropyga dubitata*, nest under large tree root in riparian forest near Fun-Fun Cave; USNM (nest DR6: prep JSL090803-05A) • 1 adult ♀; same data as previous; UNAB (nest DR6: prep JSL090803-05B) • 1 adult ♀; San Francisco Mountains, Loma Quita Espuela Reserve, 19.3386, -70.1482, elev. 290 m; 30.vii.2009; JS LaPolla, SA Schneider leg.; associated with *Acropyga dubitata* in mixed forest/cacao plantation, host *Theobroma* sp.; MNHNSD (nest DR3: prep JSL090730-08A) • 4 adult ♀♀; same data as previous; USNM (nest DR3: preps S0436A; JSL090730-05B,C; JSL090730-08D) • 1 adult ♀; San Francisco Mountains, Loma Quita Espuela Reserve, 19.3386, -70.1482, elev. 290 m; 31.vii.2009; JS LaPolla, SA Schneider leg.; associated with *Acropyga dubitata* in mixed forest/cacao plantation, host *Theobroma* sp.; UKMNH (nest DR4: prep JSL090731-01A) • 1 adult ♀; same data as previous; MNHNSD (nest DR4: prep JSL090731-01B) • 1 adult ♀; same data as previous; UKNMH (nest DR4: prep JSL090731-01C) • 3 adult ♀♀; same data as previous; USNM (nest DR4: preps JSL090731-02D,E,F) • 1 adult ♀; same data as previous; USNM (nest DR5: prep S0437A).

Description. Adult female ($N = 17$). In life, body bright white to cream colored and free of obvious waxy secretions, small deposits of wax from trilocular pores visible under SEM (Fig. 3), tending to gather in intersegmental regions of the body and appendages.

General. Mounted on microscope slide, body broadly oval and membranous, 0.86–1.03 (0.93) mm long, widest near abdominal segments III–V, 0.50–0.70 (0.60) mm wide. Abdomen slightly constricted between segments VII and VIII or smoothly tapering; abdominal segment VIII 186–251 (210) μm wide at base. Anal lobes poorly

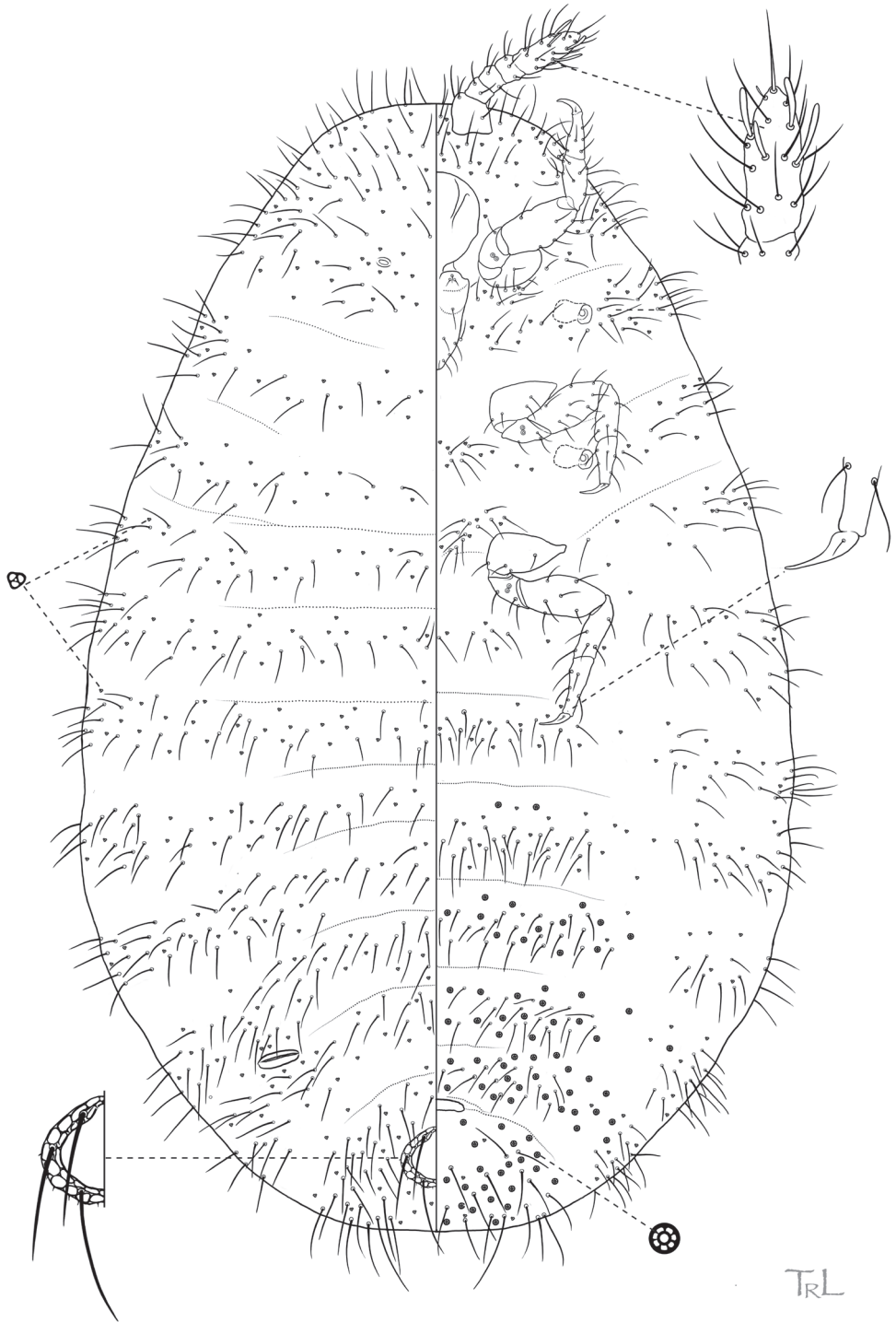


Figure 2. *Ripersiella campensis* Schneider & LaPolla sp. nov. Adult female, full body view, illustrated from holotype by T. Litwak (USDA ARS SEL), with edits by SAS.

developed with several flagellate setae on venter and dorsum, ranging from 23–75 μm long, with 1 or 2 longer setae situated near dorsal margin. Body setae flagellate, 14–40 μm on head, 13–33 μm on thorax, 14–37 μm on abdominal segments. Trilocular pores abundant and distributed among body setae; bitubular cereres absent; oral collar tubular ducts absent. Microtrichia present on abdominal segments; rounded dermal micro-bumps abundant in intersegmental areas and surroundings of appendages. Eyes absent.

Venter. Cephalic plate absent. Labium with 3 segments; 71 μm long and 43 μm at widest point. Antennae geniculate, 5-segmented, closely situated near midline on ventral submargin of head; overall length 140–156 (146) μm ; length of segment I: 33–43 (34) μm ; segment II: 17–21 (17) μm ; segment III: 14–19 (16) μm ; segment IV: 14–19 (18) μm ; segment V: 53–60 (58) μm ; apical antennal segment with 1 spine-like seta, 4 falcate stout sensory setae, and what appears to be 1 minute sensory seta at terminal apex; few flagellate setae on each antennal segment, 25–35 μm long; sensorium present on second antennal segment. Legs well developed; overall length of hind leg 266–292 (280) μm ; length of hind coxa 34–49 (34) μm ; hind trochanter + femur 101–115 (103) μm ; hind tibia + tarsus 103–108 (105) μm ; hind claw 23–27 (26) μm ; each claw with short setose digitule 2–3 μm long; flagellate setae present on each segment, around 27 μm long. Circulus absent. Multilocular disc pores in irregular rows or groups on segments III–VIII, sometimes missing from segments III or IV but always present at least as far anterior as V, pores with 7 loculi in the outer ring.

Dorsum. Anal ring on dorsal surface separated from posterior body margin by approximately 1 \times diameter of ring, 49–59 μm in diameter; with oval cells, some cells bearing spicules; with 3 pairs of setae 40–54 μm long. Posterior pair of dorsal ostioles present, diameter of orifice measured along longitudinal axis approximately 45 μm ; anterior pair present but much smaller than posterior pair and poorly developed, diameter of orifice approximately 10 μm . Multilocular disc pores absent.

Informal synonyms. Specimens of *R. campensis* have been previously referred to in the literature as “*Rhizoecus* new sp.” (Schneider and LaPolla 2011). At the time, collections from the Dominican Republic were thought to comprise a single species associated with *A. dubitata* and the generic assignment was uncertain.

Etymology. The species epithet is an adjective formed from the Latin noun *campus* referring to “a level place or surface” with the suffix *-ensis* denoting “of or from a place” alluding to the type series being collected only from lowland areas of Hispaniola.

Diagnosis. *Ripersiella campensis* sp. nov. is similar in appearance to *R. montanae* sp. nov., described below. Morphological differences between the two species are subtle, but they can be distinguished based on the following suite of characteristics. In *R. campensis*, multilocular disc pores are present on abdominal segments V–VIII and usually present on segments III–IV as well, body setae are comparatively longer and sparsely distributed, antennal segments II–IV are subequal in length (average lengths in μm : 19, 16, 17), and segment V is approximately 57 μm long. In *R. montanae*, multilocular disc pores are restricted to abdominal segments VI–VIII, body setae are comparatively shorter and densely distributed, antennal segments II–IV differ in length (average lengths in μm : 13, 24, 20), and segment V is approximately 40 μm long.

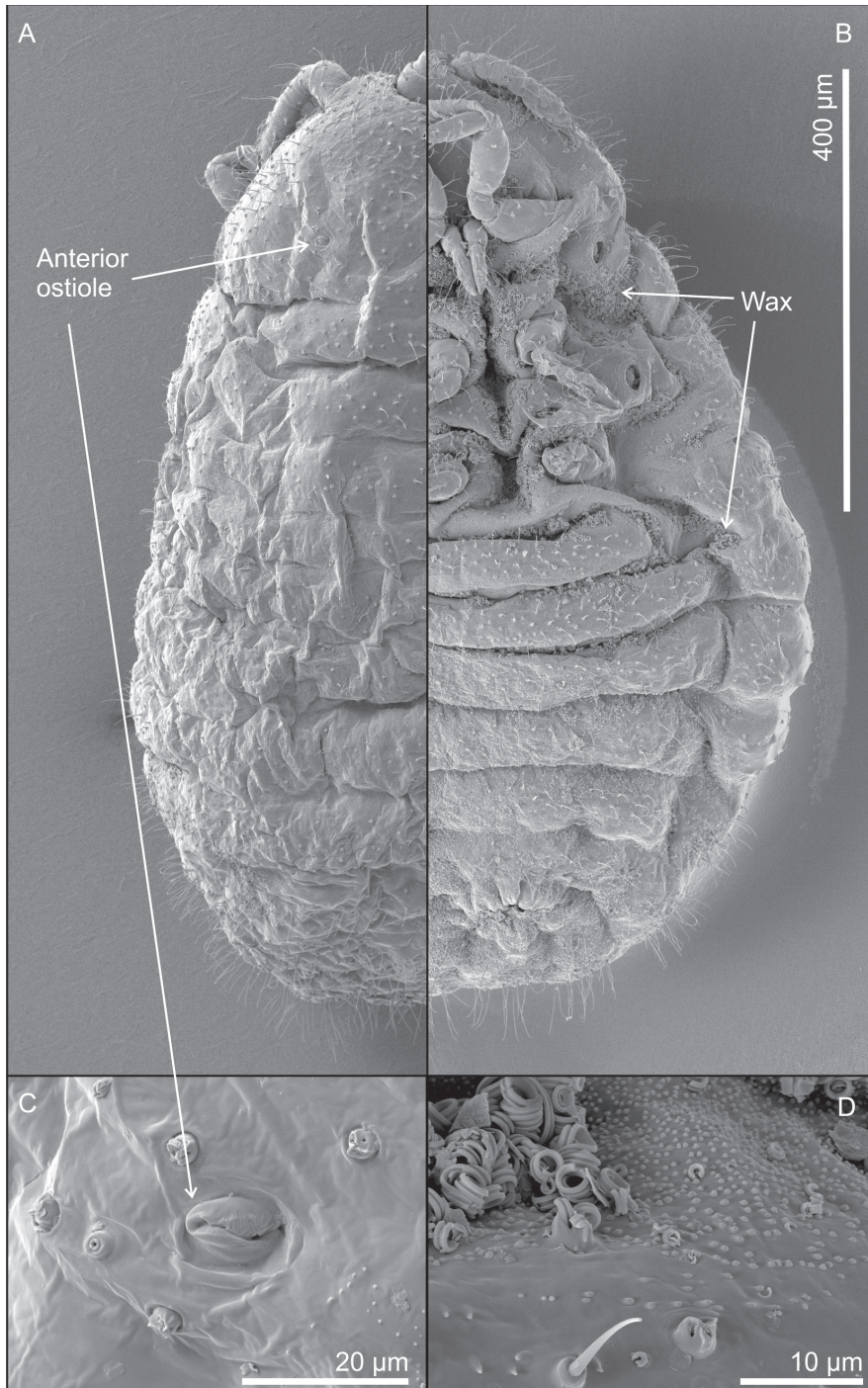


Figure 3. *Ripersiella campensis* Schneider & LaPolla sp. nov. Scanning electron micrographs (SEM) by J. Mowery (USDA ARS SEL) **A** dorsal view **B** ventral ½ view of adult female **C** magnified view of miniscule anterior dorsal ostiole **D** magnified view of curled wax deposits, trilobular pores, spine-like microtrichia, and abundant domed dermal micro-bumps in intersegmental region.

Ripersiella campensis is also similar in appearance to *R. andensis*. The two species can be distinguished as follows (character states for *R. andensis* are given in parentheses): having multilocular disc pores on any of segments III–V (absent on these segments); having anal lobe setae as long as 75 μm (as long as 35 μm); setae on the head, thorax, and abdomen are exceeding 30 μm (not exceeding 25 μm); hind legs are approximately 280 μm long (240 μm); and antennae are approximately 146 μm long (128 μm).

Comments. *Ripersiella campensis* was discovered from five nests of *Acropyga dubitata* (Wheeler & Mann) (nests DR3–6,8). The nests were located in lowland (between 112–290 m) forested areas, including a mixed forest/cacao plantation, riparian forest, and secondary growth forest near agricultural fields. We verified direct species-to-species association (trophobiosis) between the scale insects and ants through observation of attendance by worker ants and by the fact that all colonies contained numerous individuals of the same root mealybug species within their nest chambers and no additional species of scale insects were present. In the Dominican Republic, *R. montanae* also associates with *A. dubitata* but potentially only in areas of high elevation (>1000 m) in the mountains near the shared border with Haiti.

Ripersiella colombiensis (Hambleton)

Figure 4

Neorhizoecus colombiensis Hambleton, 1946: 43.

Rhizoecus colombiensis (Hambleton); Hambleton 1977: 372.

Ripersiella colombiensis (Hambleton); Kozár and Konczné Benedicty 2003: 236.

Material examined. Holotype. COLOMBIA • 1 adult ♀; La Esperanza; ii.1936; R Roba coll.; USNM. **Other material.** UNITED STATES • 1 adult ♀; Arizona, Cochise Co., Chiricahua Mtns, SW Res. Sta., 5 miles W. Portal; 31.8833, -109.2063, 1646 m; 5–15.viii.2001; JS LaPolla; with *Acropyga epedana*; USNM • 1 adult ♀; Arizona, Cochise Co., near Portal; 31.8838, -109.2229, 1645 m; 31.vii.2005; CR Smith; collected from colony of *Acropyga epedana*; USNM.

Description. Adult female, based on holotype. Appearance in life not reported; extent of wax production unknown.

General. Mounted on microscope slide, body broadly oval and membranous, 1.09 mm long, widest at metathorax and abdominal segments I–II, 0.91 mm wide. Abdomen rounded and gently tapering toward posterior apex; abdominal segment VIII approximately 270 μm wide at base. Anal lobes poorly developed with several flagellate setae on dorsum and venter, 18–28 μm long; lacking differentiated group of 3 long anal lobe setae. Body setae flagellate, 17–25 μm on head, 15–20 μm on thorax, 16–21 μm on abdominal segments. Trilocular pores scarcely distributed among body setae; multilocular disc pores absent; bitubular cerores absent; oral collar tubular ducts absent. Microtrichia present on abdominal segments and thorax. Eyes absent.

Venter. Cephalic plate absent. Labium with 3 segments; 88–110 μm long and 69 μm at widest point. Antennae geniculate, 5-segmented, closely situated near midline on

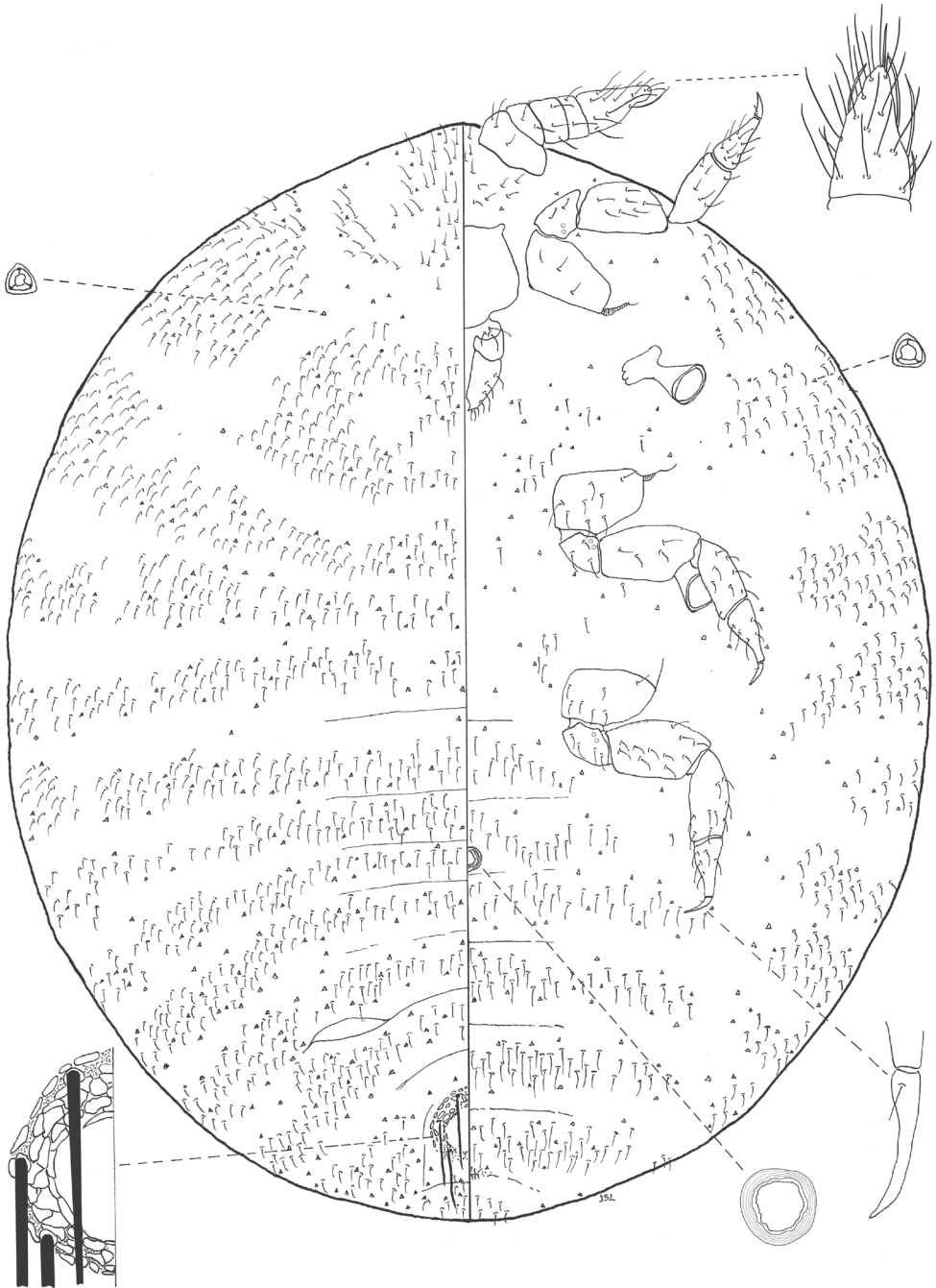


Figure 4. *Ripersiella colombiensis* (Hambleton). Adult female, full body view, re-illustrated by JSL from Williams and Granara de Willink (1992) and Kozár and Konczné Benedicty (2007), with edits by SAS.

ventral submargin of head; overall length 182 μm ; length of segment I: 36 μm ; segment II: 26 μm ; segment III: 28 μm ; segment IV: 22 μm ; segment V: 70 μm ; apical segment with 1 spine-like and 4 falcate sensory setae; flagellate setae on each antennal segment 18–40 μm long. Legs well developed; overall length of hind leg 394 μm ; length of hind coxa 48 μm ; length of hind trochanter + femur 158 μm ; length of hind tibia + tarsus 152 μm ; length of hind claw 36 μm ; each claw with setose digitule 4 μm long; flagellate or stout setae present on each segment 18–28 μm long. Single conical circulus present between abdominal segments III and IV, 28 μm wide; inner margin of orifice slightly crenulated.

Dorsum. Anal ring situated on dorsal surface separated from posterior body margin by approximately 1 \times diameter of ring, 80 μm in diameter; with oval cells lacking spicules; bearing three pairs of setae about 63 μm long. Posterior pair of ostioles present, diameter of orifice measured along longitudinal axis approximately 68 μm ; anterior pair of ostioles apparently absent.

Diagnosis. *Ripersiella colombiensis* is most similar in appearance to the newly described species *R. illicians*. Consult the diagnosis of *R. illicians* for a discussion on how to distinguish them.

Comments. *Ripersiella colombiensis* is confirmed to associate with *Acropyga epedana* and is one of few species of Rhizoecidae with a published record of *Acropyga* queens carrying gravid female trophobionts on their nuptial flight (Smith et al. 2007; Schneider and LaPolla 2020). Specimens from Colombia and Arizona appear likely to be conspecific, although those from Arizona have noticeably longer and thinner legs relative to their body size.

Ripersiella illicians Schneider & LaPolla, sp. nov.

<https://zoobank.org/7A49B97A-43A7-48D4-B8DF-8D9408E9A882>

Figures 5, 6

Material examined. Holotype. PERU • 1 adult ♀; Madre de Dios, Manu National Park, Cocha Cashu Biological Station, near trail marker 27:1150; -11.8833, -71.4000; 10.vi.2019; JS LaPolla, SA Schneider leg.; upland forest, from large nest of *Acropyga goeldii* (group) at base of tree; USNM (nest PER25-01: prep S0426E). **Paratypes.** PERU • 3 adult ♀♀; same data as holotype; USNM (nest PER25-01: preps S0426B,D,F) • 1 adult ♀; same data as holotype; UNMSM (nest PER25-01: prep S0426C) • 1 adult ♀; same data as holotype; UNAB (nest PER25-01: prep S0426G) • 1 adult ♀; same data as holotype; UKMNH (nest PER25-01: prep S0426A).

Description. Adult female ($N = 7$). In life, body bright white to cream colored and visibly coated in powdery white wax.

General. Mounted on microscope slide, body broadly oval and membranous, 0.70–0.83 (0.78) mm long, widest at metathorax and abdominal segments I–II, 0.46–0.61 (0.55) mm wide. Abdomen rounded and gently tapering toward posterior apex; abdominal segment VIII 148–196 (196) μm wide at base. Anal lobes poorly developed with several flagellate setae on dorsum, 57–60 μm long. Body setae flagellate, 15–

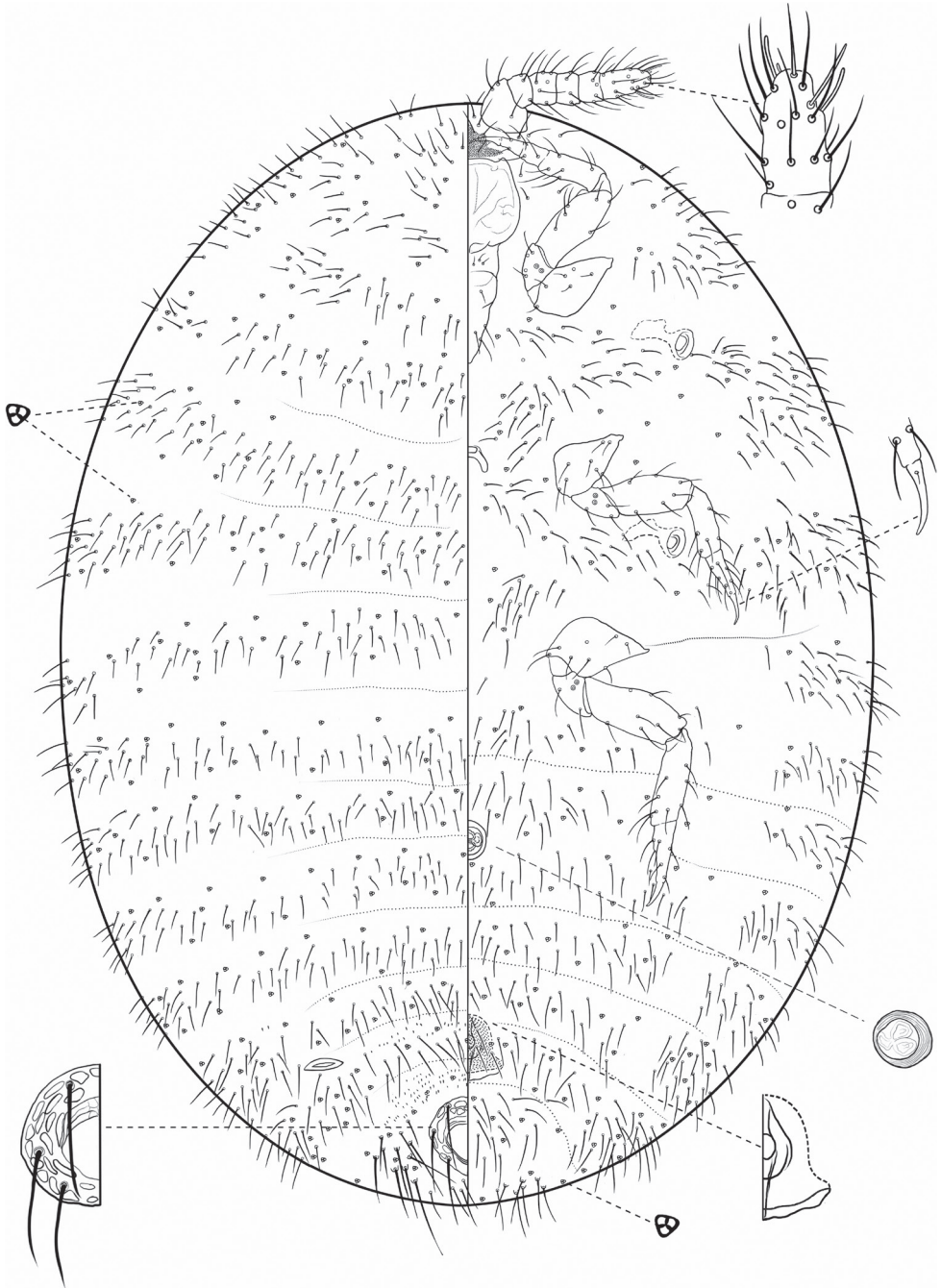


Figure 5. *Ripersiella illicians* Schneider & LaPolla sp. nov. Adult female, full body view, illustrated from holotype by T. Litwak (USDA ARS SEL), with edits by SAS.

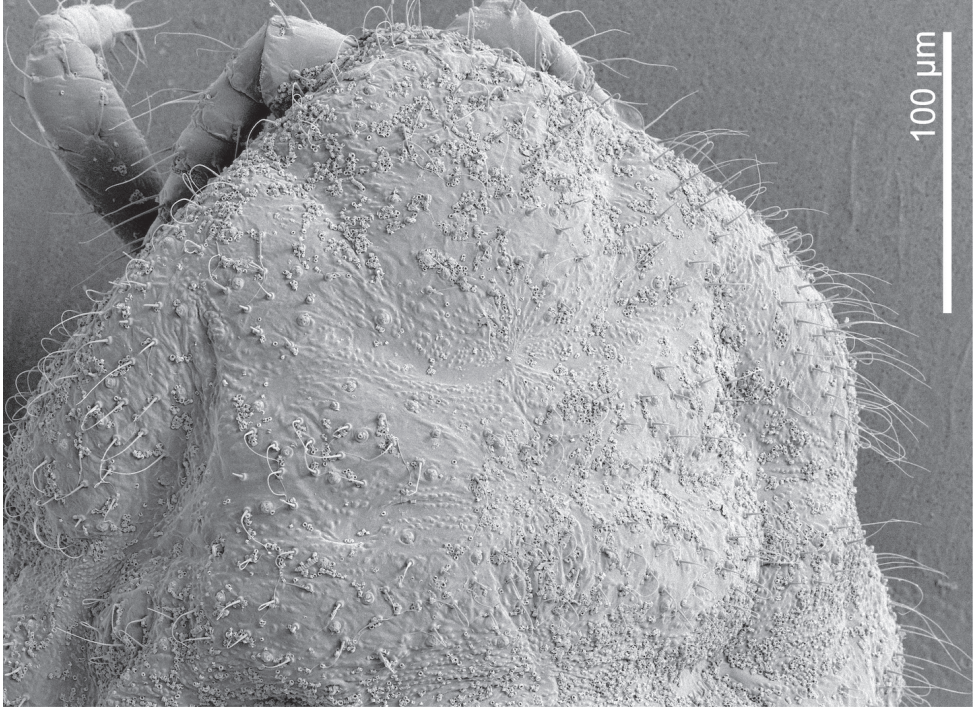


Figure 6. *Ripersiella illicians* Schneider & LaPolla sp. nov. Scanning electron micrograph (SEM) by J. Mowery (USDA ARS SEL). Dorsal anterior view of adult female head and thorax, showing the absence of anterior ostioles and the presence of curled wax deposits and domed dermal micro-bumps in intersegmental areas.

27 μm on head, 17–33 μm on thorax, 15–40 μm on abdominal segments. Trilocular pores abundant and distributed among body setae; multilocular disc pores absent; bitubular cerores absent; oral collar tubular ducts absent. Microtrichia apparently present only on dorsum of segments VI–VIII; rounded dermal micro-bumps present in intersegmental areas and surroundings of appendages. Internal genital organ sclerotized in some specimens of type series. Eyes absent.

Venter. Cephalic plate present. Labium with 3 segments; 82 μm long and 41 μm at widest point. Antennae geniculate, 6-segmented, closely situated near midline on ventral submargin of head; overall length 130–151 (151) μm ; length of segment I: 30–37 (37) μm ; segment II: 14–18 (18) μm ; segment III: 17–20 (20) μm ; segment IV: 14–19 (19) μm ; segment V: 13–17 (17) μm ; segment VI: 39–40 (40) μm ; apical segment with 4 falcate stout sensory setae; a few flagellate setae present on each antennal segment, 19–30 μm long. Legs well developed; overall length of hind leg 274–290 (288) μm ; length of hind coxa 43–44 (44) μm ; length of hind trochanter + femur 102–108 (106) μm ; length of hind tibia + tarsus 102–110 (110) μm ; length of hind claw 26–31 (28) μm ; each claw with stout setose digitule 1–2 μm long; flagellate setae present on each segment approximately 23 μm long. Single conical circulus present between abdominal segments III and IV, 22 μm in diameter; inner margin of orifice crenulated or with rugose projections.

Dorsum. Anal ring situated on dorsal surface separated from posterior body margin by approximately one-half diameter of ring, 59–61 μm in diameter; with oval cells lacking spicules; bearing 3 pairs of setae about 50 μm long. Posterior pair of ostioles present, diameter of orifice measured along longitudinal axis approximately 39 μm ; anterior pair of ostioles absent.

Informal synonyms. Specimens of *R. illicians* have been previously referred to in the literature as “*Ripersiella* undescribed (i)” (Schneider et al. 2022).

Etymology. The species epithet is an adjective formed from *illicium*, meaning attraction or enticement, and its use alludes to the apparent tendency of *Acropyga* colonies to gain rhizoecid partners through horizontal acquisitions. Such colonies have been figuratively attracted away from their primary associates in Xenococcidae.

Diagnosis. *Ripersiella illicians* sp. nov. is similar to *R. colombiensis* as both species have a subcircular body shape, bearing one circulus, and both are lacking multilocular disc pores and an anterior pair of dorsal ostioles. However, *R. illicians* can be distinguished from *R. colombiensis* as follows (character states for *R. colombiensis* are given in parentheses): having 6-segmented antennae (5-segmented antennae); having comparatively long body setae, ranging from 15–40 μm (comparatively short, ranging from 15–25 μm); and having anal lobe setae that are distinctly longer than body setae, 57–60 μm (similar in length to body setae, 18–28 μm).

Comments. *Ripersiella illicians* was discovered from a large nest of *Acropyga goeldii* (group). Root mealybugs were abundant in the nest, and wax could be seen on their body using a hand lens. Their direct association was confirmed through observation of the colony using a nest-box, as described by Schneider et al. (2022). After specimens were collected into a nest-box, worker ants gathered trophobionts into a protective cluster and were actively engaged in attending to them.

***Ripersiella montanae* Schneider & LaPolla, sp. nov.**

<https://zoobank.org/82F8E9C9-49A4-4436-A8C6-9817CBE46D76>

Figures 7, 8

Material examined. Holotype. DOMINICAN REPUBLIC • 1 adult ♀; W. of Hondo Valley, 13 m off road; 18.7229, -71.7061, elev. 1032 m; 24.vii.2009; JS LaPolla, SA Schneider leg.; associated with *Acropyga dubitata*, nest under a stone in coffee plantation next to road, host *Coffea* sp.; USNM (nest DR2: prep JSL090724-13A). **Paratypes.** DOMINICAN REPUBLIC • 5 adult ♀♀; same data as holotype; USNM (nest DR1: preps S0434A; S0435A; JSL090724-08A,B; JSL090724-10F) • 1 adult ♀; same data as holotype; MNHNSD (nest DR1: prep JSL090724-05E) • 1 adult ♀; same data as holotype; UNAB (nest DR1: prep JSL090724-08C) • 1 adult ♀; same data as holotype; UKMNH (nest DR1: prep JSL090724-08D).

Description. Adult female ($N = 9$). In life, body bright white to cream colored and free of obvious waxy secretions, small deposits of wax from trilocular pores

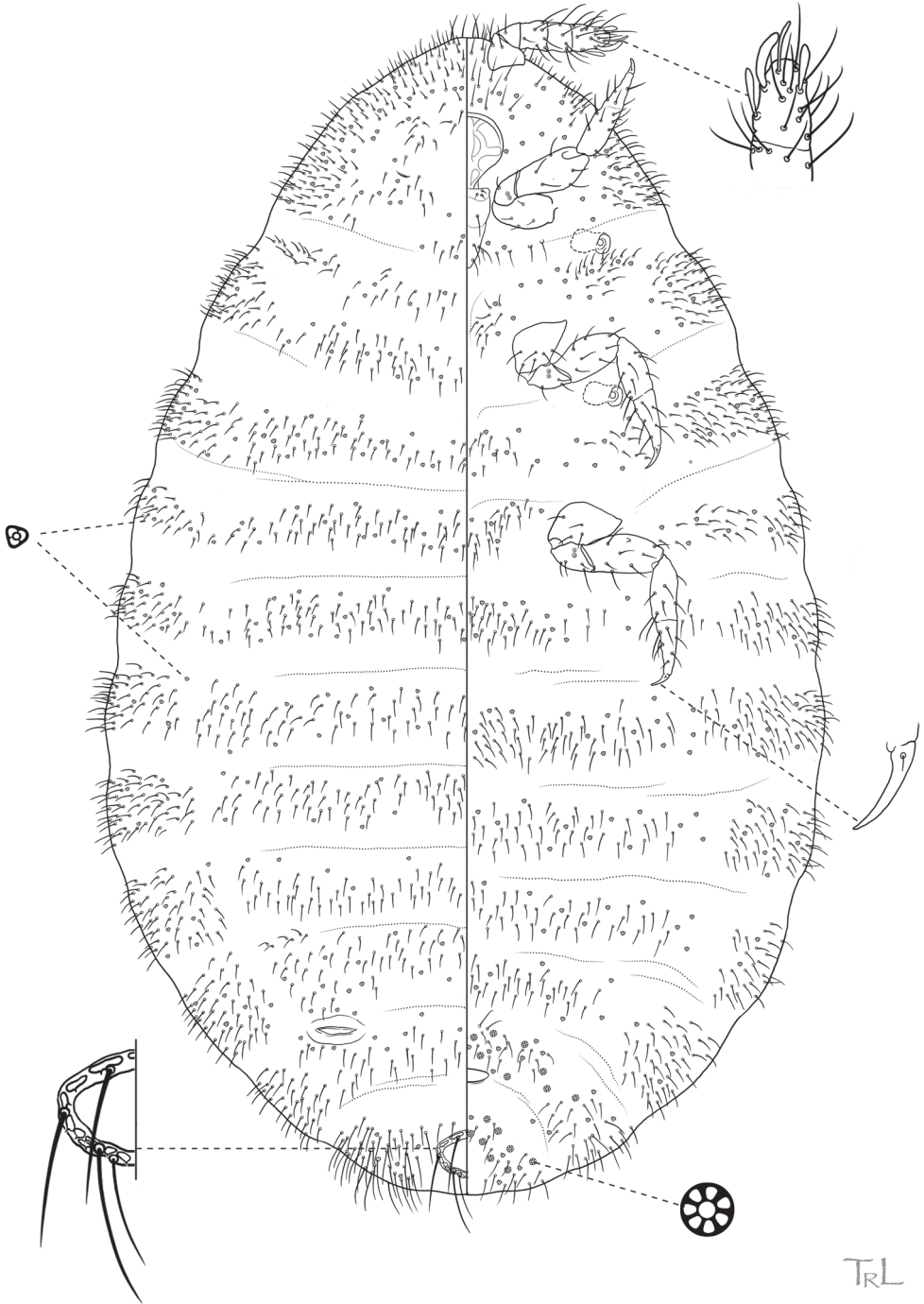


Figure 7. *Ripersiella montanae* Schneider & LaPolla sp. nov. Adult female, full body view, illustrated from holotype by T. Litwak (USDA ARS SEL), with edits by SAS.

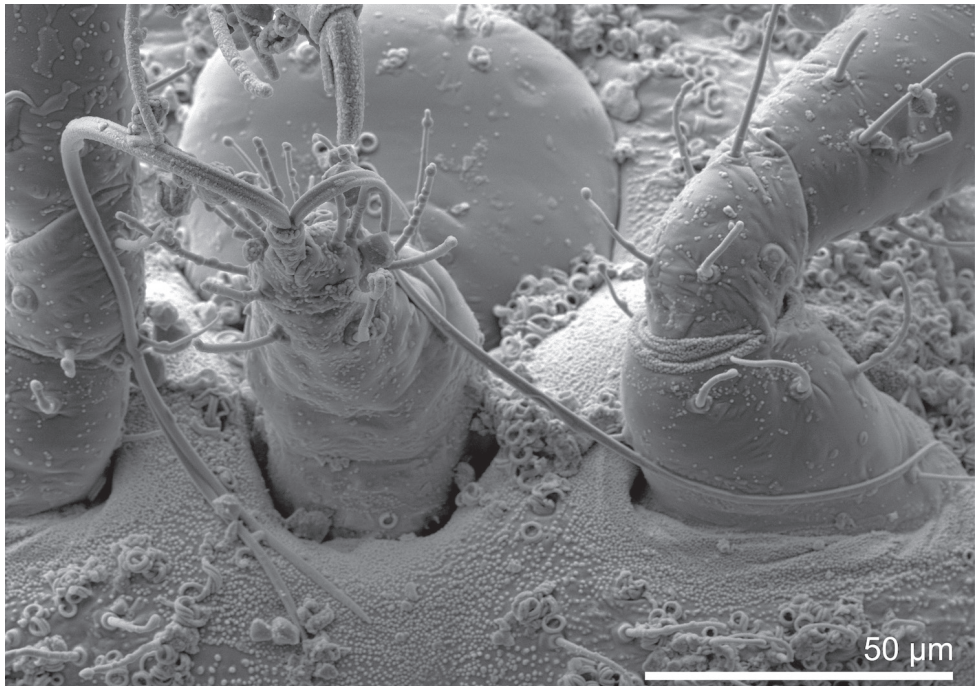


Figure 8. *Ripersiella montanae* Schneider & LaPolla sp. nov. Scanning electron micrograph (SEM) by J. Mowery (USDA ARS SEL). Ventral view of adult female labium and prothoracic legs, showing curled wax deposits and an abundance of domed dermal micro-bumps surrounding the attachment points of appendages.

visible under SEM (Fig. 8), tending to gather in intersegmental regions of the body and appendages.

General. Mounted on microscope slide, body broadly oval and membranous, 0.91–1.03 (0.99) mm long, widest near abdominal segments III–V, 0.51–0.68 (0.62) mm wide. Abdomen slightly constricted between segments VII and VIII or smoothly tapering; abdominal segment VIII 199–250 (199) μ m wide at base. Anal lobes poorly developed with several flagellate setae on venter and dorsum, ranging from 16–59 μ m long, with longest setae situated near dorsal margin; lacking differentiated set of 3 longer stout setae common to the group. Body setae short and flagellate, 10–22 μ m on head, 12–20 μ m on thorax, 14–24 μ m on abdominal segments. Trilocular pores abundant and distributed among body setae; bitubular ceroses absent; oral collar tubular ducts absent. Microtrichia present on abdominal segments; rounded dermal micro-bumps abundant in intersegmental areas and surroundings of appendages (Fig. 8). Eyes absent.

Venter. Cephalic plate absent. Labium with 3 segments; 70 μ m long and 42 μ m at widest point. Antennae geniculate, 5-segmented, closely situated near midline on ventral submargin of head; overall length 126–133 (129) μ m; length of segment I: 30–34 (34) μ m; segment II: 12–19 (13) μ m; segment III: 20–26 (24) μ m; segment

IV: 17–21 (18) μm ; segment V: 36–42 (40) μm ; apical antennal segment with 1 spine-like and 4 falcate stout sensory setae; a few flagellate setae on each antennal segment, 20–30 μm long; sensorium present on second antennal segment. Legs well developed; overall length of hind leg 253–277 (275) μm ; length of hind coxa 32–48 (48) μm ; hind trochanter + femur 86–101 (95) μm ; hind tibia + tarsus 101–111 (111) μm ; hind claw 21–26 (21) μm ; each claw with short setose digitule 2–3 μm long; flagellate or stout setae present on each segment, about 25 μm long. Circulus absent. Multilocular disc pores in irregular rows or groups on segments VI–VIII, sometimes absent from segment VI, pores with 7 loculi in the outer ring.

Dorsum. Anal ring on dorsal surface separated from posterior body margin by approximately one-half diameter of ring, 40–53 μm in diameter; with oval cells, some cells bearing spicules; typically with three pairs of setae, although one specimen in type series (JSL090724-05E) has four pairs, each 40–50 μm long. Posterior pair of dorsal ostioles present, diameter of orifice measured along longitudinal axis approximately 40 μm ; anterior pair present but barely perceptible except under SEM, reduced compared to posterior pair and poorly developed, diameter of orifice approximately 15 μm . Multilocular disc pores absent.

Informal synonyms. Specimens of *R. montanae* have been previously referred to in the literature as “*Rhizoecus* new sp.” (Schneider and LaPolla 2011). At the time, *R. campensis* and *R. montanae* were thought to comprise a single species associated with *A. dubitata* and the generic assignment was uncertain.

Etymology. The species epithet is derived from the Latin adjective *montanus* (of mountains), indicating that the type series was collected from a mountainous area of Hispaniola.

Diagnosis. *Ripersiella montanae* sp. nov. is similar in appearance to *R. campensis* sp. nov. The diagnosis section under *R. campensis* explains how the two species may be distinguished. *Ripersiella montanae* is also similar in appearance to *R. andensis* but the two species can be distinguished as follows (character states for *R. andensis* are given in parentheses): having antennal segments II–IV differing in length (subequal in length); having a comparatively short terminal antennal segment, 40 μm long (comparatively long, 53 μm); having hind legs approximately 275 μm long (240 μm); having the hind trochanter+femur shorter than the tibia+tarsus (the reverse); and having anal lobe setae as long as 59 μm (as long as 33 μm).

Comments. *Ripersiella montanae* was discovered from two nests of *A. dubitata* (nests DR1–2). The nests were located under stones in a coffee plantation within a few meters of one another. We verified direct species-to-species association (trophobiosis) between the scale insects and ants through observation of attendance by worker ants and by the fact that both colonies contained numerous individuals of the same root mealybug species within their nest chambers and no additional species of scale insects were present. This species was only discovered at high elevation (>1000 m) in the mountainous region of western Dominican Republic near the border with Haiti. Several nests of *A. dubitata* were collected throughout the lowland regions (112–290 m) of Dominican Republic but these nests contained a different associated root mealybug species, *R. campensis*.

***Ripersiella pediandensis* Schneider & LaPolla, sp. nov.**

<https://zoobank.org/00D70A87-8894-4D9B-BDF2-B79BD397D643>

Figure 9

Material examined. *Holotype*. PERU • 1 adult ♀; Madre de Dios, Dept. Cusco, Cosnipata Valley, Carretera a Manu; -13.0685, -71.5539; 3.viii.2012; TR Schultz leg. (TRS120803-05); collected from *Acropyga goeldii* (group) colony; host not recorded; USNM (nest TRS1: prep S0092B). *Paratypes*. PERU • 1 adult ♀; same data as holotype; USNM (nest TRS1: prep S0092A) • 1 adult ♀; same data as holotype; UNAB (nest TRS1: prep TRS120803-05A).

Description. Adult female ($N = 3$). Appearance in life not recorded.

General. Mounted on microscope slide, body membranous, broadly oval in young adults to nearly circular in more mature specimens, 1.31–1.53 (1.43) mm long, widest near abdominal segments III–V, 1.01–1.44 (1.21) mm wide. Abdomen smoothly rounded; abdominal segment VIII 258–275 (258) μm wide at base. Anal lobes poorly developed with several flagellate setae on venter and dorsum, ranging from 10–40 μm long, each with group of 3 distinctly stouter setae situated near dorsal margin 71–108 μm long. Body setae flagellate, 11–33 μm on head, 11–15 μm on thorax, 10–40 μm on abdominal segments. Trilocular pores abundant and distributed among body setae; bitubular ceroses absent. Microtrichia present; presence of rounded dermal micro-bumps uncertain. Eyes absent.

Venter. Cephalic plate present, with few setae on the plate and several setae and trilocular pores surrounding the ventral and lateral margins. Labium with 3 segments; 92 μm long and 49 μm at widest point. Antennae geniculate, 5-segmented, closely situated near midline on ventral submargin of head; overall length 188–201 (192) μm ; length of segment I: 45–50 (48) μm ; segment II: 19–24 (19) μm ; segment III: 19–21 (19) μm ; segment IV: 19–23 (23) μm ; segment V: 79–88 (79) μm ; apical antennal segment with 1 spine-like and 4 falcate stout sensory setae; a few flagellate setae on each antennal segment, 30–45 μm long; sensorium present on second antennal segment. Legs well developed; overall length of hind leg 346–381 (346) μm ; length of hind coxa 42–63 (42) μm ; hind trochanter + femur 132–137 (132) μm ; hind tibia + tarsus 136–144 (136) μm ; hind claw 36–37 (36) μm ; each claw with short setose digitule 7.5 μm long; flagellate setae present on each segment, about 25 μm long; 3 stout spine-like setae on inner margin of tibia and tarsus. Circulus absent. Multilocular disc pores present near the vulva on abdominal segments VII–VIII with 9 loculi in the outer ring; near each spiracle a multilocular disc pore with 6 or 7 loculi present. Oral collar tubular ducts present in singular rows or sparsely scattered on median to submedian areas of ventral abdominal segments, 1 or 2 present on thoracic segments near each spiracle.

Dorsum. Anal ring on dorsal surface separated from posterior body margin by approximately 1 \times diameter of ring, 66–73 μm in diameter; with oval cells, some cells bearing spicules; with three pairs of setae 30–42 μm long. Posterior pair of dorsal ostioles present, diameter of orifice measured along longitudinal axis approximately 44 μm ; anterior pair present but smaller than posterior pair, diameter of orifice approximately 29 μm . Multilocular disc pores absent. Oral collar tubular ducts absent.

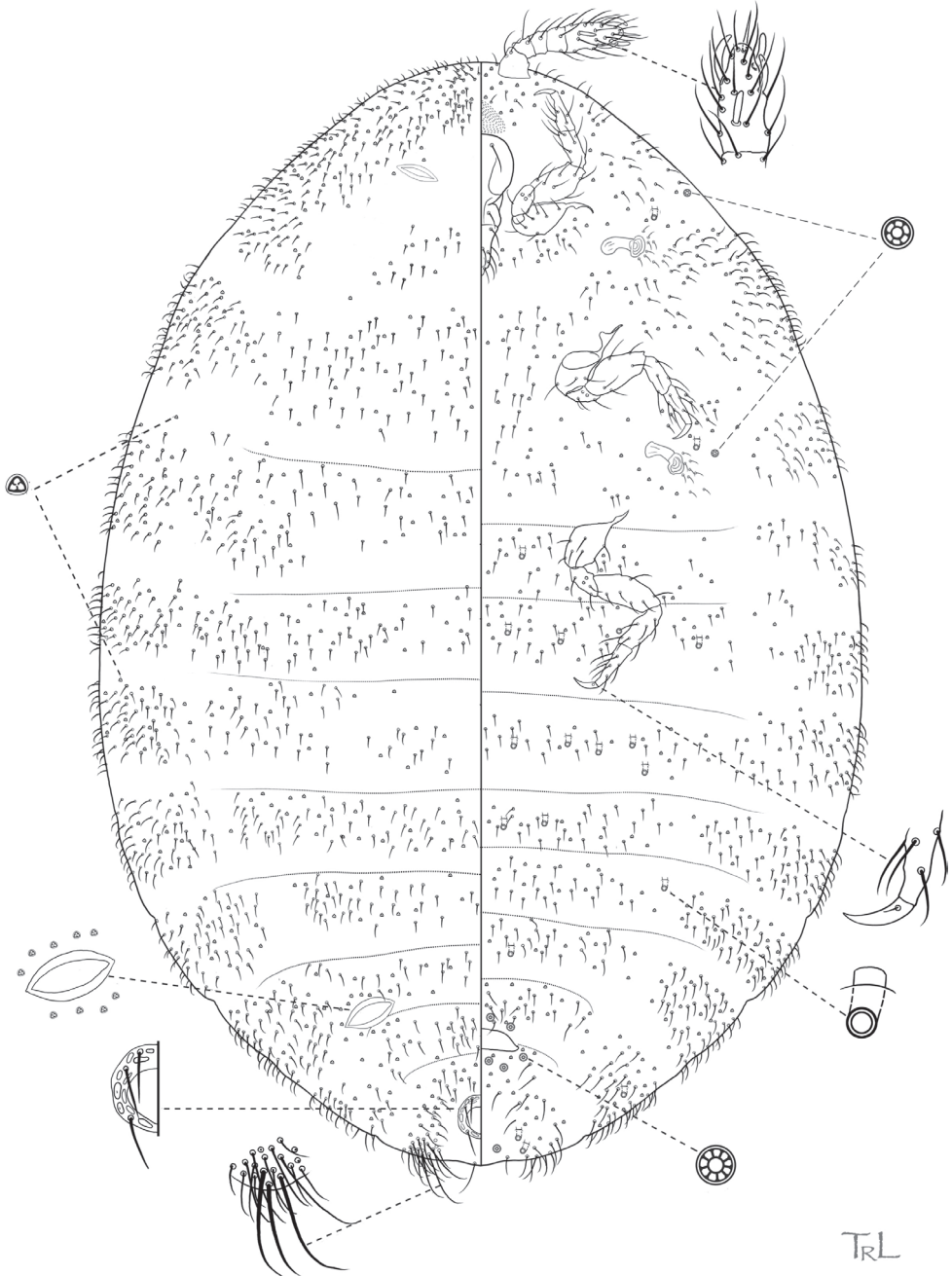


Figure 9. *Ripersiella pediandensis* Schneider & LaPolla sp. nov. Adult female, full body view, illustrated from holotype by T. Litwak (USDA ARS SEL), with edits by SAS.

Etymology. The species epithet is an adjective meaning “from the foot of the Andes”, which combines the noun *pedis* (foot), the adjective *andinus* (pertaining to the Andes Mountains), and suffix *-ensis* (of or from a place).

Diagnosis. *Ripersiella pediandensis* sp. nov. is similar in appearance to *R. andensis* but the two species can be distinguished as follows (character states for *R. andensis* are given in parentheses): having oral collar tubular ducts present on the venter (absent); having comparatively long claws, 37 μm (comparatively short, 24 μm); having comparatively long anal lobe setae, 71–108 μm (comparatively short, 33 μm). The body and appendages of *R. pediandensis* are also longer in comparison. Compared to *R. kelloggi* (character states in parentheses), the legs of *R. pediandensis* are larger in proportion to the body (smaller in proportion), the cephalic plate is present (absent), multilocular disc pores are present near the vulva (absent), it is lacking a circulus (bears 2 small circuli), and the longest anal lobe setae are 71–108 μm long (less than 30 μm long). See the diagnosis under *R. telalia* sp. nov. for a comparison to that species.

Comments. The association between *R. pediandensis* and a species of *Acropyga* (within the *goeldii* group) is lacking information on observations that were made to confirm direct trophobiosis between these partners, and only a single nest was collected. Thus, as in some other cases discussed by Schneider and LaPolla (2020), we consider this relationship to be speculative (however likely) until it can be confirmed through further collections and observations.

***Ripersiella telalia* Schneider, sp. nov.**

<https://zoobank.org/9BF4827C-F919-49E2-8BBC-B76E3B87B0EA>

Figures 10, 11

Material examined. Holotype. PERU • 1 adult ♀; Madre de Dios, Manu National Park, Cocha Cashu Biological Station, trail intersection of 1:306 and 5A; -11.8833, -71.4000; 10.vi.2019; JS LaPolla, SA Schneider leg.; from large *Acropyga* (possibly *decedens*) nest; USNM (nest PER24-01: prep S0425D). **Paratypes.** PERU • 3 adult ♀♀; same data as holotype; USNM (nest PER24-01: preps S0425A,C,F) • 1 adult ♀; same data as holotype; UNMSM (nest PER24-01: prep S0425B) • 1 adult ♀; same data as holotype; UNAB (nest PER24-01: prep S0425E) • 1 adult ♀; same data as holotype; UKNMH (nest PER24-01: prep S0425G).

Description. Adult female ($N = 7$). In life, body bright white to cream colored and visibly coated in powdery white wax (Fig. 11).

General. Mounted on microscope slide, body broadly oval and membranous, 0.85–1.07 (0.95) mm long, widest near abdominal segment III, 0.55–0.72 (0.65) mm wide. Abdomen smoothly tapering toward posterior end; abdominal segment VIII about 250 μm wide at base. Anal lobes poorly developed with several stout flagellate setae on venter and dorsum, 16–25 μm long, with longest setae on margin; lacking differentiated set of 3 longer stout setae common to the group. Body setae short and flagellate, 9–12 μm on head, 8–12 μm on thorax, 9–19 μm on abdominal segments. Trilocular pores abundant and distributed among body setae; bitubular cereros absent; 1–4 oral collar tubular ducts present on margins of each abdominal segment VI–VIII and extending as far anterior as III on some specimens. Microtrichia present; rounded dermal micro-bumps apparently absent. Eyes absent.

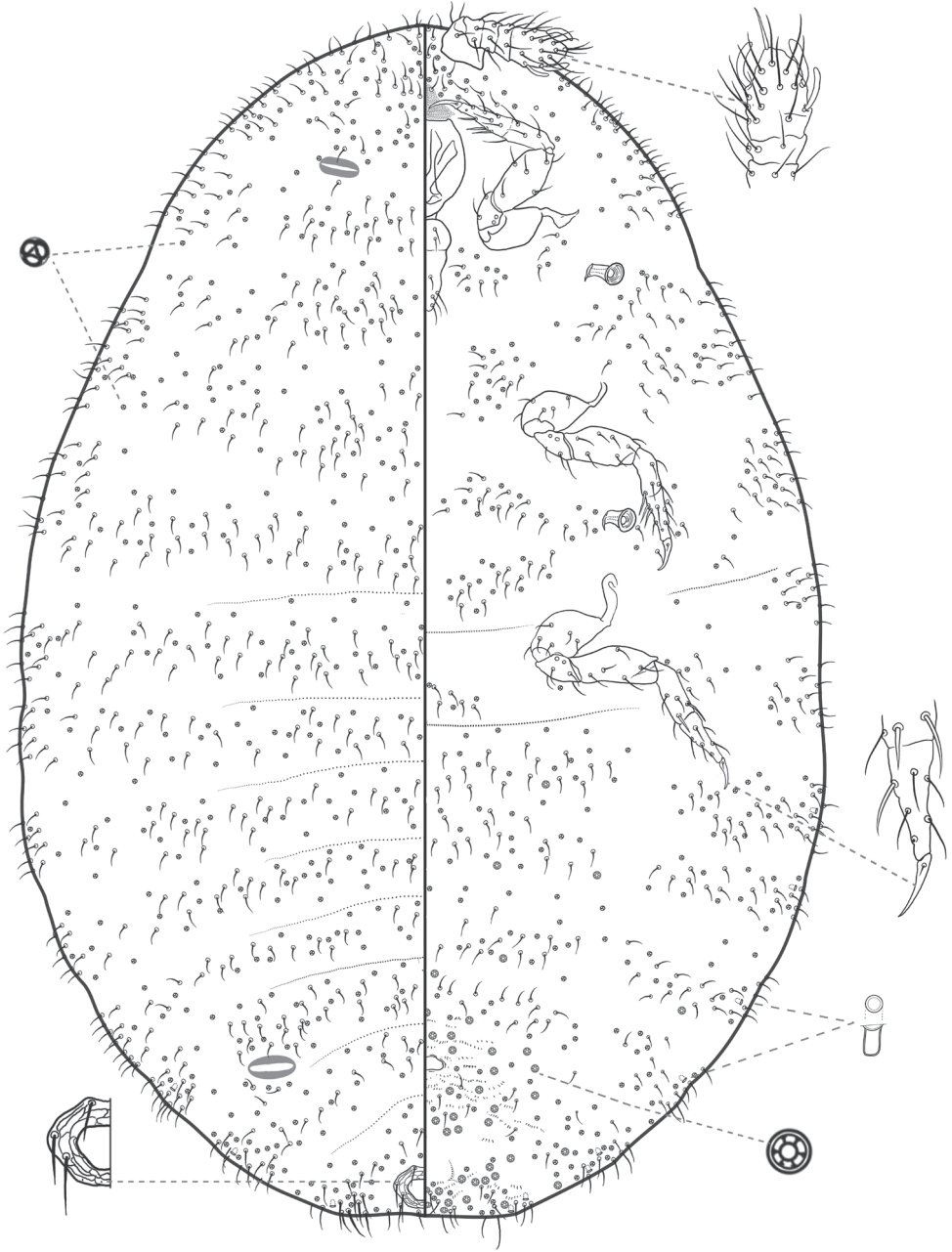


Figure 10. *Ripersiella telalia* Schneider sp. nov. Adult female, full body view, illustrated from holotype by T. Litwak (USDA ARS SEL), with edits by SAS.

Venter. Cephalic plate present. Labium with 3 segments; 76 μm long and 39 μm at widest point. Antennae geniculate, 5-segmented, closely situated near midline on ventral submargin of head; overall length about 126–129 (128) μm ; length of segment I: 32–35 (32) μm ; segment II: 13–16 (16) μm ; segment III: 14–17 (15) μm ; segment IV:

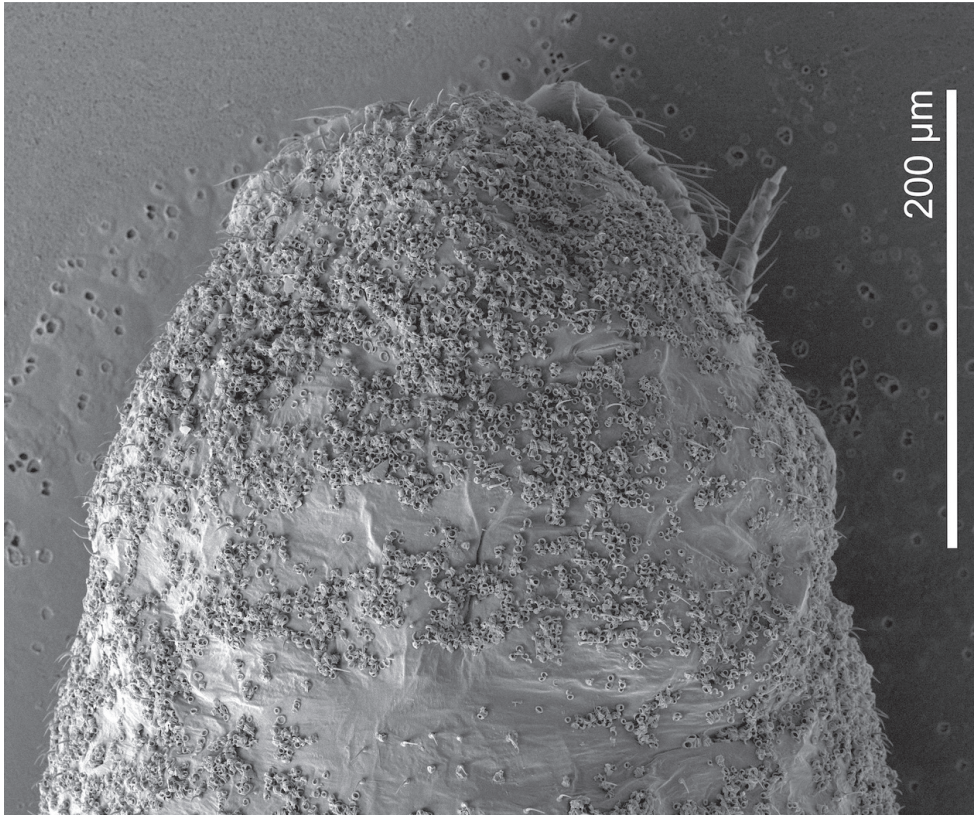


Figure 11. *Ripersiella telalia* Schneider sp. nov. Scanning electron micrograph (SEM) by J. Mowery (USDA ARS SEL). Dorsal anterior view of adult female head and thorax, showing the presence of anterior ostioles, relatively heavy coating of curled wax deposits, and apparent absence of domed dermal microbumps in intersegmental areas.

12–14 (13) μm ; segment V: 50–52 (52) μm ; on some specimens apical antennal segment retains partial intersegmental line marking obsolete segment VI; with 1 spine-like and 3 falcate stout sensory setae on apical segment; a few flagellate setae on each antennal segment, 15–30 μm long; sensorium present on second antennal segment. Legs well developed; overall length of hind leg 267–284 (270) μm ; length of hind coxa 41–52 (41) μm ; hind trochanter + femur 101–105 (102) μm ; hind tibia + tarsus 97–101 (101) μm ; hind claw 26–30 (28) μm ; each claw with short setose digitule 2–3 μm long; flagellate setae present on each segment, around 13–20 μm long; 3 stout spine-like setae on inner margin of tibia and tarsus. Circulus absent. Multilocular disc pores in irregular rows or groups on median to submedian of III–VIII, sparse on III–VI, abundant on segments VII and VIII with some located on submargins, pores with 6 or 7 loculi in the outer ring.

Dorsum. Anal ring near dorsal margin, 41–46 μm in diameter; with oval cells, some cells bearing spicules; with 3 pairs of setae 26 μm long. Posterior pair of dorsal ostioles present, diameter of orifice measured along longitudinal axis approximately

42 µm; anterior pair present and slightly smaller than posterior pair, diameter of orifice approximately 33 µm. Multilocular disc pores absent.

Informal synonyms. Specimens of *R. telalia* have been previously referred to in the literature as “*Ripersiella* near *andensis* (ii)” (Schneider et al. 2022).

Etymology. The species epithet is a genitive noun meaning “distant conversation”, combining the Greek noun *lalia* (conversation, talk) with the suffix *tele* (at a distance). Throughout the isolation of the modern pandemic, quarantine chat groups helped us maintain a much-needed sense of community. This species is named in tribute to these groups, and is specifically dedicated to Josh, Justin, and Mark. The name can be considered a double entendre, as it also alludes to the species’ symbiosis with ants as an ongoing conversation between distantly related partners.

Diagnosis. *Ripersiella telalia* sp. nov. is similar to *R. pediandensis* sp. nov. in possessing oral collar tubular ducts, but the distribution of ducts differs between species. In *R. telalia* these ducts are restricted to the margins of abdominal segments with only 1–4 present per segment, whereas in *R. pediandensis* they are present in ventral bands often exceeding four per segment. The anterior pair of dorsal ostioles are large and more obviously developed in *R. telalia* relative to the other species discussed in this work.

Comments. *Ripersiella telalia* was discovered from quite a large nest of *Acropyga* (probably *decedens*). We estimated in the field that the nest comprised thousands of individual ants and scales. Their direct association was confirmed through observation of the colony using a nest-box, as described by Schneider et al. (2022). After specimens were collected into a nest-box, worker ants gathered trophobionts into a protective cluster and were actively engaged in attending to them.

Key to the Neotropical species of *Ripersiella* lacking bitubular cerores

In Szita et al. (2020), the first couplet in their key to adult females from the Neotropical region distinguishes between species with and species without bitubular cerores (bitubular ducts). Our key to adult females below, restricted to the species lacking bitubular cerores, would substitute their couplets 18–19.

1	Ventral multilocular disc pores absent.....	2
–	Ventral multilocular disc pores present.....	4
2	Oral collar tubular ducts present; abdomen bearing 2 circuli	
 <i>R. kelloggi</i> Ehrhorn & Cockerell	
–	Oral collar tubular ducts absent; abdomen bearing 1 circulus	3
3	Antennae 5-segmented, about 180 µm long; metathoracic legs about 350 µm long; anal lobe setae short, 18–28 µm	<i>R. colombiensis</i> (Hambleton)
–	Antennae 6-segmented, about 135 µm long; metathoracic legs about 285 µm long; anal lobe setae long, 57–60 µm	
 <i>R. illicians</i> Schneider & LaPolla sp. nov.	
4	Oral collar tubular ducts absent	5
–	Oral collar tubular ducts present.....	7

- 5 Antennal segment V shorter than combined length of segments II–IV; antennal segments II–IV differing in length
 ***R. montanae* Schneider & LaPolla sp. nov.**
- Antennal segment V equal to or exceeding combined length of segments II–IV; antennal segments II–IV subequal in length..... **6**
- 6 Ventral multilocular disc pores present on abdominal segments III, IV, or V; longest anal lobe setae distinctly longer than body setae, up to 75 µm long...
 ***R. campensis* Schneider & LaPolla sp. nov.**
- Ventral multilocular disc pores always absent from segments III–IV and rarely on V; longest anal lobe setae similar in length to body setae, up to 35 µm long ***R. andensis* (Hambleton)**
- 7 Oral collar tubular ducts present on medial and submedial areas of abdominal segments; longest anal lobe setae distinctly longer than body setae
 ***R. pediandensis* Schneider & LaPolla sp. nov.**
- Oral collar tubular ducts restricted to submarginal and marginal areas of abdominal segments; longest anal lobe setae similar in length to body setae
 ***R. telalia* Schneider sp. nov.**

Discussion

With the inclusion of several new species in this complex, we can begin to recognize shared traits that may relate to their intimate association with *Acropyga* ants. Structures relating to wax production are of interest. Species in the *andensis*-complex are all conspicuously lacking tubular cerores, which is an uncommon trait among the Rhizoecidae (Kozár and Konczné Benedicty 2007). Loss and reduction of wax-producing structures is suspected to coincide with ant-association among sternorrhynchous insects (Way 1963; Delabie 2001; Ivens 2015); for example, the Xenococcidae have no wax pores, with one unusual exception (Williams 2004). Along these lines, multiple (though not all) species in the *andensis*-complex seem to produce little to no wax from their trilocular pores. Certain species were at first thought to be free of wax until closer inspection under SEM showed that wax deposits are indeed present (Figs 3, 8) but only apparent under high magnification. Why some species produce visible amounts of wax (e.g., *R. illicians* and *R. telalia*) and others do not (e.g., *R. campensis* and *R. montanae*) may relate to abiotic conditions within the nest or perhaps to the duration of their lineage's association with *Acropyga* ants, assuming the loss of wax production occurs gradually over generations.

The trend toward reduction of ostioles among the *andensis*-complex appears to be related to ant association as well. The anterior pair of dorsal ostioles is reduced in size compared to the posterior pair or they are lost entirely among species in the complex. We also note a gradient in the degree of ostiole development among species, ranging from *R. telalia* (Figs 10, 11) and *R. pediandensis* (Fig. 9) with the most prominent pairs

at 33 μm and 29 μm in diameter, respectively, down to two species (*R. colombiensis* and *R. illicians*) who have lost them entirely. *Ripersiella campensis* and *R. montanae* have anterior ostioles reduced in size (10–15 μm in diameter) and poorly developed to the point that they are essentially undetectable when viewed under a light microscope; we only recognized their presence due to SEM imaging (Fig. 3). Ostioles are missing entirely among other scale groups associated with *Acropyga* including the Xenococcidae and some other species of Rhizoecidae (Tanaka 2016; Schneider and LaPolla 2020), further suggesting that reduction of ostioles among the *andensis*-complex is due to their relationship with ants. Ostioles are likely involved in predator defense (discussed in detail by Williams 1978), and these root mealybugs have outsourced their defense against natural enemies to their mutualist partner. Furthermore, reduction in ostiole size among mealybugs is typically correlated with increased dorsal wax production or the production of a felted ovisac covering the body, as in *Antonina* Signoret (Williams 1978); species in the *andensis*-complex produce little to no wax at all. Interestingly, mealybugs from the tribe Allomyrmococcini Williams (Hemiptera, Pseudococcidae), the obligate associates of herdsmen ants (Dill et al. 2002), have trended in the opposite direction and possess dramatically enlarged ostioles that may exude ant attractants (Williams 1978). Therefore, the degree of ostiole development in either direction, whether becoming enlarged or reduced, apparently correlates to a close ecological relationship with ants.

Finally, the “hairiness” of species seems potentially important among groups of trophobiotic mealybugs. For example, members of Xenococcidae tend to be densely covered in setae and/or microtrichia (Williams 1998, 2004; Schneider and LaPolla 2011), as are species of Allomyrmococcini. Williams (1978) suggested that a dense covering of setae may trap a layer of air and act as an alternative to waterproofing in the absence of wax production. Microtrichia can similarly provide waterproofing (Neumann and Woermann 2009). Anecdotally, we note that certain species in the *andensis*-complex appear slightly more densely covered in setae than is typical (e.g., *R. montanae* and *R. pediandensis*). However, further study is required to determine if the relative densities of setae or microtrichia significantly differ among ant-associated rhizoecids compared to those that are free-living. Their setae are clearly less densely distributed than trophobionts from other groups, like the Xenococcidae and Allomyrmococcini. High-resolution SEM images of *R. campensis*, *R. illicians*, and *R. montanae* (Figs 3, 6, 8) captured an abundance of domed dermal micro-bumps, similar to microtrichia, which are concentrated in intersegmental regions and the attachment points of appendages and are not visible under light microscopy. This feature could be typical within the family, which we will only discover through further sampling and imaging of free-living and ant-associated species. Such dermal micro-bumps are not apparent on *R. telalia*, which coincidentally has a relatively dense coating of wax (Fig. 11) compared to the other species and the largest anterior ostioles. Determining the identity and function of these dermal micro-bumps and their correlation to waxiness and ant association offers interesting directions for future research.

Acknowledgements

We thank Dr Roxana Arauco Aliaga for accommodation at Cocha Cashu Biological Station and for assistance with permitting (SERFOR #003620). We thank Kelvin Guerrero for assisting with travel, accommodations, and field work in the Dominican Republic. Thanks to Joe Mowery (USDA ARS SEL) for assistance with SEM imaging. And we thank Imre Foldi for suggesting terminology to describe the unfamiliar domed intersegmental dermal structures visible under SEM. Éva Szita, Hirotaka Tanaka, and Alejandro Caballero kindly provided reviews, and their suggestions helped to improve this manuscript. Support for this research was provided by the National Science Foundation (award number 1754242 to JSL and SAS; DEB-0743542 to JSL). The research was supported also in part by the U.S. Department of Agriculture, Agricultural Research Service. Mention of trade names or commercial products in this publication is solely for the purpose of providing specific information and does not imply recommendation or endorsement by the U.S. Department of Agriculture; USDA is an equal opportunity provider and employer.

The authors have declared that no competing interests exist.

References

- Blaimer BB, LaPolla JS, Branstetter MG, Lloyd MW, Brady SG (2016) Phylogenomics, biogeography and diversification of obligate mealybug-tending ants in the genus *Acropyga*. *Molecular Phylogenetics and Evolution* 102: 20–29. <https://doi.org/10.1016/j.ympev.2016.05.030>
- Bolton SJ, Bauchan GR, Ochoa R, Pooley C, Klompen H (2014) The role of the integument with respect to different modes of locomotion in the Nematolycidae (Endeostigmata). *Experimental & Applied Acarology* 65(2): 149–161. <https://doi.org/10.1007/s10493-014-9857-0>
- Caballero A, Ramos-Portilla AA, Suárez-González D, Serna F, Gil ZN, Benavides P (2019) Scale insects (Hemiptera: Coccoomorpha) on coffee roots (*Coffea arabica* L.) in Colombia, with records of associated ants (Hymenoptera: Formicidae). *Ciencia y Tecnología Agropecuaria. Mosquera (Colombia)* 20: 93–116. https://doi.org/10.21930/rcta.vol20_num1_art:1250
- Choi J, Lee S (2022) Higher classification of mealybugs (Hemiptera: Coccoomorpha) inferred from molecular phylogeny and their endosymbionts. *Systematic Entomology* 47(2): 354–370. <https://doi.org/10.1111/syen.12534>
- Cockerell TDA (1899) Tables for the determination of the genera of Coccidae. *Canadian Entomologist* 31(10): 273–279. <https://doi.org/10.4039/Ent31273-10>
- Delabie JH (2001) Trophobiosis between Formicidae and Hemiptera (Sternorrhyncha and Auchenorrhyncha): An overview. *Neotropical Entomology* 30(4): 501–516. <https://doi.org/10.1590/S1519-566X2001000400001>
- Dill M, Williams DJ, Maschwitz U (2002) Herdsmen ants and their mealybug partners. *Abhandlungen der Senckenbergischen Naturforschenden Gesellschaft* 557: 1–373.

- Goux L (1941) Description d'un *Rhizoecus* nouveau et de sa larve néonate (!). (Note sur les coccides (Hem. Coccoidea) de la France. 31^{me} note.). Bulletin du Muséum d'Histoire Naturelle de Marseille 1: 197–203.
- Goux L (1943) Notes sur les coccides (Hem. Coccoidea) de la France (33^{me} note). Nouvelle contribution à l'étude des *Parahizoecus* avec description de deux espèces nouvelles et de leur larve néonate. Bulletin du Muséum d'Histoire Naturelle de Marseille 3: 41–55.
- Hambleton EJ (1946) Studies of hypogeic mealybugs. Revista de Etologia 17: 1–77.
- Hambleton EJ (1977) Notes on the species of *Neorhizoecus* Hambleton, a synonym of *Rhizoecus* Künckel D'Herculeis (Homoptera: Pseudococcidae). Proceedings of the Entomological Society of Washington 79: 367–376.
- Ivens AB (2015) Cooperation and conflict in ant (Hymenoptera: Formicidae) farming mutualisms—a review. Myrmecological News 21: 19–36.
- Johnson C, Agosti D, Delabie JH, Dumpert K, Williams D, Tschirnhaus MV, Maschwitz U (2001) *Acropyga* and *Azteca* ants (Hymenoptera: Formicidae) with scale insects (Sternorrhyncha: Coccoidea): 20 million years of intimate symbiosis. American Museum Novitates 3335: 1–18. [https://doi.org/10.1206/0003-0082\(2001\)335%3C0001:AAAAHF%3E2.0.CO;2](https://doi.org/10.1206/0003-0082(2001)335%3C0001:AAAAHF%3E2.0.CO;2)
- Kozár F, Konczné Benedicty Z (2003) Description of four new species from Australian, Austro-oriental, New Zealand and South Pacific regions (Homoptera, Coccoidea, Pseudococcidae, Rhizoecinae), with a review, and a key to the species *Ripersiella*. Bollettino di Zoologia Agraria e di Bachicoltura (Milano) 35: 225–239.
- Kozár F, Konczné Benedicty Z (2007) Rhizoecinae of the World. Plant Protection Institute, Hungarian Academy of Sciences, Budapest, 617 pp.
- LaPolla JS (2004) *Acropyga* (Hymenoptera: Formicidae) of the world. Contributions of the American Entomological Institute 33: 1–130.
- LaPolla JS (2005) Ancient trophophoresy: a fossil *Acropyga* (Hymenoptera: Formicidae) from Dominican amber. Transactions of the American Entomological Society 131: 21–28.
- LaPolla JS, Cover SP, Mueller UG (2002) Natural history of the mealybug-tending ant, *Acropyga epedana*, with descriptions of the male and queen castes. Transactions of the American Entomological Society 128: 367–376.
- LaPolla JS, Burwell C, Brady SG, Miller DR (2008) A new ortheziid (Hemiptera: Coccoidea) from Australia associated with *Acropyga myops* Forel (Hymenoptera: Formicidae) and a key to Australian Ortheziidae. Zootaxa 1946(1): 55–68. <https://doi.org/10.11646/zootaxa.1946.1.3>
- Neumann D, Woermann D (2009) Physical conditions for trapping air by a microtrichia-covered insect cuticle during temporary submersion. Naturwissenschaften 96(8): 933–941. <https://doi.org/10.1007/s00114-009-0551-8>
- Normark BB, Okusu A, Morse GE, Peterson DA, Itioka T, Schneider SA (2019) Phylogeny and classification of armored scale insects (Hemiptera: Coccoidea: Diaspididae). Zootaxa 4616: 001–098. <https://doi.org/10.11646/zootaxa.4616.1.1>
- Page RD (2003) Tangled Trees: Phylogeny, Cospeciation, and Coevolution. University of Chicago Press, Chicago, 378 pp.
- Schneider SA, LaPolla JS (2011) Systematics of the mealybug tribe Xenococcini (Hemiptera: Coccoidea: Pseudococcidae), with a discussion of trophobiotic associations with *Acropyga*

- Roger ants. *Systematic Entomology* 36(1): 57–82. <https://doi.org/10.1111/j.1365-3113.2010.00546.x>
- Schneider SA, LaPolla JS (2020) Trophobiosis between a new species of *Williamsrhizoecus* (Hemiptera: Coccoomorpha: Rhizoecidae) and *Acropyga silvestrii* (Hymenoptera: Formicidae) in Tanzania. *Zootaxa* 4853(2): 283–291. <https://doi.org/10.11646/zootaxa.4853.2.9>
- Schneider SA, Sodano J, LaPolla JS (2022) Distinguishing symbiotic partners of *Acropyga* ants from free-living soil inhabitants. *Neotropical Entomology* 51(4): 641–647. <https://doi.org/10.1007/s13744-022-00948-9>
- Smith CR, Oettler J, Kay A, Deans C (2007) First recorded mating flight of the hypogeic ant, *Acropyga epedana*, with its obligate mutualist mealybug, *Rhizoecus colombiensis*. *Journal of Insect Science* 7(11): 1–5. <https://doi.org/10.1673/031.007.1101>
- Szita É, Konczné Benedicty Z, Kondo T, Ramos-Portilla AA, Kaydan MB (2020) Studies on the genus *Ripersiella* Tinsley (Hemiptera: Coccoomorpha: Rhizoecidae) in the Neotropical region, with description of a new species. *Zootaxa* 4851(3): 573–582. <https://doi.org/10.11646/zootaxa.4851.3.7>
- Tanaka H (2016) A new genus and species of Rhizoecidae (Hemiptera, Sternorrhyncha, Coccoomorpha) associated with *Acropyga yaeyamensis* (Hymenoptera, Formicidae, Formicinae). *ZooKeys* 616: 115–124. <https://doi.org/10.3897/zookeys.616.9442>
- Way MJ (1963) Mutualism between ants and honeydew-producing Homoptera. *Annual Review of Entomology* 8(1): 307–344. <https://doi.org/10.1146/annurev.en.08.010163.001515>
- Williams DJ (1978) The anomalous ant-attended mealybugs (Homoptera: Pseudococcidae) of south-east Asia. *Bulletin of the British Museum (Natural History). Entomology* 37: 1–72.
- Williams DJ (1998) Mealybugs of the genera *Eumyrmococcus* Silvestri and *Xenococcus* Silvestri associated with the ant genus *Acropyga* Roger and a review of the subfamily Rhizoecinae (Hemiptera, Coccoidea, Pseudococcidae). *Bulletin of the Natural History Museum London (Entomology)* 67: 1–64.
- Williams DJ (2004) A synopsis of the subterranean mealybug genus *Neochavesia* Williams and Granara de Willink (Hemiptera: Pseudococcidae: Rhizoecinae). *Journal of Natural History* 38(22): 2883–2899. <https://doi.org/10.1080/00222930310001657856>
- Williams DJ, Granara de Willink MC (1992) *Mealybugs of Central and South America*. CAB International, Wallingford, 635 pp.

GPS tracking data of Eurasian oystercatchers (*Haematopus ostralegus*) from the Netherlands and Belgium

Henk-Jan van der Kolk^{1,2,3,4}, Peter Desmet⁵, Kees Oosterbeek⁶,
Andrew M. Allen^{1,3,4}, Martin J. Baptist⁷, Roeland A. Bom⁸,
Sarah C. Davidson⁹, Jan de Jong¹⁰, Hans de Kroon³, Bert Dijkstra¹¹,
Rinus Dillerop¹¹, Adriaan M. Dokter^{12,13}, Magali Frauendorf^{1,3,4}, Tanja Milotić⁵,
Eldar Rakhimberdiev¹³, Judy Shamoun-Baranes¹³, Geert Spanoghe⁵,
Martijn van de Pol^{1,4,14}, Gunther Van Ryckegem⁵, Joost Vanoverbeke⁵,
Eelke Jongejans^{1,3,4}, Bruno J. Ens^{4,6}

1 Netherlands Institute of Ecology, Department of Animal Ecology, Wageningen, Netherlands **2** Dutch Bryological and Lichenological Society (BLWG), Utrecht, Netherlands **3** Radboud University, Nijmegen, Netherlands **4** Centre of Avian Population Studies (CAPS), Wageningen, Netherlands **5** Research Institute for Nature and Forest (INBO), Brussels, Belgium **6** Sovon Dutch Centre for Field Ornithology, Nijmegen, Netherlands **7** Wageningen Marine Research, Wageningen University and Research, Den Helder, Netherlands **8** Royal Netherlands Institute for Sea Research, Coastal Systems, 't Horntje, Netherlands **9** Department of Animal Migration, Max Plank Institute of Animal Behaviour, Radolfzell, Germany **10** WetlandWacht, Vogelbescherming, Zeist, Netherlands **11** Vogelwerkgroep Assen, Assen, Netherlands **12** Cornell Lab of Ornithology, Cornell University, Ithaca, USA **13** Institute for Biodiversity and Ecosystem Dynamics, University of Amsterdam, Amsterdam, Netherlands **14** College of Science and Engineering, James Cook University, Townsville, Australia

Corresponding author: Henk-Jan van der Kolk (henk-janvdkolk@hotmail.com)

Academic editor: George Sangster | Received 20 July 2022 | Accepted 5 September 2022 | Published 3 October 2022

<https://zoobank.org/6FF1E82D-9849-4A34-B1EC-45753EBA9CCC>

Citation: van der Kolk H-J, Desmet P, Oosterbeek K, Allen AM, Baptist MJ, Bom RA, Davidson SC, de Jong J, de Kroon H, Dijkstra B, Dillerop R, Dokter AM, Frauendorf M, Milotić T, Rakhimberdiev E, Shamoun-Baranes J, Spanoghe G, van de Pol M, Van Ryckegem G, Vanoverbeke J, Jongejans E, Ens BJ (2022) GPS tracking data of Eurasian oystercatchers (*Haematopus ostralegus*) from the Netherlands and Belgium. ZooKeys 1123: 31–45. <https://doi.org/10.3897/zookeys.1123.90623>

Abstract

We describe six datasets that contain GPS and accelerometer data of 202 Eurasian oystercatchers (*Haematopus ostralegus*) spanning the period 2008–2021. Birds were equipped with GPS trackers in breeding and wintering areas in the Netherlands and Belgium. We used GPS trackers from the University of Amsterdam

Bird Tracking System (UvA-BiTS) for several study purposes, including the study of space use during the breeding season, habitat use and foraging behaviour in the winter season, and impacts of human disturbance. To enable broader usage, all data have now been made open access. Combined, the datasets contain 6.0 million GPS positions, 164 million acceleration measurements and 7.0 million classified behaviour events (i.e., flying, walking, foraging, preening, and inactive). The datasets are deposited on the research repository Zenodo, but are also accessible on Movebank and as down-sampled occurrence datasets on the Global Biodiversity Information Facility (GBIF) and Ocean Biodiversity Information System (OBIS).

Keywords

Acceleration measurements, animal movement, behaviour, bio-logging, bird tracking, habitat use, machine observation, Movebank, oystercatchers, time budget, UvA-BiTS

Described datasets

- Oosterbeek K, Bom RA, Shamoun-Baranes J, Desmet P, van der Kolk H, Bouten W, Ens BJ (2022) O_SCHIERMONNIKOOG - Eurasian oystercatchers (*Haematopus ostralegus*, Haematopodidae) breeding on Schiermonnikoog (the Netherlands). Dataset. <https://doi.org/10.5281/zenodo.6603183>
- Oosterbeek K, de Jong J, Desmet P, van der Kolk H, Bouten W, Ens BJ (2022) O_AMELAND - Eurasian oystercatchers (*Haematopus ostralegus*, Haematopodidae) breeding on Ameland (the Netherlands). Dataset. <https://doi.org/10.5281/zenodo.6656937>
- Dokter AM, Oosterbeek K, Baptist M, Desmet P, van der Kolk H, Bouten W, Ens BJ (2022) O_BALGZAND - Eurasian oystercatchers (*Haematopus ostralegus*, Haematopodidae) wintering on Balgzand (the Netherlands). Dataset. <https://doi.org/10.5281/zenodo.6603023>
- van der Kolk H, Oosterbeek K, Jongejans E, Frauendorf M, Allen AM, Bouten W, Desmet P, de Kroon H, Ens BJ, van de Pol M (2022) O_VLIELAND - Eurasian oystercatchers (*Haematopus ostralegus*, Haematopodidae) breeding and wintering on Vlieland (the Netherlands). Dataset. <https://doi.org/10.5281/zenodo.5653891>
- Dijkstra B, Dillerop R, Oosterbeek K, Bouten W, Desmet P, van der Kolk H, Ens BJ (2022) O_ASSEN - Eurasian oystercatchers (*Haematopus ostralegus*, Haematopodidae) breeding in Assen (the Netherlands). Dataset. <https://doi.org/10.5281/zenodo.5653311>
- Spanoghe G, Desmet P, Milotic T, Van Ryckegem G, Vanoverbeke J, Ens BJ, Bouten W (2022) O_WESTERSCHELDE - Eurasian oystercatchers (*Haematopus ostralegus*, Haematopodidae) breeding in East Flanders (Belgium). Dataset. <https://doi.org/10.5281/zenodo.5879096>

Introduction

The nominate subspecies of the Eurasian oystercatcher (*Haematopus ostralegus ostralegus* Linnaeus, 1758) is a well-studied, long-lived wader that breeds in coastal areas, and locally inland, in large parts of Europe and winters in coastal areas in

Europe and northern Africa (van de Pol et al. 2014). In coastal areas, oystercatchers largely rely on intertidal mudflats where they forage on shellfish and worms. The behavioural ecology and population ecology of oystercatcher are well understood, as showcased by numerous studies on individual variation in dominance, foraging techniques (Goss-Custard 1996) and life history (Ens et al. 2014a), long-term population studies (Allen et al. 2022) and development of models that predict winter mortality from individual-based models (Stillman and Goss-Custard 2010). The Netherlands harbours approximately 10% of the global breeding population and 20% of the wintering population of the Eurasian oystercatcher, whereas Belgium harbours a small part of the breeding and winter population (-0.1%; van de Pol et al. 2014). The population of oystercatchers increased during the second half of the 20th century, stabilized in the 1980's, but afterwards declined strongly (van de Pol et al. 2014). There is an increasing concern about the ongoing decline in the Netherlands, for which potential causes include (mechanical and non-mechanical) fisheries, disturbance, agricultural intensification and rising sea levels due to climate change (van de Pol et al. 2014).

The datasets described here include all GPS tracking efforts of Eurasian oystercatchers in the Netherlands and Belgium. Research on oystercatchers in the Netherlands intensified in 2008, which was declared as the “Year of the Oystercatcher” by BirdLife Netherlands and the Sovon Dutch Centre for Field Ornithology. In that year, ringing groups were established through the country and they started to colour-band oystercatchers at their breeding grounds, such that they could be resighted in the wintering areas. In the same year, the first trials were completed using GPS trackers from the University of Amsterdam Bird Tracking System (UvA-BiTS; Bouten et al. 2013) on oystercatchers on Schiermonnikoog, an island in the Wadden Sea where a breeding population of oystercatchers has been monitored since 1983. In 2010, new UvA-BiTS tracking studies on oystercatchers began on the Wadden island of Ameland and in the tidal basin of Balgzand. In 2016, the CHIRP (Cumulative Human Impact on biRd Populations) project started (Allen et al. 2018), which aimed to quantify the cumulative impact of human activities on the oystercatcher population. Within this project oystercatchers were equipped with UvA-BiTS GPS trackers on the Wadden island of Vlieland. In 2018, two smaller UvA-BiTS GPS tracking projects were initiated in the city of Assen (Drenthe, the Netherlands) and in agricultural areas near the city of Antwerp (Belgium, in close proximity to the estuary of the Scheldt River).

The research objectives of the GPS tracking studies presented here were diverse, and included studying the territory size and territory use of breeding oystercatchers on saltmarshes and roof-nesting birds in cities, studying the spatial use of mudflats in winter with regard to the presence of benthic prey and to quantify the impacts of aircraft disturbance. To enable further use of the tracking data, we have now published all of the collected data as open data under Creative Commons Zero (CC0 1.0) waiver.

Coverage

Taxonomic coverage

The six datasets collectively contain 6.0 million GPS locations and 164 million accelerometer measurements of 202 individuals of the nominate subspecies of the Eurasian oystercatcher *Haematopus ostralegus ostralegus*, collected using UvA-BiTS (Fig. 1).

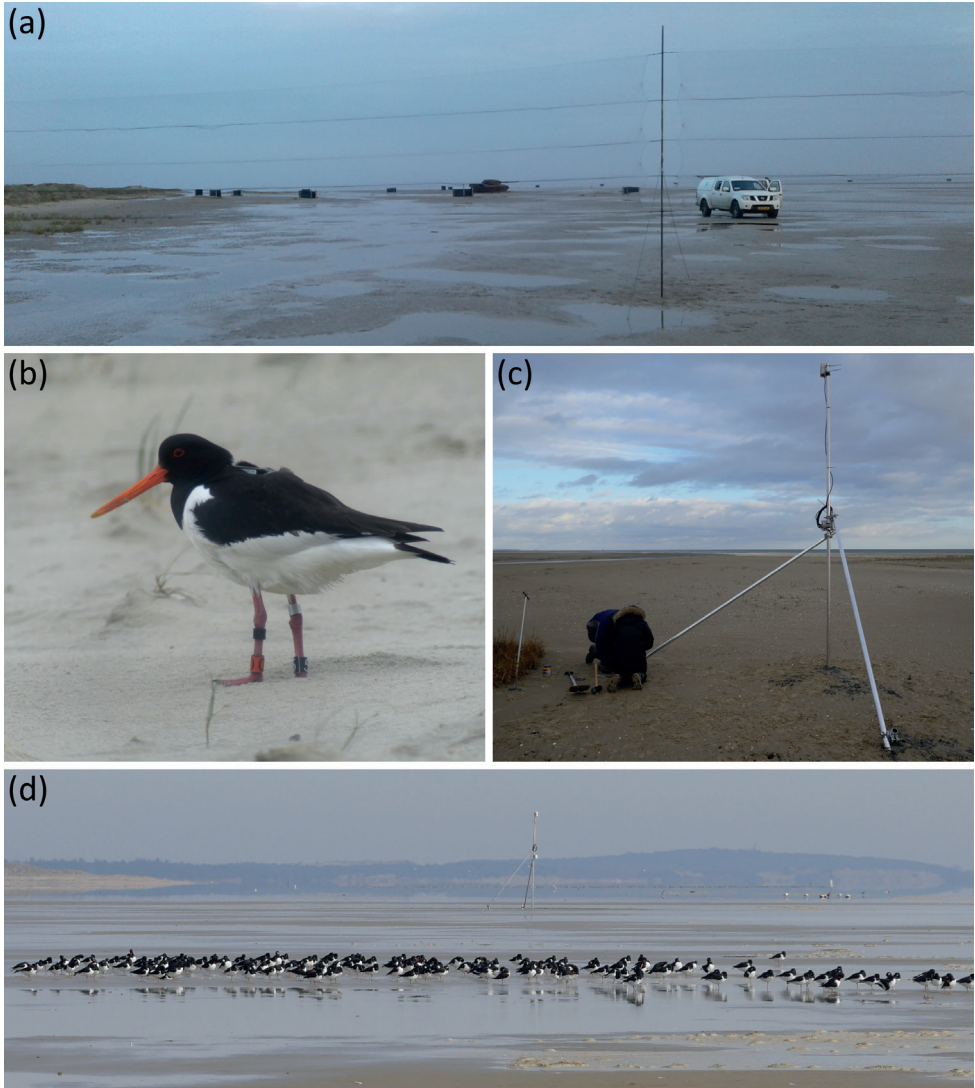


Figure 1. Collecting GPS data of Eurasian oystercatchers using the UvA-BiTS system. **a** mistnets at a high tide roost site on Vlieland, with which birds were trapped **b** Eurasian oystercatcher equipped with colour-rings and UvA-BiTS GPS tracker **c** installation of a relay station via which data from trackers could be retrieved **d** a high tide roost site of Eurasian oystercatchers, showing a relay station in the background.

Geographic coverage

The datasets contain data from breeding and wintering individuals. A total of 98 breeding individuals were tagged on the Dutch Wadden islands, specifically on the saltmarshes of Schiermonnikoog (O_SCHIERMONNIKOOG), the polder meadows on Ameland (O_AMELAND) and on sandflats on Vlieland (O_VLIELAND). A total of 104 wintering individuals were tagged in the Dutch Wadden Sea at Balgzand (O_BALGZAND) and on sandflats on Vlieland (O_VLIELAND). Inland populations were studied in the Dutch city Assen (O_ASSEN) and in urban and agricultural areas near Antwerp in Belgium (O_WESTERSCHELDE) (Table 1; Fig. 2a). The dataset O_BALGZAND also contains one bird (animal-id: 5331220) that was captured on the nest on the saltmarsh of Schiermonnikoog. The number of tracked individuals per dataset can be found in Table 1. Since many oystercatchers migrate between their breeding and wintering sites, the data coverage extends beyond the sites where birds were tagged. Specifically, the breeding sites of tagged individuals ranged from Antwerp to Scandinavia and Russia, and wintering sites spanned from northern France to the Dutch Wadden Sea (Fig. 2b).

Temporal coverage

The datasets collectively cover a time period from 2008 until 2021 (Table 1, Fig. 3).

Methodology

Study extent

Oystercatchers were trapped either in summer on the nest or in winter on their feeding grounds and roost sites. Oystercatchers in breeding populations were always adults that were caught on the nest using walk-in cages. Oystercatchers in wintering populations were caught using mistnets at night, either at low tide (O_BALGZAND) or at high tide (O_VLIELAND). The age of captured birds in winter was classified as either juvenile (1st winter), subadult (2nd winter) or adult (>2nd winter) based on morphology (Cramp et al. 1983). At study sites on Schiermonnikoog and Vlieland, the sex of most birds was determined by DNA analysis of a small blood sample taken from the wing vein and, if available, sex is included in the datasets. Biometrics of trapped birds were taken and included in the datasets, including wing length, tarsus-toe length, bill length, bill tip height, bill tip width (all in mm) and bill tip shape (B = chisel-shaped, H = blunt or hammer-shaped, P = pointed, combined letters indicate intermediate bill tip shapes; van de Pol et al. 2009). Body mass of trapped birds was measured at all study sites and provided for all birds. All birds were equipped with colour rings and with an UvA-BiTS GPS-tracker (Bouten et al. 2013), attached on the back with a harness of Teflon tape that looped around the neck and wings.

Table 1. Dataset characteristics. **Coordinates** are the median coordinates of the catching locations of birds per project; **Individuals** indicates the number of birds that was equipped with a GPS tracker; **Individuals > 100 records** indicates the number of individuals for which at least 100 GPS records are available; **GPS records** the total number of GPS positions; **ACC records** indicates the number of accelerometer measurements; **Classified behaviour records** indicate the number of classified behaviours, derived from accelerometer samples (i.e., bursts of consecutive ACC measurements).

	O. AMELAND	O. BALGZAND	O. VLIELAND	O. ASSEN	O. WESTERSCHELDE
Title	Eurasian oystercatchers (<i>Haematopus ostralegus</i>) Haematopodidae) breeding on Schiermonnikoog (the Netherlands)	Eurasian oystercatchers (<i>Haematopus ostralegus</i>) Haematopodidae) wintering in Balgzand (the Netherlands)	Eurasian oystercatchers (<i>Haematopus ostralegus</i>) Haematopodidae) breeding and wintering on Vlieland (the Netherlands)	Eurasian oystercatchers (<i>Haematopus ostralegus</i>) Haematopodidae) breeding in Assen (the Netherlands)	Eurasian oystercatchers (<i>Haematopus ostralegus</i>) Haematopodidae) breeding in East Flanders (Belgium)
Movebank study ID	1605799506	1605798640	1605802367	1605797471	1099562810
First publication date	2022-01-02	2022-01-19	2022-01-21	2022-01-17	2022-01-19
DOI of version described in this paper	https://doi.org/10.5281/zenodo.6603183	https://doi.org/10.5281/zenodo.6603023	https://doi.org/10.5281/zenodo.5653891	https://doi.org/10.5281/zenodo.5653311	https://doi.org/10.5281/zenodo.5879096
DOI for all versions	https://doi.org/10.5281/zenodo.5647596	https://doi.org/10.5281/zenodo.5653441	https://doi.org/10.5281/zenodo.5653890	https://doi.org/10.5281/zenodo.5653310	https://doi.org/10.5281/zenodo.3734898
Dataset on GBIF	https://www.gbif.org/dataset/361adb42-c1ea-46ed-979c-281ef027cf8f	https://www.gbif.org/dataset/833c03c5-fc23-4e77-a700359e-a4fa-47d2-9bca-0b8500528cea	https://www.gbif.org/dataset/cd15902d-3ded-41c2-893d-8840e146cbb3	https://www.gbif.org/dataset/226421f2-1d29-4950-901c-aba9d0e882bc	https://www.gbif.org/dataset/20bbbd36e-d1a1-4169-8663-59feaa2641c0
Dataset on OBIS	https://obis.org/dataset/01dbcb2a-e166-4752-8547-6db4542cc039	https://obis.org/dataset/2c6aa97e-e886-4564-a53a-48c2e506f014	https://obis.org/dataset/c633b08b-90bb-43f2-8680-65ac26dd8400	https://obis.org/dataset/550b4ccl-c40d-4070-a0cb-26e010eca9d4	https://obis.org/dataset/132cfdf6e-097d-4ee4-b737-58a596dcbe27
Coordinates	53.478°N, 6.209°E	52.943°N, 4.856°E	53.248°N, 4.964°E	53.001°N, 6.570°E	51.275°N, 4.205°E
Individuals	43	22	103	6	13
Individuals > 100 records	39	20	88	4	7
GPS records	602,396	165,897	4,829,950	20,156	73,047
First GPS record	2008-05-31	2010-06-18	2016-12-02	2018-05-04	2018-05-24
Last GPS record	2014-09-02	2014-04-23	2021-09-06	2019-05-25	2020-04-11
Outliers	16	6	1,051	4	0
ACC records	23,157,229	6,266,870	123,034,944	221,802	1,688,085
Classified behaviour records			6,977,784		

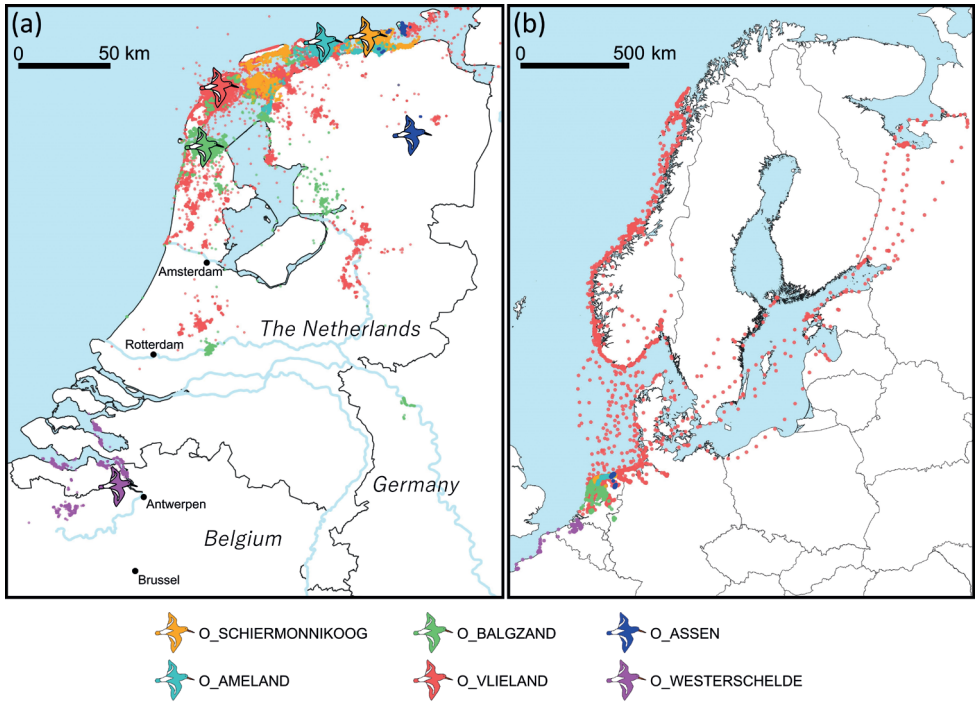


Figure 2. Maps of GPS positions collected from the six different datasets **a** map of the Netherlands and bordering areas of Belgium and Germany showing locations of study sites (indicated by bird symbols) and GPS locations **b** map of northwest Europe showing the full extent of the GPS locations. Maps show GPS locations with hourly intervals; higher frequencies in between GPS locations are omitted in this visualisation.

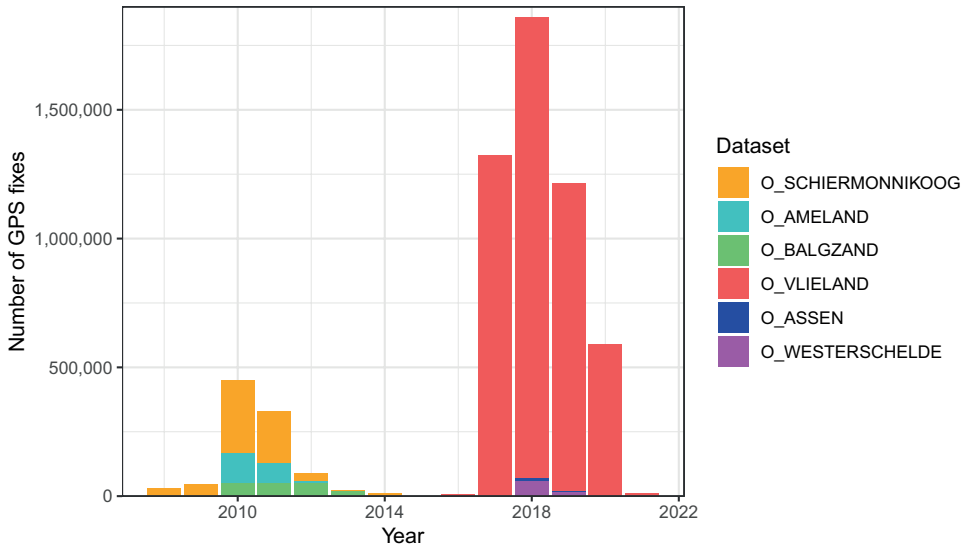


Figure 3. Number of GPS records per dataset per year.

A total of 202 individuals were equipped with a GPS tracker (Table 1), but for several individuals no data were registered, possibly due to the tracker malfunctioning. A minimum of 100 GPS records are available for 172 birds. Information on the end of a tracking session is included in the datasets when malfunctioning trackers were removed or when birds were found dead. In the project O_ASSEN, on one bird (animal-id: 5515867) a malfunctioning tracker was replaced by a new tracker.

Sampling methodology

The UvA-BiTS (Bouten et al. 2013) trackers used for these studies were all solar powered and had a weight of 18.0 g (O_SCHIERMONNIKOOG), 15.0 g (O_SCHIERMONNIKOOG, O_AMELAND, O_BALGZAND) or 13.5 g (O_SCHIERMONNIKOOG, O_VLIELAND, O_ASSEN, O_WESTERSCHELDE). The trackers record 3D GPS positions and include a tri-axial accelerometer that measures surge X, sway Y and heave Z. Accelerometer measurements were collected in samples of up to 10 s with a frequency of 20 Hz (i.e., a 2.00 s sample consists of 40 consecutive accelerometer measurements; Bouten et al. 2013).

All data collected by the GPS trackers were stored in the internal memory. The data were transmitted remotely to a base station, sometimes via in-between relay stations (Fig. 1c–d). A network of base and relay stations was set up around nesting sites (during the breeding season) or covering high tide roosts (during the non-breeding season). Mobile base stations were occasionally used to download data of birds that were found by colour-ring sightings and resided outside the station network. Data that were downloaded were automatically removed from trackers, thereby freeing up storage for new data. Due to the design of the GPS tracking system, no data could be downloaded from birds that left the study areas with station networks and never returned, except when birds were located based on colour-ring sightings for mobile download, or when trackers were retrieved from dead birds and data was subsequently downloaded from the tracker.

The settings of the GPS trackers, i.e., the intervals between successive GPS fixes, intervals between successive accelerometer samples and length of accelerometer samples, were flexible and could be changed anytime a GPS tracker connected to a base station. Accelerometer samples could follow directly upon a GPS fix or be taken in between GPS fixes. Different settings were used in different seasons and projects. In general, more data were collected when the memory of GPS trackers was empty, i.e., when birds resided within the area covered by receiving stations and data were frequently transmitted to base stations, and when the battery of the GPS trackers was fully charged, i.e., in summer when there is more sunlight. In winter, the battery of the trackers often drained, pausing data collection and consequently, there were data gaps for many birds each winter from November to January. When trackers were collecting data, GPS fixes were recorded at least once per hour, and often at higher frequencies (i.e., every 5, 10 or 15 mins). Sometimes, GPS trackers were set to record bursts with high frequency GPS fixes (i.e., every 16 s) for one or two hours per day during daytime. A total of 6.0 million GPS fixes were collected between 2008 and 2021 (Fig. 3).

Data received by the base stations were automatically extracted, post-processed, and stored in a central PostgreSQL database which is part of UvA-BiTS, and accessible to participating researchers only.

The accelerometer samples (i.e., a burst of consecutive accelerometer measurements) can be used to derive movement and behaviour. Typically, behaviour was classified based on summary characteristics (e.g., mean X, standard deviation of Z, etc.) of the accelerometer samples, using a machine learning program that was calibrated with a training dataset. Within these projects, training datasets were acquired by annotating accelerometer samples based on detailed field observations (Shamoun-Baranes et al. 2012) or based on videos that were taken from birds with GPS trackers (van der Kolk et al. 2020a). For O_VLIELAND, a Random Forest model was trained to distinguish five behaviours (flying, walking, foraging, preening, and inactive) and had a prediction accuracy of 94.6% (van der Kolk et al. 2020a). A total of 7.0 million behavioural classifications based on the random forest model were included in the dataset O_VLIELAND, enabling the study of individual variation in behaviour and time budgets (Fig. 4). Note that the classification models were based on annotated behavioural data obtained in intertidal areas mainly in the non-breeding season, and that some behaviours are therefore not distinguished (e.g., no territorial display behaviour was included and incubating behaviour was grouped with inactive behaviour).

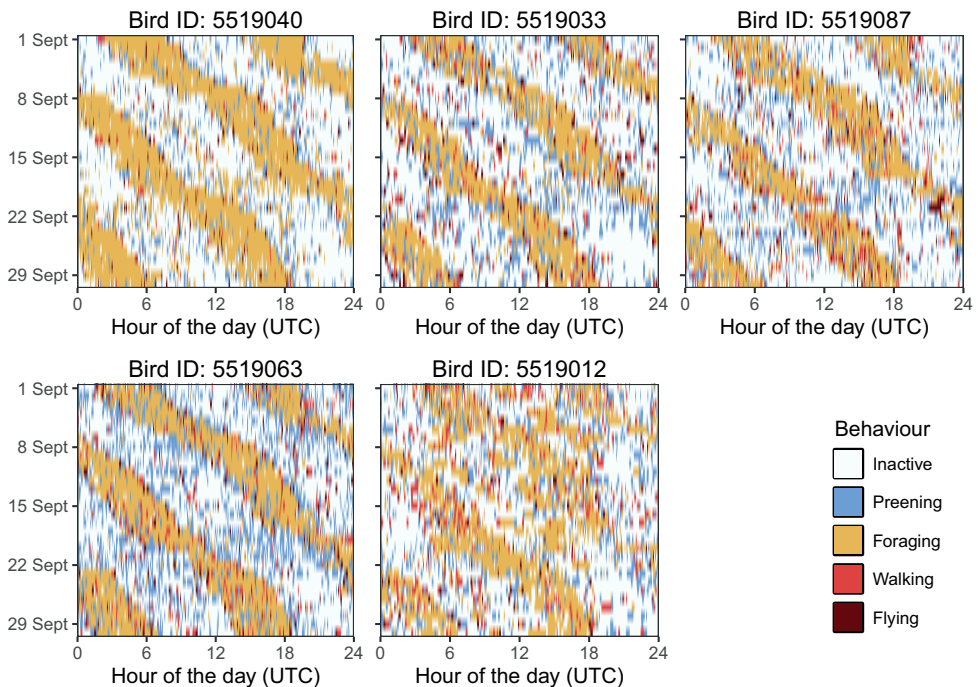


Figure 4. Example of how behavioural classifications included in dataset O_VLIELAND can be used to study time budgets. Time budgets are shown for five individuals in September 2018, which is the non-breeding season when birds were present in intertidal areas on or near Vlieland. The time when birds are foraging shifts every day by 0.5-1.0 hours, as the moments of low tide shifts with the lunar cycle.

Quality control

GPS fixes that were likely incorrect (i.e., outliers) were marked in two ways: manually by the researcher in the UvA-BiTS database (indicated as TRUE in *manually-marked-outlier*) and automatically (in <https://github.com/inbo/bird-tracking>) before uploading to Movebank for GPS-fixes with speed above 45 ms^{-1} or GPS-fixes with an angle below 30° and speed above 15 ms^{-1} (indicated as TRUE in *import-marked-outlier*). The outlier count for each study is provided in Table 1. The rationale for these criteria is that migrating oystercatchers can travel at speeds up to around 30 ms^{-1} but then move in a more or less straight direction (translating into a large angle). Outliers are typically characterised by high speed and a sharp angle (i.e., a movement towards the outlier is followed by a movement back to the original location). These criteria target mostly the largest outliers, and depending on the goal of data use, stricter filtering criteria may need to be applied.

Data publication

To make the data openly available, all data were uploaded to Movebank (<https://www.movebank.org>), an online platform and database specialized in storing animal tracking and bio-logging data. The Movebank data model enables the description of animals, tags, deployments, detections, and other measurements recorded by or derived from animal-borne sensors, such as acceleration data (Kays et al. 2022). For the six datasets, reference data containing information about the animals, tags and deployments, as well as GPS and acceleration data were downloaded from the UvA-BiTS database and transformed to the Movebank data format (Movebank 2021) using SQL queries and R scripts (<https://github.com/inbo/bird-tracking>). This guarantees a consistent approach for all datasets and allows for repeating the process when new data become available for active studies. These data (and for O_VLIELAND additional behavioural classifications) were then uploaded to the Movebank database, with one study-identifier for each dataset (Table 1), documented with metadata and made available under an open Creative Commons Zero waiver.

To enable long-term and low-tech data preservation, data were also deposited as CSV files on the research repository Zenodo (<https://zenodo.org>). GPS, acceleration and behavioural data were split into separate files per year and compressed, making it easier to download data in manageable chunks. A `datapackage.json` file was included for each deposit, making it a Frictionless Data Package (<https://specs.frictionlessdata.io/data-package/>), a simple container format for tabular data. This file references all CSV files, organizes them into resources (reference-data, gps, acceleration, and biometric-measurements) and describes each of their fields, including data type, format and definition according to the Movebank Attribute Dictionary (Movebank 2021). The `datapackage.json` file also facilitates programmatic access to the dataset, such as with the R package ‘frictionless’ (Desmet and Oldoni 2022). Each deposited version on Zenodo is assigned a DOI upon publication, as well as a versionless DOI that always points to the latest version of the deposit (see Table 1 for their Zenodo identifiers).

Movement data can be used as general-purpose occurrence data. To enable wider discoverability and use, we reformatted our datasets to incorporate them

in the Global Biodiversity Information Facility (GBIF, <https://www.gbif.org>) and the Ocean Biodiversity Information System (OBIS, <https://obis.org>). Reference and GPS data (excluding outliers; including fields informing on accuracy, e.g., *coordinateUncertaintyInMeters*) were transformed to Darwin Core (Wieczorek et al. 2012), and down-sampled to the first record per hour, to not needlessly flood GBIF and OBIS with high-frequency movement data. Metadata were transformed to the Ecological Metadata Language (EML) and included the same authors, keywords and DOI, and explained that data are down-sampled. The transformation process to Darwin Core and EML was automated with the custom developed R package ‘movepub’ (Desmet 2022). This automated approach includes fields that are not available for the datasets described in this study (*organismName* and *reproductiveCondition*), but could be included for future datasets that are transferred using this process. The datasets on Zenodo, GBIF and OBIS cross reference each other as well as the datasets on Movebank.

Method steps

Sampling

1. Researcher defines a GPS tracker measurement scheme, which could be updated anytime GPS trackers were connected to a base station.
2. Researcher captures bird, takes biometrics, attaches UvA-BiTS GPS tracker, and releases bird.
3. Researcher records or updates metadata about bird, GPS tracker and deployment in UvA-BiTS database.
4. GPS tracker records data.
5. GPS tracker automatically transmits recorded data when connected with a base station.
6. Recorded data were automatically extracted, post-processed, and stored in the central PostgreSQL database of UvA-BiTS.
7. Data stream stops when a bird no longer returns to the study area, if a bird dies, if a GPS tracker malfunctions or if receiver stations are removed.

Data publication

1. Data (reference, GPS and acceleration) were exported from UvA-BiTS in the Movebank data format.
2. GPS outliers were marked.
3. Data were uploaded to the appropriate study on Movebank and made publicly available.
4. Data were exported from Movebank and archived on Zenodo as a Frictionless Data Package, where each update has a version with a DOI.
5. Data were downsampled to one location per hour and formatted as Darwin Core, allowing exports to GBIF and OBIS.

Additional information

The following information is not included in the datasets and is available upon request: (1) resightings of tagged birds based on colour-ring observations by volunteers; and (2) manually annotated accelerometer data and a classification model to classify behaviour based on accelerometer samples following van der Kolk et al. (2020a), or classifications for specific time periods and datasets that are not already included.

Related publications

The described datasets were used in the following publications: O_SCHIERMONNIKOOG (Shamoun-Baranes et al. 2012; Ens et al. 2014b; Bakker et al. 2021), O_AMELAND (Ens et al. 2014b; Bakker et al. 2021), O_BALGZAND (Dokter et al. 2017; Bakker et al. 2021), O_VLIELAND (Linssen et al. 2019; van der Kolk et al. 2020a, b, 2021a, b, 2022; Bakker et al. 2021; van der Kolk 2021), O_ASSEN (Dijkstra and Dillerop 2018, 2019), O_WESTERSCHELDE (Vanoverbeke et al. 2020).

Acknowledgements

We thank Jakob Schwalb-Willmann and one anonymous reviewer for their constructive comments, which helped to improve the manuscript. The datasets were published with funding from Stichting NLBIF - Netherlands Biodiversity Information Facility (nlbif2021.004). The UvA-BiTS virtual lab is supported by the Dutch national e-infrastructure, built with support of LifeWatch, the Netherlands eScience Center, SURFsara and SURF foundation. Funding for O_SCHIERMONNIKOOG and O_AMELAND was provided by NAM gas exploration. Funding for O_BALGZAND was provided by the project Monitoring abundance, composition, development and spatial variation in macrozoobenthos and birds of the national programme for sea and coastal research (ZKO) of the Netherlands Organization for Scientific Research (NWO) and additional funding by NAM gas exploration. Funding for O_VLIELAND was provided by the Applied and Engineering Sciences domain of the Netherlands Organisation for Scientific Research (NWO-TTW 14638) and co-funding via NWO-TTW by Royal Netherlands Air Force, Birdlife Netherlands, NAM gas exploration and Deltares. Funding for O_ASSEN was provided by the Prins Bernard Cultuurfonds Drenthe, municipality of Assen, IJsvogelfonds (from Birdlife Netherlands and Nationale PostcodeLoterij) and the Waterleiding Maatschappij Drenthe. Funding for O_WESTERSCHELDE was provided by the Flemish-Dutch Scheldt Commission (VNSC) and Research Foundation - Flanders (FWO) as part of the Belgian contribution to LifeWatch, and part of the tags was funded by the Sovon Dutch Centre for Field Ornithology. SCD acknowledges support from the NASA Ecological Forecasting Program Grant 80NSSC21K1182.

References

- Allen A, Ens BJ, van de Pol M, Frauendorf M, van der Kolk HJ, de Kroon H, Jongejans E (2018) Cumulative Human Impacts on biRd Populations (CHIRP): A multi-tiered approach to conserving the near-threatened Eurasian Oystercatcher. 5th European Congress of Conservation Biology. <https://doi.org/10.17011/conference/eccb2018/107685>
- Allen AM, Jongejans E, van de Pol M, Ens BJ, Frauendorf M, van der Sluijs M, de Kroon H (2022) The demographic causes of population change vary across four decades in a long-lived shorebird. *Ecology* 103(4): e3615. <https://doi.org/10.1002/ecy.3615>
- Bakker W, Ens BJ, Dokter AM, van der Kolk HJ, Rappoldt K, van de Pol M, Troost K, van der Veer HW, Bijleveld AI, van der Meer J, Oosterbeek K, Jongejans E, Allen AM (2021) Connecting foraging and roosting areas reveals how food stocks explain shorebird numbers. *Estuarine, Coastal and Shelf Science* 259: 107458. <https://doi.org/10.1016/j.ecss.2021.107458>
- Bouten W, Baaij EW, Shamoun-Baranes J, Camphuysen KC (2013) A flexible GPS tracking system for studying bird behaviour at multiple scales. *Journal of Ornithology* 154(2): 571–580. <https://doi.org/10.1007/s10336-012-0908-1>
- Cramp S, Simmons KLE, Brooks DC, Collar NJ, Dunn E, Gillmor R, Hollom PAD, Hudson R, Nicholson EM, Ogilvie MA, Olney P, Roselaar C, Voous KH, Wallace D, Wattle J, Wilson M (1983) Handbook of the birds of Europe, the Middle East and North Africa. The birds of the Western Palearctic: 3. Waders to gulls. Oxford University Press, Oxford.
- Desmet P (2022) movepub: Prepare Movebank data for publication. R package version 0.1.0. <https://github.com/inbo/movepub>
- Desmet P, Oldoni D (2022) frictionless: Read and Write Frictionless Data Packages. R package version 0.10.0. <https://doi.org/10.5281/zenodo.5815355>
- Dijkstra B, Dillerop R (2018) Eerste bevindingen zenderonderzoek Scholeksters *Haematopus ostralegus* in Assen. *Drentse vogels* 32: 39–52.
- Dijkstra B, Dillerop R (2019) Over de reis van twee Drentse Scholeksters *Haematopus ostralegus* naar hun overwinteringsgebied in de Waddenzee. *Drentse vogels* 33: 30–35.
- Dokter AM, van Loon EE, Rappoldt C, Oosterbeek K, Baptist MJ, Bouten W, Ens BJ (2017) Balancing food and density-dependence in the spatial distribution of an interference-prone forager. *Oikos* 126(8): 1184–1196. <https://doi.org/10.1111/oik.04139>
- Ens BJ, van de Pol M, Goss-Custard JD (2014a) Chapter Eight - The Study of Career Decisions: Oystercatchers as Social Prisoners In: Naguib M, Barrett L, Brockmann HJ, Healy S, Mitani JC, Roper TJ, Simmons LW (Eds) *Advances in the study of behavior*. Academic Press, Vol 46, 343–420. <https://doi.org/10.1016/B978-0-12-800286-5.00008-0>
- Ens BJ, Bom RA, Dokter AM, Oosterbeek K, de Jong J, Bouten W (2014b) Nieuwe ontdekkingen en mogelijkheden in het onderzoek aan Scholeksters dankzij het UvA Bird Tracking Systeem. *Limosa* 87(2–3): 117–128.
- Goss-Custard JD (1996) *The Oystercatcher. From Individuals to Populations*. Oxford University Press, Oxford.
- Kays R, Davidson SC, Berger M, Bohrer G, Fiedler W, Flack A, Hirt J, Hahn C, Gauggel D, Russell B, Kölzsch A, Lohr A, Partecke J, Quetting M, Safi K, Scharf A, Schneider

- G, Lang I, Schaeuffelhut F, Landwehr M, Storhas M, van Schalkwyk L, Vinciguerra C, Weinzierl R, Wikelski M (2022) The Movebank system for studying global animal movement and demography. *Methods in Ecology and Evolution* 13(2): 419–431. <https://doi.org/10.1111/2041-210X.13767>
- Linssen H, van de Pol M, Allen AM, Jans M, Ens BJ, Krijgsveld KL, Frauendorf M, Van der Kolk HJ (2019) Disturbance increases high tide travel distance of a roosting shorebird but only marginally affects daily energy expenditure. *Avian Research* 10(1): 1–11. <https://doi.org/10.1186/s40657-019-0171-8>
- Movebank (2021) Movebank attribute dictionary. World Wide Web electronic publication. <http://vocab.nerc.ac.uk/collection/MVB/current/> [accessed in January 2022]
- Shamoun-Baranes J, Bom R, van Loon EE, Ens BJ, Oosterbeek K, Bouten W (2012) From sensor data to animal behaviour: An oystercatcher example. *PLoS ONE* 7(5): e37997. <https://doi.org/10.1371/journal.pone.0037997>
- Stillman RA, Goss-Custard JD (2010) Individual-based ecology of coastal birds. *Biological Reviews of the Cambridge Philosophical Society* 85(3): 413–434. <https://doi.org/10.1111/j.1469-185X.2009.00106.x>
- van de Pol M, Ens BJ, Oosterbeek K, Brouwer L, Verhulst S, Tinbergen JM, Rutten AL, Jong MD (2009) Oystercatchers' bill shapes as a proxy for diet specialisation: More differentiation than meets the eye. *Ardea* 97(3): 335–347. <https://doi.org/10.5253/078.097.0309>
- van de Pol M, Atkinson P, Blew J, Crowe O, Delany S, Duriez O, Ens BJ, Hälterlein B, Hötter H, Laursen K, Oosterbeek K, Petersen A, Thorup O, Tjørve K, Triplet P, Yésou P (2014) A global assessment of the conservation status of the nominate subspecies of Eurasian Oystercatcher *Haematopus ostralegus ostralegus*. *International Wader Studies* 20: 47–61.
- van der Kolk H (2021) Stay or fly away? Impact of human disturbance on shorebird individuals and populations. PhD Thesis. Radboud University, Nijmegen.
- van der Kolk H, Ens BJ, Oosterbeek K, Bouten W, Allen AM, Frauendorf M, Lameris TK, Oosterbeek T, Deuzeman S, de Vries K, Jongejans E, van de Pol M (2020a) Shorebird feeding specialists differ in how environmental conditions alter their foraging time. *Behavioral Ecology* 31(2): 371–382. <https://doi.org/10.1093/beheco/arz189>
- van der Kolk H, Allen AM, Ens BJ, Oosterbeek K, Jongejans E, van de Pol M (2020b) Spatiotemporal variation in disturbance impacts derived from simultaneous tracking of aircraft and shorebirds. *Journal of Applied Ecology* 57(12): 2406–2418. <https://doi.org/10.1111/1365-2664.13742>
- van der Kolk H, Ens BJ, Frauendorf M, Jongejans E, Oosterbeek K, Bouten W, van de Pol M (2021a) Why time-limited individuals can make populations more vulnerable to disturbance. *Oikos* 130(4): 637–651. <https://doi.org/10.1111/oik.08031>
- van der Kolk H, Ens BJ, Jongejans E, Frauendorf M, Allen AM, de Kroon H, van de Pol M (2021b) Conclusies uit vier jaar onderzoek naar vliegtuigverstoring van Scholeksters (*Haematopus ostralegus*) op Vlieland. *Twirre* 31(2): 9–18.
- van der Kolk H, Ens BJ, Oosterbeek K, Jongejans E, van de Pol M (2022) The hidden cost of disturbance: Eurasian Oystercatchers (*Haematopus ostralegus*) avoid a disturbed roost site during the tourist season. *The Ibis* 164(2): 437–450. <https://doi.org/10.1111/ibi.13035>

- Vanoverbeke J, Spanoghe G, De Regge N, Van Ryckegem G (2020) Foerageergedrag van scholeksters op de Westerschelde. Rapporten van het Instituut voor Natuur- en Bosonderzoek: 23. <https://doi.org/10.21436/inbor.18345084>
- Wieczorek J, Bloom D, Guralnick R, Blum S, Döring M, Giovanni R, Robertson T, Vieglais D (2012) Darwin Core: An evolving community-developed biodiversity data standard. PLoS ONE 7(1): e29715. <https://doi.org/10.1371/journal.pone.0029715>

A survey of the genus *Himalaphantes* Tanasevitch, 1992 (Araneae, Linyphiidae) with description of three new species from Yunnan, China

Meng-ting Zhang¹, Ping Liu¹, Muhammad Irfan^{1,2}, Xian-jin Peng¹

1 College of Life Sciences, Hunan Normal University, Changsha, Hunan 410081, China **2** Key Laboratory of Eco-environments in Three Gorges Reservoir Region (Ministry of Education), School of Life Sciences, Southwest University, Chongqing 400715, China

Corresponding authors: Ping Liu (pingzi129@126.com), Xian-jin Peng (xjpeng@126.com)

Academic editor: Dragomir Dimitrov | Received 7 May 2022 | Accepted 8 September 2022 | Published 3 October 2022

<https://zoobank.org/F36D19E8-F921-405A-AF3E-DB4D8E722724>

Citation: Zhang M-t, Liu P, Irfan M, Peng X-j (2022) A survey of the genus *Himalaphantes* Tanasevitch, 1992 (Araneae, Linyphiidae) with description of three new species from Yunnan, China. ZooKeys 1123: 47–62. <https://doi.org/10.3897/zookeys.1123.86261>

Abstract

Three new species of *Himalaphantes* Tanasevitch, 1992 from Yunnan province, China, are described: *H. arcuatus* **sp. nov.** (♀), *H. lingulatus* **sp. nov.** (♂♀), and *H. uncatus* **sp. nov.** (♂♀). The diagnosis of the genus is clarified, and extended detailed descriptions, photographs of somatic features and copulatory organs, and a distribution map are provided.

Keywords

Gaoligong Mountains, morphology, Southwest China, taxonomy

Introduction

The genus *Himalaphantes* was erected by Tanasevitch (1992) to accommodate four ex-*Lepthyphantes* species: *Himalaphantes azumiensis* (Oi, 1979), *H. grandiculus* (Tanasevitch, 1987), *H. magnus* (Tanasevitch, 1987), and *H. martensi* (Thaler, 1987), which are distributed in China, India, Japan, Nepal, and Russia (WSC 2022). *Himalaphantes azumiensis* was reported from the Qinghai, Henan, Sichuan, and Hunan provinces of China (Zhu et al. 1986; Hu 2001; Zhu and Zhang 2011; Yin et al. 2012).

While examining specimens collected from the Gaoligong Mountains, Yunnan, three new species of the genus *Himalaphantes* were recognized and are described here. The genus diagnosis is clarified and extended due to the appearance of new congeners.

Materials and methods

Specimens were stored in 75% ethanol. Epigynes were cleared in trypsin enzyme solution before examination and photography. Left male palps were used for description and color photographs. Specimens were examined and measured with a Leica M205C stereomicroscope. Photographs were taken using Kuy Nice E31SPM digital camera mounted on an Olympus BX53. Compound focus images were generated using Helicon Focus v. 7.6.1.0. A map was created using the online mapping software SimpleMappr (Shorthouse 2010) and then modified in Adobe Photoshop CS2. Leg chaetotaxy is given in the following order: (dorsal, proximal lateral, distal lateral, ventral). Leg measurements are given in the following order: total length (femur, patella + tibia, metatarsus, tarsus). All measurements are given in millimeters (mm). All type specimens treated in this study are deposited at the College of Life Sciences, Hunan Normal University, Changsha, China. The terminology used in the text and figures follows Tanasevitch (1992).

Abbreviations used in the text and figures are as follows: **ALE** = anterior lateral eyes; **AME** = anterior median eyes; **AME–ALE** = distance between AME and ALE; **AME–AME** = distance between AME; **apo** = anterior pocket of paracymbium; **appo** = apical pocket of paracymbium; **DSA** = distal suprategular apophysis; **E** = embolus; **EP** = embolus proper; **LC** = lamella characteristica; **LP** = lateral pocket; **fg** = Fickert's gland; **MM** = median membrane; **PC** = paracymbium; **PCA** = proximal cymbial apophysis; **PLE** = posterior lateral eyes; **PME** = posterior median eyes; **PME–PLE** = distance between PME and PLE; **PME–PME** = distance between PME; **PMP** = posterior median plate; **ppo** = posterior pocket of paracymbium; **PS** = proscapus; **R** = radix; **S** = spermatheca; **ST** = subtegulum; **St** = stretcher; **T** = tegulum; **TA** = terminal apophysis; **TH** = thumb.

Taxonomy

Family Linyphiidae Blackwall, 1859

Genus *Himalaphantes* Tanasevitch, 1992

Diagnosis. *Himalaphantes* is closely related to *Herbiphantes* Tanasevitch, 1992 in having the similar long legs, male palp tibia, modified male chelicerae and similar morphology of embolic division in palp (Tanasevitch 1992: fig. 1b, d, f), but it can be distinguished by the following features: posterior pocket of paracymbium with well-developed projection with blunt (Zhu and Zhang 2011: fig. 80D, E) to bifurcated end

(Figs 4B, D, 7B, D), whereas posterior pocket of paracymbium absent in *Herbiphantes* (Tanasevitch 1992: fig. 1a, c, e). Well-developed proximal cymbial apophysis in *Himalaphantes* species (Figs 4A–C, 7A–C; Tanasevitch 1987: figs 1–3), whereas absent in *Herbiphantes* (Irfan and Peng 2019: figs 4A, B, D, 5A, B; Tanasevitch 1992: fig. 1a, c, e). Female epigyne can be distinguished from *Herbiphantes* species by the proscape small/enlarged with posterior margin smooth and/or posterior margin with small protuberance laterally in *Himalaphantes* species (Figs 1A, B, 5A, B, 8A, B; Tanasevitch 1992: figs 4–9), whereas posterior margin of proscape lacks any of small protuberance laterally in *Herbiphantes* (Irfan and Peng 2019: figs 6A–C, 7A, B; Tanasevitch 1992: fig. 2a–h); stretcher present in *Himalaphantes* species (Figs 1A–C, 5A–C, 8A–C; Tanasevitch 1992: figs. 4–9), whereas stretcher absent in *Herbiphantes* (Irfan and Peng 2019: figs 6A–C, 7A, B; Tanasevitch 1992: fig. 2a–h); posterior median plate relatively reduced and unmodified in *Himalaphantes* species (Figs 1C, 5C, 8C; Tanasevitch 1992: fig. 3e), whereas enlarged and modified in *Herbiphantes* (Irfan and Peng 2019: figs 6A–C, 7A, B; Tanasevitch 1992: fig. 2b, f, i).

Composition. By addition of three new congeners, the genus *Himalaphantes* now comprises of seven species: *H. arcuatus* sp. nov. ♀, from China; *H. azumiensis* from Russia, Japan, and China; *H. grandiculus* from Nepal; *H. lingulatus* sp. nov. ♂♀, from China; *H. magnus* from Nepal; *H. martensi* (Thaler, 1987) from India and Nepal; and *H. uncatatus* sp. nov. ♂♀, from China.

Distribution. China, India, Japan, Nepal and Russia.

Himalaphantes arcuatus sp. nov.

<https://zoobank.org/F23021F9-AAA4-4CFF-974F-07AD6B200EEB>

Figs 1, 2, 10

Type material. Holotype ♀: CHINA, Yunnan Province: Longling County, Xiaoheishan Village, 24.5035°N, 98.4571°E, 2106 m, 29.X.2003, Guo Tang leg. (031029).

Paratypes: 17♀♀, same data as holotype (031029).

Etymology. The specific epithet is derived from the Latin adjective “*arcuata*” (arched), referring to the arched spermatheca.

Diagnosis. This new species resembles *Himalaphantes uncatatus* sp. nov. (Fig. 8), but can be distinguished by: (1) stretcher wider than long, with rounded end in *H. arcuatus* sp. nov. (Fig. 1C), whereas as wide as long, posterior margin with depression medially in *H. uncatatus* sp. nov. (Fig. 8C); (2) spermathecae C-shaped in *H. arcuatus* sp. nov. (Fig. 1C), whereas sinuous in *H. uncatatus* sp. nov. (Fig. 8C); (3) chelicerae with four retromarginal teeth in *H. arcuatus* sp. nov., whereas with five retromarginal teeth in *H. uncatatus* sp. nov.

Description. Female (holotype) (Fig. 2A, B). Total length 3.60. Carapace 1.12 long, 1.16 wide, yellow, sides brown, cephalic region slightly elevated, fovea, cervical and radial grooves distinct; clypeus 0.19 high. Sternum scutiform, brown. Endites brown, distal end broad with scopulae. Labium brown, wider than long. Chelicerae

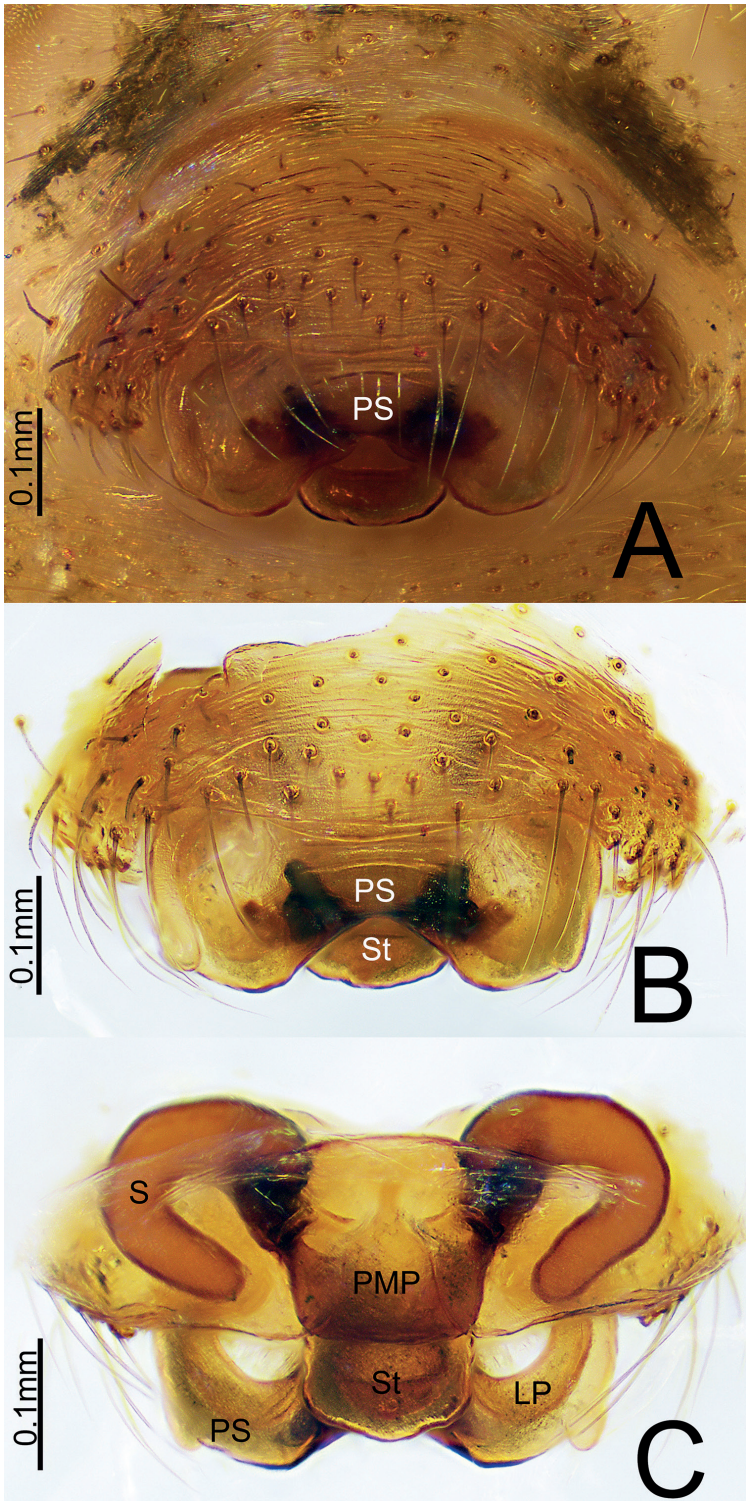


Figure 1. *Himalaphantes arcuatus* sp. nov., holotype ♀ **A, B** epigyne, ventral view **C** epigyne, dorsal view.



Figure 2. *Himalaphantes arcuatus* sp. nov., holotype ♀ **A** habitus, dorsal view **B** habitus, ventral view.

brown, with three promarginal and four retromarginal teeth. Eye sizes and interdistances: AME: 0.09, ALE: 0.11, PME: 0.07, PLE: 0.09, AME–AME: 0.06, AME–ALE: 0.08, PME–PME: 0.04, PME–PLE: 0.06, ALE–PLE: 0.03. Legs yellow with dark annuli. Spines: femur I–II: 1-1-0-0, III–IV: 0-0-0-0; tibia I–II: 2-2-2-2, III: 2-1-2-1, IV 2-2-2-1; metatarsus I, IV: 1-1-1-0, II–III: 1-1-1-1. Leg measurements: I, 8.01 (2.17, 2.77, 2.39, 0.68); II, 7.07 (1.75, 2.19, 1.97, 1.16); III, 4.98 (1.28, 1.46, 1.47, 0.77); IV, 6.65 (1.21, 2.07, 1.81, 1.56); leg formula 1243. Abdomen 2.41 long, 1.73 wide, oval, dorsum greyish yellow, with a dark longitudinal band and light spots dispersed anteriorly, irregular dark markings posteriorly; ventrum grayish yellow, with irregular dark or light spots.

Epigyne (Fig. 1A–C). Wider than long, proscapus wider than long, posterior margin with a deep depression medially, each side with one small protuberance; stretcher longer than wide, with rounded end. Posterior median plate trapezoid, covering most of the stretcher. Copulatory opening present in the middle of proscapus posteriorly. Copulatory ducts short, slightly curved. Spermathecae C-shaped.

Male. Unknown.

Distribution. Known only from the type locality (Fig. 10).

***Himalaphantes lingulatus* sp. nov.**

<https://zoobank.org/9D6376F1-6F50-4DD1-AC61-A2A7262A55A1>

Figs 3–6, 10

Type material. *Holotype* ♂: CHINA, Yunnan Province: Baoshan City, Yakou Village, 24.4372°N, 98.4605°E, 2186 m, 31.X.2003, Guo Tang leg. (Tang031031). *Paratypes*: 1♂22♀♀, same data as holotype (Tang031031).

Etymology. The specific epithet is derived from the Latin adjective “*lingulate*” (tongue-shaped), referring to the tongue-shaped stretcher.

Diagnosis. This new species resembles *H. grandiculus* (Tanasevitch 1987: figs 2, 4–7, 10–12, 1992: fig. 3a–c) but can be distinguished by the following characters: (1) distal end of proximal cymbial apophysis depression medially in *H. lingulatus* sp. nov. (Fig. 4A), whereas rounded in *H. grandiculus* (Tanasevitch 1992: fig. 11); (2) distal branch of paracymbium near cymbiform in ventro-retrolateral view and with three teeth at midlength in *H. lingulatus* sp. nov. (Fig. 4B), whereas near flag-shaped and with one tooth in *H. grandiculus* (Tanasevitch 1987: fig. 2); (3) distal end of embolus blunt and curved in *H. lingulatus* sp. nov. (Fig. 3A), whereas pointed and straight in *H. grandiculus* (Tanasevitch 1992: fig. 3a); (4) stretcher about one-quarter width of scapus in *H. lingulatus* sp. nov. (Fig. 5A), whereas about one-fifth width of scapus in *H. grandiculus* (Tanasevitch 1987: fig. 4); (5) shape of anterior and lateral margins of epigyne arched in *H. lingulatus* sp. nov. (Fig. 5A); whereas varies from rounded to angular in *H. grandiculus* (Tanasevitch 1992: figs 4, 6)

Description. Male (holotype) (Fig. 6A, B). Total length 3.59. Carapace 1.41 long, 1.18 wide, yellowish brown, with a brown longitudinal band medially, lateral sides brown, cephalic region slightly elevated, fovea, cervical and radial grooves distinct; clypeus 0.20 high. Sternum scutiform, yellowish brown with dark margin. Endites yellow, distal end broad with scopulae. Labium wider than long, yellowish brown. Chelicerae yellowish brown, with three promarginal and four retromarginal teeth. Eye sizes and interdistances: AME: 0.09, ALE: 0.11, PME: 0.12, PLE: 0.09, AME–AME: 0.04, AME–ALE: 0.05, PME–PME: 0.06, PME–PLE: 0.08, ALE–PLE: 0.06. Legs yellow with dark annuli. Spines: femur I: 0-1-0-0, II–IV: 0-0-0-0; tibia I: 2-2-1-2, II: 2-0-1-2 III–IV 2-0-1-1; metatarsus I–IV: 1-1-1-0. Leg measurements: I, 11.5 (2.68, 3.66, 3.54, 1.62); II, 8.89 (2.46, 2.61, 2.60, 1.22); III, 7.43 (1.27, 2.49, 2.41, 1.26); IV, 7.42 (2.60, 1.60, 2.27, 0.95); leg formula 1234. Abdomen 1.83 long, 0.88 wide, oval, yellow, dorsum with a dark longitudinal band and light spots dispersed anteriorly, dark herringbones posteriorly; ventral yellow, with lots of irregular dark or light patches.

Palp (Figs 3A, B, 4A–D). Tibia longer than wide. Cymbium longer than wide, median part of prolateral side bulged, proximal cymbial apophysis columnar, distal end as wide as base, with a shallow depression medially. Paracymbium sclerotized, apical pocket near cymbiform in in ventro-retrolateral and prolateral view, anterior pocket unmodified with smooth margin, posterior pocket with three teeth. Distal suprategular apophysis C-shaped, with pointed tip in retrolateral view. Radix longer than wide. Fickert’s gland present within radix. Lamella characteristically S-shaped, with V-shaped tip. Median membrane wider than long. Terminal apophysis proximally

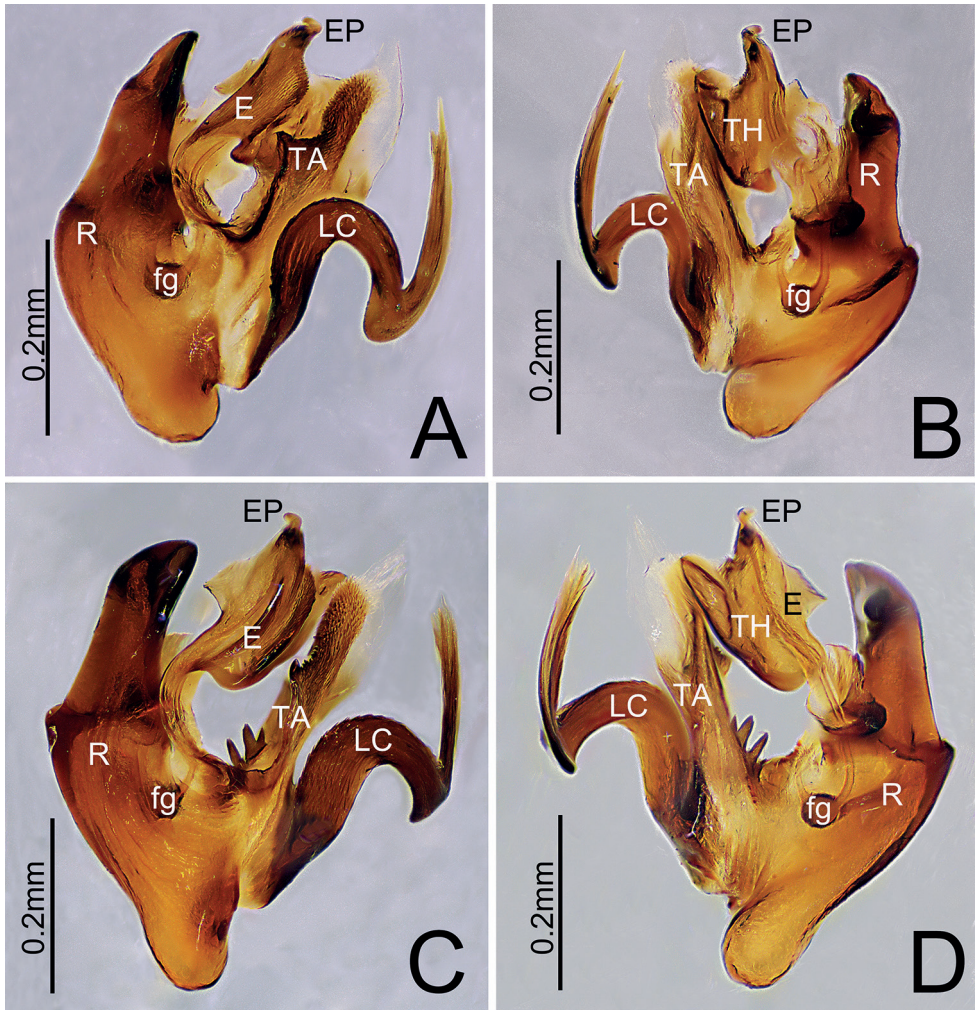


Figure 3. **A, B** *Himalaphantes lingulatus* sp. nov., holotype ♂ **C, D** *Himalaphantes uncatus* sp. nov., holotype ♂ **A, C** embolus, prolatateral view **B, D** embolus, retrolateral view.

strongly sclerotized and distal end relatively membranous. Embolus broad and extending upwards, with curved and blunt end.

Female (one paratype of Tang031031) (Fig. 6C, D). Total length 3.99. Carapace 1.51 long, 1.22 wide, cervical and radial grooves indistinct; clypeus 0.25 high. Chelicerae with four promarginal and five retromarginal teeth. Eye sizes and interdistances: AME: 0.11, ALE: 0.13, PME: 0.12, PLE: 0.10, AME–AME: 0.03, AME–ALE: 0.04, PME–PME: 0.05, PME–PLE: 0.05, ALE–PLE: 0.02. Spines: femur I: 1-1-0-0, II–IV: 1-0-0-0; tibia I: 2-2-2-2, II: 2-1-2-2, III: 2-2-1-1, IV: 2-2-2-1; metatarsus I–IV: 1-1-1-0. Leg measurements: I, 6.84 (1.79, 2.78, 1.28, 0.99); II, 6.61 (1.92, 2.32, 1.32, 1.05); III, 5.43 (1.64, 1.57, 1.42, 0.80); IV, 6.01 (2.06, 2.10, 1.08, 0.77); leg formula 1243. Abdomen 2.42 long, 1.67 wide. Patterns same as in male, but darkly colored.

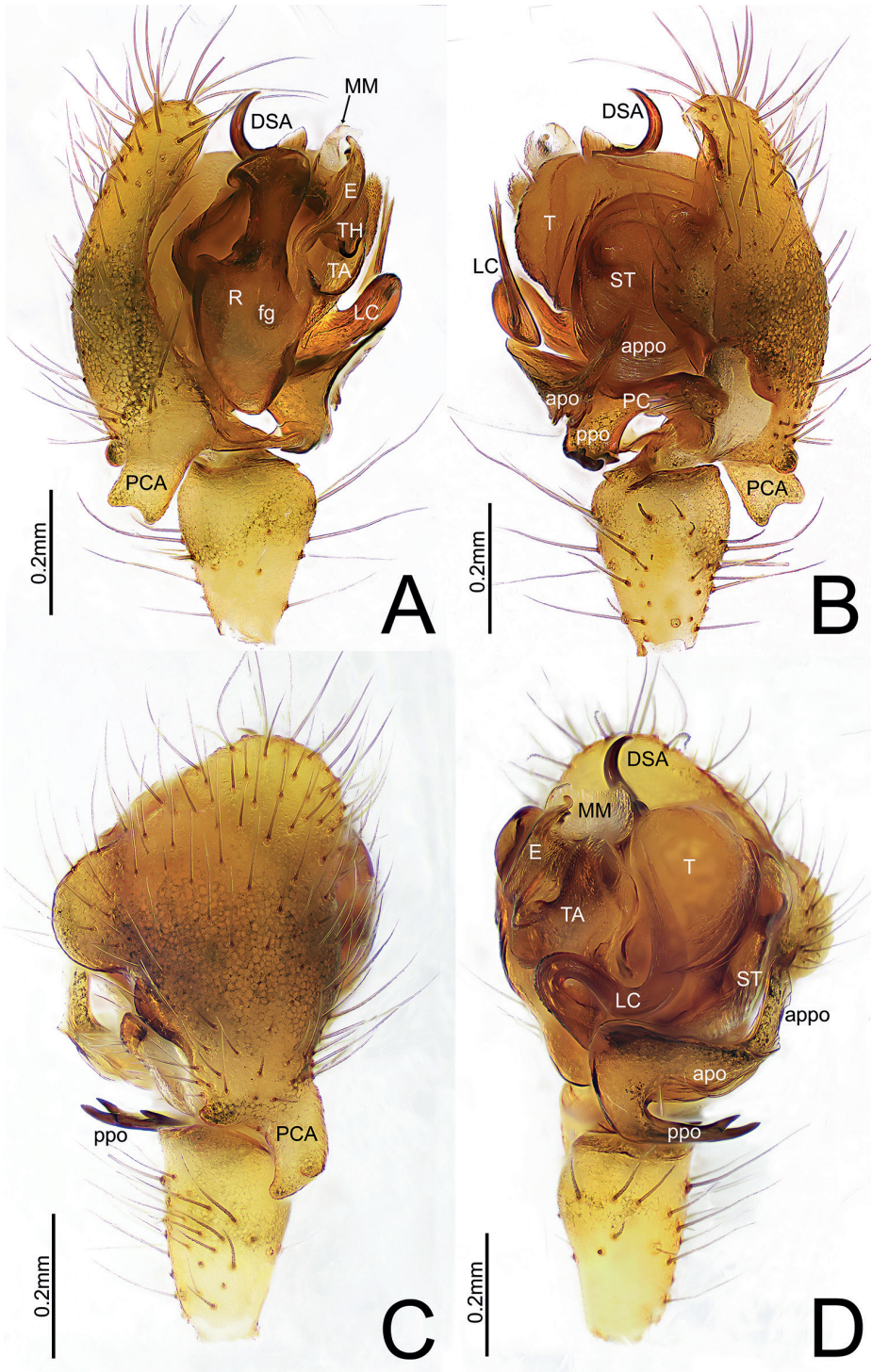


Figure 4. *Himalaphantes lingulatus* sp. nov., holotype ♂ **A** palp, prolateral view **B** palp, retrolateral view **C** palp, dorsal view **D** palp, ventral view.

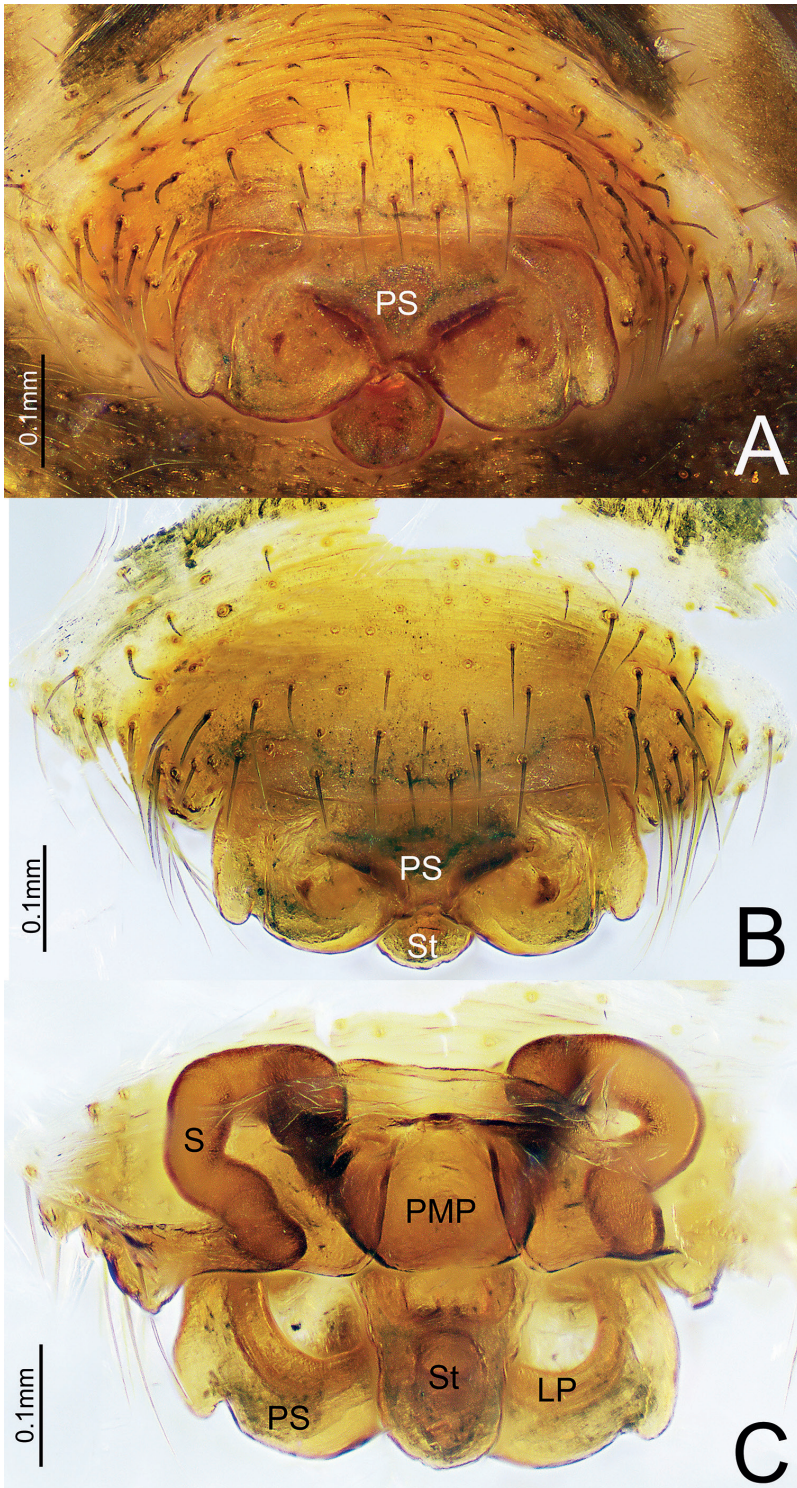


Figure 5. *Himalaphantes lingulatus* sp. nov., paratype ♀ **A, B** epigyne, ventral view **C** epigyne, dorsal view.

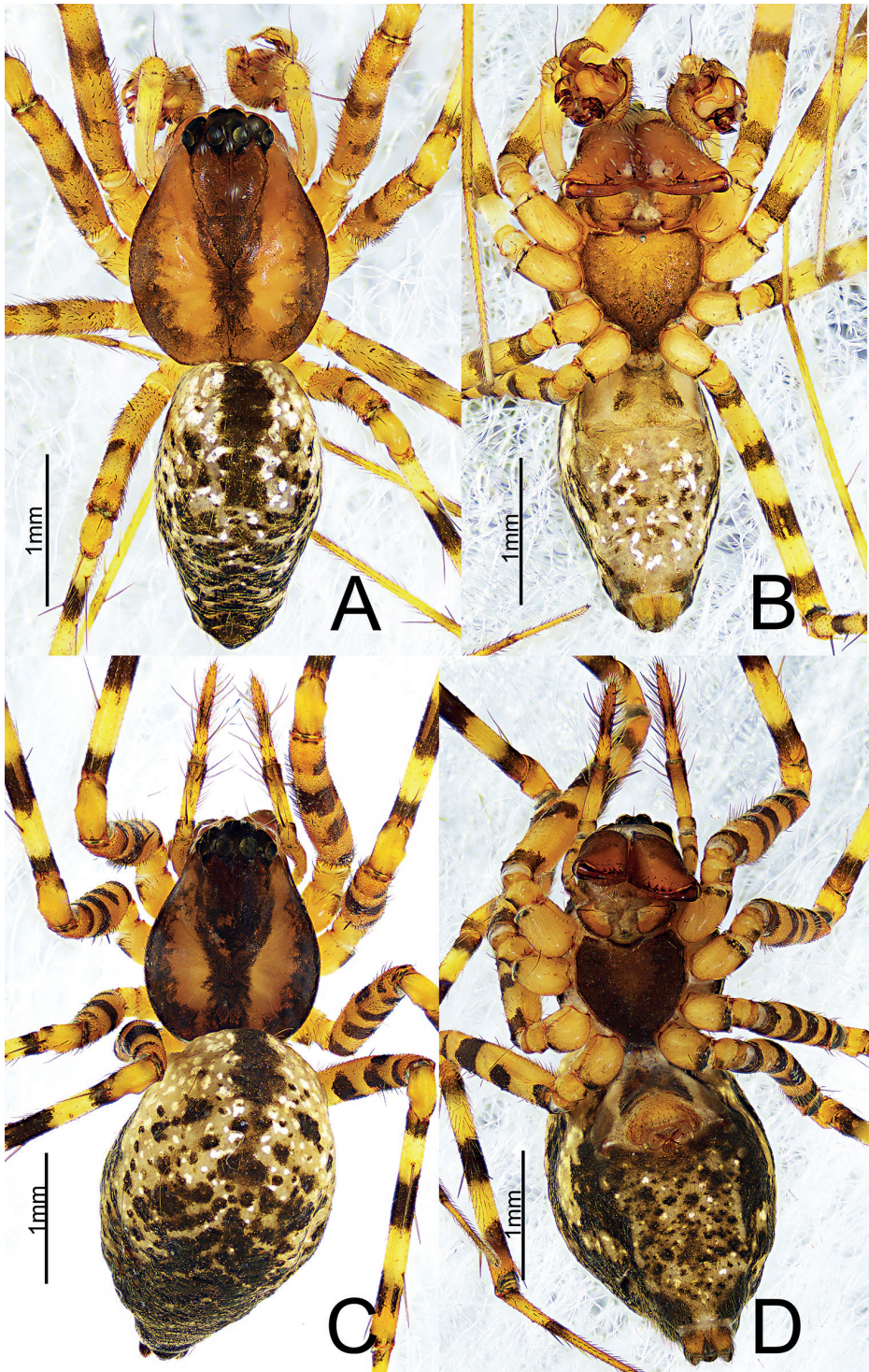


Figure 6. *Himalaphantes lingulatus* sp. nov., holotype ♂ and paratype ♀ **A** habitus, dorsal view **B** habitus, ventral view **C** habitus, dorsal view **D** habitus, ventral view.

Epigyne (Fig. 5A–C). Wider than long, proscapus wider than long, posterior margin with a deep depression medially, each side with a small protuberance; stretcher much longer than wide in dorsal view, tongue-shaped with rounded end. Posterior median plate somewhat oval. Copulatory opening present in lateral pockets at the middle of proscapus posteriorly. Copulatory ducts short, slightly curved. Spermathecae tubular and sinuous.

Distribution. Known only from the type locality (Fig. 10).

***Himalaphantes uncatu* sp. nov.**

<https://zoobank.org/F5C7648F-B52F-4684-AAD7-F53C4F979A0C>

Figs 3, 7–10

Type material. *Holotype* ♂: CHINA, Yunnan Province: Tengchong County, Dashaoping Village, km 41–46 on the road from Bawan to Tengchong, 24.5563°N, 99.4516°E, 2416 m, 18.X.2003, Guo Tang leg. (Tang031018). Paratypes: 1♂18♀♀, same data as holotype (Tang031018).

Etymology. The specific epithet is derived from the Latin adjective “*uncatus*” (hook-shaped), referring to the hook-shaped distal suprategular apophysis.

Diagnosis. The new species resembles *Himalaphantes lingulatus* sp. nov. (Figs 3–6) but can be distinguished by the following characters: (1) proximal cymbial apophysis narrowing posteriorly in prolateral view in *H. uncatu* sp. nov. (Fig. 7A), whereas somewhat rectangular in *H. lingulatus* sp. nov. (Fig. 4A); (2) anterior pocket of paracymbium triangular in retrolateral view in *H. uncatu* sp. nov. (Fig. 7B), whereas somewhat cymbiform in *H. lingulatus* sp. nov. (Fig. 4B); (3) posterior margin of proscapus with a deep inverted V-shaped depression in *H. uncatu* sp. nov. (Fig. 8A–C), whereas with a transverse arc-shaped depression in *H. lingulatus* sp. nov. (Fig. 5A–C); (4) stretcher almost as long as wide, posterior margin slightly depressed medially in dorsal view in *H. uncatu* sp. nov. (Fig. 8B), whereas much longer than wide, with rounded end in *H. lingulatus* sp. nov. (Fig. 5B).

Description. Male (holotype) (Fig. 9A, B). Total length 3.13. Carapace 1.36 long, 1.06 wide, yellowish brown, with brown lateral side, cephalic region slightly elevated, with brown lines from posterior lateral eyes to fovea, fovea, cervical and radial grooves distinct; clypeus 0.17 high. Sternum scutiform, brown. Endites yellowish brown, distal end broad with scopulae. Labium wider than long, brown. Chelicerae yellowish brown, with three promarginal and five retromarginal teeth. Eye sizes and interdistances: AME: 0.08, ALE: 0.10, PME: 0.12, PLE: 0.11, AME–AME: 0.03, AME–ALE: 0.05, PME–PME: 0.04, PME–PLE: 0.05, ALE–PLE: 0.06. Legs yellow with dark annuli. Spines: femur I–IV: 1-0-0-0; tibia I–II: 2-1-1-2, III: 2-1-2-1, IV: 2-1-1-1; metatarsus I–IV: 1-1-1-0. Leg measurements: I, 10.88 (2.96, 3.28, 3.36, 1.28); II, 8.13 (2.45, 2.13, 2.33, 1.22); III, 5.77 (1.42, 1.57, 1.71, 1.07); IV, 6.81 (1.88, 1.85, 2.12, 0.96); leg formula 1243. Abdomen 1.69 long, 0.95 wide, oval, dorsum greyish yellow, with three or four dark herringbones posteriorly and irregular white patches at median and lateral sides; ventral greyish yellow with a few white patches medially.

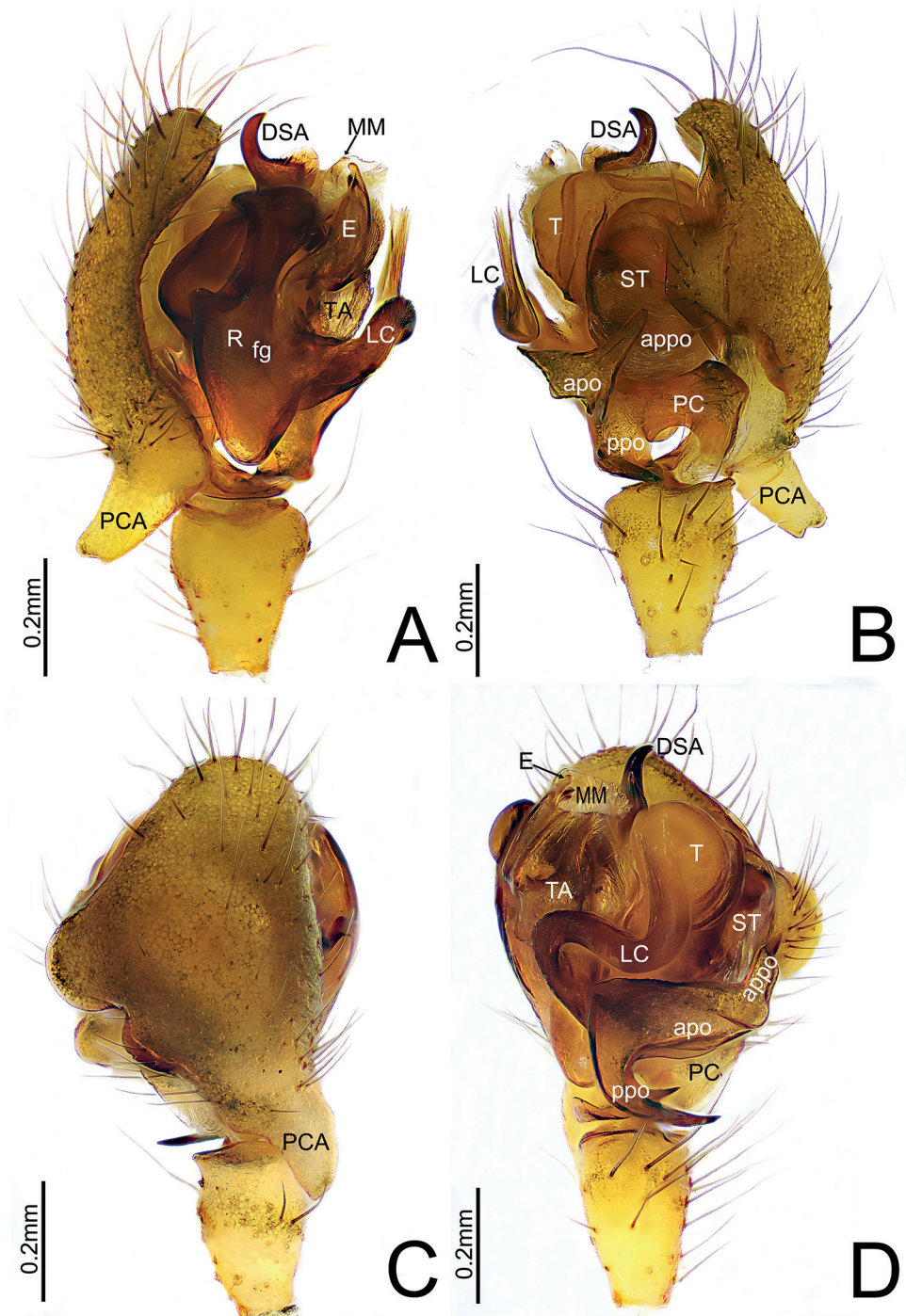


Figure 7. *Himalaphantes uncatatus* sp. nov., holotype ♂ **A** palp, prolateral view **B** palp, retrolateral view **C** palp, dorsal view **D** palp, ventral view.

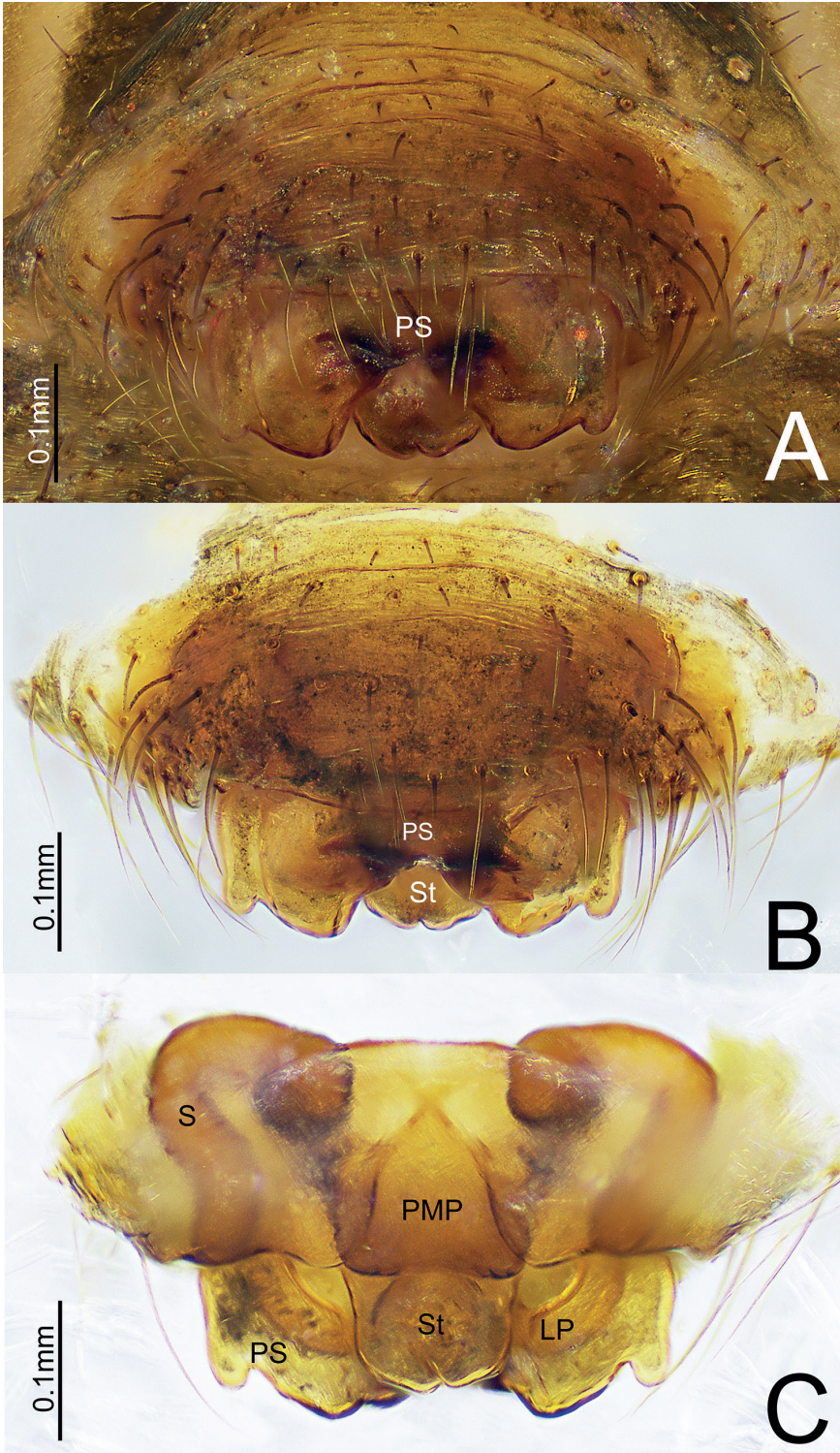


Figure 8. *Himalaphantes uncatus* sp. nov., paratype ♀ **A, B** epigyne, ventral view **C** epigyne, dorsal view.

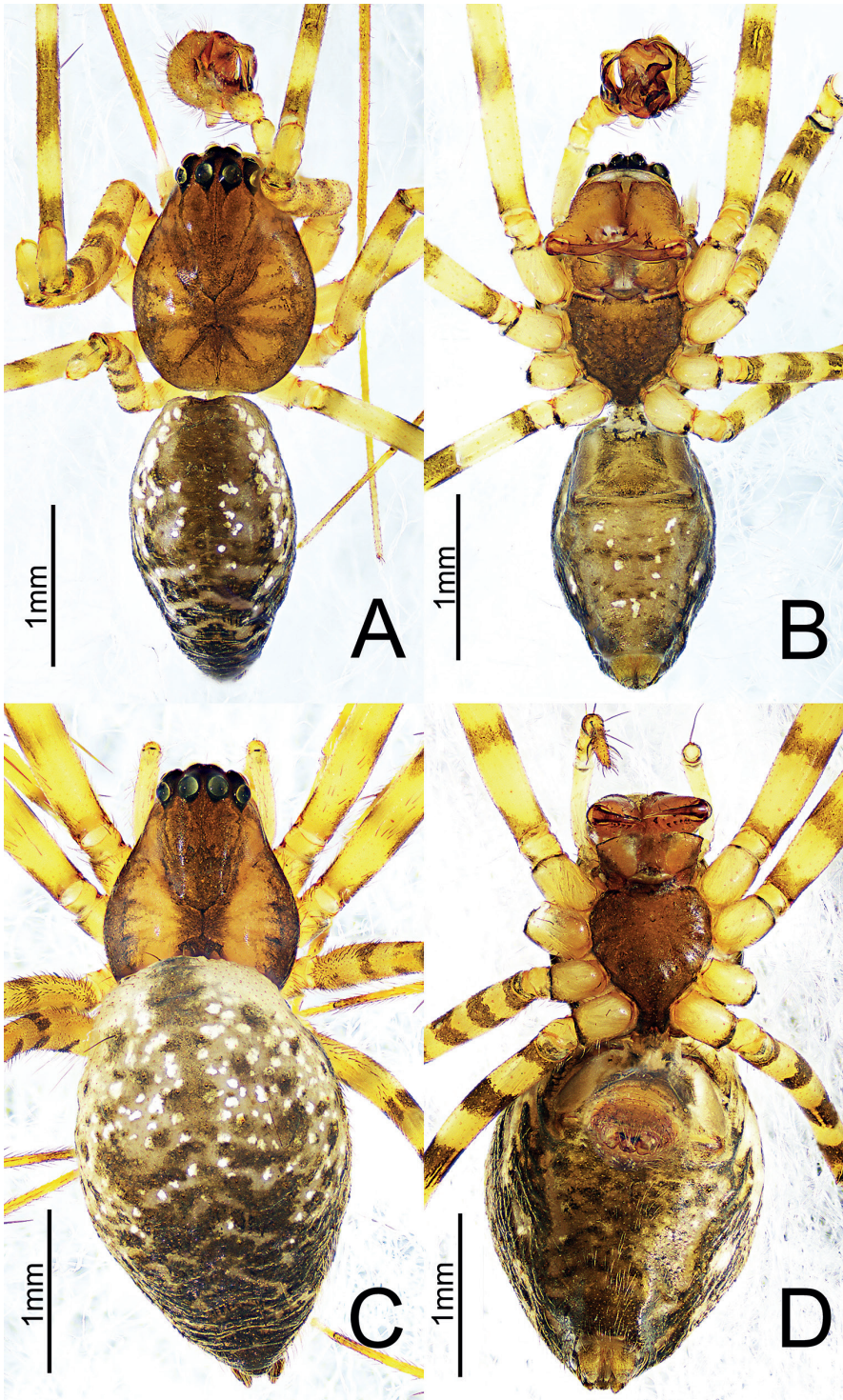


Figure 9. *Himalaphantes uncatus* sp. nov., holotype ♂ and paratype ♀ **A** habitus, dorsal view **B** habitus, ventral view **C** habitus, dorsal view **D** habitus, ventral view.

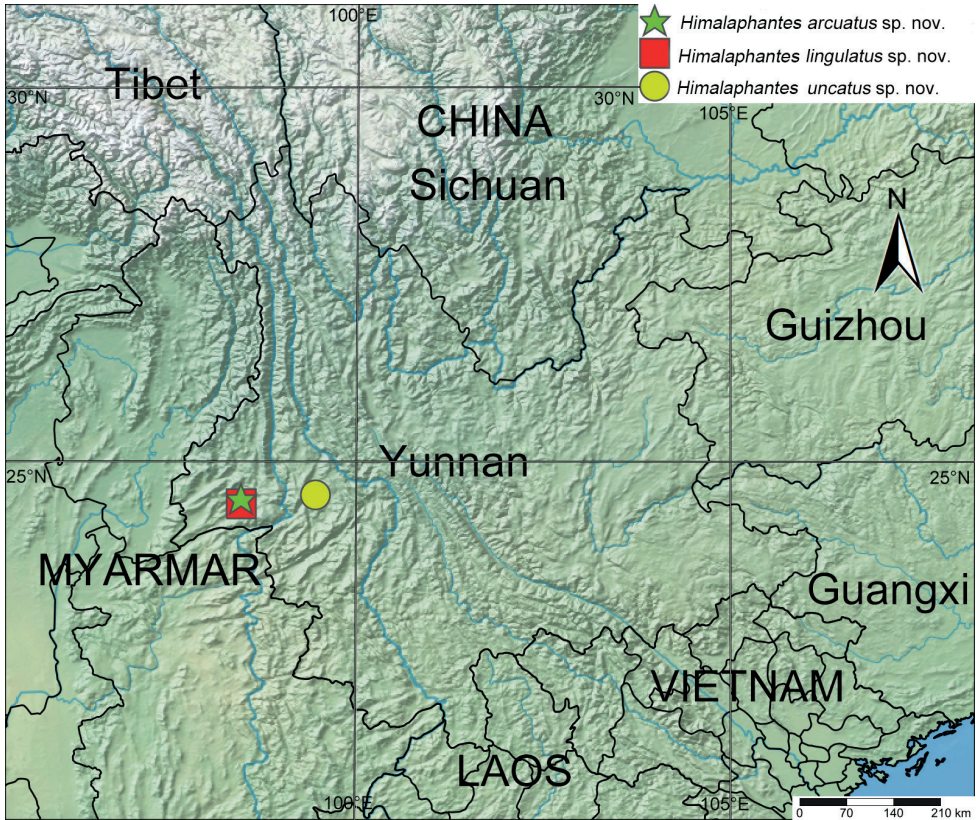


Figure 10. Type localities of *Himalaphantes arcuatus* sp. nov., *Himalaphantes lingulatus* sp. nov. and *Himalaphantes uncatus* sp. nov.

Palp (Figs 3C, D, 7A–D). Tibia longer than wide. Cymbium longer than wide, median part of retrolateral margin bulged, proximal cymbial apophysis almost cylindrical, distal end narrower than base, with a shallow depression medially. Paracymbium sclerotized, apical pocket finger-shaped with blunt end, anterior pocket somewhat triangular in retrolateral view, posterior pocket with three teeth at mid length. Distal suprategular apophysis hook-shaped, with pointed tip in retrolateral view. Radix much longer than wide. Fickert's gland present within radix. Lamella characteristically S-shaped in ventral view. Median membrane wider than long. Terminal apophysis with four teeth at the base, proximally strongly sclerotized and distal end relatively membranous. Embolus broad and extending upwards, with curved and blunt tip, thumb well-developed.

Female (one paratype of Tang031018) (Fig. 9C, D). Total length 3.63. Carapace 1.09 long, 1.11 wide, cervical and radial grooves indistinct; clypeus 0.14 high. Chelicerae with three promarginal and five retromarginal teeth. Eye sizes and interdistances: AME: 0.09, ALE: 0.10, PME: 0.11, PLE: 0.12, AME–AME: 0.03, AME–ALE: 0.07, PME–PME: 0.05, PME–PLE: 0.04, ALE–PLE: 0.01. Spines: femur I: 0-1-0-0, II–IV: 0-0-0-0; tibia I: 2-2-1-3, II–IV: 2-2-2-1; metatarsus I–II: 1-1-1-0, III–IV: 1-1-1-1.

Leg measurements: I, 6.36 (2.22, 1.55, 1.66, 0.93); II, 9.24 (1.74, 2.80, 3.20, 1.50); III, 4.61 (1.44, 1.39, 0.97, 0.81); IV, 5.31 (1.70, 1.40, 1.44, 0.77); leg formula 2143. Abdomen 2.42 long, 1.66 wide. Color and patterns same as in male.

Epigyne (Fig. 8A–C). Wider than long, proscapus wider than long, posterior margin with a deep depression medially, each side with a small protuberance; stretcher almost as long as wide, posterior margin slightly depressed medially. Posterior median plate somewhat rectangular. Copulatory opening present in the middle of scapus posteriorly. Copulatory ducts short, slightly curved. Spermathecae tubular, sinuous.

Distribution. Known only from the type locality (Fig. 10).

Acknowledgements

We are grateful to Andrei Tanasevitch (A.N. Severtsov Institute of Ecology and Evolution, Moscow, Russia) and one anonymous reviewer for their high quality and constructive reviews. We also thank Stephanie F. Loria (American Museum of Natural History, New York, USA) for reviewing the English of manuscript and Guo Tang for collecting the specimens. This research was sponsored by the National Natural Sciences Foundation of China (NSFC-30970327, 31272271, 31272272, 31301861), and the Scientific Research Projects of Hunan Education Department (no. 21B0055).

References

- Hu JL (2001) Spiders in Qinghai-Tibet Plateau of China. Henan Science and Technology Publishing House, Zhengzhou, 658 pp.
- Shorthouse DP (2010) Simple Mappr, an online tool to produce publication-quality point maps. <https://www.simplemappr.net> [accessed on 28 April 2022]
- Tanasevitch AV (1987) The spider genus *Lepthyphantes* Menge 1866 in Nepal (Arachnida: Araneae: Linyphiidae). Courier Forschungsinstitut Senckenberg 93: 43–64.
- Tanasevitch AV (1992) New genera and species of the tribe Lepthyphantini (Aranei Linyphiidae Micronetinae) from Asia (with some nomenclatorial notes on linyphiids). Arthropoda Selecta 1(1): 39–50.
- World Spider Catalog (2022) World Spider Catalog, Version 23.0. Natural History Museum Bern. <http://wsc.nmbe.ch> [accessed 15 June 2022]
- Yin CM, Peng XJ, Yan HM, Bao YH, Xu X, Tang G, Zhou QS, Liu P (2012) Fauna Hunan: Araneae in Hunan, China. Hunan Science and Technology Press, Changsha, 1590 pp.
- Zhu CD, Li ZS, Sha YH (1986) Three new species of spiders of Linyphiidae from Qinghai Province, China (Araneae). Acta Zootaxonomica Sinica 11: 264–269.
- Zhu MS, Zhang BS (2011) Spider Fauna of Henan: Arachnida: Araneae. Science Press, Beijing, 558 pp.

First contribution to *Labiobaetis* Novikova & Kluge in Cambodia (Ephemeroptera, Baetidae), with description of two new species

Thomas Kaltenbach^{1,2}, Jhoana Garces³, Jean-Luc Gattolliat^{1,2}

1 Museum of Zoology, Palais de Rumine, Place Riponne 6, CH-1005 Lausanne, Switzerland **2** University of Lausanne (UNIL), Department of Ecology and Evolution, CH-1015 Lausanne, Switzerland **3** Ateneo Biodiversity Research Laboratory, Department of Biology, School of Science and Engineering, Ateneo de Manila University, Quezon City, 1108 Metro Manila, Philippines

Corresponding author: Thomas Kaltenbach (thomas.kaltenbach@bluewin.ch)

Academic editor: Eduardo Dominguez | Received 13 July 2022 | Accepted 20 August 2022 | Published 4 October 2022

<https://zoobank.org/13556B2A-BE87-44F6-9A43-FCDAFE1C68CB>

Citation: Kaltenbach T, Garces J, Gattolliat J-L (2022) First contribution to *Labiobaetis* Novikova & Kluge in Cambodia (Ephemeroptera, Baetidae), with description of two new species. ZooKeys 1123: 63–81. <https://doi.org/10.3897/zookeys.1123.90308>

Abstract

Material collected in 2018 in Cambodia gives us first insights into the diversity of *Labiobaetis* Novikova & Kluge, 1987 in this country. No species has been reported so far. We identified two new species using a combination of morphology and genetic distance (COI, Kimura 2-parameter). They are described and illustrated based on their larvae. A key to all *Labiobaetis* species of continental Southeast Asia is provided. The interspecific K2P distance between the two new species is 20–21%, the intraspecific distance of one of them is 1%. The total number of *Labiobaetis* species worldwide is augmented to 156.

Keywords

COI, genetic distance, integrated taxonomy, Southeast Asia

Introduction

The genus *Labiobaetis* Novikova & Kluge, 1987 (Novikova and Kluge 1987) is one of the richest genera of mayflies with 154 previously described species (Barber-James et al. 2013; Kaltenbach and Gattolliat 2021; Sivaruban et al. 2022). The distribution of *Labiobaetis* is nearly worldwide, except for the Neotropical realm, New Zealand, and New Caledonia; its

main diversity is found in Southeast Asia (Kaltenbach and Gattolliat 2019, 2020, 2021; Kaltenbach et al. 2020) and New Guinea (Kaltenbach and Gattolliat 2018, 2021; Kaltenbach et al. 2021). The history and concept of the genus *Labiobaetis* were recently summarized in detail (Shi and Tong 2014; Kaltenbach and Gattolliat 2018). Together with *Pseudopannota* Waltz & McCafferty, 1987, it belongs to the tribe Labiobaetini, established by Kluge and Novikova (2016) based on a unique combination of imaginal and larval characters. *Labiobaetis* is part of Baetidae, the family with the highest species diversity among mayflies, comprising over 1160 species in 118 genera (Sartori and Brittain 2015; Jacobus et al. 2019; updated), which is approximately one-third of all mayfly species worldwide.

In the past years, the diversity of *Labiobaetis* in Southeast Asia was intensely studied with focus on the archipelagos of Indonesia (including the whole of Borneo) and the Philippines (Kaltenbach and Gattolliat 2019, 2020, 2021; Kaltenbach et al. 2020). Many new species were described based on morphological and molecular evidence. This contribution will shift our focus to continental Southeast Asia, starting with a first contribution to the knowledge of *Labiobaetis* in Cambodia. Further studies of the genus in the region are in preparation.

Cambodia is located in the southern part of the Indochinese Peninsula in Southeast Asia, bordering Laos in the northwest, Thailand in the north and the east, and Vietnam in the south and the west, and with a long coastline along the Gulf of Thailand in the west. It is geographically characterized by large central wetlands around Tonle Sap Lake, and by the upper reaches of the Mekong River delta towards Vietnam, surrounded by uplands and low mountains. Cambodia's rich biodiversity is based on its seasonal tropical rainforests.

So far, the specific diversity of *Labiobaetis* and of Baetidae in general in Cambodia was unknown, despite a first study on mayflies including the first general report of the genus in the country (Chhorn et al. 2020). Some work was done in the neighbouring Vietnam, including a key for the identification of Ephemeroptera (Soldán 1991; Mekong River Commission 2006), and several studies on Baetidae were recently done in the neighbouring Thailand (e.g. Kluge and Suttinun 2020; Suttinun et al. 2020, 2021, 2022). Intensive exchange between these faunas is likely, as there are only rather low mountain chains with large corridors inbetween, and no other barriers between them. In China, an important study on *Labiobaetis* was done by Shi and Tong (2014). In the present study, we describe two new species of *Labiobaetis* from Cambodia based on larval stage.

Materials and methods

Materials used in the study were obtained as part of the Cambodia Entomology Initiative aquatic insect ecological study expeditions (Freitag et al. 2018; Chhorn et al. 2020). The specimens were preserved in 96% ethanol.

Dissection of larvae was done in Cellosolve (2-Ethoxyethanol) with subsequent mounting on slides with Euparal liquid, using an Olympus SZX7 stereomicroscope.

The DNA of part of the specimens was extracted using non-destructive methods allowing subsequent morphological analysis (see Vuataz et al. 2011 for details). We

amplified a 658 bp fragment of the mitochondrial gene cytochrome oxidase subunit 1 (COI) using the primers LCO 1490 and HCO 2198 (Folmer et al. 1994; see Kaltenbach and Gattolliat 2020 for details). Sequencing was done with Sanger's method (Sanger et al. 1977). The genetic variability between specimens was estimated using Kimura-2-parameter distances (K2P; Kimura 1980), calculated with the program MEGA 7 (Kumar et al. 2016; <http://www.megasoftware.net>).

GenBank accession numbers are given in the sections of examined material.

Drawings were made with an Olympus BX43 microscope. To facilitate the determination of species and the comparison of important structures, we partly use a combination of dorsal and ventral aspects in one drawing. Explanations are given in Kaltenbach et al. (2020: fig. 1).

Photographs of larvae were taken using a Canon EOS 6D camera and processed with the programs Adobe Photoshop Lightroom (<http://www.adobe.com>) and Helicon Focus v. 5.3 (<http://www.heliconsoft.com>). Photographs were subsequently enhanced with Adobe Photoshop Elements 13.

The distribution maps were generated with the program SimpleMapper (<https://simplemapper.net>; Shorthouse 2010).

The dichotomous key was elaborated with the support of the program DKey v. 1.3.0 (<http://drawing.org/dkey>; Tofilski 2018).

The terminology follows Hubbard (1995) and Kluge (2004).

Abbreviations

RUPP Cambodia Entomology Initiative, Royal University of Phnom Penh (RUPP), temporarily stored in Ateneo de Manila University, Quezon City, Philippines (AdMU);

MZL Musée de Zoologie Lausanne (Switzerland).

Results

Definition of groups and description of their characters

Labiobaetis operosus group (*L. brao* sp. nov.) and *sumigarensis* group (*L. kui* sp. nov.) were defined and characterized in Kaltenbach and Gattolliat (2019) and Kaltenbach et al. (2020).

Labiobaetis brao sp. nov.

<https://zoobank.org/A5F61492-39FC-4FBC-A77F-C5620E5EDC1E>

Figs 1, 2, 6b

Diagnosis. Larva. Following combination of characters: A) antennal scape with well developed distolateral process (Fig. 2g); B) dorsal surface of labrum with submarginal

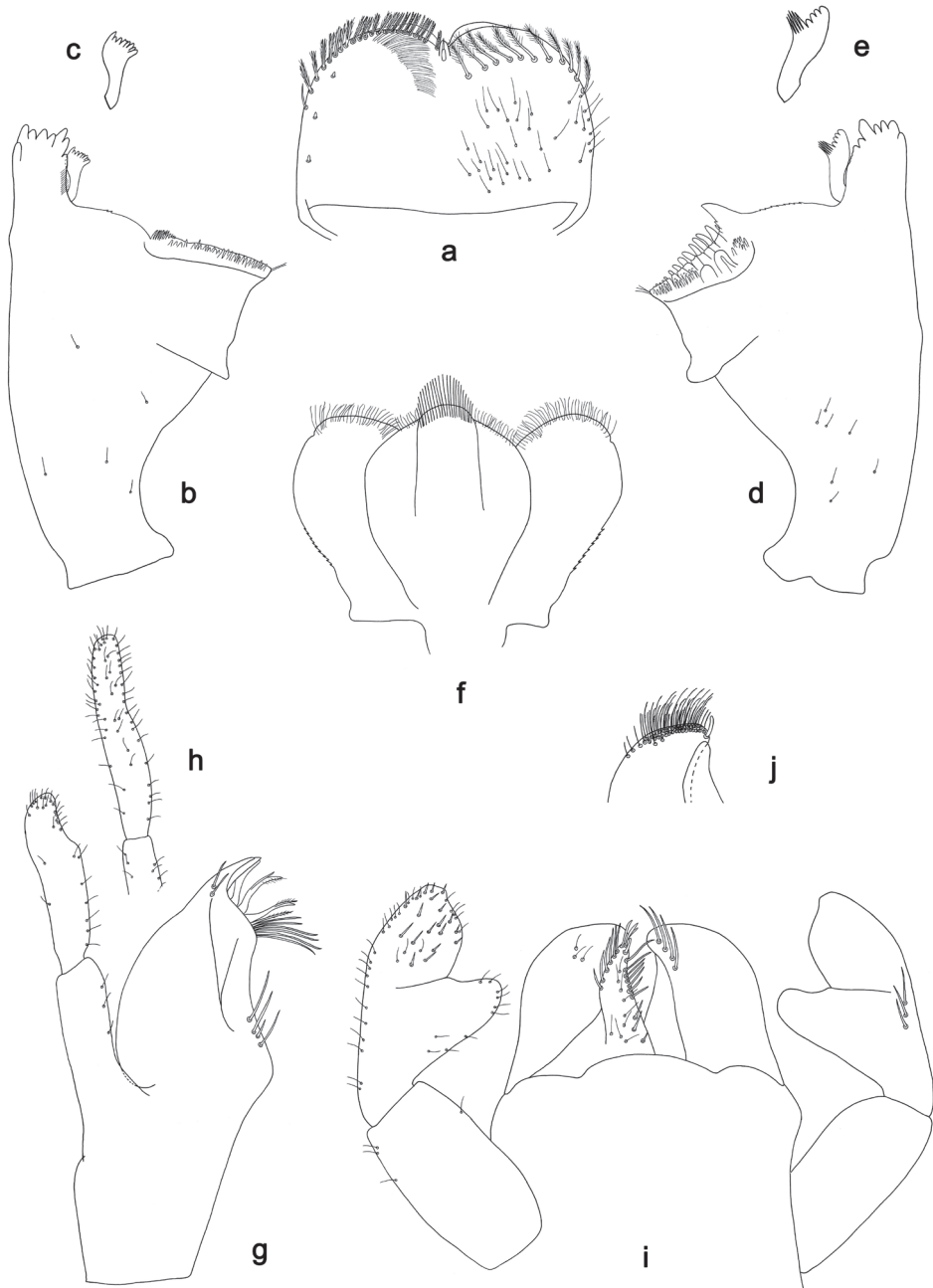


Figure 1. a–g, i, j *Labiobaetis brao* sp. nov., larva morphology **a** labrum (left: ventral view, right: dorsal view) **b** right mandible **c** right prosthema **d** left mandible **e** left prosthema **f** hypopharynx and superlinguae **g** maxilla **i** labium (left: ventral view, right: dorsal view) **j** apex of paraglossa **h** *Labiobaetis paraoperosus*: maxillary palp.

arc of 9–11 feathered setae (Fig. 1a); B) labial palp segment II with broad, extended, thumb-like distomedial protuberance; segment III rather oblong, apically truncate (Fig. 1h); C) fore femur rather broad, length ca $3\times$ maximum width, dorsal margin with 11–25 curved, short, spine-like setae (Fig. 2a); D) hind protoptera well developed; E) seven pairs of tergalii; F) paraproct distally not expanded, with ca 34 marginal spines and additional row of minute spines along inner, proximal margin (Fig. 2e, f).

Description. Larva (Figs 1a–g, i, j, 2 a–c, e–h, 5a, b). Body length 6.4–8.4 mm. Cerci: ca $2/3$ of body length. Paracercus: ca $2/3$ of cerci length. Antenna: approximately twice as long as head length.

Colouration (Fig. 5a, b). Head, thorax and abdomen dorsally grey-brown, with pattern as in Figure 6a. Abdominal tergites I and X brighter. Fore protoptera light grey-brown with dark striation. Head ventrally brownish, thorax and abdomen ventrally light grey-brown. Legs ecru to light brown, femur with grey-brown distomedial spot, apex and dorsal margin grey-brown. Caudalii grey-brown.

Antenna (Fig. 2h) with scape and pedicel subcylindrical, with well-developed distolateral process at scape.

Labrum (Fig. 1a). Subrectangular, length $0.65\times$ maximum width. Distal margin with medial emargination and a small process. Dorsally with medium, fine, simple setae scattered over surface; submarginal arc of setae composed of 9–11 long, feathered setae. Ventrally with marginal row of setae composed of lateral and anterolateral long, feathered setae and medial long, bifid, pectinate setae; ventral surface with ca three short, spine-like setae near lateral and anterolateral margin.

Right mandible (Fig. 1b, c). Incisor and kinetodontium fused. Incisor with five denticles; kinetodontium with three denticles, inner margin of innermost denticle with a row of thin setae. Prosthema robust, apically denticulate. Margin between prosthema and mola slightly convex, with few minute denticles. Tuft of setae at apex of mola present.

Left mandible (Fig. 1d, e). Incisor and kinetodontium fused. Incisor with four denticles; kinetodontium with three denticles. Prosthema robust, apically with small denticles and comb-shaped structure. Margin between prosthema and mola slightly convex, with minute denticles. Tuft of setae at apex of mola present.

Both mandibles with lateral margins almost straight. Basal half with fine, simple setae scattered over dorsal surface.

Hypopharynx and superlinguae (Fig. 1f). Lingua approx. as long as superlinguae. Lingua longer than broad; medial tuft of stout setae well developed, broad; distal half laterally expanded. Superlinguae distally rounded; lateral margin rounded; fine, long, simple setae along distal margin.

Maxilla (Fig. 1g). Galea-lacinia ventrally with two simple, apical setae under canines. Inner dorsal row of setae with three denti-setae, distal denti-seta tooth-like, middle and proximal denti-setae slender, bifid and pectinate. Medially with one spine-like seta and three long, simple setae. Maxillary palp $1.3\times$ as long as length of galea-lacinia; 2-segmented; palp segment II approximately as long as segment I; setae on maxillary palp fine, simple, scattered over surface of segments I and II; apex of last segment rounded, with excavation at inner distolateral margin.

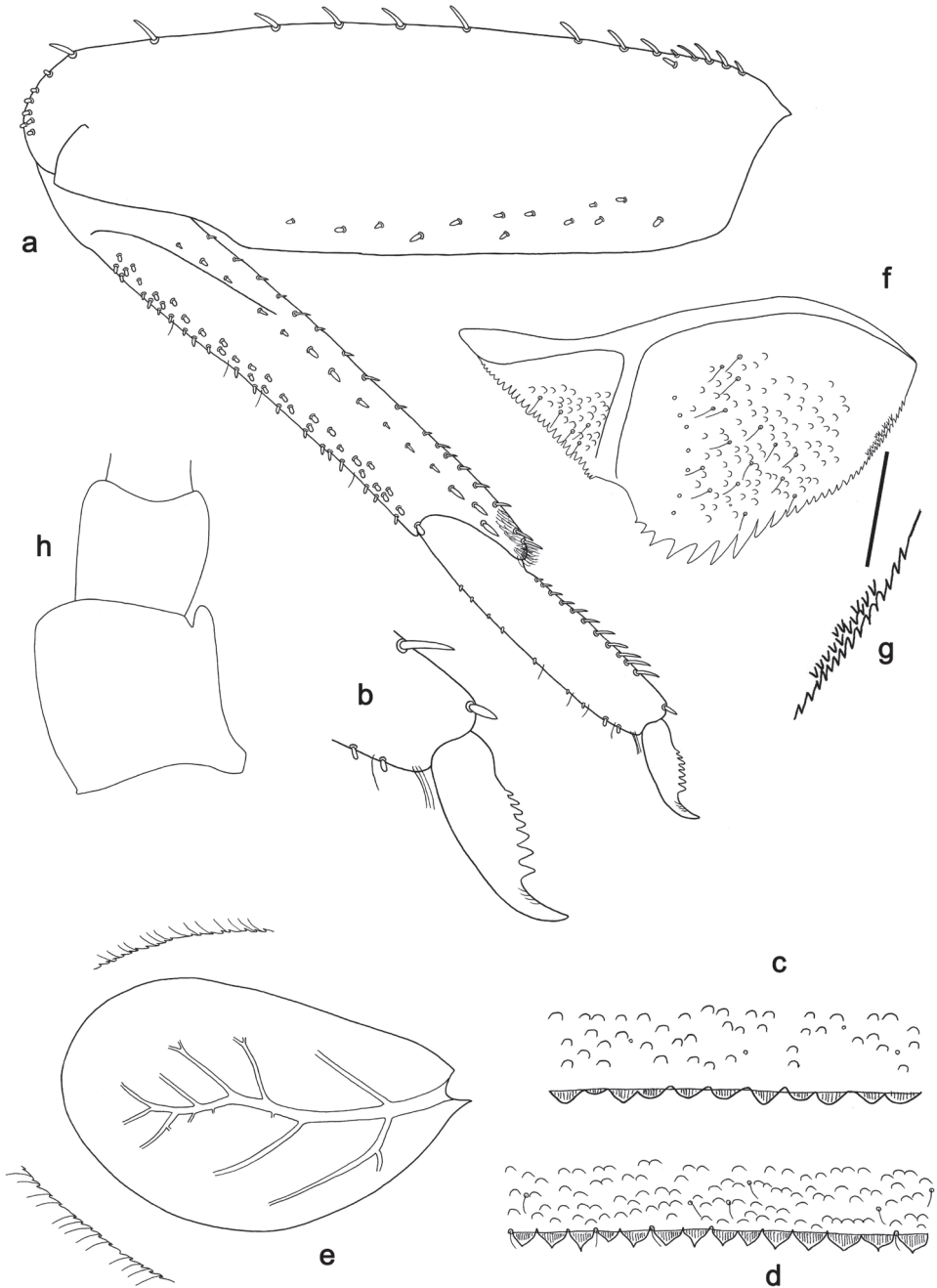


Figure 2. a–c, e–h *Labiobaetis brao* sp. nov., larva morphology **a** foreleg **b** fore claw **c** tergum IV **e** tergalium IV **f** paraproct **g** spines along paraproct margin **h** antennal base **d** *Labiobaetis paraoperosus*: tergum IV.

Labium (Fig. 1i, j). Glossa basally broad, narrowing toward apex; shorter than paraglossa; inner margin with 8–10 spine-like setae, distalmost seta much longer than other setae; apex with three medium and one short, robust setae; outer margin with ca 6 spine-like setae; ventral surface with fine, simple, scattered setae. Paraglossa subrectangular, curved inward; apex rounded; with three rows of long, robust, distally pectinate setae in apical area and three medium, simple setae in anteromedial area; dorsally with a row of four long, spine-like, simple setae near inner margin. Labial palp with segment I $0.8\times$ length of segments II and III combined. Segment I ventrally with short, fine, simple setae. Segment II with broad, extended, thumb-like distomedial protuberance; distomedial protuberance $0.7\times$ width of base of segment III; ventral surface with short, fine, simple setae; dorsally with a row of three long, spine-like setae near outer margin. Segment III rather oblong, apically truncate; length $1.1\times$ width; ventrally covered with short, spine-like, simple setae and short, fine, simple setae.

Hind protoptera well developed.

Foreleg (Fig. 2a, b). Ratio of foreleg segments 1.4:1.0:0.6:0.2. **Femur**. Length ca $3\times$ maximum width. Dorsal margin with 11–25 curved, short, spine-like setae, often one seta additionally near margin in basal area; length of setae $0.14\times$ maximum width of femur. Apex rounded, with a spine-like seta and some short, stout setae. Many stout, lanceolate setae scattered along ventral margin; femoral patch absent. **Tibia**. Dorsal margin with row of short, stout, apically rounded setae, and some fine, simple setae; many more stout, apically rounded setae along dorsal margin; on apex one seta of same type. Ventral margin with row of short, curved, spine-like setae, on apex some longer setae and a tuft of fine, simple setae. Anterior surface with row of stout, lanceolate setae near ventral margin. Patellatibial suture present on basal $1/3$ area. **Tarsus**. Dorsal margin with row of short, stout setae and some fine, simple setae. Ventral margin with row of curved, spine-like setae. Claw with one row of 7–10 denticles; distally pointed; with ca four stripes; subapical setae absent.

Middle and hind legs. As foreleg, but with reduced or rudimentary femoral patch on middle femur, and reduced or well developed on hind femur.

Terga (Fig. 2c). Surface with irregular rows of U-shaped scale bases. Posterior margin of tergum IV with spines varying between mostly triangular to mostly rounded, wider than long.

Tergalii (Fig. 2e). Present on segments I–VII. Margins with small denticles intercalating fine simple setae. Tracheae extending from main trunk to inner and outer margins. Tergalius I ca $2/3$ length of segment II. Tergalius IV as long as length of segments V and $1/2$ VI combined. Tergalius VII as long as length of segment VIII.

Paraproct (Fig. 2f, g). Distally not expanded, with ca 34 stout, marginal spines, and additional row of minute spines along inner, proximal margin. Surface scattered with U-shaped scale bases and fine, simple setae. Cercotractor with numerous small, marginal spines.

Etymology. The new species is dedicated to the indigenous Brao people from northeastern Cambodia.

Distribution. Cambodia (Fig. 6b).

Biological aspects. The specimens were mainly collected in secondary forest remnants at altitudes of 100 m, partly on littoral gravel.

Type material. *Holotype.* CAMBODIA • larva; Kampong Speu Province, Kokie waterfall, sec. forest remnants; 110 m; 11°12'11"N, 104°03'49"E; 12.07.2018; leg. H. Freitag and J. Garces; on slide; GBIFCH00592700; MZL. *Paratypes.* CAMBODIA • 8 larvae; same data as holotype; 1 on slide; GenBank ON982739; GBIFCH00829878; RUPP; 1 on slide; GBIFCH00975576; MZL; 6 in alcohol; GBIFCH00975580, GBIFCH00975581; MZL • 1 larva; Kampong Speu Province, Chambok River, 1.83 Km from Chambok Community, sec. forest, littoral gravel; 240 m; 11°21'58"N, 104°06'17"E; 11.07.2018; leg. H. Freitag and J. Garces; on slide; GBIFCH00592730; RUPP.

***Labiobaetis kui* sp. nov.**

<https://zoobank.org/03B09E8B-57E2-40AA-8BAD-911A6D969606>

Figs 3, 4, 5c, d, 6b

Diagnosis. Larva. Following combination of characters: A) antennal scape without process (Fig. 4g); B) dorsal surface of labrum with submarginal arc of 16–18 long, clavate setae (Fig. 3a); C) labial palp segment II with an extended, slightly hooked, thumb-like distomedial protuberance (Fig. 3i); D) left mandible without setae at apex of mola (Fig. 3e); E) fore femur rather slender, length ca 4× maximum width, dorsal margin with 10–15 curved, spine-like setae (Fig. 4a); F) hind protoptera absent; G) six pairs of tergellii; H) paraproct distally slightly expanded, with 33–38 stout, marginal spines (Fig. 4f).

Description. Larva (Figs 3, 4, 5c, d). Body length ca 4.9 mm. Caudalii broken. Antenna broken.

Colouration (Fig. 5c, d). Head, thorax, and abdomen dorsally uniform brown. Head, thorax, and abdomen ventrally light brown. Legs light brown; femur with a brown medial spot, darker on ventral margin, dorsal margin and apex brown. Caudalii light brown.

Antenna (Fig. 4g) with scape and pedicel subcylindrical, without distolateral process at scape.

Labrum (Fig. 3a, b). Rectangular, length 0.7× maximum width. Distal margin with medial emargination and a small process. Dorsally with medium, fine, simple setae scattered over surface; submarginal arc of setae composed of 16–18 long, clavate setae. Ventrally with marginal row of setae composed of anterolateral long, feathered setae and medial long, bifid setae; ventral surface with ca three short, spine-like setae near lateral and anterolateral margin.

Right mandible (Fig. 3c, d). Incisor and kinetodontium fused. Incisor with five denticles; kinetodontium with three denticles, inner margin of innermost denticle with a row of thin setae. Prostheda robust, apically denticulate. Margin between prostheda and mola slightly convex. Tuft of setae at apex of mola present.

Left mandible (Fig. 3e, f). Incisor and kinetodontium fused. Incisor with five denticles; kinetodontium with three denticles. Prostheda robust, apically with small denticles and comb-shaped structure. Margin between prostheda and mola straight, with minute denticles towards subtriangular process. Tuft of setae at apex of mola absent.

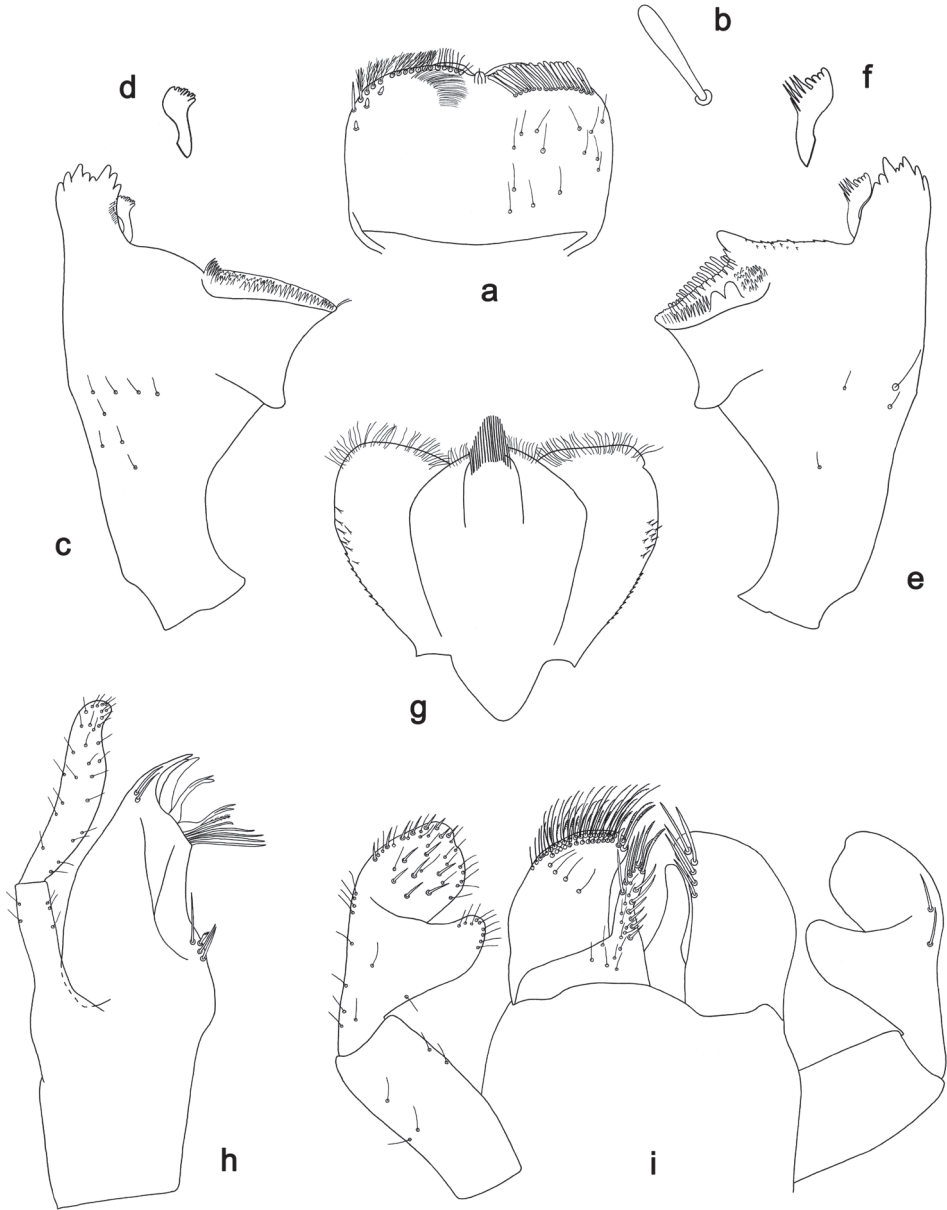


Figure 3. *Labiobaetis kui* sp. nov., larva morphology **a** labrum (left: ventral view, right: dorsal view) **b** seta of submarginal arc **c** right mandible **d** right prostheca **e** left mandible **f** left prostheca **g** hypopharynx and superlinguae **h** maxilla **i** labium (left: ventral view, right: dorsal view).

Both mandibles with lateral margins almost straight. Basal half with fine, simple setae scattered over dorsal surface.

Hypopharynx and superlinguae (Fig. 3g). Lingua approx. as long as superlinguae. Lingua longer than broad; medial tuft of stout setae well developed; distal half laterally

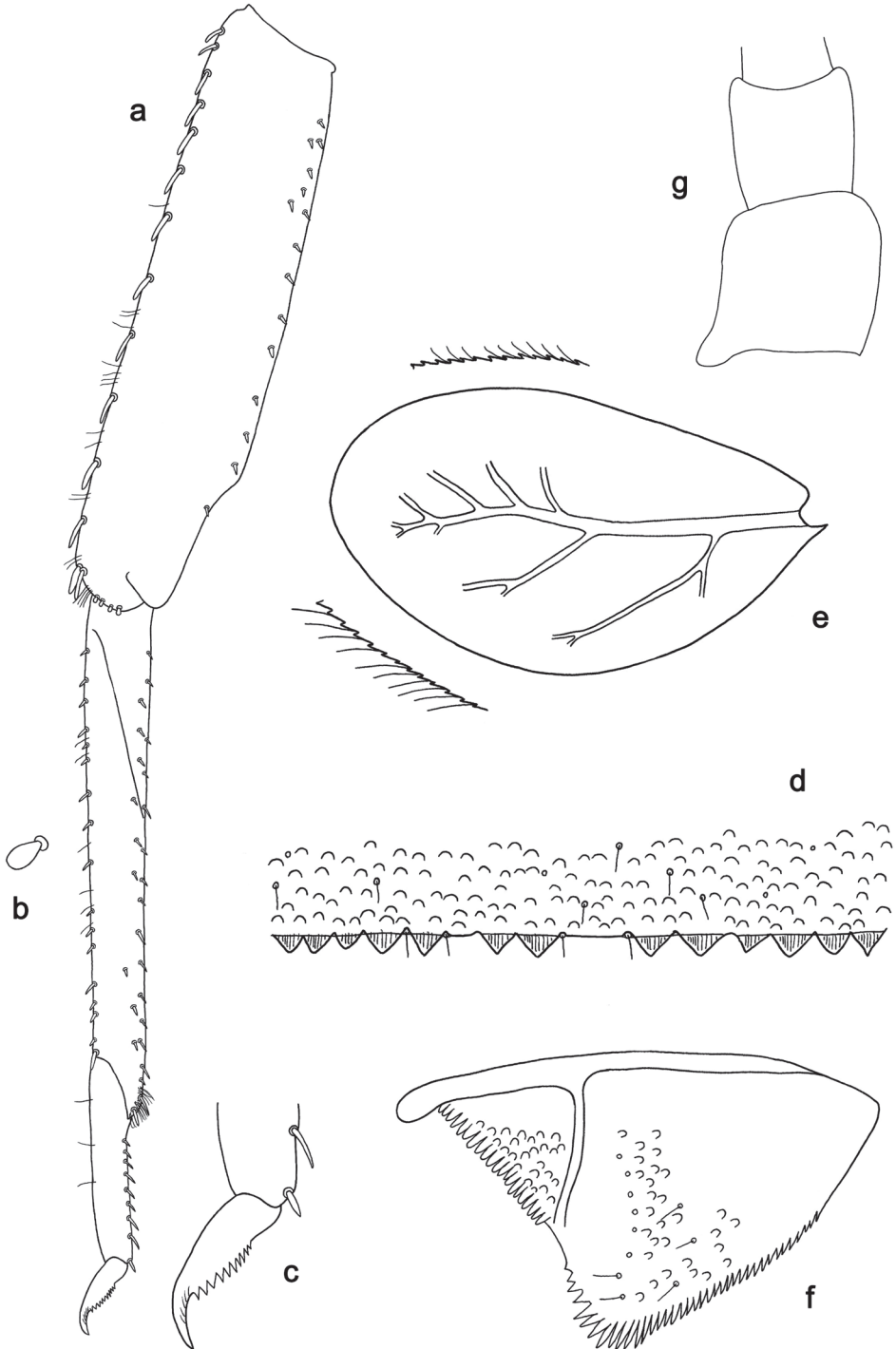


Figure 4. *Labiobaetis kui* sp. nov., larva morphology **a** foreleg **b** seta of tibia dorsal margin **c** fore claw **d** tergum IV **e** tergalium IV **f** paraproct **g** antennal base.

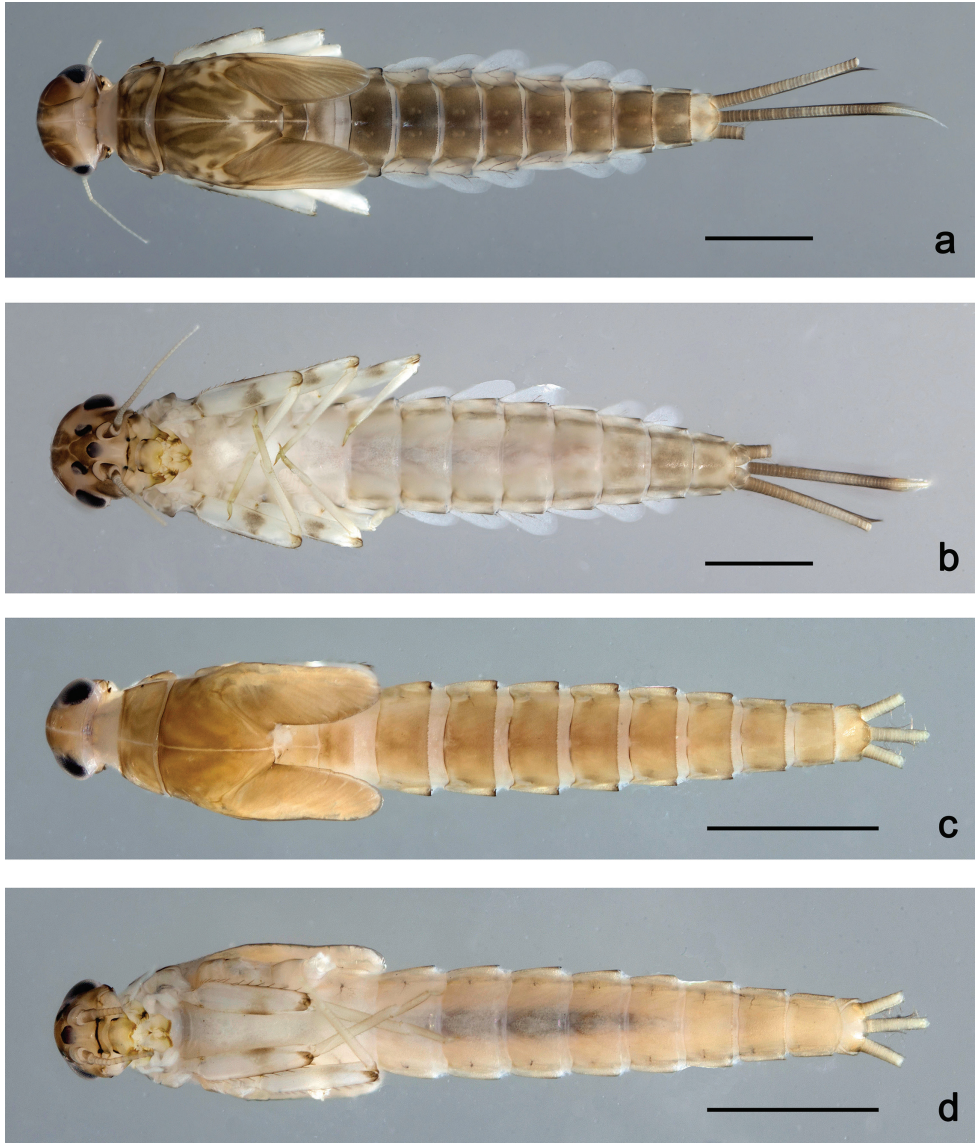


Figure 5. Habitus, larvae **a** *Labiobaetis brao* sp. nov., dorsal view **b** *Labiobaetis brao* sp. nov., ventral view **c** *Labiobaetis kui* sp. nov., dorsal view **d** *Labiobaetis kui* sp. nov., ventral view. Scale bar: 1 mm.

expanded. Superlinguae distally almost straight; lateral margin rounded; fine, long, simple setae along distal margin.

Maxilla (Fig. 3h). Galea-lacinia ventrally with two simple, apical setae under canines. Inner dorsal row of setae with three denti-setae, distal denti-seta tooth-like, middle and proximal denti-setae slender, bifid. Medially with one pectinate, spine-like seta and three or four medium, simple setae. Maxillary palp 1.2× as long as length of

galea-lacinia; 2-segmented; palp segment II 1.2× length of segment I; setae on maxillary palp fine, simple, scattered over surface of segments I and II; apex of last segment rounded, with excavation at inner distolateral margin.

Labium (Fig. 3i). Glossa basally broad, narrowing toward apex; shorter than paraglossa; inner margin with ca six spine-like setae increasing in length distally; apex with two long and one medium, robust, pectinate setae; outer margin with ca four spine-like setae; ventral surface with fine, simple, scattered setae. Paraglossa subrectangular, curved inward; apex rounded; with three rows of long, robust, distally pectinate setae in apical area and a row of 2–4 medium, simple setae in anteromedial area; dorsally with a row of four or five long, spine-like, simple setae near inner margin. Labial palp with segment I 0.8× length of segments II and III combined. Segment I ventrally with short, fine, simple setae. Segment II with extended, slightly hooked, thumb-like distomedial protuberance; distomedial protuberance 0.7× width of base of segment III; ventral surface with short, fine, simple setae; dorsally with two long, spine-like, simple setae near outer margin. Segment III slightly pentagonal; apex rounded, inner apical margin slightly concave; length subequal to width; ventrally covered with short, spine-like, simple setae and short, fine, simple setae.

Hind protoptera absent.

Foreleg (Fig. 4a–c). Ratio of foreleg segments 1.3:1.0:0.4:0.2. **Femur**. Length ca 4× maximum width. Dorsal margin with 10–15 long, curved, spine-like setae; length of setae 0.23× maximum width of femur. Apex rounded, with a pair of long, curved, spine-like setae and some short, stout setae. Many stout, lanceolate setae scattered along ventral margin; femoral patch absent. **Tibia**. Dorsal margin with row of short, stout, apically rounded setae, on apex one longer, spine-like seta. Ventral margin with row of short, curved, spine-like setae, on apex some longer setae and a tuft of fine, simple setae. Anterior surface scattered with stout, lanceolate setae near ventral margin. Patellatibial suture present on basal 1/3 area. **Tarsus**. Dorsal margin with some fine, simple setae. Ventral margin with row of curved, spine-like setae. Claw with one row of nine or ten denticles; distally pointed; with ca. five stripes; subapical setae absent.

Terga (Fig. 4d). Surface with irregular rows of U-shaped scale bases and scattered fine, simple setae. Posterior margin of tergum IV with triangular spines, wider than long.

Tergalii (Fig. 4e). Present on segments II–VII. Margins with small denticles intercalating fine simple setae. Tracheae extending from main trunk to inner and outer margins. Tergalium IV as long as length of segments V and 1/3 VI combined. Tergalium VII as long as length of segment VIII.

Paraproct (Fig. 4f). Distally slightly expanded, with 33–38 stout, marginal spines. Surface scattered with U-shaped scale bases, fine, simple setae and micropores. Cercotractor with numerous small, marginal spines.

Etymology. The new species is dedicated to the indigenous Kui people from northeastern Cambodia.

Distribution. Cambodia (Fig. 6b).

Biological aspects. The specimens were collected from 100 m to 640 m, mostly on littoral gravel.



Figure 6. Distribution of *Labiobaetis* in Cambodia a overview map b *Labiobaetis* species.

Type material. *Holotype.* CAMBODIA • larva; Kampong Speu Province, Chambok River, 1.83 Km from Chambok Community; 240 m; 11°21'58"N, 104°06'17"E; 11.07.2018; leg. H. Freitag and J. Garces; on slide; GBIFCH00592702; MZL.
Paratypes. CAMBODIA • 14 larvae; same data as holotype; 1 on slide; GBIFCH00592701; MZL; 13 in alcohol; GenBank ON982737, ON982738; GBIFCH00515681, GBIFCH00829876, GBIFCH00829877, GBIFCH00975577, GBIFCH00975578; MZL • 7 larvae; Kampong Speu Province, waterfall at Kirirom National Park; 640 m; 11°20'26"N, 104°02'14"E; 13.07.2018; leg. H. Freitag and J. Garces; 1 on slide; GBIFCH00592698; RUPP; 6 in alcohol; GBIFCH00975579; MZL • 1 larva; Kampong Speu Province, Kokie waterfall, secondary forest remnants; 110 m; 11°12'11"N, 104°03'49"E; 12.07.2018; leg. H. Freitag and J. Garces; on slide; GBIFCH00592699; RUPP.

Key to *Labiobaetis* species of continental Southeast Asia (larvae)

- 1 Setae of submarginal arc dorsally on labrum simple, pointed (Kaltenbach et al. 2020: fig. 2a).....2
- Setae of submarginal arc dorsally on labrum feathered or clavate (clavate setae apically pectinate or smooth) (Figs 1a, 3a, b; Shi and Tong 2014: fig. 7).....4
- 2 Right mandible with pronounced hump between prostheca and mola (Shi and Tong 2014: fig. 24)***L. numeratus* (Müller-Liebenau, 1984)**
- Right mandible without hump between prostheca and mola3
- 3 Tergalii present on abdominal segments I-VII; hind protoptera well developed (Müller-Liebenau 1984: fig. 9i); femoral patch present.....***L. multus* (Müller-Liebenau, 1984)**
- Tergalii present on abdominal segments II-VII; hind protoptera minute (Müller-Liebenau 1984: fig. 10i); femoral patch absent ***L. moriharai* (Müller-Liebenau, 1984)**
- 4 Setae of submarginal arc dorsally on labrum feathered (Fig. 1a) 5
- Setae of submarginal arc dorsally on labrum clavate (apically smooth or pectinate) (Fig. 3a, b)7
- 5 Hind protoptera absent..... ***L. difficilis* (Müller-Liebenau, 1984)**
- Hind protoptera present, well developed (Müller-Liebenau 1984: fig. 8i) ...6
- 6 Distomedial protuberance of labial palp segment II slightly curved upwards (Fig. 1i); paraproct with additional rows of minute spines at distal margin (Fig. 2f, g).....***L. brao* sp. nov.**
- Distomedial protuberance of labial palp segment II slightly curved downwards (Müller-Liebenau 1984: fig. 8g); paraproct without extra rows of spines (Müller-Liebenau 1984: fig. 8l)..... ***L. operosus* (Müller-Liebenau, 1984)**
- 7 Hind protoptera present, well developed (Shi and Tong 2014: fig. 5).....***L. ancoralis* Shi & Tong, 2014**
- Hind protoptera absent..... 8

- 8 Antennal scape with slightly developed distolateral process (Müller-Liebenau 1984: fig. 6f); tarsus ventrally with row of feathered, spine-like setae; posterior margin of tergite IV with triangular spines, apically sharply pointed (Müller-Liebenau 1984: fig. 39).....***L. diffundus* (Müller-Liebenau, 1984)**
- Antennal scape without distolateral process (Fig. 4g); tarsus ventrally with row of spine-like setae (not feathered); posterior margin of tergite IV with triangular spines, apically mostly blunt (Fig. 4d).....***L. kui* sp. nov.**

Genetics

COI sequences were obtained from both new species (see type material sections). The genetic distance (K2P) between them is 20–21%, and therefore much higher than 3.5%, which is generally considered as a likely maximal value for intraspecific divergence (Hebert et al. 2003; Ball et al. 2005). A very limited genetic distance of 1% was found between two specimens of *L. kui* sp. nov., as expected for the same location.

Discussion

Assignment to *Labiobaetis* and to species groups

For the assignment of the new species to *Labiobaetis* we refer to Kluge and Novikova (2014), Müller-Liebenau (1984), and McCafferty and Waltz (1995). *Labiobaetis* is characterized by a number of characters, some of which are not found in other taxa (Kluge and Novikova 2014): antennal scape sometimes with a distolateral process (Fig. 2h); maxillary palp two segmented with excavation at inner distolateral margin of segment II, excavation may be poorly developed or absent (Figs 1g, 3h); labium with paraglossae widened and glossae diminished; labial palp segment II with distomedial protuberance (Figs 1i, 3i). All these characters vary and may be secondarily lost (Kluge and Novikova 2014). The concept of *Labiobaetis* is also based on additional characters, summarized and discussed by Kaltenbach and Gattolliat (2018, 2019).

The morphological groups within *Labiobaetis* are primarily a working tool but could also serve as a basis for future studies on the generic or subgeneric delimitations and phylogeny of this genus. The inclusion of nuclear gene sequences may prove that some of them are natural groups. The two species in Cambodia belong to different groups, one to the *operosus* group and one to the *sumigarensis* group. The *operosus* group is mainly characterized by A) labrum dorsally with submarginal arc of feathered setae; B) distolateral process at scape well developed; C) seven pairs of tergalii; D) hind protoptera well developed (see Kaltenbach et al. 2020: 40). The *sumigarensis* group is mainly characterized by A) labrum dorsally with submarginal arc of clavate setae; B) left mandible without setae at mola apex; C) six pairs of tergalii; D) hind protoptera absent; E) colour dorsally uniform brown (see Kaltenbach et al. 2020: 63).

These groups are widespread and highly diversified in Asia. Species of the *operosus* group are also known from India, Malaysia, Indonesia, and the Philippines; and species of the *sumigarensis* group from India, Sri Lanka, Malaysia, Indonesia, Brunei, China, Taiwan, and the Philippines (Müller-Liebenau 1984; Müller-Liebenau and Hubbard 1985; Kang et al. 1994; Shi and Tong 2014; Kubendran et al. 2015; Kaltenbach and Gattolliat 2019, 2020; Kaltenbach et al. 2020; Sivaruban et al. 2022). None of these groups are known from New Guinea (Kaltenbach and Gattolliat 2018, 2021; Kaltenbach et al. 2021).

Apart from *Labiobaetis brao* sp. nov. (*operosus* group), there is another species of this group in continental Southeast Asia, *L. operosus* (Müller-Liebenau, 1984). *Labiobaetis brao* sp. nov. is different from *L. operosus* by a labial palp segment II protuberance slightly directed distad (slightly directed proximad in *operosus*, Müller-Liebenau 1984: fig. 8g) and by minute additional spines along the inner proximal margin of the paraproct (Fig. 2g; absent in *operosus*, Kaltenbach and Gattolliat 2019: fig. 35d). The most similar species to *L. brao* sp. nov. is *L. paraoperosus* Kaltenbach & Gattolliat from Sumatra. It is different by a maxillary palp with slight distolateral excavation (Fig. 1h; strong excavation in *L. brao* sp. nov.); labial palp segment II with thumb-like protuberance very broad, not narrowing toward apex (Kaltenbach and Gattolliat 2019: fig. 36h; less broad and narrowing toward apex in *L. brao* sp. nov.); spines at posterior margin of tergite IV triangular, pointed (Fig. 2d; rounded spines in *L. brao* sp. nov.). Apart from *L. kui* sp. nov., there is also another species of group *sumigarensis* in continental Southeast Asia, *L. diffundus* (Müller-Liebenau, 1984). *Labiobaetis kui* sp. nov. is different by the absence of a distolateral process at antennal scape (Fig. 4g; small process in *diffundus*, Müller-Liebenau 1984: fig. 6f), by a labial palp segment II protuberance relatively narrow with distinctly rounded apex (Fig. 3i; broader with less rounded apex in *diffundus*, Müller-Liebenau 1984: fig. 6g), and by spines at proximal margin of tergum IV much wider than long (Fig. 4d; slightly wider than long in *diffundus*, Müller-Liebenau 1984: fig. 39).

Genetic distance

The genetic distances between the two new species of *Labiobaetis* in the Cambodia (20–21%, K2P) is rather high, which is in line with the genetic distances found in Indonesia (11–24%; Kaltenbach and Gattolliat 2019), Borneo (19–25%; Kaltenbach and Gattolliat 2020), and the Philippines (15–27%; Kaltenbach et al. 2020). Ball et al. (2005) reported a mean interspecific, congeneric distance of 18% for mayflies from the United States and Canada.

The number of sampled localities and different habitats is until now very limited and the vast majority of the country was not covered by collection activities so far (Fig. 6b). Therefore, we can expect that the number of *Labiobaetis* species in Cambodia will substantially increase with further collections.

Acknowledgements

We are grateful to Soksan Chhorn (Cambodia Entomology Initiative, Phnom Penh) for the donation of the materials as part of BIO-PHIL Biodiversity Training Module. Biodiversity module training and course expeditions in Cambodia were kindly enabled through funding by the German Academic Exchange Service (DAAD project BIO-PHIL 57393541). We are also thankful to Michel Sartori (MZL) for his constant interest and support for our project, and to Marion Podolak (MZL) and Céline Stoffel (MZL, UNIL) for their support with lab work and preparation of the COI barcodes.

Lastly, we are grateful to the reviewers for their valuable comments on the manuscript.

References

- Ball SL, Hebert PDN, Burian SK, Webb JM (2005) Biological identifications of mayflies (Ephemeroptera) using DNA barcodes. *Journal of the North American Benthological Society* 24(3): 508–524. <https://doi.org/10.1899/04-142.1>
- Barber-James HM, Sartori M, Gattolliat J-L, Webb J (2013) World checklist of freshwater Ephemeroptera species. <http://fada.biodiversity.be/group/show/35>
- Chhorn S, Chan B, Sopha S, Doeurk B, Chhy T, Phauk S, Sor R (2020) Diversity, abundance and habitat characteristics of mayflies (Insecta: Ephemeroptera) in Chambok, Kampong Speu Province, southwest Cambodia. *Cambodian Journal of Natural History* 2020: 61–68.
- Folmer O, Black M, Hoeh W, Lutz R, Vrijenhoek R (1994) DNA primers for amplification of mitochondrial cytochrome c oxidase subunit I from diverse metazoan invertebrates. *Molecular Marine Biology and Biotechnology* 3: 294–299. http://www.mbari.org/staff/vrijen/PDFS/Folmer_94MMBB.pdf
- Freitag H, Doeurk B, Chhorn S, Khin C, Sopha S, Ehlers S, Voges J, Garces JM, Phauk S (2018) Aquatic Polyphaga (Insecta: Coleoptera) from Kampong Speu Province, Cambodia. *Cambodian Journal of Natural History* 2018: 90–100.
- Hebert PDN, Cywinska A, Ball SL, DeWaard JR (2003) Biological identifications through DNA barcodes. *Proceedings of the Royal Society B: Biological Sciences* 270(1512): 313–321. <https://doi.org/10.1098/rspb.2002.2218>
- Hubbard MD (1995) Towards a standard methodology for the description of mayflies (Ephemeroptera). In: Corkum LD, Ciborowski JJH (Eds) *Current Directions in Research on Ephemeroptera*. Canadian Scholar's Press, Toronto, 361–369.
- Jacobus LM, Macadam CR, Sartori M (2019) Mayflies (Ephemeroptera) and their contributions to ecosystem services. *Insects* 10(6): 1–26. <https://doi.org/10.3390/insects10060170>
- Kaltenbach T, Gattolliat J-L (2018) The incredible diversity of *Labiobaetis* Novikova & Kluge in New Guinea revealed by integrative taxonomy (Ephemeroptera, Baetidae). *ZooKeys* 804: 1–136. <https://doi.org/10.3897/zookeys.804.28988>

- Kaltenbach T, Gattolliat J-L (2019) The tremendous diversity of *Labiobaetis* Novikova & Kluge in Indonesia (Ephemeroptera, Baetidae). *ZooKeys* 895: 1–117. <https://doi.org/10.3897/zookeys.895.38576>
- Kaltenbach T, Gattolliat J-L (2020) *Labiobaetis* Novikova & Kluge in Borneo (Ephemeroptera, Baetidae). *ZooKeys* 914: 43–79. <https://doi.org/10.3897/zookeys.914.47067>
- Kaltenbach T, Gattolliat J-L (2021) New species of *Labiobaetis* Novikova & Kluge from South-east Asia and New Guinea (Ephemeroptera, Baetidae). *ZooKeys* 1067: 159–208. <https://doi.org/10.3897/zookeys.1067.72251>
- Kaltenbach T, Garces JM, Gattolliat J-L (2020) The success story of *Labiobaetis* Novikova & Kluge in the Philippines (Ephemeroptera, Baetidae), with description of 18 new species. *ZooKeys* 1002: 1–114. <https://doi.org/10.3897/zookeys.1002.58017>
- Kaltenbach T, Surbakti S, Kluge NJ, Gattolliat J-L, Sartori M, Balke M (2021) Discovery of a new mayfly species (Ephemeroptera, Baetidae) near Cenderawasih University campus in Papua, Indonesia. *Treubia* 48(1): 37–54. <https://doi.org/10.14203/treubia.v48i1.4020>
- Kang C-H, Chang H-C, Yang C-T (1994) A revision of the genus *Baetis* in Taiwan (Ephemeroptera, Baetidae). *Journal of Taiwan Museum* 47: 9–44.
- Kimura M (1980) A simple method for estimating evolutionary rates of base substitutions through comparative studies of nucleotide sequences. *Journal of Molecular Evolution* 16(2): 111–120. <https://doi.org/10.1007/BF01731581>
- Kluge NJ (2004) *The Phylogenetic System of Ephemeroptera*. Academic Publishers, Dordrecht, 1–442. <https://doi.org/10.1007/978-94-007-0872-3>
- Kluge NJ, Novikova EA (2014) Systematics of *Indobaetis* Müller-Liebenau & Morihara 1982, and related implications for some other Baetidae genera (Ephemeroptera). *Zootaxa* 3835(2): 209–236. <https://doi.org/10.11646/zootaxa.3835.2.3>
- Kluge NJ, Novikova EA (2016) New tribe Labiobaetini tribus n., redefinition of *Pseudopannota* Waltz & McCafferty 1987 and descriptions of new and little known species from Zambia and Uganda. *Zootaxa* 4169(1): 1–43. <https://doi.org/10.11646/zootaxa.4169.1.1>
- Kluge NJ, Suttinun C (2020) Review of the Oriental genus *Indocloeon* Müller-Liebenau 1982 (Ephemeroptera: Baetidae) with descriptions of two new species. *Zootaxa* 4779(4): 451–484. <https://doi.org/10.11646/zootaxa.4779.4.1>
- Kubendran T, Balasubramanian C, Selvakumar C, Gattolliat J-L, Sivaramakrishnan KG (2015) Contribution to the knowledge of *Tenuibaetis* Kang & Yang 1994, *Nigrobaetis* Novikova & Kluge 1987 and *Labiobaetis* Novikova & Kluge (Ephemeroptera: Baetidae) from the Western Ghats (India). *Zootaxa* 3957: 188–200. <https://doi.org/10.11646/zootaxa.3957.2.3>
- Kumar S, Stecher G, Tamura K (2016) MEGA 7: Molecular evolutionary genetics analysis version 7.0 for bigger data sets. *Molecular Biology and Evolution* 33(7): 1870–1874. <https://doi.org/10.1093/molbev/msw054>
- McCafferty WP, Waltz RD (1995) *Labiobaetis* (Ephemeroptera: Baetidae): new status, new North American species, and related new genus. *Entomological News* 106: 19–28.
- Mekong River Commission (2006) Identification of Freshwater Invertebrates of the Mekong River and its Tributaries. Mekong River Commission, 274 pp.
- Müller-Liebenau I (1984) New genera and species of the family Baetidae from West-Malaysia (River Gombak) (Insecta: Ephemeroptera). *Spixiana* 7: 253–284.

- Müller-Liebenau I, Hubbard MD (1985) Baetidae from Sri Lanka with some general remarks on the Baetidae of the Oriental Region (Insecta: Ephemeroptera). *The Florida Entomologist* 68(4): 537–561. <https://doi.org/10.2307/3494855>
- Novikova EA, Kluge NJ (1987) Systematics of the genus *Baetis* (Ephemeroptera, Baetidae), with descriptions of new species from Middle Asia. *Vestnik Zoologii* 1987(4): 8–19. [in Russian]
- Sanger F, Nicklen S, Coulson AR (1977) DNA sequencing with chain-terminating inhibitors. *Proceedings of the National Academy of Sciences of the United States of America* 74(12): 5463–5467. <https://doi.org/10.1073/pnas.74.12.5463>
- Sartori M, Brittain JE (2015) Order Ephemeroptera. In: Thorp J, Rogers DC (Eds) *Ecology and General Biology: Thorp and Corvich's Freshwater Invertebrates*. Academic Press, 873–891. <https://doi.org/10.1016/B978-0-12-385026-3.00034-6>
- Shi W, Tong X (2014) The genus *Labiobaetis* (Ephemeroptera: Baetidae) in China, with description of a new species. *Zootaxa* 3815: 397–408. <https://doi.org/10.11646/zootaxa.3815.3.5>
- Shorthouse DP (2010) SimpleMappr, an online tool to produce publication-quality point maps. <https://www.simplemappr.net>
- Sivaruban T, Pandarian Srinivasan, Barathy S, Rajasekaran Isack (2022) A new species and record of *Labiobaetis* Novikova and Kluge, 1987 (Ephemeroptera: Baetidae) from India. *Aquatic Insects*. <https://doi.org/10.1080/01650424.2022.2070217>
- Soldán T (1991) An annotated list of mayflies (Ephemeroptera) found in the Nam Cat Tien National Park. In: Spitzer K, Leps J, Zahrada M (Eds) *Nam Cat Tien: Czechoslov. Vietnam. Exped. Nov 1989. Research Report*, Institute of Entomology, Czechoslovakian Academy of Science, 4–9.
- Suttinun C, Gattolliat J-L, Boonsong B (2020) *Cymbalcloeon* gen. nov., an incredible new mayfly genus (Ephemeroptera: Baetidae) from Thailand. *PLoS ONE* 15(10): e0240635. <https://doi.org/10.1371/journal.pone.0240635>
- Suttinun C, Kaltenbach T, Gattolliat J-L, Boonsong B (2021) A new species and first record of the genus *Procerobaetis* Kaltenbach & Gattolliat, 2020 (Ephemeroptera, Baetidae) from Thailand. *ZooKeys* 1023: 13–28. <https://doi.org/10.3897/zookeys.1023.61081>
- Suttinun C, Gattolliat J-L, Boonsoong B (2022) First report of the genus *Tenuibaetis* (Ephemeroptera, Baetidae) from Thailand revealing a complex of cryptic species. *ZooKeys* 1084: 165–182. <https://doi.org/10.3897/zookeys.1084.78405>
- Tofilski A (2018) DKey software for editing and browsing dichotomous keys. *ZooKeys* 735: 131–140. <https://doi.org/10.3897/zookeys.735.21412>
- Vuataz L, Sartori M, Wagner A, Monaghan MT (2011) Toward a DNA taxonomy of Alpine *Rhithrogena* (Ephemeroptera: Heptageniidae) using a mixed Yule-Coalescent Analysis of mitochondrial and nuclear DNA. *PLoS ONE* 6(5): e19728. <https://doi.org/10.1371/journal.pone.0019728>

Revision of the genus *Urvaschia* Hopp (Hemiptera, Lygaeoidea, Oxycarenidae), with descriptions of two new species from China and Nepal

Cuiqing Gao¹, Shiya Xiao¹, Előd Kondorosy²

1 Co-Innovation Center for Sustainable Forestry in Southern China, College of Forestry, Nanjing Forestry University, Long Pan Road, Nanjing, Jiangsu 210037, China **2** Department of Conservation Biology, Georgikon Campus, Hungarian University of Agriculture and Life Sciences, H-8360 Keszthely, Hungary

Corresponding authors: Cuiqing Gao (cqgao@njfu.edu.cn), Előd Kondorosy (kondorosy.ee@gmail.com)

Academic editor: Wenjun Bu | Received 16 June 2022 | Accepted 12 September 2022 | Published 4 October 2022

<https://zoobank.org/0C665F99-B681-4C66-9336-9F65E33B0995>

Citation: Gao C, Xiao S, Kondorosy E (2022) Revision of the genus *Urvaschia* Hopp (Hemiptera, Lygaeoidea, Oxycarenidae), with descriptions of two new species from China and Nepal. ZooKeys 1123: 83–97. <https://doi.org/10.3897/zookeys.1123.87863>

Abstract

The species of *Urvaschia* Hopp, 1987 are reviewed. The following taxonomic change is proposed: *Urvaschia obscuripennis* (Kiritshenko, 1914), **comb. nov.** (transferred from *Microplax* Fieber, 1860). The genus *Urvaschia* Hopp is newly recorded from Afghanistan, China, Iran, and Tadjhikistan. Two new species of *Urvaschia*, *Urvaschia convexa* **sp. nov.** and *U. recta* **sp. nov.** are described from China and Nepal. A diagnosis of the genus, a key to all of the included species, habitus photographs, and male genitalia illustrations of selected species are presented.

Keywords

Asia, distribution, Heteroptera, key, *Microplax*, new combination, taxonomy, true bugs

Introduction

The lygaeoid family Oxycarenidae (Hemiptera: Heteroptera) includes, until now, 27 genera and approximately 140 species worldwide (Dellapé and Henry 2022). The genus *Urvaschia* Hopp, 1987 (Hemiptera: Heteroptera: Lygaeoidea: Oxycarenidae) currently contains only one described species occurring in the high mountains of Nepal and Kashmir (Hopp 1987). The authors studied the Oxycarenidae material of several

Eurasian collections and found two new species which are described. Furthermore, a species currently belonging to *Microplax* Fieber, 1860, is more closely related to *Urvaschia pterosticta* Hopp, 1987 than to any other known species.

Materials and methods

Composite images were obtained with an M205FA Leica stereomicroscope and camera using the Leica Application Suite software (ver. 4.5.0). Localities were mapped using SimpleMapp (Shorthouse 2010).

Label data are cited verbatim, lines on the same label are divided by a slash (/), and different labels are divided by double slashes (//). Printed [pr] and handwritten [hw] texts are indicated. Details of male dissection methods and terminologies used in this article follow those given in Ashlock (1957) and O'Donnell (1991). The vein terminologies used in this article are those provided in Wootton and Betts (1986). All measurements in the text are given in millimetres.

Abbreviations

BMNH	Natural History Museum, London, United Kingdom;
CEHI in TLMF	Collection Ernst Heiss in Tiroler Landesmuseum Ferdinandeum, Innsbruck, Austria;
HNHM	Hungarian Natural History Museum, Budapest, Hungary;
IZAS	Institute of Zoology, Academia Sinica, Beijing, China;
NHMB	Naturhistorisches Museum, Basel, Switzerland;
NKUM	Institute of Entomology, Nankai University, Tianjin, China;
NMPC	National Museum of Natural History, Prague, Czech Republic;
TNHM	Tianjin Natural History Museum, Tianjin, China;
ZIN	Zoological Institute, Russian Academy of Sciences, St. Petersburg, Russia.

Taxonomy

Urvaschia Hopp, 1987

Figs 1–4

Urvaschia Hopp, 1987: 225–240; Slater and O'Donnell 1995: 78.

Type species. *Urvaschia pterosticta* Hopp, 1987.

Diagnosis (modified from Hopp 1987) (Figs 1, 2). Body elongate oval. Less than half length of first segment of antenna exceeding clypeus. Head short with eyes near to pronotum (less than one half diameter of eyes); bucculae short, only reaching

base of antennae; labium almost reaching mesocoxae. Forewing slightly exceeding tip of abdomen; corium clearly punctate, at least between Cu vein and clavus; clavus punctate; membrane with thick veins, with distal ends fused to form four closed cells on membrane; corium and membrane between the veins covered with conspicuous brown spots. Profemur unarmed or sometimes with one very tiny spine.

Differential diagnosis. *Urvaschia* differs from *Microplax* Fieber, 1860 by lacking any spine or with a very tiny spine at the distal part of the profemur (vs. one distinct spine and some tiny spines present at the distal part of profemur in *Microplax*); head short with a short postocular part which is less than 1/2 longitudinal diameter of the eyes (vs. head elongate with a long postocular part which is approximately as long as the diameter of eyes in *Microplax*); corium is clearly punctate and with many tiny spots (vs. corium lacking any punctures and unicolourous or with large spots in *Microplax*).

Urvaschia is also similar to *Camptotelus* Fieber, 1860 but it can be distinguished from the latter by bucculae not enlarged laterad, first segment of antennae exceeding clypeus, and clavus punctate (vs. the bucculae enlarged laterad, first segment of antennae not exceeding clypeus, and clavus impunctate in *Camptotelus*).

Urvaschia can be distinguished from *Leptodemus* Reuter, 1900 by the first segment of the antennae exceeding clypeus and the hemelytra punctate (vs. the first segment of antennae not exceeding clypeus and the hemelytra are impunctate in *Leptodemus*).

The key of Péricart (1999) contains all Palearctic Oxycarenidae genera except *Urvaschia*. *Urvaschia* runs to couplet 16 (15) (to *Leptodemus*) but they differ in the above-mentioned features. The other possibility if we choose that the specimen has at least one tiny spine on the profemur, we run either to *Leptodemus* at couplet 22 (23) (again) or to *Microplax* at couplet 24 (25) if we choose “profemur has at least one distinct tooth”. Therefore, no described genus has identical characters shared with *Urvaschia*.

Urvaschia pterosticta Hopp, 1987

Figs 1a, d, 4

Urvaschia pterosticta: Hopp, 1987: 226: original description; Slater and O'Donnell 1995: 78: catalogue.

Type material examined. *Holotype* (Fig. 1a, d) • NEPAL ♂; Bumra-Chhurchi [pr] / Logna 3350m [pr] / Pina 2370m // Nepal, 1977 / W. Wittmer [pr] 29. V. [hw] // *Urvaschia* [hw] / *pterodiasticta* [hw] / HOPP [hw] / det. Hopp. I. 1987 [hw] // *Holotype* [hw] / *Typus* [pr] [red label] (NHMB).

Redescription. Colouration. Head black. Antennae blackish brown with segments II and III yellowish brown. Anterior lobe of pronotum black, with a yellow mid spot in the anterior margin; posterior lobe brown with darker punctures. Scutellum black. Corium pale yellowish brown, with sparse obscure pale brown spots including exocorium; veins thick and brown; apical angle of corium with single small blackish brown spot. Colour of membrane similar to corium, with dark brown spots on distal

margin and between brown veins. Femora blackish brown; tibiae yellow with both ends brown; colour of tarsi similar to apices of tibiae.

Structure. Head slightly declined, both dorsally and ventrally with very dense, deep, large punctures. Dorsal surface flat. Eyes slightly protruding laterally. Distance between posterior margin of eyes and anterior margin of pronotum approximately one fourth of diameter of eyes. Antennae covered with short dense oblique setae; apical 1/2 of segment I surpassing clypeus.

Pronotum trapezoid, swollen, calli slightly emergent. Anterior and posterior margin straight; lateral margins slightly arched. Pronotum covered with large, dense punctures. Clavus with three distinct shallow rows of large punctures, with middle row incomplete.

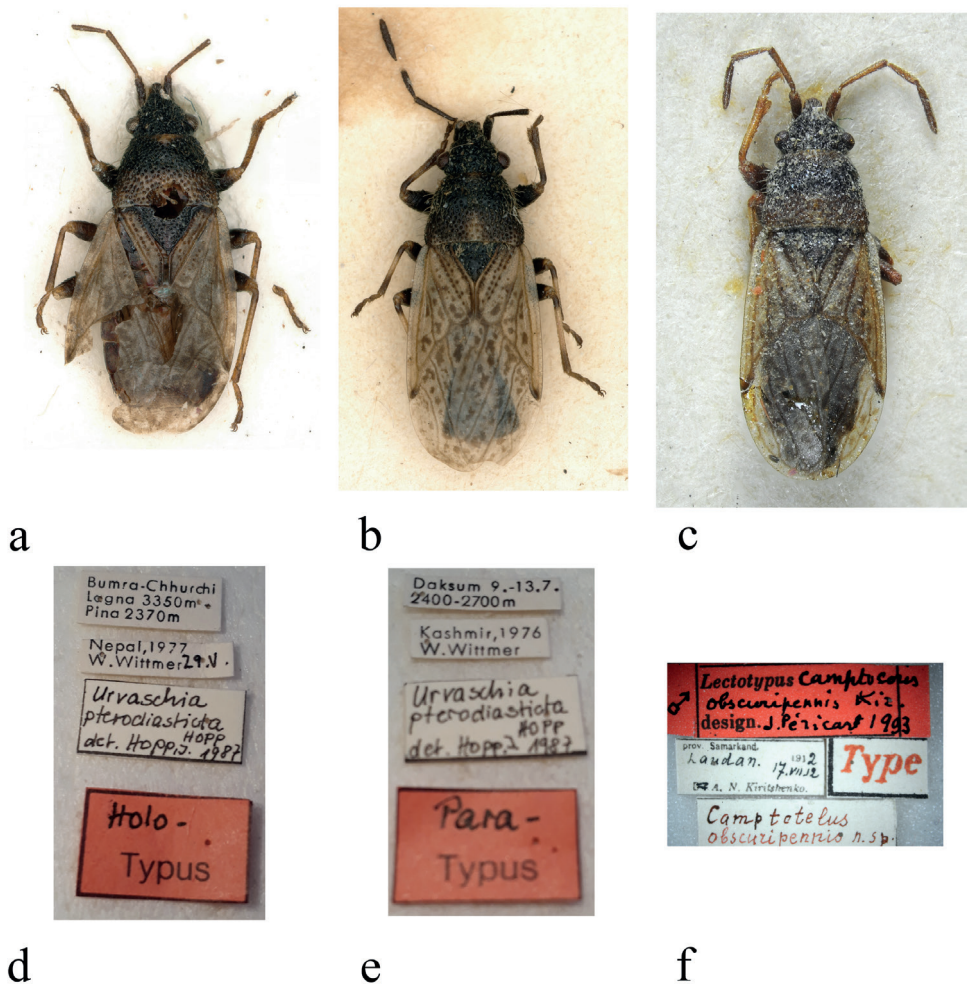


Figure 1. Type photographs **a, d** *Urvashia pterosticta*, holotype, habitus, and labels **b, e** *Urvashia pterosticta* paratype, habitus, and labels **c, f** *Urvashia obscuripennis* comb. nov., habitus and type labels (photographed by F. Konstantinov, ZIN (**c, f**) and I. Zürcher, NHMB (**a, b, d, e**)).

Corium with scattered punctures between vein Cu and clavus; apical margin strongly concave, costal margin convex; apical angle elongated and narrow; total length of corium ~ 2/3 of hemelytra. Membrane relatively long and broad (Fig. 1a); membranal veins thick and obvious; apex of membrane surpassing abdomen. Fore femora slightly thickened, without any spines (Fig. 1a). Abdominal connexivum not exposed.

Pygophore (based on Hopp 1987): posterior margin of pygophore and cup-like sclerite fused; distal margin of cup-like sclerite without a deep incision. Parameres: outer projection large and rounded; inner projection very small and pointed.

Distribution. Nepal (Hopp 1987) (Fig. 4).

Remarks. The female paratype from Kashmir (Fig. 1b) of *U. pterosticta* has a straight and unicolourous exocorium, and the anterior margin of its pronotum and the antenna are uniformly dark. Therefore, it is identical with *U. obscuripennis* and not the holotype of *U. pterosticta* (Fig. 1a); hence, Kashmir should be deleted from locality records of *U. pterosticta*.

It needs to be clarified that the labels of the holotype and paratype (Fig. 1d, e) showed “*Urvaschia pterodiasticta* Hopp” instead of “*Urvaschia pterosticta*” as used in the original description.

Urvaschia obscuripennis (Kiritshenko, 1914) comb. nov.

Figs 1b, c, e, f, 2a, d, 3a–c, 4

Camptotelus obscuripennis Kiritshenko, 1914: 411.

Microplax obscuripennis: Muminov 1973: 75; Hoberlandt 1987: 18; Slater and O’Donnell 1995: 76; Péricart 1998: 128; Péricart 1999: 84B: 48; Péricart 2001: 114.

Type material examined. Lectotype: TADZHIKISTAN • ♂; prov. Samarkand. [pr] / Laudan. 17.VII. 12 [hw] / A. N. Kiritshenko. [pr] // *Camptotelus* / *obscuripennis* n. sp. // Type [pr, red] // Lectotypus [pr] *Camptotelus* [hw] / *obscuripennis* Kir. [hw] / design. [pr] J. Péricart 1993 [hw, red label] (ZIN) (Fig. 1c, f).

Paratype of *U. pterosticta* Hopp. INDIA, KASHMIR • ♀; Daksum 9.-13.7. [pr] / 2400–2700m [pr] // Kashmir, 1976 [pr] / W. Wittmer [pr] // *Urvaschia* [hw] / *pterodiasticta* [hw] / HOPP [hw] / det. Hopp. I. 1987 [hw] // Para- [hw] / Typus [pr] [red label] (NHMB) (Fig. 1b, e).

Other material examined. CHINA • 2♂♂, Yunnan, Yulongshan, Lijiang, Yunnan / 14.vi.1996 / 2700m. leg. Leyi Zheng [all pr] (NKUM); 1♂, Heishui, Yulongshan, Lijiang, Yunnan / 15.vi.1996 / 3000m. leg. Leyi Zheng [all pr] (NKUM); 2♂♂1♀, Shizishan, Wuding, YUNNAN / 2200m / 10.viii.1986 [all hw] (NKUM); 2♂♂1♀, Shizishan, Wuding, YUNNAN / 2300m / 10.viii.1986 [all hw] (NKUM); 1♀, Yulongshan, Lijiang, YUNNAN [all hw] / 13.viii.1979 [hw] / 2800m [hw] leg. Leyi Zheng [pr] (NKUM); 1♀, Yulongshan, Lijiang, YUNNAN / 14.viii.1979 / 2700m [all hw] leg. Zuopei Ling [pr] (NKUM); 1♀, Fenghuangshan, Nanjian, YUNNAN / 2.xi.2001 / 2400m, leg. Wenjun Bu [all pr] (NKUM); 1♂, Fenghuangshan, Nanjian, YUNNAN / 3.xi.2001 / 2400m

[all pr] (NKUM); 1♂, Fenghuangshan, Nanjian, YUNNAN / 3.xi.2001 / 2400m, leg. Weibing Zhu [all pr] (NKUM); 1♂, Sheyaojing, Wuliang Mountain, Nanjian, YUNNAN / 7.xi.2001 / 2400m, leg. Weibing Zhu [all pr] (NKUM); 1♀, Xujiaba, Ailao Mountain [YUNNAN, pr] / 82-007466 [hw] / 22.iii.1982 [hw] (NKUM) ; INDIA• 1♂ 1♀ Nainital, / Kumaon, U. P. / India, H. G. C. // Nainital, / W. Almora, / India, H. G. C. // Champion / Coll. B. M. / 1927–409 (BMNH); AFGHANISTAN• 1♂, J. Klapperich / Sarakanda, 3500 m / 26.7.53, Gebirge / Badakschan / NO-Afghanistan [pr] // Microplax ♂ / obscuripennis K [hw] / Det.L.Hoberlandt, 198[pr]4[hw]; 2♀♀, same data except sex [Microplax ♀ / obscuripennis K]; TADZHIKISTAN 1♂, п б. Искандер- / дарья бл. истоков [=Iskander-darya near source] / *Кириченко* [p] 5 VIII [hw]947 [p] // Microplax / obscuripennis Kir. [hw]; 1♀, р. Сары-таг, оз. / Искандер-куль / *Кириченко* [p] 21 VII [hw]947 [p]; IRAN• 2♀♀, N. Iran, 4.-9.7 1977 / Kandavan, pass / 3000m, 11.8.70 [p] // Loc. No. 395 / Exped Nat. Mus. / Praha [p] // Microplax ♀ / obscuripennis K [hw] / Det.L.Hoberlandt, 198[p]4[hw]; 1♂, N Iran, C Elburz / Kandavan - pass, / 2700–2900 m, S-slope [p] // Loc. no. 87 / Exp. Nat. Mus. / Praha [p] // Microplax ♂ / obscuripennis K [hw] / Det.L.Hoberlandt, 198[p]4[hw]; 1♀, Энарик – Тамин, / в Кирман, в Перс. / *Зарудн* [p] 21. [hw] VIII98 [p] // Microplax / melanocera n. sp. [hw] / *Oshanin* det. [p].

Examined material (digital photograph). China, Sichuan Province, Ganzi Tibetan Autonomous Prefecture, Jiulong County, Wulaxi Town, S215, 28.620355°N, 101.670542°E, photographed by Lu Feng. The image can be found on the iNaturalist website (<https://www.inaturalist.org/observations/59187411>).

Redescription. Colouration. Head black. Antennae blackish brown, sometimes with segments II and III yellowish brown. Bucculae and labium blackish brown, concolourous with clypeus. Anterior lobe of pronotum black, sometimes with anterior margin yellow; posterior lobe dark blackish brown, with a short yellow midline mark near posterior margin. Scutellum black. Corium pale yellowish brown, with sparse, obscure, pale brown spots except exocorium; veins thick and brown; apical angle of corium with single blackish brown spot. Colour of membrane similar to corium, with dark brown spots between brown veins. Thoracal sterna black. Supracoxal lobe of prosternum blackish brown. Ostiolar peritreme of metathoracic scent gland blackish brown. Posterior 1/2 of mesopleuron and metapleuron broadly yellowish white. Femora blackish brown; tibiae yellow with both ends yellowish brown to blackish brown; colour of tarsi similar to apexes of tibiae. Abdominal sterna dark reddish brown.

Structure. Head slightly declined, both dorsally and ventrally, with very dense, deep, large punctures and erect white setae (ventrally decumbent). Dorsal surface flat. Eyes slightly protruding laterally. Distance between posterior margin of eyes and anterior margin of pronotum ~ 1/2 diameter of eyes. Bucculae high, covering labium, with sparse punctures. Antennae covered with short dense oblique setae; apical one quarter of segment I surpassing clypeus. Labium reaching base of mesocoxae, first segment of labium almost reaching posterior margin of bucculae.

Pronotum trapezoid, flat, calli slightly emergent. Anterior and posterior margin straight; lateral margins of pronotum slightly sinuate; both anterolateral and postero-

lateral pronotal angles round. Pronotum covered with large, dense punctures (smaller on calli) and long, white, erect setae, slightly leaning posteriad. Base of scutellum sunken, basal 1/2 covered with small punctures and with similar setae as pronotum; apical 1/2 of scutellum without middle ridge, only lateral margins with small punctures. Hemelytra flat, sparsely covered with short white setae; clavus with three clear rows of large shallow punctures, with middle row incomplete. Corium with scattered punctures between vein Cu and clavus, and a row of dense punctures along inner margin of exocorium, apically being superficial, sometimes absent there; apical margin strongly concave, costal margin almost straight; corium evenly broadening posteriad, body broadest near apex of corium; apical angle elongated and narrow; total length of corium $\sim 2/3$ of hemelytra. Membrane comparatively long, broad, inner ca 1/3 overlapping each other (Figs 1c, 2a); membranal veins thick and obvious; apex of membrane surpassing abdomen. Prosternum, propleura, and lateral part of mesopleura punctate, similarly to pronotum, meso- and metasternum with metapleura impunctate. Ostiolar peritreme of metathoracic scent gland strongly protruding, apically rounded, evaporatorium rounded, reaching $> 3/4$ over metapleura laterad. Fore femora slightly thickened, sometimes with a tiny spine (Fig. 2d). Abdominal connexivum not exposed. Abdomen impunctate, abdominal sternum covered with sparse setae.

Pygophore: posterior margin of pygophore and cup-like sclerite fused; distal margin of cup-like sclerite with a deep incision (Fig. 3a). Parameres (Fig. 3b, c): outer projection small and rounded; inner projection very small and pointed; blade approximately bent rectangularly to shank of paramere in lateral view.

Measurements (mm, $N = 8$). Body length 2.68–3.50. Head length 0.34–0.47, width across eyes 0.60–0.72; antennal segments I–IV length: 0.17–0.26; 0.37–0.56; 0.27–0.32; 0.40–0.45; labium length 0.96, first segment length 0.23. Pronotum length 0.55–0.68, width of anterior margin 0.48–0.54, width of posterior margin 0.68–0.88; scutellum length 0.31–0.39, width 0.33–0.50. Distance apex clavus–corium apex 0.74–0.97; distance apex corium – apex membrane 0.70–0.88.

Distribution. China (Sichuan, Yunnan); India (Kashmir, Uttarakhand) (Hopp 1987); Iran (Alborz, Sistan and Baluchestan); Afghanistan (Badakshan); Tadjikistan (Fig. 4).

Remarks. As mentioned above, the female paratype of *U. pterosticta* from Kashmir (Fig. 1b) was transferred to this species. Meanwhile, the original distribution information from China of this species should be considered a misidentification; see the detailed comments of *Urvaschia convexa* sp. nov.

Differential diagnosis. *Urvaschia obscuripennis* is similar to *U. pterosticta* in having similar brown spots on the hemelytra and apex of the corium conspicuously concave, but the lateral margin of the corium is almost straight and the exocorium spotless, the lateral margins of pronotum are slightly sinuate (vs. lateral margin of the corium more arched and exocorium with brown spots; the lateral margins of the pronotum more arched in *U. pterosticta*), and the distal margin of the cup-like sclerite with a deep incision (vs. distal margin of cup-like sclerite without any incision but with a median keel in *U. pterosticta*).

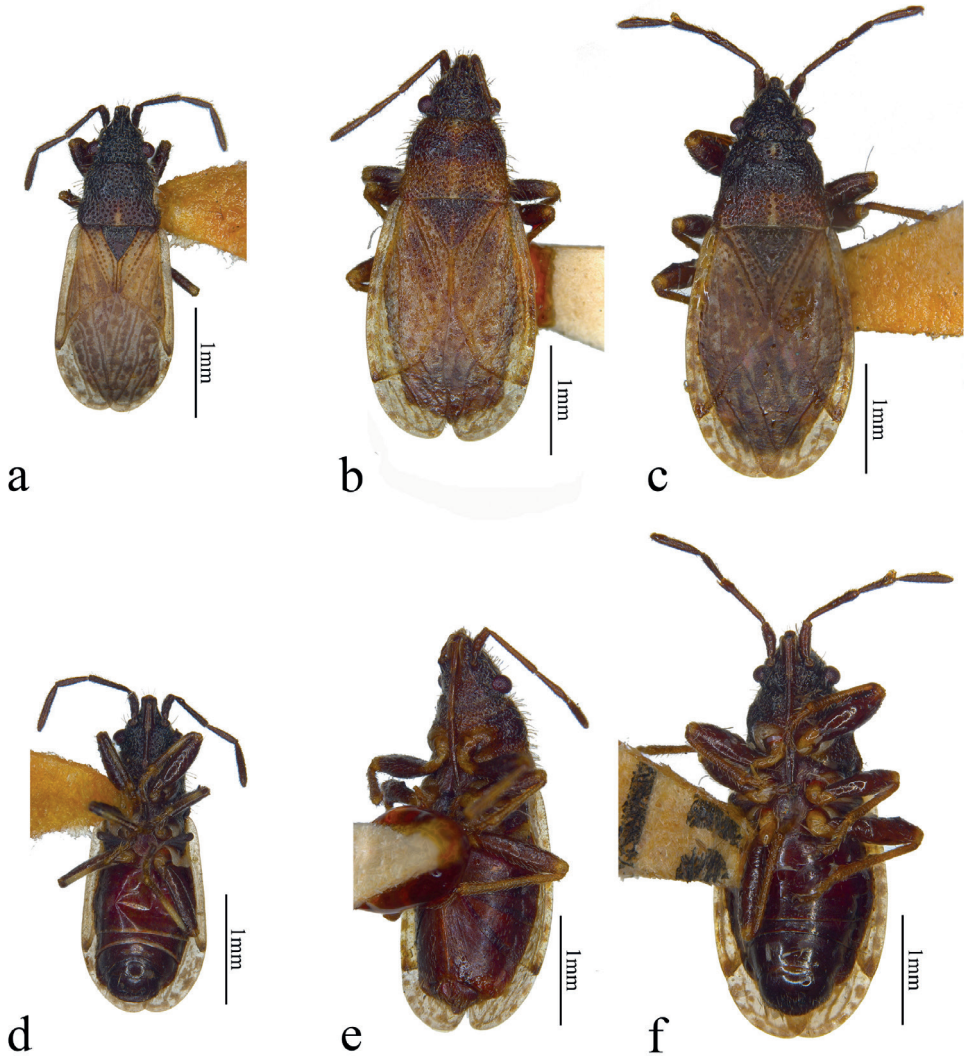


Figure 2. Dorsal and ventral views **a, d** *Urvaschia obscuripennis* comb. nov. **b, e** *Urvaschia convexa* sp. nov., holotype **c, f** *Urvaschia recta* sp. nov., holotype.

***Urvaschia convexa* sp. nov.**

<https://zoobank.org/4060CA49-013C-4BE2-80C6-2353010E1247>

Figs 2b, e, 3d–f, 4

Camptotelus obscuripennis: Zheng and Zou 1981: 91, fig. 323, pl.13: 129. Misidentification.

Type material examined. Holotype. CHINA • ♀; Maerkang [pr], Sichuan [pr] / 2600–2800m / 13.viii.1963 [hw] (TNHM) // leg. Jiang Xiong [pr] // *Camptotelus obscuripennis* Kiritschenko [hw]/ det. Leyi Zheng [hw]. **Paratype.** CHINA • ♂;

Maerkang [pr], Sichuan [pr] / 2600–2800m / 11.viii.1963 [hw] (TNHM) // leg. Jiang Xiong [pr].

Description. Colouration. Head blackish brown; bucculae and labium brown; antennae dark brown. Pronotum brown, with a pale brown midline; callar area of pronotum blackish brown. Scutellum blackish brown, distal 3/4 with a brown midline. Corium pale yellowish brown, evenly covered with obscure brown spots; distal margin of corium dark brown; apical angle of corium with a small blackish brown spot. Colour of membrane similar to that of corium, with brown spots between brown veins. Thoracic sterna blackish brown except posterior 1/2 of prosterna yellowish brown. Supracoxal lobe of prosternum yellow. Mesopleuron blackish brown; inner 1/2 of ostiolar peritreme of metathoracic scent gland yellowish white, outer 1/2 of ostiolar peritreme brown. Posterior 1/2 of metapleura broadly yellowish white. Abdominal sterna dark reddish brown. Femora dark brown, tibiae ochraceous.

Structure. Head slightly declined, covered very densely with deep and large punctures and long white erect setae both dorsally and ventrally; vertex comparatively flat. Eyes slightly protruding laterally. Distance between posterior margin of eyes and anterior margin of pronotum \sim 1/3 of diameter of eyes. Bucculae high, covering labium, with sparse punctures. Antennae covered with dense oblique setae; apical quarter of segment I surpassing clypeus. Labium reaching base of mesocoxae, first segment of labium surpassing posterior margin of bucculae. Venter of head comparatively flat, covered with dense punctures and dense decumbent setae.

Pronotum trapezoid, flat, calli slightly emergent. Anterior margin straight; middle part of posterior margin slightly concave; lateral margins of pronotum sinuate; both of anterolateral and posterolateral pronotal angles rounded. Pronotum covered with dense punctures and with long erect setae, slightly leaning posteriad. Base of scutellum slightly sunken, covered with punctures and setae except midline, slightly emergent in apical 1/2. Hemelytra flat, sparsely covered with white short setae; clavus with inner and outer rows of strong and shallow punctures, scattered with many irregular punctures between them. Corium with sparse scattered punctures. Apical margin of corium convex, costal margin evenly arched; body broadest near apex of clavus, length of corium almost three fourth of hemelytra. Membrane short and small, only overlapping each other on inner edge (Fig. 2b); membranal veins remarkable; apex of membrane surpassing tip of abdomen. Ostiolar peritreme of metathoracic scent gland strongly protruding, apically rounded. Fore femora slightly thickened, unarmed (Fig. 2e). Abdominal connexivum not exposed. Abdominal sternum impunctate, covered with comparatively dense setae.

Pygophore (Fig. 3d): Posterior margin of pygophore and cup-like sclerite fused. Parameres (Fig. 3e, f): outer projection large and slightly sharp; inner projection very small; blade nearly rectangularly bent to shank of paramere in lateral view.

Measurements (mm, $N = 2$). **Holotype.** ♀ (**Paratype.** ♂), Body length 3.44 (3.08). Head length 0.53 (0.45), width across eyes 0.65 (0.69); antennal segments I–IV length: 0.20: 0.50: 0.36: 0.41 (0.17: 0.42: 0.31: 0.43); labium length 1.26 (covered), first segment length 0.31. Pronotum length 0.71 (0.66), width of anterior margin 0.58 (0.53), width of posterior margin 1.01 (0.85); scutellum length 0.44 (0.39),

width 0.57 (0.40). Distance apex clavus–apex corium 1.03 (0.92); distance apex corium–apex membrane 0.76 (0.65).

Etymology. The species epithet, *convexa*, is an adjective and refers to the convex distal margin of corium.

Distribution. China (Sichuan) (Fig. 4).

Differential diagnosis. Based on the description and figures, we conclude that the new species was always misidentified as “*Camptotelus obscuripennis* Kiritshenko, 1914” in China (Zheng and Zou 1981, 1987; Zheng 1988). When we examined the photographs of the type of *Camptotelus obscuripennis*, we found they are different but closely related species. The new species differs from *U. obscuripennis* in the following combination of characters: antennae unicolourous (vs. antennae not unicolorous in *U. obscuripennis*); distal margin of corium convex and apical angle of corium not elongated (vs. distal margin of corium concave; apical angle elongated and pointed in *U. obscuripennis*); inner 1/2 of ostiolar peritreme of metathoracic scent gland yellowish white, outer 1/2 brown (vs. ostiolar peritreme of metathoracic scent gland black in *U. obscuripennis*); profemur unarmed (vs. profemur with a spine).

***Urvaschia recta* sp. nov.**

<https://zoobank.org/E6FF0F07-0BAB-4014-B183-858C6A2FE4F8>

Figs 2c, f, 3g–i, 4

Type material examined. Holotype. CHINA • ♂; Lijiang [hw], Yunnan [pr] / 11.viii. [hw]1979 [pr] / leg. Jianxin Cui [pr] (NKUM). **Paratypes.** CHINA • 1♀, Bayi town, Xizang / 6.viii.2003 / leg. Huaijun Xue, Xinpu Wang [all pr] (NKUM); 1♀, Xiaonanchuan Forestry Centre, Erlonghe, Liupanshan, Ningxia / 28.vi.2008 / 1900m. leg. Gengping Zhu [all pr] (NKUM); 1♀, Zhongreniao, Xiangcheng [all hw], Sichuan [pr] / 3950m // 1982.VII.4 [all hw] / leg. Huaicheng Chai [hw] (IZAS).

Other material examined. CHINA • pr. Beijing / Mentougou Dist. / Beijing 130 km NW / Liyan Ling // Linshan Mt. / 1749 m, 115°30'E / 40°00', 2.VIII.2002 // leg. G. Melika (HNHM); NEPAL • 1♂ 1♀ Umg. Alm Darghari / b. Maharigaon, 4000m // Gebiet von Jumla / Westnepal, lg. H. Franz // COLLECTION / ERNST HEISS / Innsbruck – Austria (CEHI in TLMF).

Description. Colouration. Head blackish brown. Antennae dark blackish brown. Bucculae and labium dark brown. Pronotum with a yellowish white midline except area of calli. Anterior lobe of pronotum blackish brown, posterior lobe dark brown. Scutellum blackish brown. Hemelytra pale yellowish brown, with dense dark brown spots between brown veins covering exocorium as well; distal margin of corium dark brown; apical angle of corium with a blackish brown spot. Thoracal sterna blackish brown. Supracoxal lobes yellowish white to yellow. Mesopleuron black; inner 1/2 of ostiolar peritreme of metathoracic scent gland yellowish white, outer 1/2 of ostiolar peritreme brown. Posterior 1/2 of metapleura broadly yellowish white. Femora blackish brown; tibiae and tarsi ochraceous. Abdominal sterna dark reddish brown.

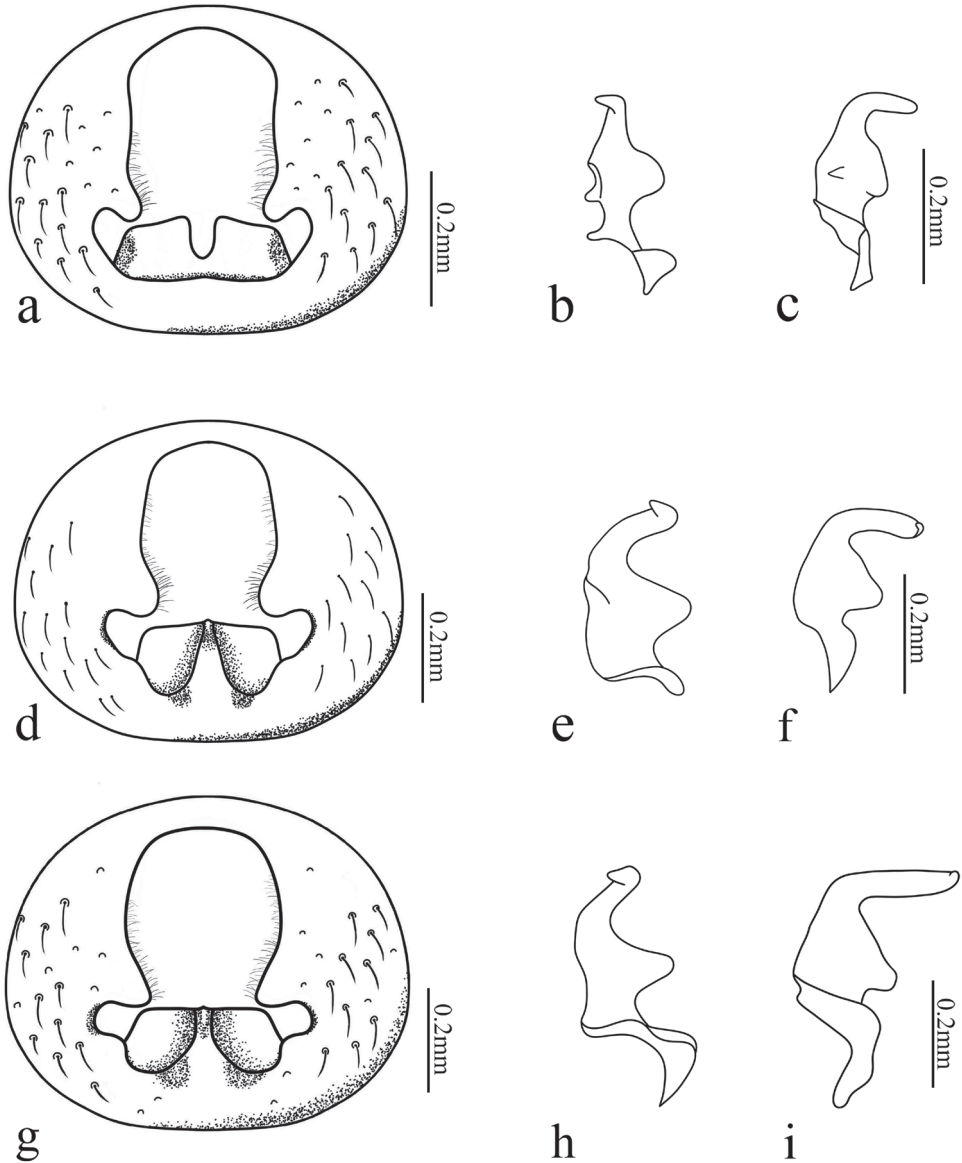


Figure 3. Pygophore (dorsal views, parameres removed) and left paramere (dorsal and lateral views): **a–c** *Urvaschia obscuripennis* comb. nov. **d–f** *Urvaschia convexa* sp. nov., paratype **g–i** *Urvaschia recta* sp. nov., holotype.

Structure. Head slightly declined, covered with large deep punctures and erect white setae. Eyes slightly protruding laterally. Distance between posterior margin of eyes and anterior margin of pronotum $1/2$ diameter of eyes. Bucculae high, almost parallel to labium, visible laterad of clypeus from dorsal view. Antennae covered with dense oblique setae, apical $1/3$ of segment I surpassing clypeus. First segment of

labium surpassing bucculae, segment II surpassing base of head, labium reaching middle of mesocoxae. Venter of head flat, covered with punctures and dense white decumbent setae.

Pronotum trapezoid, flat, covered with large dense punctures and long white erect setae, slightly leaning posteriad; calli slightly emergent. Anterior margin of pronotum straight; posterior margin of pronotum straight with posterolateral pronotal angles slightly protruding posteriad. Base of scutellum slightly sunken; each margin covered with dense punctures, smaller than on pronotum and sparse setae, central area with sparse punctures and inconspicuous median carina. Hemelytra flat, sparsely covered with white and short setae; clavus with inner and outer rows of punctures, scattered with irregular one or two rows of punctures in middle. Corium with several punctures between vein Cu and clavus, and a row of punctures along inner margin of exocorium (Fig. 2c); cubital vein inconspicuous. Apical margin of corium straight, costal margin evenly arched; body broadest near apex of clavus; corium longer than 2/3 of hemelytra. Membrane comparatively broad, almost fully overlapping each other (Fig. 2c); membranal veins thick and conspicuous; apex of membrane surpassing abdomen. Femora slightly thickened, profemora sometimes with one small spine (Fig. 2f). Abdominal connexivum not exposed. Abdominal sternum impunctate, covered with sparse setae.

Pygophore (Fig. 3g): Posterior margin of pygophore and cup-like sclerite fused. Parameres (Fig. 3h, i): outer projection large, triangular; inner projection inconspicuous; blade bent rectangularly with shank of paramere from lateral view.

Measurements (mm, $N = 3$). **Holotype**. ♂ (**Paratypes**. 2♀♀); Body length 3.49 (3.72–3.81). Head length 0.46 (0.50–0.51), width across eyes 0.77 (0.73–0.76); antennal segments I–IV length: 0.22: 0.46: 0.33: 0.40 (I–IV: 0.18–0.25: 0.54: 0.35: 0.45); labium length 1.34, first segment length 0.32. Pronotum length 0.73 (0.73–0.76), width of anterior margin 0.60 (0.64), width of posterior margin 1.04 (1.12–1.15); scutellum length 0.51 (0.48–0.50), width 0.56 (0.67–0.71). Distance apex clavus–apex corium 1.08 (1.08–1.18); distance apex corium–apex membrane 0.78 (0.98–1.05).

Etymology. The species epithet *recta*, derived from Latin adjective *rectus* (= straight), alludes to the straight apical margin of the corium.

Distribution. China (Beijing, Ningxia, Sichuan, Xizang, Yunnan), Nepal (Fig. 4). The locality of the Nepalese specimen is very near to the type locality of *U. pterosticta*; therefore, it cannot be seen separately on Fig. 4.

Differential diagnosis. The new species is similar to *U. convexa* sp. nov. in having brown spots on the hemelytra and oval body shape, but the corium is not elongated, with the length of the corium almost twice the length of the membrane from the apical angle of the corium to the apex, and its apex is almost straight (vs. corium conspicuously elongated, with the length of the corium almost three times the length of the membrane from the apical angle of the corium to the apex, and the apex of the corium is conspicuously convex in *U. convexa* sp. nov.); membrane almost fully overlapping (vs. membrane only overlapping on the inner edge in *U. convexa* sp. nov.).

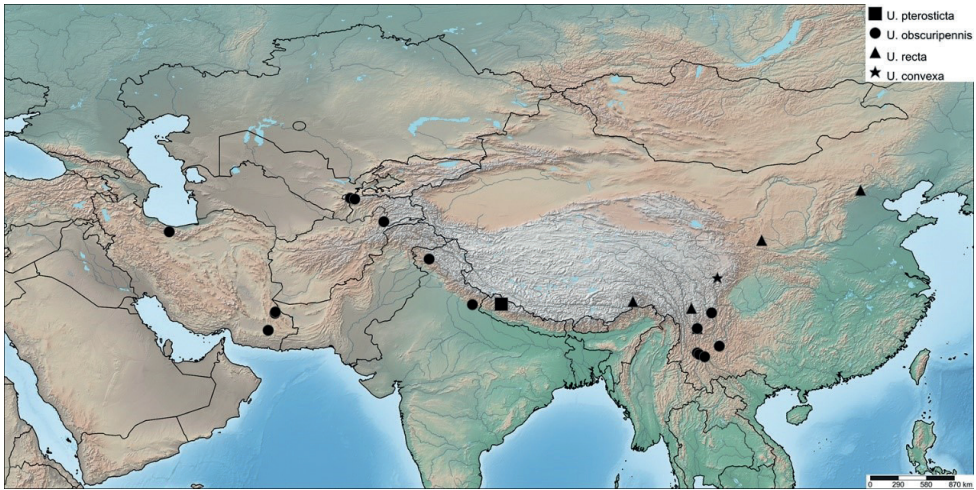


Figure 4. Distribution of the species of *Urvaschia*.

Key to species of *Urvaschia*

- 1 Distal margin of corium markedly concave, apex of corium elongated (Figs 1, 2a) **2**
- Distal margin of corium convex or straight, apex of corium not elongated (Fig. 2b, c) **3**
- 2 Costal margin of corium convex, with brown spots; lateral margin of pronotum slightly arched, not sinuate (Fig. 1a); distal margin of cup-like plate carinate, acute..... ***U. pterosticta* Hopp, 1987**
- Costal margin of corium straight, excorium unicolourous, spotless; lateral margin of pronotum slightly sinuate (Fig. 2a); distal margin of cup-like plate with a deep incision (Fig. 3a) ***U. obscuripennis* (Kiritshenko, 1914) comb. nov.**
- 3 Distal margin of corium convex; membrane only overlapping on inner edge (Fig. 2b)..... ***U. convexa* sp. nov.**
- Distal margin of corium almost straight; membrane fully overlapping each other (Fig. 2c)..... ***U. recta* sp. nov.**

Discussion

Until now, the regional Palaearctic *Urvaschia* species seemed to be endemic in Nepal and Kashmir, but four species distributed in six countries documented here indicate a more widely-distributed taxon. It is interesting that the shape of the corial apical margin of *Urvaschia* species varies between different species, from concave, straight, to convex. This demands further investigations using both morphological and molecular evidence of species of related oxycarenid genera.

Acknowledgements

We thank Wenjun Bu (NKUM), Mick Webb (BMNH), Anna Ágnes Somogyi (HNHM), Hong Liu (IZAS) and Ernst Heiss (TLMF) for the loan of specimens. We are grateful to Isabelle Zürcher (NHMB) for photographs of the holotype and paratype of *Urvaschia pterosticta*; to Fedor Konstantinov (ZIN) for photographing the lectotype of *Camptotelus obscuripennis* and checking the types for important features; to Petr Kment (NMPC) for kindly photographing some specimens of Oxycarenidae in the Hoberlandt collection, including *Urvaschia* specimens, and to Feng Lu (College of Life Sciences and Oceanography, Shenzhen University, Shenzhen China) for agreeing to use the locality data of his picture of *U. obscuripennis*. We are grateful to M. B. Malipatil (AgriBio, Melbourne, Australia) and Wenjun Bu (NKUM) for the detailed valuable comments on the manuscript. This study received financial support from the Natural Science Foundation of the Jiangsu Higher Education Institutions of China (19KJB510009), the Program of the Ministry of Science and Technology of the People's Republic of China (2015FY210300), the National Natural Science Foundation of China (grant no. 31402010), and the Highly Educated Talents Foundation in Nanjing Forestry University (grant no. G2014002).

References

- Ashlock PD (1957) An investigation of the taxonomic value of the phallus in the Lygaeidae (Hemiptera-Heteroptera). *Annals of the Entomological Society of America* 50(4): 407–426. <https://doi.org/10.1093/aesa/50.4.407>
- Dellapé PM, Henry TJ (2022) Lygaeoidea Species File. Version 5.0/5.0. <http://Lygaeoidea.SpeciesFile.org/> [accessed 7 June 2022]
- Hoberlandt L (1987) Results of the Czechoslovak-Iranian Entomological Expeditions to Iran 1970, 1973 et 1977. Heteroptera, Lygaeidae, Oxycareninae. *Acta Entomologica Musei Nationalis Pragae* 42: 11–29.
- Hopp I (1987) *Urvaschia* n. gen., eine neue Wanzen-gattung aus dem Himalaya (Heteroptera: Lygaeidae: Oxycareninae). *Entomologische Zeitung* 97(16): 225–240. [In German]
- Kiritshenko AN (1914) Hemiptera-Heteroptera turanica nova. II. *Revue Russe d'Entomologie* 13: 397–415.
- Muminov NN (1973) New and little-known Oxycareninae (Heteroptera, Lygaeidae) of central Asia. *Doklady Akademii Nauk Tadzhikskoi SSR* 16(9): 74–76. [In Russian]
- O'Donnell JE (1991) A survey of male genitalia in lethaeine genera (Heteroptera: Lygaeidae: Rhyparochrominae). *Journal of the New York Entomological Society* 99: 441–470.
- Péricart J (1998) Désignation de lectotypes et paralectotypes pour des Lygaeidae paléarctiques et commentaires (Heteroptera). 4. Les types des auteurs russes. *Revue Française d'Entomologie (N.S.)* 19 (1997): 123–129.
- Péricart J (1999) Hémiptères Lygaeidae euro-méditerranéens 2. Faune de France 84B. Fédération Française des sociétés de sciences naturelles, Paris, 453 pp.

- Péricart J (2001) Lygaeidae. In: Aukema B, Rieger C (Eds) Catalogue of the Heteroptera of the Palaearctic Region, Vol 4: The Netherlands Entomological Society, Amsterdam, 113–114.
- Shorthouse DP (2010) SimpleMappr, an online tool to produce publication-quality point maps. [Retrieved from] <https://www.simplemappr.net> [Accessed 07 May 2022]
- Slater JA, O'Donnell JE (1995) A Catalogue of the Lygaeidae of the World (1960–1994). New York Entomological Society, New York, 410 pp.
- Wootton RJ, Betts CR (1986) Homology and function in the wings of Heteroptera. *Systematic Entomology* 11(3): 389–400. <https://doi.org/10.1111/j.1365-3113.1986.tb00191.x>
- Zheng LY (1988) Hemiptera: Lygaeoidea, Miridae (Stenodemini). In: *Insects of Mt. Namjagbarwa region of Xizang*: Science Press, Beijing, 95–100. [In Chinese, English summary]
- Zheng LY, Zou HG (1981) Lygaeidae. In: Hsiao TY, Ren SZ, Zheng LY, Jing XL, Zou HG, Liu SL (Eds) *A handbook for the determination of the Chinese Hemiptera-Heteroptera, Volume 2*: Science Press, Beijing, 91–92. [In Chinese, English summary]
- Zheng LY, Zou HG (1987) Lygaeoidea. In: Zhang SM (Ed.) *Agricultural diseases, insect pests and weeds in Tibet, Volume 1: the Tibet people's Publishing House, Lhasa*, 85–88. [In Chinese, English summary]

Description of two species of the genus *Astrodia* Verrill, 1899 (Ophiuroidea, Euryalida, Asteronychidae), including a new species from seamounts in the West Pacific

Xiaojun Xie¹, Bo Lu¹, Jie Pang¹, Dongsheng Zhang^{1,2,3}

1 Key Laboratory of Marine Ecosystem Dynamics, Second Institute of Oceanography, Ministry of Natural Resources, Hangzhou, China **2** Southern Marine Science and Engineering Guangdong Laboratory (Zhuhai), Zhuhai, Guangdong, China **3** School of Oceanography, Shanghai Jiao Tong University, Shanghai, China

Corresponding author: Dongsheng Zhang (dszhang@sio.org.cn)

Academic editor: Sabine Stöhr | Received 8 June 2022 | Accepted 1 September 2022 | Published 4 October 2022

<https://zoobank.org/DF436107-268C-4011-9D57-02B8C83C35ED>

Citation: Xie X, Lu B, Pang J, Zhang D (2022) Description of two species of the genus *Astrodia* Verrill, 1899 (Ophiuroidea, Euryalida, Asteronychidae), including a new species from seamounts in the West Pacific. ZooKeys 1123: 99–122. <https://doi.org/10.3897/zookeys.1123.87397>

Abstract

Five specimens of Ophiuroidea from deep-sea seamounts in the West Pacific were collected and identified as two species, *Astrodia duospina* sp. nov. and *Astrodia abyssicola*. The new species, *Astrodia duospina* sp. nov., can be distinguished from its congeners by having indistinct or underdeveloped oral papillae, relatively short genital slits, crescent-shaped lateral arm plates, and plate-shaped external ossicles on the aboral surface of the disc. One specimen was identified as *Astrodia abyssicola*, which has been reported in the north-western Pacific and the north-eastern coast of Japan. The most recent tabular key of *Astrodia* was revised with two more key characteristics added, the shape and presence of oral papillae and the number of arm spines. The phylogenetic relationship of *Astrodia* and *Asteronyx* was analyzed based on 16S and COI sequences. The discovery of the two species further expanded the geographical distribution of the genus *Astrodia*.

Keywords

Deep sea, molecular phylogeny, morphology, ophiuroids, taxonomy

Introduction

Class Ophiuroidea, as the largest group among echinoderms, with 2126 valid species (Stöhr et al. 2022), are widely distributed from the tropics to polar seas, and from the intertidal to the deep ocean. The Indo-Pacific, North Pacific, and South Pacific regions are reported to have relatively high ophiuroid species richness (Stöhr et al. 2012). Due to the technical limitations of deep sea exploration, the deep-sea ophiuroid fauna remains poorly known (Rodrigues et al. 2011). Seamounts are often of volcanic origin, with elevated topography from the deep-sea floor, which alters the flow of ocean currents and provides highly heterogeneous habitats serving as “hotspots” for deep-sea animals, especially for suspension-feeding epibenthic organisms (e.g. corals, sponges, and ophiuroids) (Yesson et al. 2011). Understanding the biodiversity of ophiuroids from seamounts will provide key information for the protection of this vulnerable ecosystem.

The order Euryalida Lamarck, 1816 comprises about 200 species from three families, Euryalidae Gray, 1840, Asteronychidae Ljungman, 1867, and Gorgonocephalidae Ljungman, 1867 (Stöhr et al. 2022). Among these, Asteronychidae is the smallest family with only 12 extant species from four genera (*Asteronyx* Müller & Troschel, 1842, *Astrodia* Verrill, 1899, *Astronebris* Downey, 1967 and *Ophioschiza* H.L. Clark, 1911). The genus *Astrodia* was erected by Verrill, in 1899 and currently comprises four species, *Astrodia abyssicola* (Lyman, 1879), *Astrodia excavata* (Lütken & Mortensen, 1899), *Astrodia plana* (Lütken & Mortensen, 1899) and *Astrodia tenuispina* (Verrill, 1884). *Astrodia tenuispina* was first described by Verrill (1884) under the name *Asteronyx tenuispina*, and was transferred to *Astrodia* by Verrill (1899). Koehler (1922) described a new species, *Astrodia bispinosa*, which was later regarded as a junior synonym of *Astrodia tenuispina* (Baker 1980). The most recent description of *Astrodia plana* was published by Döderlein (1927). Recently, Okanishi and Fujita (2014) reviewed this genus and transferred *Ophiocreas abyssicola* Lyman, 1879 to *Astrodia*. In their review, Okanishi and Fujita (2014) provided interspecific distinguishing characteristics including the shape and arrangements of external ossicles on the aboral surface of the disc, length of genital slits in relation to the height of the disc, the shape of the lateral arm plates, presence or absence of a projection of the lateral arm plates on the middle to the distal portion of the arms. Additionally, the geographical distribution of the four species was summarized (Okanishi and Fujita 2014).

In this study, we describe a new species, *Astrodia duospina* sp. nov., and redescribe *Astrodia abyssicola*, from seamounts of the West Pacific. New interspecific diagnostic characteristics were identified, and the tabular key of Okanishi and Fujita (2014) for the genus *Astrodia* was updated. DNA sequences were used to infer the phylogenetic relationship of the two species with their congeners.

Materials and methods

Sample collection

Five specimens of *Astrodia* were collected by ROV *HAILONG III*, ROV *HAILONG IV*, and HOV *JIAOLONG*, from seamounts in the Philippine Sea and the Northwest Pacific, during several COMRA's cruises in 2013, 2020, and 2021 (Fig. 1). All specimens were preserved in 95% ethanol on board the vessels and photographed using a digital camera (Canon EOS 5D), then deposited in the repository of the Second Institute of Oceanography, Hangzhou, China (RSIO).

Morphological analysis

Morphological characters were examined and photographed using a stereoscopic microscope (Zeiss Axio Zoom V16). Arm skeletons were examined with a Hitachi TM1000 scanning electron microscope. Skeletal elements were prepared by submerging in commercial bleach (2.5% NaOCl). Washed in distilled water and ethanol, air-dried, and mounted on a stub using dissolved carbon tapes.

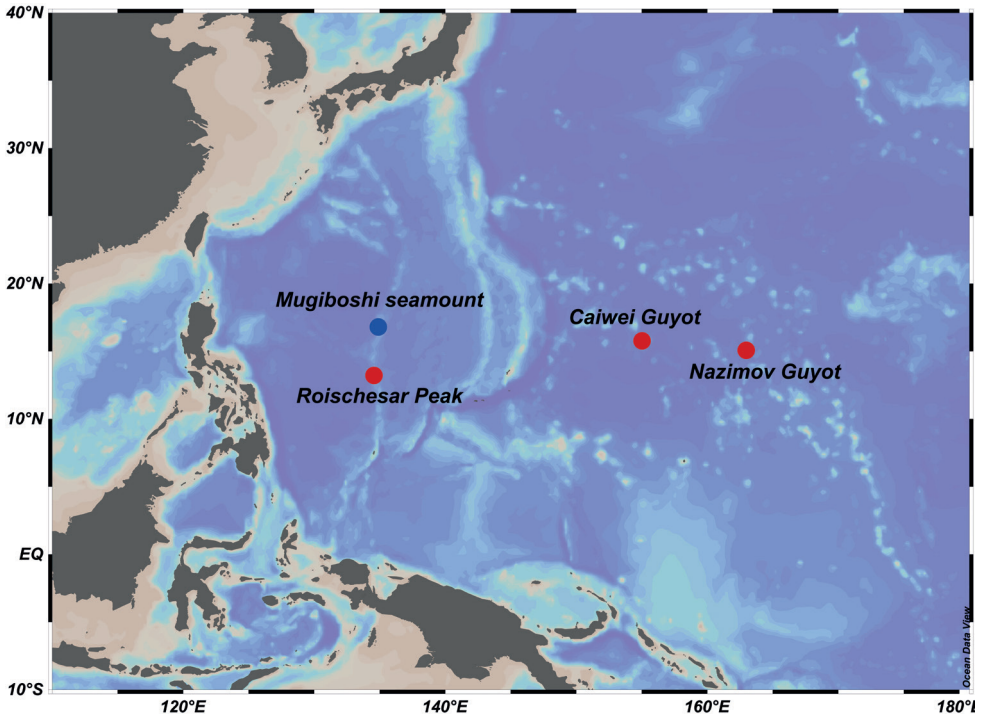


Figure 1. Sampling sites of two species in the Philippine Sea and the Northwest Pacific (red circles represent the sampling sites of *Astrodia duospina* sp. nov., the blue circle represents the sampling site of *Astrodia abyssicola*).

The following literature was used as references for the morphological analysis: Okanishi and Fujita (2014), Okanishi et al. (2018), Manso (2010), Baker (1980), and Martynov (2019).

Molecular analysis

Several arm segments were dissected from each individual for genomic DNA extraction using DNeasy Blood & Tissue Kit (QIAGEN) following the manufacturer's protocols. The COI sequences and 16S rRNA sequences were amplified with primers listed in Table 1. The PCR procedures were as follows: an initial denaturation step at 95 °C for 4 min followed by 35 cycles of 94 °C for 15 s, 50 °C for 30 s, and 72 °C for 1 min, and a final extension step at 72 °C for 10 min, for COI; an initial denaturation at 95 °C for 4 min, followed by 35 cycles of 94 °C for 15 s, 50 °C for 30 s, and 72 °C for 30 s, and a final extension at 72 °C for 7 min, for 16S. PCR reactions were performed using 25 µL volumes containing: 1 µL of DNA template, 1 µL of each primer, 9.5 µL of dd H₂O, and 12.5 µL of 2 × Phanta Max Master Mix (Vazyme, China). PCR products were purified with a QIAquick PCR purification kit (QIAGEN) following the protocol supplied by the manufacturer. Sequencing was performed by Sangon Biotech (Shanghai, China) on an ABI 3730XL DNA analyzer (Applied Biosystems, Foster City, CA, USA). Forward and reverse sequences were de novo assembled and edited using Geneious Prime 2021 (<https://www.geneious.com>), deposited in GenBank (COI: OP328780–OP328783; 16S: OP325290–OP325293).

Seventy-two 16S sequences and 28 COI sequences of Asteronychidae were downloaded from the NCBI. In total, 78 16S sequences and 34 COI sequences (Table 2), including four new 16S sequences and four new COI sequences were used for phylogenetic analysis, with two species of *Asteroschema* as the outgroup. COI and 16S were aligned using Clustal Omega (Sievers and Higgins 2014) as a plug-in in Geneious with default settings, respectively. Maximum likelihood trees were inferred based on a concatenated alignment of 16S and COI, as well as an alignment of 16S and COI respectively. IQ-TREE was used to perform the maximum likelihood bootstrap method (<http://iqtree.cibiv.univie.ac.at/>) (Nguyen et al. 2015), with the substitution model GTR+I+G, bootstrap support values determined by the ultrafast bootstrap algorithm for 100,000 replicates (Hoang et al. 2018). The best substitution model was selected by ModelFinder as a plug-in in IQ-TREE websites. (Kalyanamoorthy et al. 2017).

Table 1. Information on primers used for PCR programs.

Primer	Sequence
Oph-COI-F	TTTCAACTAATCAYAAGGAYATWGG
Oph-COI-R	CTTCAGGRTGWCCRAARAAYCA
16Sar	CGCCTGTTTATCAAAAACAT
16Sbr	CCGGTCTGAACTCAGATCACGT

Table 2. Voucher specimens and accession numbers of COI and 16S sequence data used in the phylogenetic analysis (IDSSE, Institute of Deep-sea Science and Engineering, China; MV, Museums Victoria, Australia; NSMT, National Museum of Nature and Science, Japan; RSIO, Second Institute of Oceanology, China; SIO, Scripps Institution of Oceanography, USA).

Species	Locality	Voucher number	COI	16S	Code from Okanishi et al. (2018)
<i>Asteronyx longifissus</i>	Monterey, California	SIO: BIC: E6108	-	KM014337	-
<i>Asteronyx loveni</i>	South China Sea	IDSSE-EEB-SW0002	MZ198756	MZ203264	-
<i>Asteronyx loveni</i>	New Zealand	MV F188855	KU895061	-	-
<i>Asteronyx loveni</i>	Off Abashiri, Hokkaido	NSMT E-6904-A	-	LC276316	OK-226
<i>Asteronyx loveni</i>	Off Abashiri, Hokkaido	NSMT E-6904-B	-	LC276354	OK-315
<i>Asteronyx loveni</i>	Off Abashiri, Hokkaido	NSMT E-6904-C	LC276289	LC276330	OK-256
<i>Asteronyx loveni</i>	Off Abashiri, Hokkaido	NSMT E-6904-G	LC276290	LC276331	OK-257
<i>Asteronyx loveni</i>	Off Abashiri, Hokkaido	NSMT E-6904-H	LC276282	LC276317	OK-227
<i>Asteronyx loveni</i>	Off Abashiri, Hokkaido	NSMT E-6904-I	-	LC276359	OK-339
<i>Asteronyx loveni</i>	Off Abashiri, Hokkaido	NSMT E-6904-J	-	LC276350	OK-295
<i>Asteronyx loveni</i>	Off Abashiri, Hokkaido	NSMT E-6904-K	-	LC276332	OK-258
<i>Asteronyx loveni</i>	Off Abashiri, Hokkaido	NSMT E-6904-L	-	LC276358	OK-337
<i>Asteronyx loveni</i>	Off Abashiri, Hokkaido	NSMT E-6904-R	-	LC276334	OK-262
<i>Asteronyx loveni</i>	Off Abashiri, Hokkaido	NSMT E-6904-S	-	LC276353	OK-314
<i>Asteronyx loveni</i>	Off Abashiri, Hokkaido	NSMT E-6904-T	-	LC276333	OK-261
<i>Asteronyx loveni</i>	Off Abashiri, Hokkaido	NSMT E-6951-B	-	LC276343	OK-281
<i>Asteronyx loveni</i>	Off Abashiri, Hokkaido	NSMT E-6951-C	LC276292	LC276337	OK-269
<i>Asteronyx loveni</i>	Off Abashiri, Hokkaido	NSMT E-6951-D	-	LC276344	OK-284
<i>Asteronyx loveni</i>	Off Abashiri, Hokkaido	NSMT E-6951-F	-	LC276336	OK-268
<i>Asteronyx loveni</i>	Off Abashiri, Hokkaido	NSMT E-6951-G	-	LC276341	OK-279
<i>Asteronyx loveni</i>	Off Abashiri, Hokkaido	NSMT E-6951-H	LC276291	LC276335	OK-267
<i>Asteronyx loveni</i>	Off Miyako, Iwate	NSMT E-6943-A	LC276288	LC276329	PT-253
<i>Asteronyx loveni</i>	Off Miyako, Iwate	NSMT E-6256	AB758757	AB605076	PT-41
<i>Asteronyx loveni</i>	Off Miyako, Iwate	NSMT E-5641-A	LC276284	LC276320	PT-238
<i>Asteronyx loveni</i>	Off Miyako, Iwate	NSMT E-5641-B	LC276285	LC276321	PT-239
<i>Asteronyx loveni</i>	Off Miyako, Iwate	NSMT E-5641-C	-	LC276322	PT-240
<i>Asteronyx loveni</i>	Off Miyako, Iwate	NSMT E-5641-D	LC276286	LC276323	PT-241
<i>Asteronyx loveni</i>	Off Miyako, Iwate	NSMT E-5641-E	-	LC276324	PT-242
<i>Asteronyx loveni</i>	Off Miyako, Iwate	NSMT E-5638-A	LC276278	LC276308	PT-213
<i>Asteronyx loveni</i>	Off Miyako, Iwate	NSMT E-5638-B	-	LC276352	PT-306
<i>Asteronyx loveni</i>	Off Miyako, Iwate	NSMT E-5638-D	-	LC276357	PT-323
<i>Asteronyx loveni</i>	Off Miyako, Iwate	NSMT E-5638-E	-	LC276356	PT-320
<i>Asteronyx loveni</i>	Off Miyako, Iwate	NSMT E-5637-A	-	LC276310	PT-215
<i>Asteronyx loveni</i>	Off Miyako, Iwate	NSMT E-5637-B	LC276281	LC276314	PT-220
<i>Asteronyx loveni</i>	Shima Spur, Mie	NSMT E-6360	-	LC276302	PM-199
<i>Asteronyx loveni</i>	Shima Spur, Mie	NSMT E-6983	LC276280	LC276312	PM-218
<i>Asteronyx loveni</i>	Shima Spur, Mie	NSMT E-6983	-	LC276347	PM-290
<i>Asteronyx loveni</i>	Shima Spur, Mie	NSMT E-6982	-	LC276309	PM-214
<i>Asteronyx loveni</i>	Off Tosa, Kochi	NSMT E-1143-A	-	LC276318	PK-231
<i>Asteronyx loveni</i>	East China Sea, west of Japan	NSMT E-6986-A	LC276273	LC276298	ECS-195
<i>Asteronyx loveni</i>	East China Sea, west of Japan	NSMT E-6986-C	LC276272	LC276297	ECS-194
<i>Asteronyx reticulata</i>	East of Hiraji Bank, Nagasaki	NSMT E-6912	-	LC276355	ECS-316
<i>Asteronyx reticulata</i>	East of Hiraji Bank, Nagasaki	NSMT E-6915	-	LC276338	ECS-272
<i>Asteronyx reticulata</i>	East of Hiraji Bank, Nagasaki	NSMT E-7016	-	LC276301	ECS-198
<i>Asteronyx reticulata</i>	East of Naka-Kasayama Bank, Nagasaki	NSMT E-6908-C	-	LC276293	ECS-190
<i>Asteronyx reticulata</i>	East of Naka-Kasayama Bank, Nagasaki	NSMT E-6908-D	LC276271	LC276296	ECS-193
<i>Asteronyx reticulata</i>	East of Naka-Kasayama Bank	NSMT E-6931	LC276279	LC276311	ECS-217
<i>Asteronyx reticulata</i>	West of Gajajima Isl. Kagoshima	NSMT E-6354	-	LC276305	ECS-204
<i>Asteronyx reticulata</i>	East of Hiraji Bank, Nagasaki	NSMT E-6910	-	LC276300	ECS-197
<i>Asteronyx reticulata</i>	East of Hiraji Bank, Nagasaki	NSMT E-6911	-	LC276294	ECS-191
<i>Asteronyx reticulata</i>	East of Hiraji Bank, Kagoshima	NSMT E-6926	-	LC276342	ECS-280

Species	Locality	Voucher number	CO1	16S	Code from Okanishi et al. (2018)
<i>Asteronyx reticulata</i>	East of Hiraji Bank, Kagoshima	NSMT E-6929	-	LC276304	ECS-203
<i>Asteronyx reticulata</i>	West off Takarajima Isl.	NSMT E-6355	LC276274	LC276299	ECS-196
<i>Asteronyx reticulata</i>	West of Amami Ohshima Isl., Kagoshima	NSMT E-6351-A	-	LC276325	ECS-243
<i>Asteronyx reticulata</i>	West of Amami Ohshima Isl., Kagoshima	NSMT E-6942-B	-	LC276339	ECS-274
<i>Asteronyx reticulata</i>	West of Ensei Knoll, Kagoshima	NSMT E-6921	-	LC276349	ECS-294
<i>Asteronyx reticulata</i>	West of Ensei Knoll, Kagoshima	NSMT E-6922-A	LC276287	LC276328	ECS-249
<i>Asteronyx reticulata</i>	West of Ensei Knoll, Kagoshima	NSMT E-6925-A	-	LC276326	ECS-247
<i>Asteronyx reticulata</i>	West of Ensei Knoll, Kagoshima	NSMT E-6925-B	-	LC276327	ECS-248
<i>Asteronyx reticulata</i>	East China Sea, west of Japan	NSMT E-7001	LC276276	LC276306	ECS-205
<i>Asteronyx reticulata</i>	East China Sea, west of Japan	NSMT E-7002	LC276277	LC276307	ECS-206
<i>Asteronyx reticulata</i>	Off Amami Ohshima Isl. Kagoshima	NSMT E-6352	-	LC276315	ECS-223
<i>Asteronyx reticulata</i>	West of Minami-Ensei Knoll, Kagoshima	NSMT E-6916	-	LC276345	ECS-286
<i>Asteronyx reticulata</i>	West of Minami-Ensei Knoll, Kagoshima	NSMT E-6923-A	-	LC276340	ECS-278
<i>Asteronyx reticulata</i>	West of Minami-Ensei Knoll, Kagoshima	NSMT E-6923-B	LC276275	LC276303	ECS-202
<i>Asteronyx reticulata</i>	East China Sea, west of Japan	NSMT E-7003-A	-	LC276351	ECS-303
<i>Asteronyx reticulata</i>	East China Sea, west of Japan	NSMT E-7003-B	-	LC276346	ECS-288
<i>Asteronyx reticulata</i>	East China Sea, west of Japan	NSMT E-7000-A	-	LC276348	ECS-291
<i>Asteronyx reticulata</i>	West of Minami-Ensei Knoll, Kagoshima	NSMT E-6920	LC276270	LC276295	ECS-192
<i>Asteronyx reticulata</i>	Off Iejima Isl., Okinawa	NSMT E-6987	-	LC276313	ECS-219
<i>Asteronyx</i> sp.	Between Yakushima Isl and Tanegashima Isl., Kagoshima	NSMT E-3157-B	LC276283	LC276319	PSW-237
<i>Asteronyx luzonicus</i>	South China Sea	IDSSE-EEB-SW0003	MZ198757	MZ203265	-
<i>Astrodia abyssicola</i>	Miyagi, off Onahama	NSMT E-6257	AB758828	AB605077	-
<i>Astrodia abyssicola</i>	Philippine Sea, KPR Seamount	RSIO68002	OP328783	OP325293	-
<i>Astrodia duospina</i> sp. nov.	Philippine Sea, KPR Seamount	RSIO59012	OP328780	OP325290	-
<i>Astrodia duospina</i> sp. nov.	Northwest Pacific, Ko-Hakucho-Guyot Seamount	RSIO61068	OP328781	OP325291	-
<i>Astrodia duospina</i> sp. nov.	Northwest Pacific, RB Seamount	RSIO61069	OP328782	OP325292	-
<i>Asteroschema ajax</i>	Off Lord Howe Isl.	MV F99759	AB758762	AB605078	-
<i>Asteroschema clavigerum</i>	North Atlantic	haplotype 1	HM587850	HM587828	-

Results and discussion

Systematics

Class Ophiuroidea Gray, 1840

Order Euryalida Lamarck, 1816

Family Asteronychidae Ljungman, 1867

Genus *Astrodia* Verrill, 1899

Astrodia duospina sp. nov.

<https://zoobank.org/FC14B3BB-E9BB-4E61-A959-266A0CA733C8>

Figs 2–7

Material examined. Holotype: CHINA • 1 specimen; Northwest Pacific, Nazimov Guyot; 15°11.34'N, 162°49.26'E; depth 2713 m; 16 September 2020; collected by ROV HAILONG III; preserved in alcohol; RSIO61068. **Paratypes:** CHINA • 1 specimen; Northwest Pacific, Nazimov Guyot; 15°11.34'N, 162°49.26'E; depth 2713 m; 16

September 2020; collected by ROV HAILONG III; preserved in alcohol; RSIO61069 • 1 specimen; Northwest Pacific, Caiwei Guyot; 15°40.61'N, 154°53.77'E; depth 2744 m; 7 September 2013; collected by HOV JIAOLONG; preserved in alcohol; RSIO31004 • 1 specimen; the Philippine Sea, Kyushu-Palau Ridge, Roischesar Peak; 13°20.85'N, 134°32.81'E; depth 1900–2000 m; 2 August 2020; collected by ROV HAILONG IV; preserved in alcohol; RSIO59012.

Diagnosis. Disc raised high above the arm. Aboral disc with plate-shaped external ossicles in the center and on the periphery. Radial shield narrow, longer than wide. Teeth triangular, oral papillae indistinct or underdeveloped. Genital slits short, approximately one-fourth of the height of the disc. Lateral arm plates crescent and not projecting on arms. Arm spines no more than two.

Description of holotype. Disc pentagonal, notched interradial edges, 14 mm in diameter, 4.7 mm in height. Aboral surface almost flat, slightly depressed in the center, entirely covered by thickened skin with plate-shaped external ossicles in the center, about 220 μm long (Fig. 3A). Peripheral disc covered with a few plate-shaped external ossicles, similar to those in the center but larger, approximately twice in length. Radial

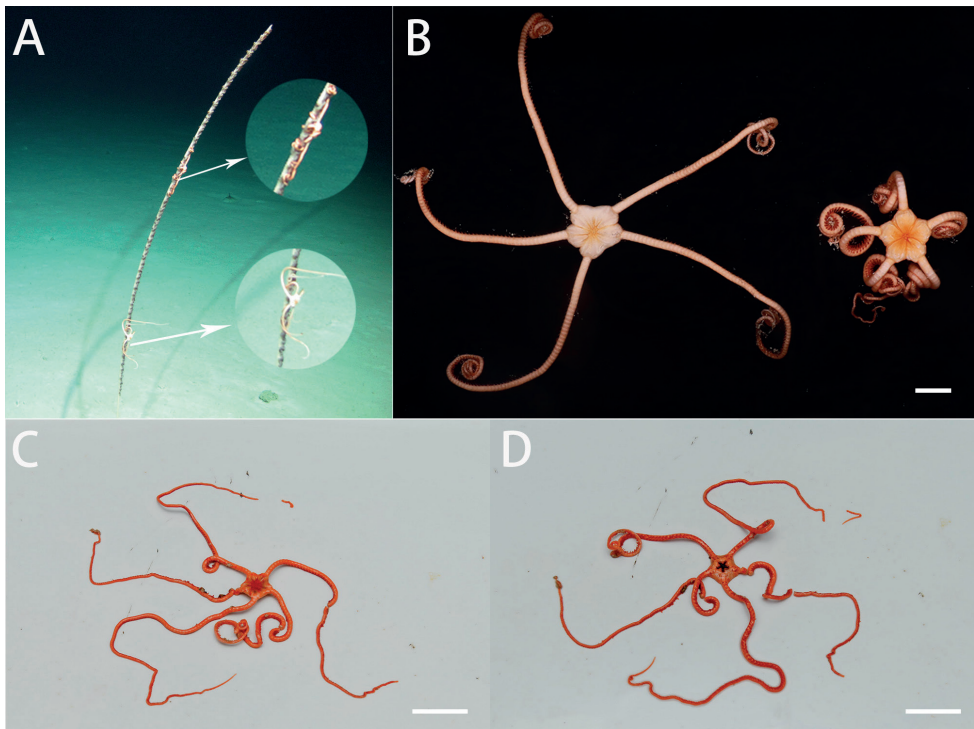


Figure 2. In situ and on-board photos of *Astrodia duospina* sp. nov. **A** photo in situ (RSIO61068: the individual below, RSIO61069: the individual above, attached to an unidentified sea pen species) **B** photo on board (RSIO61068: the individual on the left, RSIO61069: the individual on the right) **C**, **D** photos on board (RSIO31004), aboral side (**C**), oral side (**D**). Scale bars: 10 mm (**B**); 20 mm (**C**, **D**).

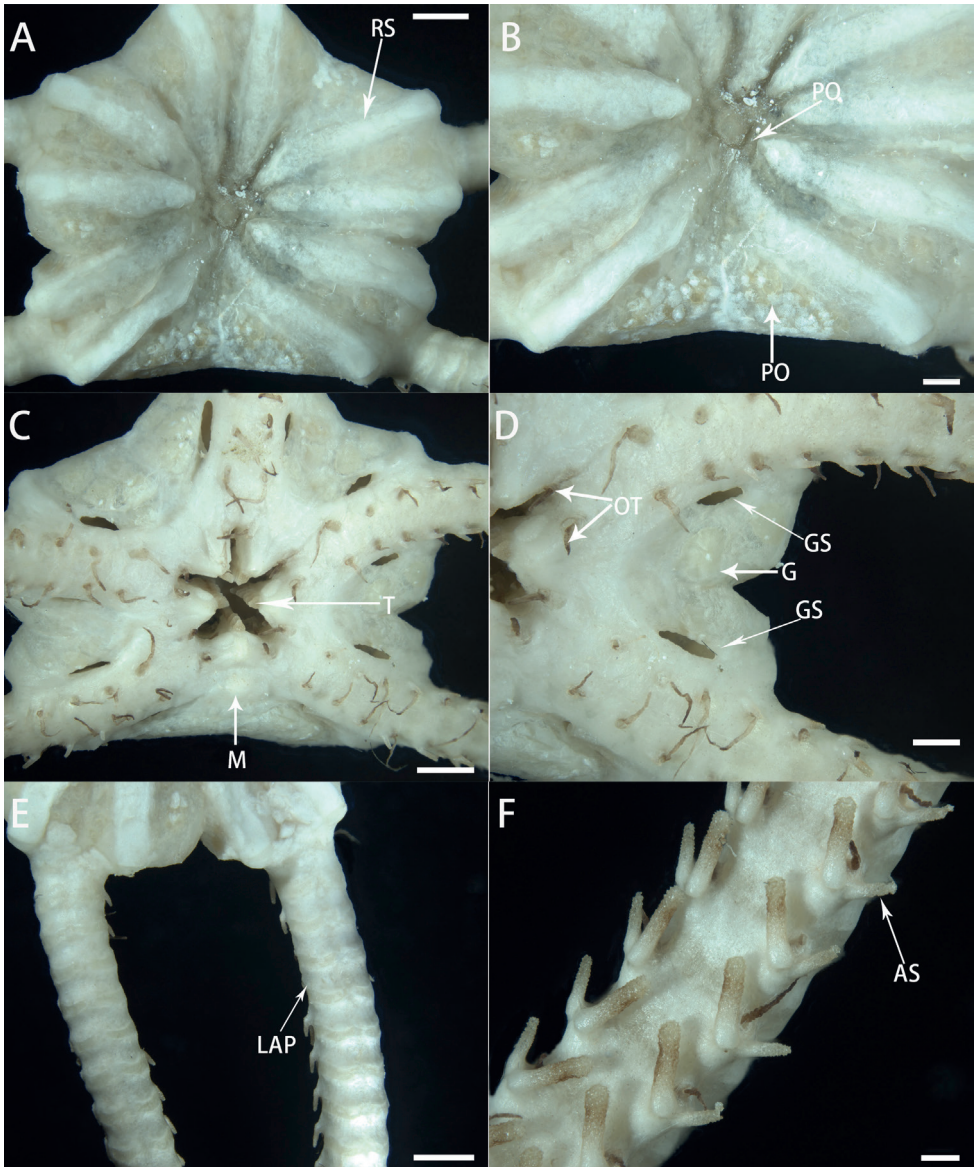


Figure 3. Morphological characters of *Astrodia duospina* sp. nov. (holotype: RSIO61068) **A** aboral view of the disc **B** periphery of the aboral disc **C** oral view of the disc **D** genital slits **E** aboral view of the arms **F** arms spines. Abbreviations: **RS** radial shield; **PO** plate-shaped ossicle; **M** madreporite; **T** teeth; **OT** oral tentacle; **GS** genital slit; **G** gonad; **LAP** lateral arm plate; **AS** arm spine. Scale bars: 2 mm (**A, C, E**); 1 mm (**B, D**); 0.5 mm (**F**).

shields narrow, tumid, bar-like, without granules or spines, and almost reach center of disc (Fig. 3A, B). Approximately 7.2 mm long and 550 μ m wide in the center and 1.1 mm wide at periphery.

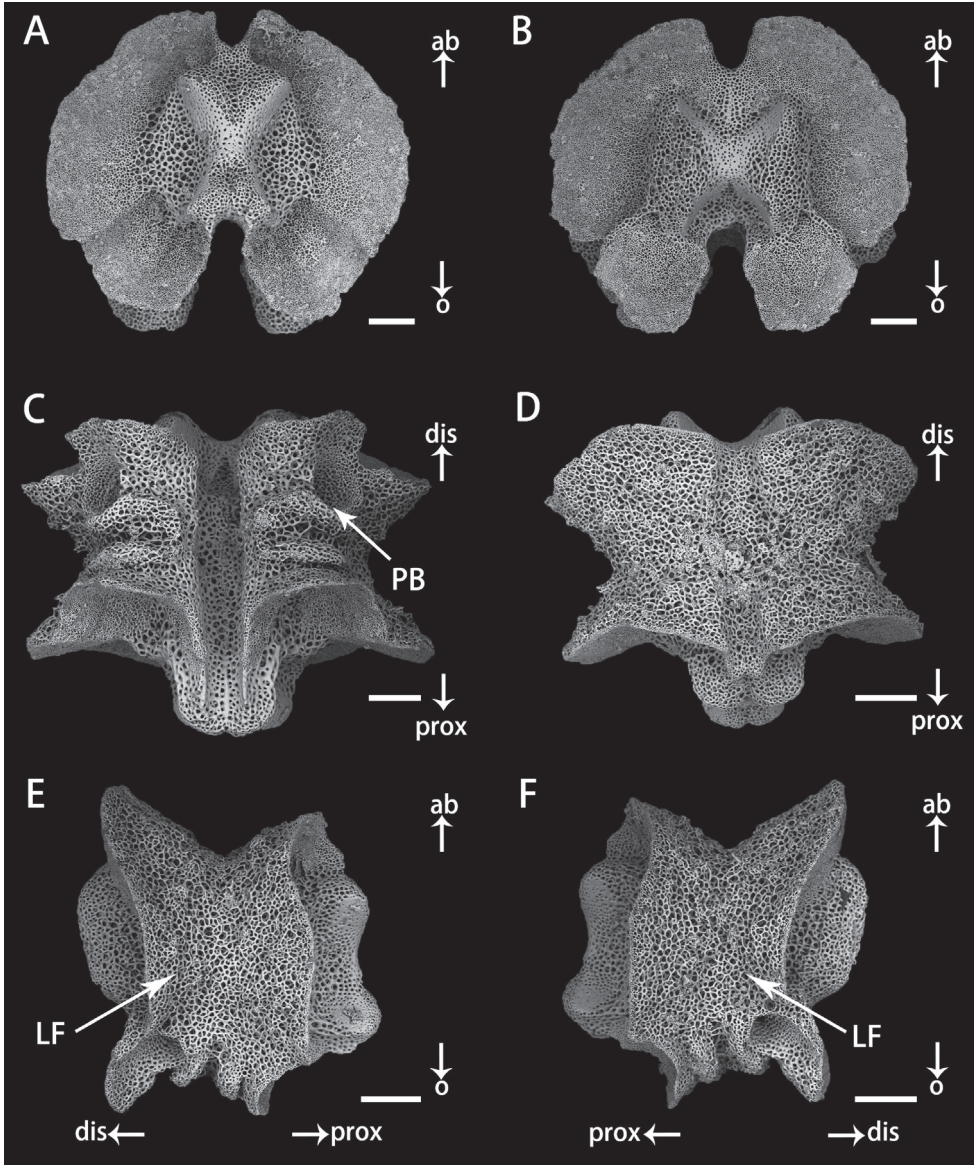


Figure 4. Vertebrae in basal arm of *Astrodia duospina* sp. nov. (holotype: RSIO61068) **A** proximal view **B** distal view **C** oral view **D** aboral view **E, F** lateral view. Abbreviations: **PB** podial basin; **LF** lateral furrow. Scale bars: 200 μ m (**A–F**).

Oral surface flat, covered by thickened skin. Oral shield small to invisible, one madreporite. Adoral shield obscured by skin (Fig. 3C). Oral interradial surface covered with several plate-shaped external ossicles (Fig. 3C). Six teeth, triangular, forming vertical row on dental plate, each jaw covered by a pair of conical oral tentacles (Fig. 3C). Oral papillae invisible or underdeveloped. Two genital slits, small, about 1/4 as long of

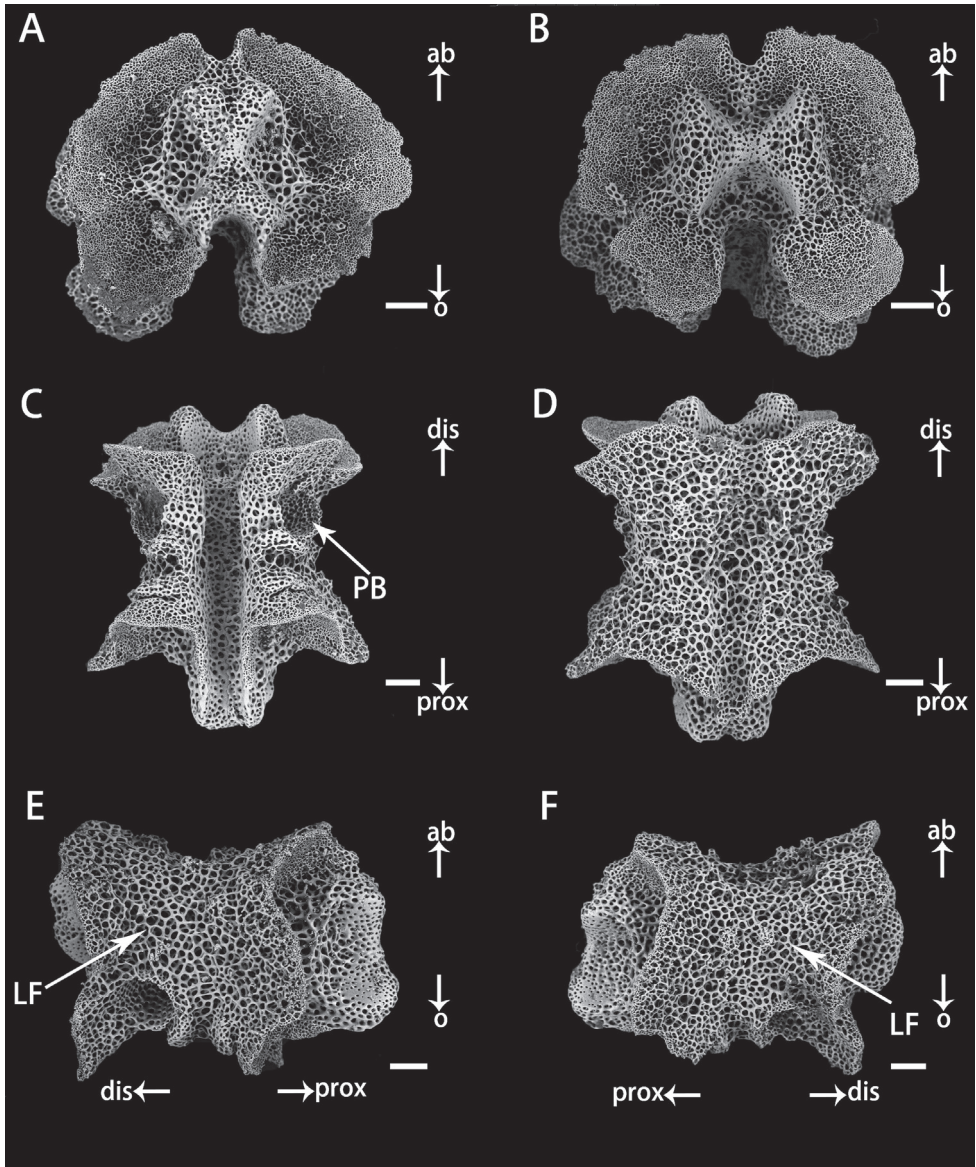


Figure 5. Vertebrae in distal arm of *Astrodia duospina* sp. nov. (holotype: RSIO61068) **A** proximal view **B** distal view **C** oral view **D** aboral view **E, F** lateral view. Abbreviations: **PB** podial basin; **LF** lateral furrow. Scale bars: 100 μ m (**A–F**).

disc height (1.3 mm long and 260 μ m wide), present on oral side of each interradius (Fig. 3D). Gonads visible on each interradius (Fig. 3C, D).

Five arms, long and slender, about eight to nine times as long as disc diameter, no abrupt change in width basally (Fig. 3E). Proximal segments 2.5 mm wide and 1.7 mm high, with arched aboral surface and flattened oral surface (Fig. 3E), gradually tapering

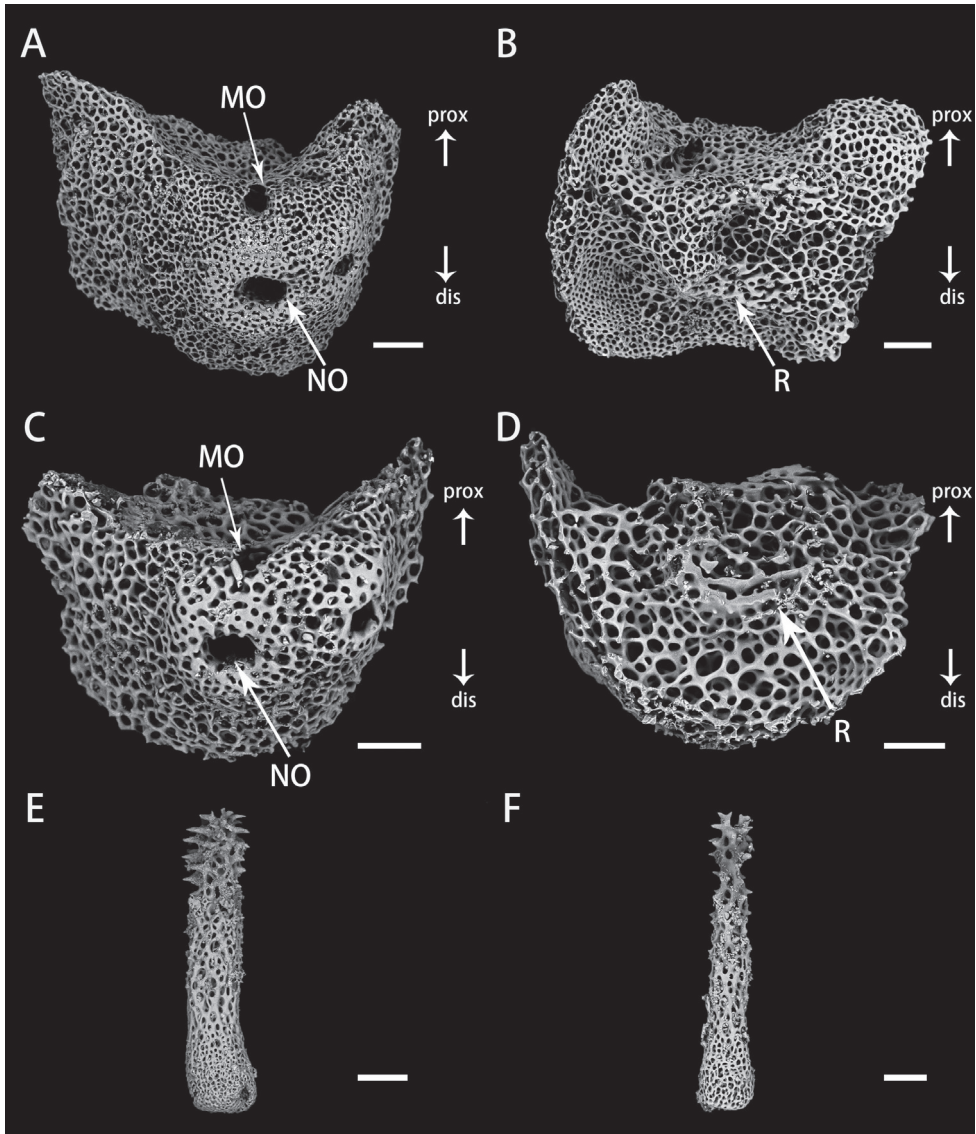


Figure 6. Lateral arm plates and arm spines of *Astrodia duospina* sp. nov. (holotype: RSIO61068) **A, B** lateral arm plates from proximal arm, outer view (**A**), inner view (**B**) **C, D** lateral arm plates from distal arm, outer view (**C**), inner view (**D**) **E, F** arm spines from proximal (**E**) and distal arm (**F**). Abbreviations: **MO** muscle opening; **NO** nerve opening; **R** ridge. Scale bars: 200 μm (**E**); 100 μm (**F**); 90 μm (**A, B**); 60 μm (**C, D**).

toward tip. Arm spines only present on ventral side. First to fourth tentacle pores with one arm spine and following tentacle pores with two arm spines. Outer arm spines slightly shorter than inner ones at proximal segments, but only three-fifths as long as inner spines on middle and distal segments (Fig. 3F).

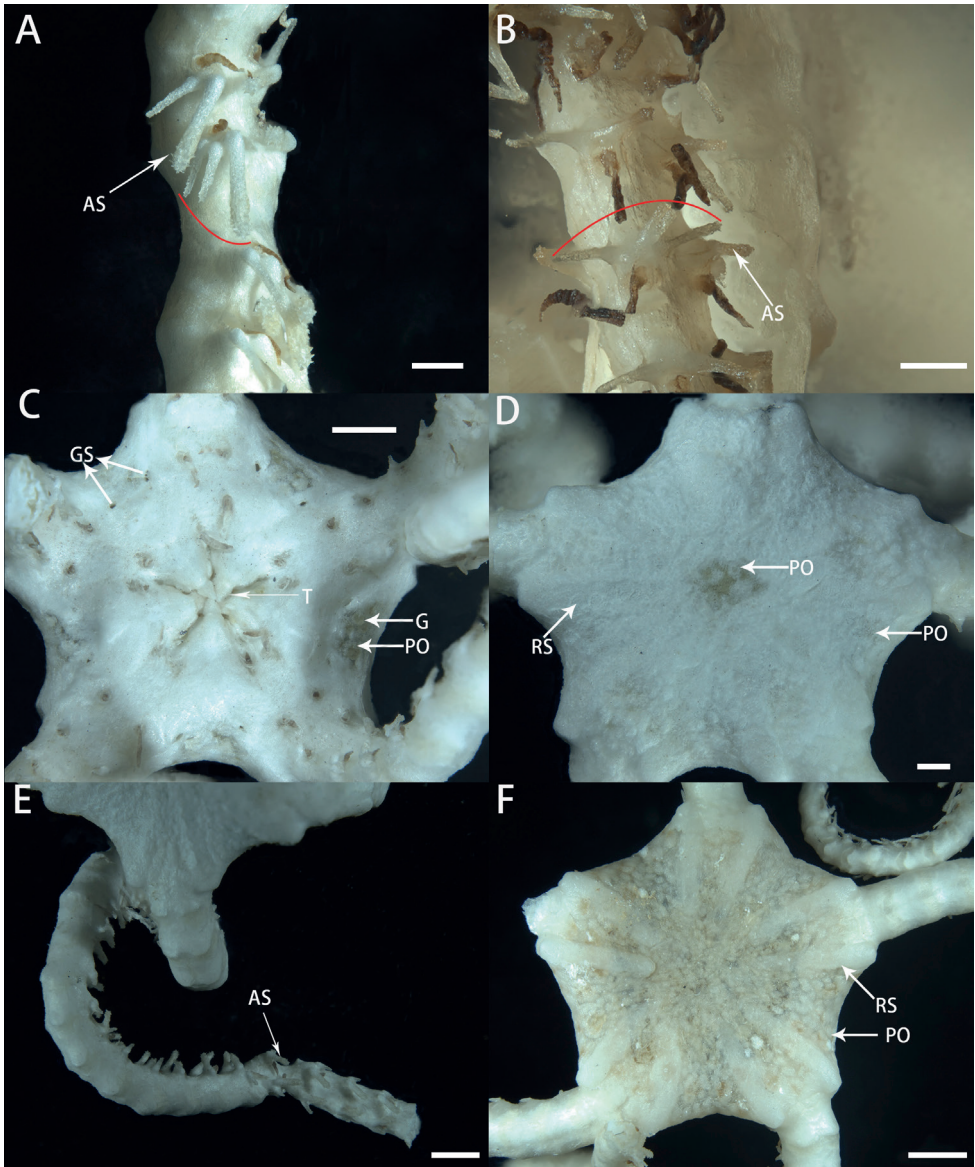


Figure 7. Morphological characters of paratypes of *Astrodia duospina* sp. nov. **A** arm spines of RSIO31004 **B** arm spines of RSIO61069 **C–E** pictures of RSIO59012, oral disc (**C**), aboral disc (**D**), arm and arm spines (**E**) **F** aboral disc of RSIO31004. These specimens have exceptionally three arm spines for an arm segment (shown by an arc in A and B). Abbreviations: **AS** arm spine; **T** teeth; **PO** plate-shaped ossicle; **GS** genital slit; **G** gonad; **RS** radial shield. Scale bars: 2 mm (**F**); 1 mm (**C, E**); 0.5 mm (**A, B, D**).

Color. Pink in situ, white in alcohol (Fig. 2).

Ossicle morphology of holotype. Vertebrae articulation streptospondylous, wider than long in proximal segments (Fig. 4A, B), longer than wide in distal segments (Fig. 5A, B). Oral side of each vertebra with longitudinal groove along midline,

deeply depressed, and no oral bridge (Figs 4C, 5C). Pair of podial basins on oral side moderate in size (Figs 4C, 5C). Aboral side of each arm vertebra with longitudinal aboral groove, moderately depressed (Figs 4D, 5D). Lateral furrow of vertebrae declining obliquely from aboral to oral side (Figs 4E–F, 5E–F). Lateral arm plates crescent-shaped, each associated with one or two arm spines and spine articulations with nerve and muscle opening separated. Spine articulation bulges outward (Fig. 6A, C). A ridge on inner side of lateral arm plate, parallel to proximal edge (Fig. 6B, D). Arm spines cylindrical, never hooked, bearing fine thorns at tip throughout arms (Figs 3F, 6E–F).

Description of paratypes. Two paratypes (RSIO31004, RSIO61069) share the same morphological characteristics as the holotype, disc diameter 10.17 and 13.94 mm, about 1/10 and 1/9 as wide as the length of the arms, respectively. However, the radial shields of RSIO31004 are shorter than the radial shields of the holotype and of

RSIO61069 (Fig. 7F). Three arm spines exceptionally occurred only once in both paratypes (RSIO31004 and RSIO61069), the innermost arm spine of RSIO61069 is the longest and the stoutest, while the middle arm spine of RSIO31004 is the stoutest. (Fig. 7A, B). The other paratype (RSIO59012) is smaller, only 6 mm in disc diameter, about 1/3 as wide as the length of the arms and may be a juvenile of this species. The radial shields and the genital slits are much shorter than in the other three specimens (Fig. 7C, D). Likewise, the arm spines are shorter than one segment (Fig. 7E)

Etymology. The species name *duo* is derived from the Latin numeral word, meaning two, and Latin feminine noun, *spina*, meaning spine, referring to the presence of no more than two arm spines throughout the arm.

Remarks. This new species falls within the genus *Astrodia* by only possessing cylindrical unhooked arm spines. The new species resembles *Astrodia abyssicola* mostly by having plate-shaped external ossicles on the aboral disc and crescent-shaped lateral arm plates. However, the oral papillae are indistinct or underdeveloped in *Astrodia duospina*, which can be used to distinguish the two species from each other (Fig. 3D). Moreover, the genital slits are very short in *Astrodia abyssicola*, which are only one-fifth of the height of the disc, while *Astrodia duospina* has larger genital slits, being longer than one-fourth the height of the disc (Fig. 3C). *Astrodia duospina* can easily be distinguished from *A. plana* and *A. excavata* by external ossicles and lateral arm plates. External ossicles are plate-shaped on the aboral surface of the disc in *Astrodia duospina* (Fig. 3A, B), but are absent in *A. plana*. Lateral arm plates are not projecting in the new species (Fig. 3E), but are distinctly projecting from the oral surface of the arm in *A. excavata*. Additionally, the new species differs from *A. tenuispina* by having distinctly smaller genital slits (Figs 3C, 7C).

Astrodia tenuispina is a widely distributed species and was characterized by having slender unhooked arm spines, small and short oral papillae, separated genital slits (Verrill 1884). Baker (1980) compared specimens from south of Australia and the northwest Atlantic, described this species with 2 or 3 arm spines, and imbricating punctate scales on the disc surface. Okanishi and Fujita (2014) redescribed this species as with plate-shaped external ossicles on the periphery of the aboral disc, granule-shaped on the central disc, genital slits half of the height of the disc, lateral arm plates

not projecting. According to these descriptions, *A. duospina* sp. nov. can be differentiated from *A. tenuispina* by having smaller genital slits and indistinct oral papillae. Furthermore, in two of the three large specimens of the new species, three arm spines were observed exceptionally at one arm segment (Fig. 7A, B), while the other three species possess three arm spines at several successive segments in the middle part of the arms. Since only a small number of specimens were examined, this characteristic was not used to distinguish the new species from its congeners, and more specimens should be examined before a robust result can be achieved.

Astrodia abyssicola (Lyman, 1879)

Figs 8–12

Ophiocreas abyssicola Lyman, 1879: 64–65, plate 17, figs 470–473.

Astrodia abyssicola: Okanishi and Fujita 2014: 188–192, figs 2–4.

Material examined. CHINA • 1 specimen; Philippine Sea, Kyushu-Palau Ridge, Mugiboshi Seamount; 16.57.14'N, 134.52.7'E; depth 3225 m; 11 August 2021; collected by an HOV JIAOLONG; preserved in alcohol; RSIO68002.

Description. Disc pentagonal and almost flat, 10 mm in diameter, 3.2 mm in height, skin wrinkled under dry conditions (Fig. 9A, B). Aboral surface of disc lacks external ossicles (Fig. 9A, B). Radial shields narrow, slightly tumid, bar-like, with-

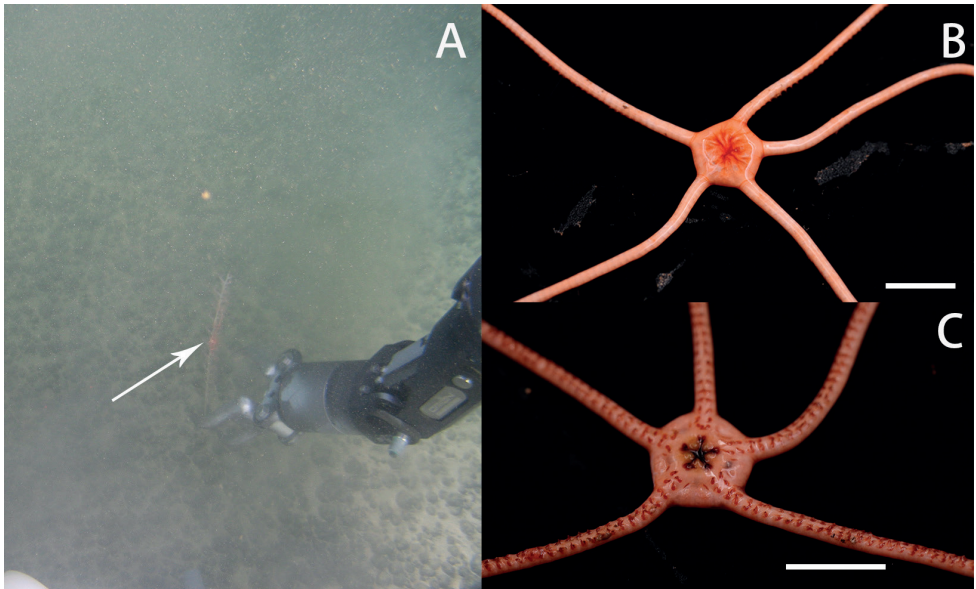


Figure 8. In situ and on-board photos of *Astrodia abyssicola* **A** photo in situ (RSIO68002, attached to an unidentified sea pen species) **B, C** photos on board (RSIO68002), aboral side (**B**), oral side (**C**). Scale bars: 10 mm (**B, C**).

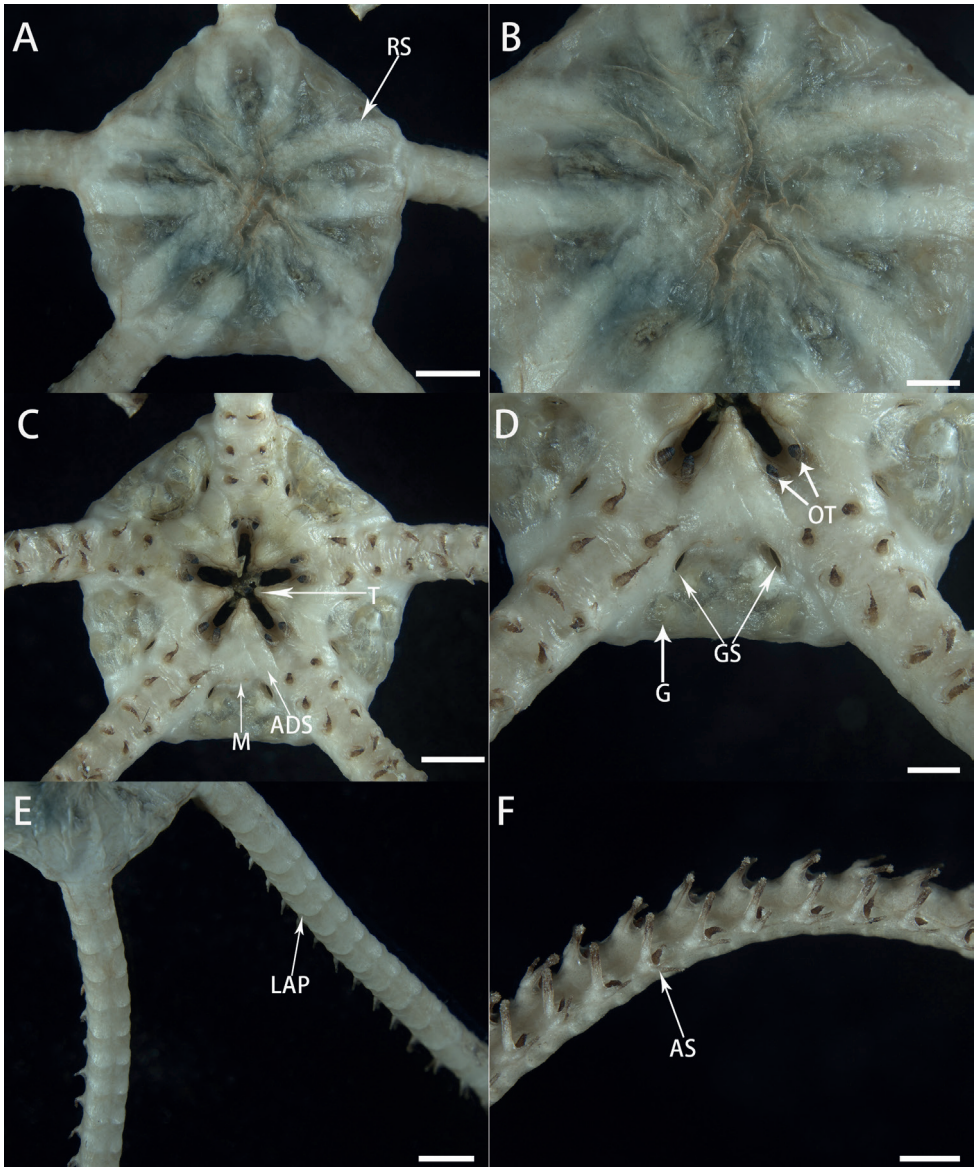


Figure 9. Morphological characters of *Astrodia abyssicola* (RSIO68002) **A** aboral view of the disc **B** center of the aboral disc **C** oral view of the disc **D** genital slits **E** aboral view of the arms **F** arms spines. Abbreviations: **RS** radial shield; **M** madreporite; **T** teeth; **ADS** adoral shield; **OT** oral tentacle; **GS** genital slit; **G** gonad; **LAP** lateral arm plate; **AS** arm spine. Scale bars: 2 mm (**A, C, E**); 1 mm (**B, D, F**).

out granules or spines, and almost reaching center of disc. (Fig. 9A). Approximately 3.8 mm long and 0.6 mm wide in center and 0.8 mm wide on periphery (Fig. 9A).

Oral surface flat, covered by thin skin, and lacking external ossicles (Fig. 9C). Oral shield triangular, one madreporite (Fig. 9D). Adoral shield big and thick, quadrangular, and longer than wide (Fig. 9D). Teeth spearhead-shaped, vertically on dental plate;

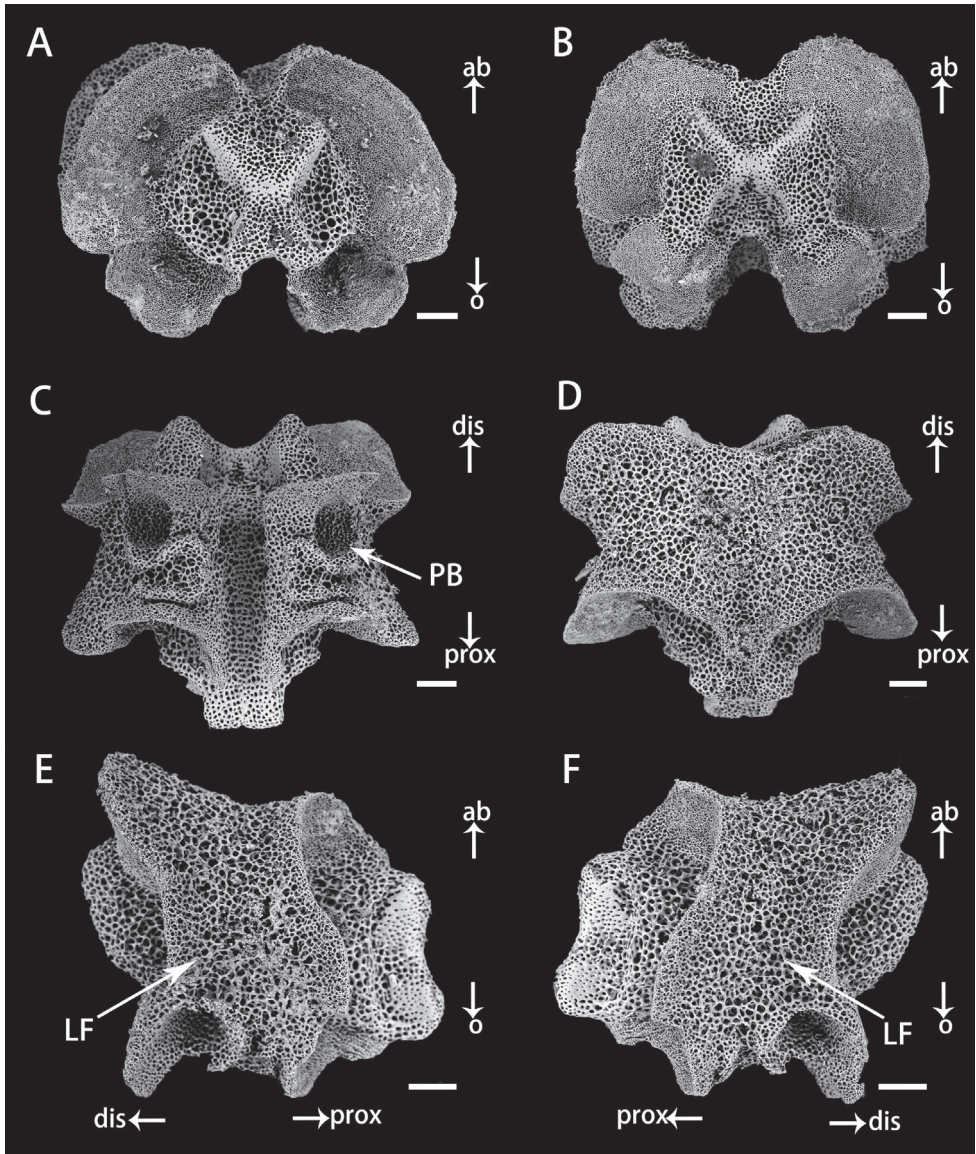


Figure 10. Vertebrae in basal arm of *Astrodia abyssicola* (RSIO68002) **A** proximal view **B** distal view **C** oral view **D** aboral view **E, F** lateral view. Abbreviations: **PB** podial basin; **LF** lateral furrow. Scale bars: 150 μm (**A–F**).

each jaw bears a pair of short, conical oral tentacles (Fig. 9C). Oral papillae indistinct or underdeveloped (Fig. 9C). Two genital slits very short, 560 μm long and 110 μm wide, present on oral side of each interradius. Gonads visible in each interradius (Fig. 9D).

Five arms, long and slender, about nine to ten times as long as disc diameter, no abrupt change in width basally (Fig. 9E). Proximal portion of arm 1.8 mm wide and 420 μm high, with arched aboral surface and flattened oral surface. Arms tapering

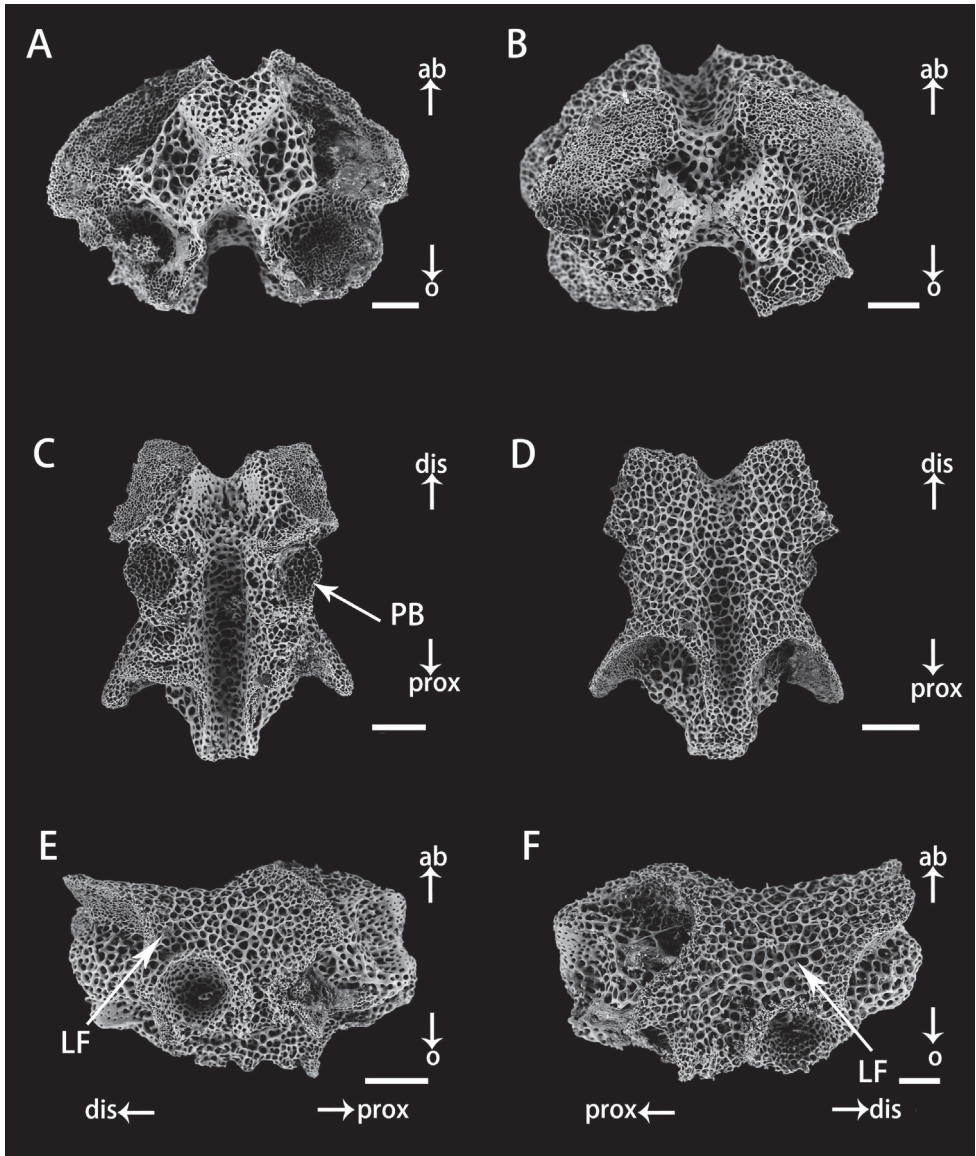


Figure 11. Vertebrae in distal arm of *Astrodia abyssicola* holotype: RSIO68002) **A** proximal view **B** distal view **C** oral view **D** aboral view **E, F** lateral view. Abbreviations: PB podial basin; LF lateral furrow. Scale bars: 150 μm (**C, D, E**); 90 μm (**A, B, F**).

gradually toward tip. Arm spines only present in ventral part of arm. First to third tentacle pores without arm spines, fourth tentacle pores with one arm spine and following tentacle pores with two arm spines. Inner arm spines longer than outer arm spines. On middle and distal part of arm, outer arm spines three-fourths as long as inner spines (Fig. 9F). Three arm spines occurred once in two of the five arms. Lateral arm plates not projecting on arms.

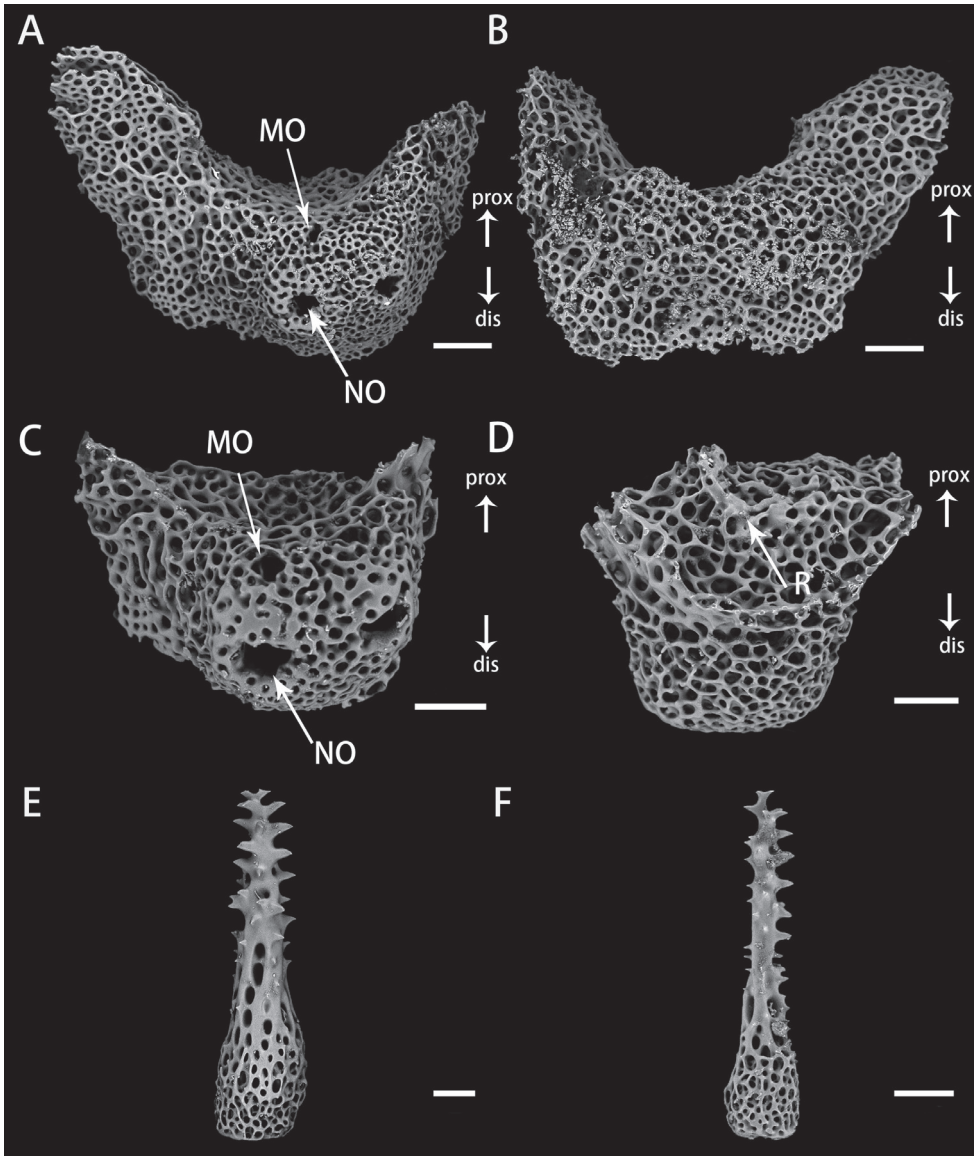


Figure 12. Lateral arm plates and arm spines of *Astrodia abyssicola* (RSIO68002) **A, B** lateral arm plates from the proximal arm, outer view (**A**), and inner view (**B**) **C, D** lateral arm plates from the distal arm, outer view (**C**), and inner view (**D**) **E, F** arm spines from proximal (**E**) and distal (**F**). Abbreviations: MO muscle opening; NO nerve opening; R ridge. Scale bars: 90 μm (**A, B, F**); 60 μm (**C, D, E**).

Color. Bright pink in situ, entirely white in alcohol (Fig. 8B, C).

Ossicle morphology. Vertebrae articulation streptospondylous, wider than long in proximal segments (Fig. 10A, B), longer than wide in distal segments (Fig. 11A, B). Oral side of each vertebra with longitudinal groove along midline, deeply depressed, and no oral bridge (Figs 10C, 11C). Pair of podial basins on oral side moderate

in size (Figs 10C, 11C). Aboral side of each arm vertebra with longitudinal aboral groove, moderately depressed (Figs 10D, 11D). Lateral furrow of vertebrae declining obliquely from aboral to oral side (Figs 10E, F, 11E, F). Lateral arm plates crescent-shaped, each associated with one or two arm spines. Spine articulations with separated nerve and muscle openings, bulging outwards (Fig. 12A, C). A ridge on inner side of lateral arm plate (Fig. 12D). Arm spines cylindrical, never hooked, bearing fine thorns at apex throughout arms (Fig. 12E, F).

Remarks. *Ophiocreas abyssicola* was first described by Lyman (1879). Okanishi and Fujita (2014) transferred *O. abyssicola* to the genus *Astrodia* and redescribed it. This specimen (RSIO68002) was identical to *Astrodia abyssicola* by having 0–2 arm spines, rather short genital slits and crescent-shaped lateral arm plates. However, this specimen lacks external ossicles on the disc and arms, which is different from previous descriptions of *Astrodia abyssicola* by Okanishi and Fujita (2014) as having plate-shaped external ossicles on the periphery. Nevertheless, the genetic distance of COI and 16S (2.9% and 1.9%) between the new collected specimen and *A. abyssicola* are too small to justify two different species. Therefore, this specimen was identified as *A. abyssicola*, thus the external ossicles on the aboral surface of the disc could be plate-shaped or absent in this species.

Key morphological characters to the species of *Astrodia*

The key morphological characters among the five species from the genus *Astrodia* based on Okanishi and Fujita (2014) were revised in this study (Table 3). Three diagnostic characteristics were proposed by Okanishi and Fujita (2014) in their key for *Astrodia*: the length of the genital slits related to the height of the disc, external ossicles on the aboral disc surface, and shape and existence of projections of lateral arm plates. All three characteristics were useful to distinguish the new species from its congeners. The external ossicle, being absent in the *A. abyssicola* specimen examined in the present study but present and plate-shaped in the previous descriptions (Okanishi and Fujita 2014), might be an intraspecific variation. Additionally, we added two morphological characters, the number of arm spines and the shape of oral papillae, as key characters for interspecific discrimination of *Astrodia*. *Astrodia abyssicola* is the only species that possesses no more than two arm spines along their arms, whereas the other four species possess up to three arm spines or occasionally four. Furthermore, oral papillae are indistinct or underdeveloped in *A. duospina* sp. nov., but are domed granule-shaped in the four known species. Thus, we consider the number of arm spines and the shape and existence of oral papillae important characteristics for interspecific discrimination within *Astrodia* (Table 3).

Molecular phylogenetic analysis

Based on the COI (583–1511 bp) and 16S (431–539 bp) sequences, the phylogenetic relationship of the two genera, *Astrodia* and *Asteronyx*, was inferred. The ML tree based on the concatenated 16S and COI sequences suggested that both *Astrodia* and *Asteronyx* were monophyletic with high bootstrap values (Fig. 13, Suppl. material 1: Fig. S1). The ML tree based on COI sequences was consistent with the tree generated

Table 3. Comparison of key morphological characters among species in the genus *Astrodia*.

Species	Arm spines	Genital slits	External ossicles	Lateral arm plates on middle to distal portion of arms	Oral papillae	Reference
<i>Astrodia abyssicola</i> (Lyman, 1879)	0–2	very short, ~1/5 (height of disc)	plate-shaped on periphery	shapes: crescent; projections: absent	domed granule-shaped	Lyman (1879), Okanishi and Fujita (2014), This study
<i>Astrodia excavata</i> (Lütken & Mortensen, 1899)	0–3	large, ~2/3 (height of disc)	granule-shaped near radial shields and genital slits	shapes: bar-like; projections: present	domed granule-shaped	Lütken and Mortensen (1899), Okanishi and Fujita (2014)
<i>Astrodia plana</i> (Lütken & Mortensen, 1899)	0–3	short, ~1/4 (height of disc)	absent	shapes: oblong; projections: absent	domed granule-shaped	Lütken and Mortensen (1899), Döderlein (1927), Okanishi and Fujita (2014)
<i>Astrodia tenuispina</i> (Verrill, 1884)	0–3, occasionally 4	short, ~1/2 (height of disc)	plate-shaped on periphery, granule-shaped in center	shapes: unknown; projections: absent	domed granule-shaped, small and short	Verrill (1884), Koehler (1906), Koehler (1922), Baker (1980), Gage et al. (1983), Manso (2010), Okanishi and Fujita (2014)
<i>Astrodia duospina</i> sp. nov.	0–2, occasionally 3	short, ~1/4 (height of disc)	plate-shaped on periphery and in center	shapes: crescent; projections: absent	indistinct or underdeveloped	This study

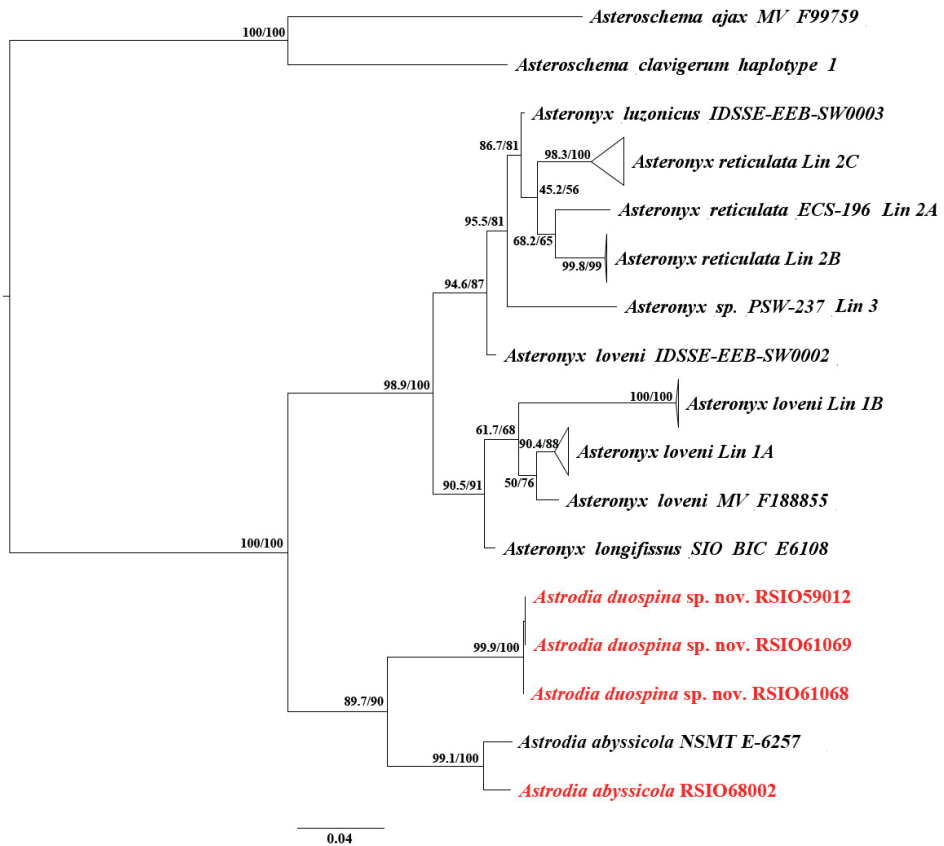


Figure 13. Maximum likelihood tree of the genus *Astrodia* based on concatenated sequences of COI and 16S (clades of Lin 1A, Lin 1B, Lin 2A, Lin 2B, Lin 2C and Lin 3 are from Okanishi et al. (2018), more detailed information about these clades showed in Suppl.materials. Values of each clade: SH-aLRT support (%) / ultrafast bootstrap support (%)).

from two genes (Suppl. material 1: Fig. S2), while in the ML tree based on 16S sequences, *Astrodia abyssicola* clustered with *Asteronyx*, with a low bootstrap value (Suppl. material 3: Fig. S3). Okanishi et al. (2018) suggested that the relationship of the two genera was unclear based on COI and 16S sequences. With newly sequenced DNA data added, our results indicated that the two genera are probably monophyletic. Additionally, the genetic distances of COI and 16S between *A. duospina* sp. nov. and *A. abyssicola* were 9.0% and 9.1%, respectively, supporting the morphological identification results. Molecular analysis also supported that the three specimens identified as *Astrodia duospina* sp. nov. are the same species, and the specimen identified as *Astrodia abyssicola* is closely related to the published sequence of this species with very small genetic distances (2.9% for COI and 1.9% for 16S) that fall into the intra-species genetic distance of Euryalida (Okanishi et al. 2018; Nethupul et al. 2022).

Conclusion

In this study, we described a new species of the genus *Astrodia* collected from seamounts in the West Pacific, and another species (*Astrodia abyssicola*) was redescribed. Through comparing the five species of *Astrodia*, the tabular key of Okanishi and Fujita (2014) was revised and two additional key characteristics, the number of arm spines and the shape of the oral papillae, were identified for interspecific discrimination of *Astrodia*. Maximum likelihood trees supported our morphological results and suggested that both *Astrodia* and *Asteronyx* were monophyletic. This study provided both morphological and molecular information of the two *Astrodia* species, and the specimens reported further expanded the known geological distribution of the genus.

Acknowledgements

We thank all the scientists and crew on the RVs DAYANGYIHAO and XIANGYANG-HONG, and the HAILONG and JIAOLONG team for their great work in the collection of the specimens. We also like to thank Dr Timothy D. O'Hara and Dr Masanori Okanishi and Ruiyan Zhang for their precious advice and kind help. This study was supported by the National Natural Science Foundation of China (42076135), the foundation of China Ocean Mineral Resources R & D Association (No. DY135-E2-2-06).

Reference

- Baker AN (1980) Euryalinid Ophiuroidea (Echinodermata) from Australia, New Zealand, and the south-west Pacific Ocean. *New Zealand Journal of Zoology* 7(1): 11–83. <https://doi.org/10.1080/03014223.1980.10423763>
- Döderlein L (1927) Indopacifische Euryalae. *Adhandlungen der Bayerischen Akademie der Wissenschaften* 31: 1–105. <https://doi.org/10.1515/9783486755459>

- Gage JD, Pearson M, Alisa MC, Paterson GLJ, Tyler PA (1983) Echinoderms of the Rockall Trough and adjacent areas I. Crinoidea, Asteroidea and Ophiuroidea. *Bulletin of the British Museum (Natural History). Zoology* 45: 263–308. <https://doi.org/10.5962/bhl.part.28002>
- Hoang DT, Chernomor O, von Haeseler A, Minh BQ, Vinh LS (2018) UFBoot2: Improving the Ultrafast Bootstrap Approximation. *Molecular Biology and Evolution* 35(2): 518–522. <https://doi.org/10.1093/molbev/msx281>
- Kalyaanamoorthy S, Minh BQ, Wong TKF, von Haeseler A, Jermin LS (2017) ModelFinder: Fast model selection for accurate phylogenetic estimates. *Nature Methods* 14(6): 587–589. <https://doi.org/10.1038/nmeth.4285>
- Koehler R (1906) Description des ophiures nouvelles recueillies par le Travailleur et le Talisman pendant les campagne de 1880, 1881, 1882, & 1883. *Mémoires de la Société Zoologique de France* 19: 6–15.
- Koehler R (1922) Echinodermata Ophiuroidea. Australian Antarctic Expedition 1911–14. Under the leadership of Sir Douglas Mawson, D.Sc., B.E. Scientific reports series C.—. *Zoology and Botany* 8(2): 1–98. <https://doi.org/10.5962/bhl.title.11722>
- Lütken CF, Mortensen T (1899) The Ophiuridae. *Memoirs of the Museum of Comparative Zoology at Harvard College* 23: 97–208. <https://www.biodiversitylibrary.org/item/91713>
- Lyman T (1879) Ophiuridae and Astrophytidae of the “Challenger” expedition. Part II. *Bulletin of the Museum of Comparative Zoology at Harvard College, Cambridge, Mass* 6: 17–83. <https://www.biodiversitylibrary.org/page/31068674#page/27/mode/1up>
- Manso CLC (2010) Deep-water Ophiuroidea (Echinodermata) from off Chile in the Eastern South Pacific. *Biota Neotropica* 10: 185–199. <https://doi.org/10.1590/S1676-06032010000200023>
- Martynov A (2019) Reassessment of the classification of the Ophiuroidea (Echinodermata), based on morphological characters. I. General character evaluation and delineation of the families Ophiomyxidae and Ophiacanthidae. *Zootaxa* 2697(1): 1. <https://doi.org/10.11646/zootaxa.2697.1.1>
- Nethupul H, Stöhr S, Zhang H (2022) Order Euryalida (Echinodermata, Ophiuroidea), new species and new records from the South China Sea and the Northwest Pacific seamounts. *ZooKeys* 1090: 161–216. <https://doi.org/10.3897/zookeys.1090.76292>
- Nguyen L-T, Schmidt HA, von Haeseler A, Minh BQ (2015) IQ-TREE: A Fast and Effective Stochastic Algorithm for Estimating Maximum-Likelihood Phylogenies. *Molecular Biology and Evolution* 32(1): 268–274. <https://doi.org/10.1093/molbev/msu300>
- Okanishi M, Fujita T (2014) A taxonomic review of the genus *Astrodia* (Echinodermata: Ophiuroidea: Asteronychidae). *Journal of the Marine Biological Association of the United Kingdom* 94(1): 187–201. <https://doi.org/10.1017/S0025315413001331>
- Okanishi M, Sentoku A, Martynov A, Fujita T (2018) A new cryptic species of *Asteronyx* Müller and Troschel, 1842 (Echinodermata: Ophiuroidea), based on molecular phylogeny and morphology, from off Pacific Coast of Japan. *Zoologischer Anzeiger* 274: 14–33. <https://doi.org/10.1016/j.jcz.2018.03.001>
- Rodrigues CF, Paterson GLJ, Cabrinovic A, Cunha MR (2011) Deep-sea ophiuroids (Echinodermata: Ophiuroidea: Ophiurida) from the Gulf of Cadiz (NE Atlantic). *Zootaxa* 2754(1): 1. <https://doi.org/10.11646/zootaxa.2754.1.1>
- Sievers F, Higgins DG (2014) Clustal Omega, Accurate Alignment of Very Large Numbers of Sequences. In: Russell DJ (Ed.), *Multiple Sequence Alignment Methods. Methods in*

- Molecular Biology. Humana Press, Totowa, NJ, 105–116. https://doi.org/10.1007/978-1-62703-646-7_6
- Stöhr S, O'Hara TD, Thuy B (2012) Global Diversity of Brittle Stars (Echinodermata: Ophiuroidea). Laudet V (Ed.). PLoS ONE 7(3): e31940. <https://doi.org/10.1371/journal.pone.0031940>
- Stöhr S, O'Hara T, Thuy B (2022) World Ophiuroidea Database. <https://doi.org/10.14284/358>
- Verrill AE (1884) Notice of the remarkable marine fauna occupying the outer banks off the southern Coast of New England. American Journal of Science 28(165): 213–220. <https://doi.org/10.2475/ajs.s3-28.165.213>
- Verrill AE (1899) Report on the Ophiuroidea collected by the Bahama expedition in 1893. Bulletin from the laboratories of natural history of the State University of Iowa 5: 1–88. <https://www.biodiversitylibrary.org/part/51087>
- Yesson C, Clark MR, Taylor ML, Rogers AD (2011) The global distribution of seamounts based on 30 arc seconds bathymetry data. Deep-sea Research. Part I: Oceanographic Research Papers 58(4): 442–453. <https://doi.org/10.1016/j.dsr.2011.02.004>

Supplementary material 1

Figure S1

Authors: Xiaojun Xie, Dongsheng Zhang

Data type: Image.

Explanation note: Maximum likelihood tree of the genus *Astrodia* and *Asteronyx* based on concatenated sequences of COI and 16S.

Copyright notice: This dataset is made available under the Open Database License (<http://opendatacommons.org/licenses/odbl/1.0/>). The Open Database License (ODbL) is a license agreement intended to allow users to freely share, modify, and use this Dataset while maintaining this same freedom for others, provided that the original source and author(s) are credited.

Link: <https://doi.org/10.3897/zookeys.1123.87397.suppl1>

Supplementary material 2

Figure S2

Authors: Xiaojun Xie, Dongsheng Zhang

Data type: Image.

Explanation note: Maximum likelihood tree of the genus *Astrodia* and *Asteronyx* based on COI sequences.

Copyright notice: This dataset is made available under the Open Database License (<http://opendatacommons.org/licenses/odbl/1.0/>). The Open Database License (ODbL) is a license agreement intended to allow users to freely share, modify, and use this Dataset while maintaining this same freedom for others, provided that the original source and author(s) are credited.

Link: <https://doi.org/10.3897/zookeys.1123.87397.suppl2>

Supplementary material 3

Figure S3

Authors: Xiaojun Xie, Dongsheng Zhang

Data type: Image.

Explanation note: Maximum likelihood tree of the genus *Astrodia* and *Asteronyx* based on 16S sequences.

Copyright notice: This dataset is made available under the Open Database License (<http://opendatacommons.org/licenses/odbl/1.0/>). The Open Database License (ODbL) is a license agreement intended to allow users to freely share, modify, and use this Dataset while maintaining this same freedom for others, provided that the original source and author(s) are credited.

Link: <https://doi.org/10.3897/zookeys.1123.87397.suppl3>

An updated checklist of Collembola in Taiwan, with DNA barcoding of *Papirioides jacobsoni* Folsom, 1924 (Symphypleona, Dicyrtomidae)

Hsin-Ju Cheng¹, Frans Janssens², Chih-Han Chang^{1,3}

1 Institute of Ecology and Evolutionary Biology, National Taiwan University, Taipei, Taiwan **2** Evolutionary Ecology, Department of Biology, University of Antwerp, Groenenborgerlaan 171, 2020 Antwerpen, Belgium **3** Department of Life Science, National Taiwan University, Taipei, Taiwan

Corresponding author: Chih-Han Chang (chihhanchang@ntu.edu.tw, chihhanchang.ntu@gmail.com)

Academic editor: Wanda M. Weiner | Received 11 July 2022 | Accepted 16 September 2022 | Published 4 October 2022

<https://zoobank.org/F52ECD74-B0D2-4E23-93DA-1986370B1F42>

Citation: Cheng H-J, Janssens F, Chang C-H (2022) An updated checklist of Collembola in Taiwan, with DNA barcoding of *Papirioides jacobsoni* Folsom, 1924 (Symphypleona, Dicyrtomidae). ZooKeys 1123: 123–146. <https://doi.org/10.3897/zookeys.1123.90202>

Abstract

From urban green space to pristine forest, Collembola is one of the most numerous and species-rich members of the soil fauna around the world. However, due to lack of taxonomic expertise and research, its diversity is poorly understood, especially in tropical and subtropical regions. Collembola biodiversity studies in Taiwan have not seen much progress since 1981, when Hsin Chi reviewed 26 species belonging to 20 genera and eight families. Additionally, reports of new records in Taiwan in the last 40 years are scattered amongst several publications and not easily accessible to most end-users. Thus, a concise summary of related research is urgently needed. In this study, we updated the checklist of Collembola in Taiwan, based on published papers as well as images recorded in 2020–2022. We concluded that 58 species of Collembola belonging to 31 genera and 12 families have been reported in Taiwan, including 13 newly-recorded species. This species richness marks a 123% increase from the 1981 review. The results have been made publicly available in the Catalog of Life in Taiwan database and the images recorded have been used to update species information in collembola.org. We also characterised morphological and genetic variations in the globular springtail species *Papirioides jacobsoni* Folsom, 1924 using DNA barcodes and highlighted potential research directions.

Keywords

Biodiversity, Entomobryomorpha, Hexapoda, Poduromorpha, springtail

Introduction

Springtails are microarthropods in the class Collembola (Arthropoda: Hexapoda). They are commonly found in leaf litter and soil and on the surface of plants, fungal sporocarp, decaying wood and rocks. They are one of the most abundant animals in the litter-soil habitat, with a density of up to 40,000 individuals per square metre in the soil in temperate grasslands or forests (Orgiazzi et al. 2016). Their morphologies are characterised by ventral tube/collophore on the first abdominal segment, which helps anchor themselves to the surface, as well as furca/furcula, the structure allowing them to jump. In some taxonomic groups, this latter structure is reduced and, therefore, species in these groups lost the ability to jump. Globally, about 9,000 species of Collembola have been described so far and the estimated number of species is about 50,000 to 65,000 (Bellinger et al. 1996–2022). Most of our knowledge about this diversity comes from studies conducted in the temperate region, whereas the subtropical region has received little attention (Potapov et al. 2020).

Taiwan is an East Asian Island located between Japan and the Philippines. It has a land area of about 32,260 km² and is divided by the Tropic of Cancer into a humid subtropical climate in the north and a tropical monsoon climate in the south, with a mean annual precipitation of approximately 2,600 mm, mostly in the form of rainfall. The terrain on the Island was shaped by the collision between the Eurasian Plate and the Philippine Sea Plate in the last five million years (Huang et al. 1997, 2000). Geographically, it is divided into the flat to gently rolling plains in the west and the rugged, forest-covered mountains in the eastern two-thirds of the Island, with over 100 mountain peaks exceeding 3,000 m in elevation. Some of these summits were covered by glaciers during the last glaciation (Ono et al. 2005) and are still regularly receiving snow and short periods of ice cover during winter nowadays. The complex terrain, climate and geological history of Taiwan, presumably, provide ample opportunity for the diversification of Collembola, as well as varying vegetation and habitats for these organisms to thrive.

Following “An Index to the Collembola” for scientific names (Salmon 1964), the first and by far the only review of Collembola in Taiwan was a Chinese-written article by Hsin Chi in 1981, which listed 26 species belonging to 20 genera and eight families (Chi 1981). As Chi noted, studies of Collembola in Taiwan during the early years were mainly conducted by Japanese researchers. The first publication was by J.R. Denis (1929), which reported three species collected from Taipei by F. Silvestri. After that, Japanese taxonomists R. Yosii and H. Uchida reported several species of Collembola in Japan and neighbouring countries and up to 37 species from Taiwan were included (Yosii 1940, 1963, 1965, 1977; Uchida 1943, 1955, 1956, 1957a, 1957b, 1958a, 1958b, 1959a, 1959b, 1960). As some of the records were later considered synonyms, the total number of species reported during this period was higher than that in the checklist compiled by Chi (1981). In addition, some Taiwanese species were occasionally recorded in entomological literature (Shiraki 1932, 1954; Asahina et al. 1965) and an article about sugar cane pests (Takano and Yanagihara 1939).

In addition to Chi's (1981) comprehensive checklist, another 22 species have been reported in Taiwan by researchers from China, Korea and Japan. Lee and Park (1989) reported 11 species and seven genera in family Entomobryidae, including four new species and three new records. A year later, Lee and Kim (1990) reported five new species and two new records in family Neanuridae. In 2010, a subspecies of *Homidia* (Entomobryidae) was re-described and elevated to species level (Shi et al. 2010). Moreover, several new records were sporadically reported (Yosii 1966, 1982; Zhao et al. 1997). In contrast, studies conducted by Taiwanese researchers were mainly about pest control or survey of ground or soil arthropods, which only recorded the total number of individuals of Collembola without any detailed taxonomic information (Chen et al. 2020).

Taken together, our knowledge on the diversity of Taiwanese collembolan fauna has changed considerably in the last 40 years since Chi's comprehensive review, including changes in scientific names and synonyms. In this study, we updated the checklist of Collembola in Taiwan, based on published papers as well as images we recorded in 2020–2022. During our field sampling, we noticed apparent variations in the colour pattern of the species *Papirioides jacobsoni* Folsom, 1924, calling into question whether the different colour morphs are, indeed, the same species. Thus, we hypothesised that these colour morphs represent two different species and conducted DNA barcode analysis to test this hypothesis.

Materials and methods

The revised checklist is based on both published studies and newly-collected samples. Most of the sampling sites are hiking trails in forests and urban areas in northern Taiwan, with only a few samples from eastern and central Taiwan. Collembola were collected using one of the two methods; (1) Litter and surface soil were collected and then transported to the laboratory within 24 hours. Collembola were extracted from litter and soil using a Berlese-Tullgren funnel for about 5–7 days. Specimens were extracted into either a jar containing 85% ethanol or a container filled with the mixture of Plaster of Paris and fine powder of activated charcoal (Plaster of Paris: activated carbon: water = 9:1:11.25); (2) For specimens that were directly spotted in the field, an aspirator was used to collect them. The collected specimens were either kept alive for as long as possible in a container filled with the mixture of Plaster of Paris and activated charcoal or stored in 85% ethanol at 4 °C for future molecular study.

Live and ethanol-preserved specimens were examined under a Nikon SMZ800N stereomicroscope, equipped with a plan Apo 1× objective lens to reduce chromatic aberration and a TOUPCAM E3ISPM12300KPA digital camera for photography. Species identification is based on Bretfeld (1999), Potapov (2001) and Jordana (2012). For families, scientific names and synonyms, we followed the Checklist of the Collembola of the World maintained by Bellinger et al. (1996–2022) and hosted in collembola.org. In most cases, junior synonyms were listed when they were related to previous records of Taiwanese Collembola. Whenever available, additional information about locations and habitats of a species was detailed in the Remarks. Species marked with an

asterisk (*) are new records identified based on photographs of live specimens collected by the Taiwanese authors.

For molecular analysis, genomic DNA was extracted from whole specimens of *Papirioides jacobsoni* using the QIAamp DNA Micro Kit (Qiagen, Hilden, Germany) following the manufacturer's instruction. Before extraction, 1 µl of carrier RNA was added into buffer AL. The extracted DNA was eluted in 50 µl elution buffer and stored at –20 °C. Polymerase chain reaction (PCR) for the mitochondrial cytochrome *c* oxidase subunit 1 gene (COI), the DNA barcode for animals, was conducted using the primers LCO1490 and HCO2198 (Folmer et al. 1994) in a 20-µl volume containing 0.2 mM dNTP, 0.5 µM of each primer, 1.5 mM MgCl₂, 1.28 µg/µl BSA and 1 U Taq polymerase. Amplification was carried out with a preheat at 94 °C for 1 min, followed by 5 cycles of 94 °C for 30 sec, 45 °C for 30 sec and 72 °C for 50 sec and then by 35 cycles of 94 °C for 30 sec, 51 °C for 30 sec and 72 °C for 50 sec, with a final extension at 72 °C for 10 min. PCR products were checked using 1.5% agarose gel electrophoresis and sequenced by Genomics (Taipei, Taiwan) using an ABI 3730X Genetic Analyzer (Applied Biosystems, CA, USA). DNA sequences were assembled in Geneious (Dotmatrix, MA, USA), double-checked by eye and deposited in GenBank under accession numbers ON602032–ON602038.

For DNA barcode analysis, COI sequences of *Dicyrtomina ornata* (Nicolet, 1842), *Ptenothrix maculosa* (Schött, 1891) and *Ptenothrix huangshanensis* Chen & Christiansen, 1996 were retrieved from GenBank (accession numbers KT808331, KU874836 and MK423965, respectively) and used as outgroups. The acquired sequences were aligned using ClustalX 2.0 (Larkin et al. 2007). A neighbour-joining analysis was conducted using Kimura's two-parameter model (Kimura 1980) in MEGA X (Kumar et al. 2018), with 1,000 bootstrap pseudo-replicates to evaluate the robustness of clades.

Results

Checklist and classification

Class Collembola Lubbock, 1870

Order Poduromorpha Börner, 1913

Family Hypogastruridae Börner, 1906

1. *Ceratophysella armata* (Nicolet, 1842)

Podura armata Nicolet 1842.

Achorutes armatus: Oudemans 1890, Yosii 1940.

Hypogastrura armata: Chi 1981.

Remarks. Mt. Taiping, Datong Township, Yilan County (Yosii 1940).

2. *Ceratophysella communis* (Folsom, 1898)

Fig. 1A

Achorutes communis Folsom, 1898.*Achorutes communis*: Yosii 1940.*Hypogastrura communis*: Uchida 1956.*Neogastrura communis*: Uchida 1965.*Hypogastrura armata communis*: Chi 1981.

Remarks. Taipei (Denis 1929). Collected in Houtong, New Taipei City (25°5'14.62"N, 121°49'38.95"E) on 22 November 2021.

Family Neanuridae Börner, 1901**3. *Crossodonthina alatoserrata* Yosii, 1965***Imparitubercula alatoserrata*: Chi 1981.

Remarks. Taipei (Yosii 1965).

4. *Crossodonthina formosana* Yosii, 1965*Imparitubercula formosana*: Chi 1981.

Remarks. Wulai, New Taipei City, from soil and litter of mixed arboreal vegetation (Lee and Kim 1990).

5. *Crossodonthina montana* Lee & Kim, 1990

Remarks. Kantaoshan, Nantou County, from soil and litter of mixed arboreal vegetation (Lee and Kim 1990).

6. *Lobella nana* Lee & Kim, 1990

Remarks. Wushe, Nantou County, from the litter of pine forest (Lee and Kim 1990).

7. *Neanura kentingensis* Lee & Kim, 1990

Remarks. Kenting Park, Pingtung County, from dry soil under shrubs (Lee and Kim 1990).

8. *Paleonura formosana* (Yosii, 1965)

Paranura formosana Yosii, 1965: Chi 1981.

Remarks. Taipei (Yosii 1965).

9. *Paralobella perfusa* (Denis, 1934)

Lobella perfusa Denis, 1934: Lee and Kim 1990.

Remarks. Xitou, Nantou County, from bamboo and pine leaf litter and litter and soil of mixed arboreal vegetation and root of herbage (Lee and Kim 1990).

10. *Pseudachorudina nepalica* Yosii, 1966

Remarks. Xitou, Nantou County, from moss and under stones (Lee and Kim 1990).

11. *Vitronura rosea* (Gervais, 1842)

Anoura rosea Gervais, 1842.

Achorutes roseus: Handschin 1929, Uchida 1956.

Biloba rosea: Uchida 1965.

Neanura rosea: Chi 1981, Lee and Kim 1990.

Neanura giselae Gisin, 1950.

Remarks. Locality not specified (Chi 1981; Lee and Kim 1990). Bellinger et al. (1996–2022) noted that “given Yoshii (1995) synonymised *rosea* Gervais with *giselae* Gisin and *mandarina* Yosii, according to ICZN rules of priority, *rosea* Gervais, 1842 takes priority on *giselae* Gisin, 1950 and *mandarina* Yosii, 1954”. Thus, we list the species as *Vitronura rosea*.

12. *Vitronura pygmaea* (Yosii, 1954)

Metanura pygmaea Yosii, 1954.

Remarks. Locality not specified (Yosii 1977).

13. *Vitronura singaporiensis* (Yosii, 1959)

Bilobella singaporiensis Yosii, 1959.

Remarks. Wulai, New Taipei City (Yosii 1976).

14. *Vitronura tubercula* Lee & Kim, 1990

Remarks. Wulai, New Taipei City, from soil and litter of mixed arboreal vegetation (Lee and Kim 1990).

15. *Womersleya formosana* Lee & Kim, 1990

Remarks. Manchou, Pingtung County, from soil under shrubs (Lee and Kim 1990).

Family Onychiuridae Lubbock, 1867**16. *Formosanonychiurus formosanus* (Denis, 1929)**

Onychiurus formosanus Denis, 1929.

Paronychiurus formosanus: Chi 1981.

Remarks. Taipei (Denis 1929).

Family Poduridae Latreille, 1804**17. *Podura aquatica* Linnaeus, 1758**

Remarks. Cosmopolitan (Usinger 1956). First recorded in Shiraki (1932).

Order Entomobryomorpha Börner, 1913**Family Entomobryidae Schäffer, 1896****18. *Dicranocentrus indicus* Bonet, 1930**

Remarks. Yosii (1966). Locality unknown.

19. *Homidia formosana* Uchida, 1943

Homidia sauteri formosana Uchida, 1943: Chi 1981.

Remarks. Meixi, Ren'ai Township, Nantou County (Uchida 1943), from leaf litter of *Liquidambar formosana* (Shi et al. 2010).

***20. *Homidia linhaiensis* Shi, Pan & Qi, 2009**

Fig. 1B

Remarks. New record. Collected in Xiaokengxi, Wenshan District, Taipei City (24°59'6.06"N, 121°35'5.82"E) on 31 December 2021.

21. *Homidia nigrocephala* Uchida, 1943

Fig. 1C

Remarks. Meixi, Ren'ai Township, Nantou County and Mt. Taiping, Datong Township, Yilan County (Uchida 1943). Collected in Baoshan, Hsinchu County (24°44'32.73"N, 121°03'28.76"E) on 8 October 2020.

22. *Homidia sauteri* (Börner, 1909)

Entomobrya (Homidia) sauteri Börner, 1909.

Remarks. Locality not specified (Aoki 2015).

23. *Homidia socia* Denis, 1929

Fig. 1D

Remarks. Kenting National Park, Pintung County, from soil under shrubs, bamboo leaves, thicket of sugar cane leaves, forest of *Aphanamixis* and lawn (Lee and Park 1989). Collected in Xindian, New Taipei City (24°58'17.12"N, 121°31'55.80"E) on 18 December 2021.

***24. *Homidia taibaiensis* Yuan & Pan, 2013**

Fig. 1E

Remarks. New record. Collected in Shiding, New Taipei City (24°57'30.8"N, 121°39'30.2"E) on 10 October 2021, from litter of *Camellia oleifera* (oil-seed camellia).

25. *Lepidocyrtus heterolepis* Yosii, 1959

Remarks. Yosii (1982). Locality unknown.

26. *Lepidocyrtus scaber* Ritter, 1911

Remarks. Zhao et al. (1997). Locality unknown.

27. *Seira oligoseta* Lee & Park, 1989

Remarks. HENCHUN, Pintung County, from sugar cane thicket, litter of bamboo forest and poor soil under shrubs (Lee and Park 1989).

28. *Sinella curviseta* Brook, 1882

Fig. 1F

Remarks. Cosmopolitan (Hopkin 1997). Xitou, Nantou County, from litter and soil of mixed arboreal vegetation, acorn, poor soil under shrubs and litter layer of



Figure 1. Photos of Collembola in Taiwan **A** *Ceratophysella communis* (Folsom, 1898) **B** *Homidia linhaiensis* Shi, Pan & Qi, 2009 **C** *Homidia nigrocephala* Uchida, 1943 **D** *Homidia socia* Denis, 1929 **E** *Homidia taibaiensis* Yuan & Pan, 2013 **F** *Sinella curviseta* Brook, 1882.

diverse arboreal composition (Lee and Park 1989). Collected in Xiayun, Taoyuan City (24°49'40.9"N, 121°22'50.3"E) on 4 November 2020.

29. *Sinhomidia bicolor* (Yosii, 1965)

Acanthocyrthus bicolor Yosii, 1965.

Achanturella bicolor: Chi 1981, Lee and Park 1989.

Remarks. Wulai, New Taipei City and Kantaoshan, Nantou County, from litter and soil of acorn stands, on mosses and under stones (Lee and Park 1989).

30. *Willowsia formosana* (Denis, 1929)

Sira formosana Denis, 1929.

Seira formosana: Chi 1981.

Remarks. Taipei (Denis 1929).

31. *Willowsia jacobsoni* (Börner, 1913)

Sira jacobsoni Börner, 1913.

Remarks. Chung Hsing University, Taichung City, from bamboo leaf litter, arboreal vegetation, acorn stands, poor soil under shrubs, outer layer of banana trees and on mosses and under stones (Lee and Park 1989).

Family Isotomidae Schäffer, 1896

*32. *Folsomia candida* Willem, 1902

Fig. 2A

Remarks. New record. Collected in Hanxi, Datong Township, Yilan County (24°36'35.64"N, 121°41'13.8"E) on 1 February 2021.

*33. *Isotoma pinnata* Börner, 1909

Fig. 2B

Remarks. New record. Collected in Wulai, New Taipei City (24°52'55.7"N, 121°32'10.67"E) on 30 October 2021.

34. *Isotoma takahashii* Yosii, 1940

Isotomurus takahashii: Yosii 1963.

Remarks. Gokwan, Xiulin Townshhip, Hualien County (Yosii 1940).

35. *Isotomurus annectens* Yosii, 1963

Remarks. Yosii (1963). Locality unknown.

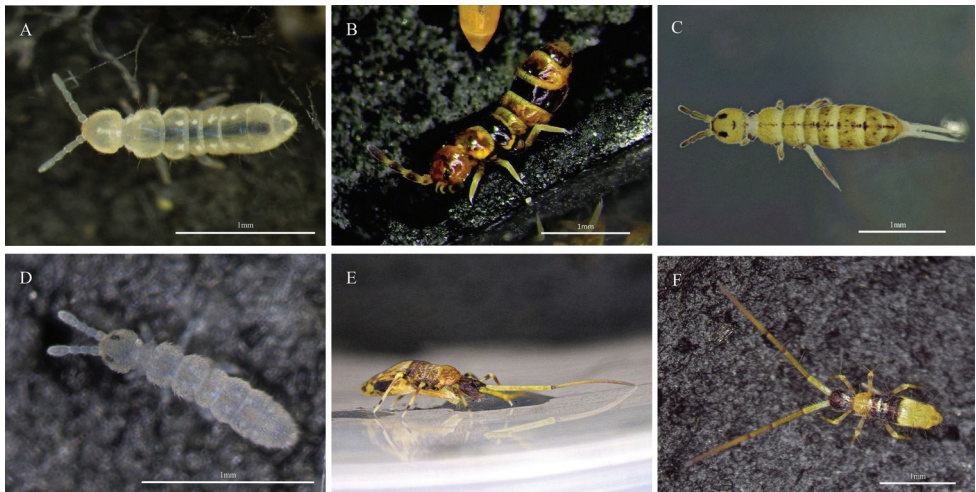


Figure 2. Photos of Collembola in Taiwan **A** *Folsomia candida* Willem, 1902 **B** *Isotoma pinnata* Börner, 1909 **C** *Isotomurus punctiferus* Yosii, 1963 **D** *Proisotoma minuta* (Tullberg, 1871) **E** *Callyntrura taiwanica* Yosii, 1965 (lateral view) **F** *Callyntrura taiwanica* Yosii, 1965 (dorsal view).

***36. *Isotomurus punctiferus* Yosii, 1963**

Fig. 2C

Remarks. New record. Collected from rocky sea shore in Waimushan, Keelung City (25°9'48.19"N, 121°43'30.24"E) on 28 May 2022.

***37. *Proisotoma minuta* (Tullberg, 1871)**

Fig. 2D

Isotoma minuta Tullberg, 1871.

Remarks. New record. Collected in Baoshan, Hsinchu County (24°44'32.73"N, 121°03'28.76"E) on 8 October 2020.

Family Paronellidae Börner, 1906**38. *Callyntrura affinis* Lee & Park, 1989**

Callyntrura (Gunungphysa) affinis Lee & Park, 1989.

Remarks. Reported in Manchou, Pintung County, from dry soil under shrubs (Lee and Park 1989).

39. *Callyntrura japonica* (Kinoshita, 1917)

Paronella japonica Kinoshita, 1917.

Handschinphysa japonica: Yosii 1956.

Aphysa japonica: Chi 1981.

Remarks. Zhiben Village, Beinan Township, Taitung County (Uchida 1943).

40. *Callyntrura microphysarum* Yosii, 1965

Callyntrura microphysarum and *Callyntrura microphysarum striata* Yosii, 1965.

Callyntrura (Gunungphysa) microphysarum and *Callyntrura (Gunungphysa) microphysarum striata*: Lee and Park 1989.

Paronella microphysarum: Chi 1981.

Remarks. Zhiben Village (Beinan Township, Taitung County), Meixi (Ren'ai Township, Nantou County), Chiayi County (Uchida 1943), Wulai (New Taipei City) (Yosii 1965) and Xitou (Nantou County), from litter and soil of mixed arboreal vegetation, on mosses and under stones, and from dry soil under shrubs (Lee and Park 1989).

41. *Callyntrura spinidentata* Lee & Park, 1989

Callyntrura (Gunungphysa) spinidentata Lee & Park, 1989.

Remarks. Xitou, Nantou County, from litter and soil of mixed arboreal vegetation (Lee and Park 1989).

42. *Callyntrura taiwanica* Yosii, 1965

Fig. 2E, F

Paronella taiwanica: Chi 1981.

Callyntrura (Gunungphysa) taiwanica: Lee and Park 1989.

Remarks. Wulai, New Taipei City, on mosses and under stones (Lee and Park 1989). Collected in Xindian, New Taipei City (24°56'47.46"N, 121°27'43.02"E) on 2 December 2021.

43. *Cyphoderus javanus* Börner, 1906

Cyphoderus assimilis: Chi 1981.

Remarks. Eluanbi, Hengchun Township, Pingtung County (Uchida 1943).

44. *Salina celebensis* (Schäffer, 1898)

Cremastocephalus celebensis Schäffer, 1898.

Remarks. Manchou, Pintung County (Lee and Park 1989) and Weishang Village, Ren'ai Township, Nantou County (Yosii 1940), from dry soil under shrubs and on mosses and under stones (Lee and Park 1989).

45. *Salina mutabilis* Lee & Park, 1989

Remarks. Xitou, Nantou County, from litter and soil of mixed arboreal vegetation, soil under bamboo leaf litter and under stones (Lee and Park 1989).

Family Tomoceridae Schäffer, 1896**46. *Tomocerus cuspidatus* Börner, 1909**

Remarks. Nenggao Village, Ren'ai Township, Nantou County and Gokwan, Xiulin Township, Hualien (Yosii 1940).

47. *Tomocerus ocreatus* Denis, 1948

Fig. 3A

Remarks. Locality not specified (Yosii 1977). Collected in National Taiwan University, Taipei City (25°1'12.69"N, 121°32'37.25"E) on 14 December 2021.

Order Symphypleona Börner, 1901**Family Dicyrtomidae Börner, 1906****48. *Calvatomina formosana* (Yosii, 1965)***Sphyrotheca formosana* Yosii, 1965.*Dicyrtomina formosana*: Chi 1981.

Remarks. Wulai, New Taipei City (Yosii 1965).

***49. *Papirioides caishijiensis* (Wu & Chen, 1996)**

Fig. 3B

Ptenothrix (Papirioides) caishijiensis Wu & Chen, 1996.

Remarks. New record. Collected in Lileng, Heping District, Taichung City (24°9'53.65"N, 120°57'12.62"E) on 7 November 2021.

50. *Papirioides mirabilis* (Denis, 1929)*Ptenothrix mirabilis* Denis, 1929: Chi 1981.*Ptenothryx mirabilis*: Yosii 1940.

Remarks. Nanshan Village, Datong Township, Yilan County (Yosii 1940).

***51. *Papirioides jacobsoni* Folsom, 1924**

Fig. 3C

Remarks. New record. Specimens used for DNA barcode analysis are archived in the Collembola collection of the Museum of Zoology, National Taiwan University, Taipei, Taiwan (NTUM-COL): four specimens collected at the Huisun Experimental Forest Station, Ren'ai Township, Nantou County on 26 February 2022 (NTUM-COL-00001, 00002, 00005, 00006); one specimen collected in Neihu Dist., Taipei City on 26 December 2021 (NTUM-COL-00011); and two specimens collected in Wulai, New Taipei City on 26 December 2021 (NTUM-COL-00026, 00027). The species has two colour-morphs: a "spotty" morph with clearly separated white spots

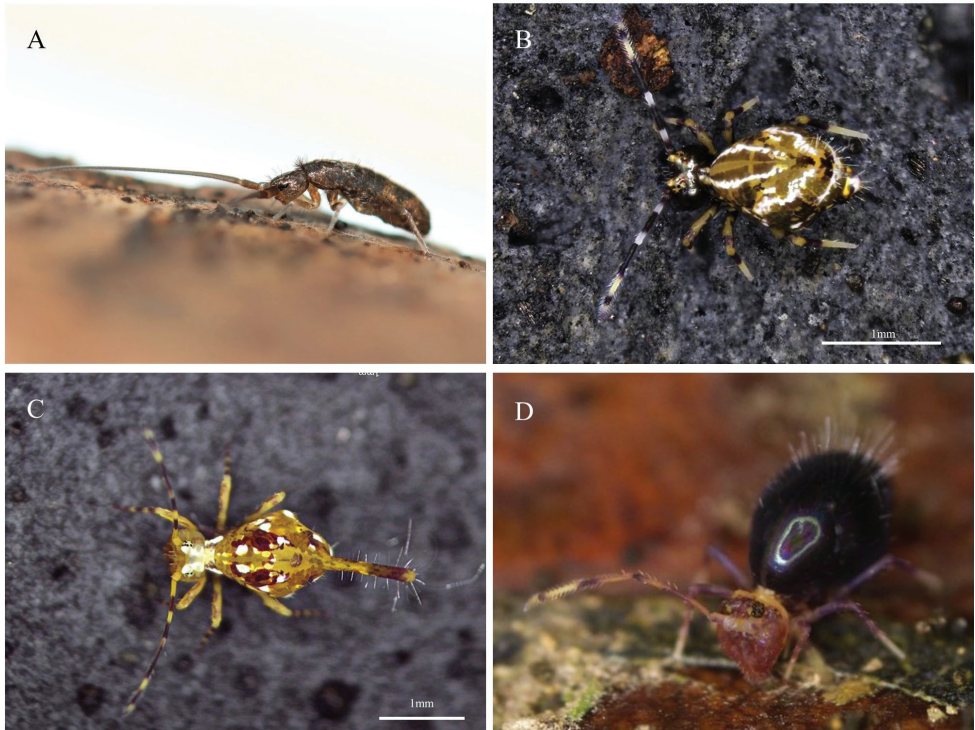


Figure 3. Photos of Collembola in Taiwan **A** *Tomocerus ocreatus* Denis, 1948 **B** *Papirioides caishijiensis* (Wu & Chen, 1996) **C** *Papirioides jacobsoni* Folsom, 1924 (spotty morph) **D** *Ptenothrix corynophora* Börner, 1909.

and a “milky” morph with irregular white patterns that are connected throughout the body (Fig. 5). DNA barcodes showed that the *P. jacobsoni* specimens analysed contain two genetically-distinct lineages, L1 and L2 (Fig. 5), corresponding to specimens collected in northern and central Taiwan, respectively. The mean *p*-distance between L1 and L2 is 8.3% (range: 7.6–8.8%). The “spotty” and “milky” colour-morphs can be found in both L1 and L2 and, thus, are not genetically distinct from each other. In fact, at one location, we found both the “spotty” and the “milky” morphs with identical COI sequences (NTUM-COL-00005 and 00006; Fig. 5).

***52. *Ptenothrix corynophora* Börner, 1909**

Fig. 3D

Remarks. New record. Collected in Houtong, New Taipei City (25°5'14.62"N, 121°49'38.95"E) on 22 November 2021.

***53. *Ptenothrix denticulata* (Folsom, 1899)**

Fig. 4A

Papirius denticulatus Folsom, 1899.

Remarks. New record. Collected in Xindian Dist., New Taipei City (24°54'53.67"N, 121°31'56.74"E) on 7 May 2022.

***54. *Ptenothrix monochroma* Yosii & Lee, 1963**

Fig. 4B

Remarks. New record. Collected in Sifenzi, New Taipei City (24°57'43.58"N, 121°39'46.92"E) on 28 November 2021.

Family Katiannidae Börner, 1913***55. *Sminthurinus trinotatus* Axelson, 1905**

Fig. 4C

Remarks. New Record. Collected in Chunri Township, Pingtung County (22°24'39.04"N, 120°44'16.77"E) on 5 June 2022.

Family Sminthuridae Lubbock, 1862**56. *Neosminthurus amabilis* (Yosii, 1965)***Lipothrix amabilis* Yosii, 1965.*Lipothrix mirabilis*(sic!) Chi 1981 lapsus.

Remarks. This species was collected in Taipei and described as *Lipothrix amabilis* Yosii, 1965. Although Yosii (1965) was cited in Chi (1981) when reviewing Taiwanese Collembola, this species was not included in Chi's checklist; nor was any reason provided for the "exclusion". Another species, *Lipothrix mirabilis* Yosii, 1965, was listed in Chi (1981), who cited Yosii (1965) as the source of the record. However, in the 1965 description of *L. mirabilis*, Yosii (1965) never mentioned anything about the presence of *L. mirabilis* in Taiwan. Thus, after carefully reviewing relevant publications, we added *N. amabilis* and removed *L. mirabilis* in the current checklist. It seems that Chi (1981) was confused by the names and listed inadvertently *mirabilis* instead of *amabilis*.

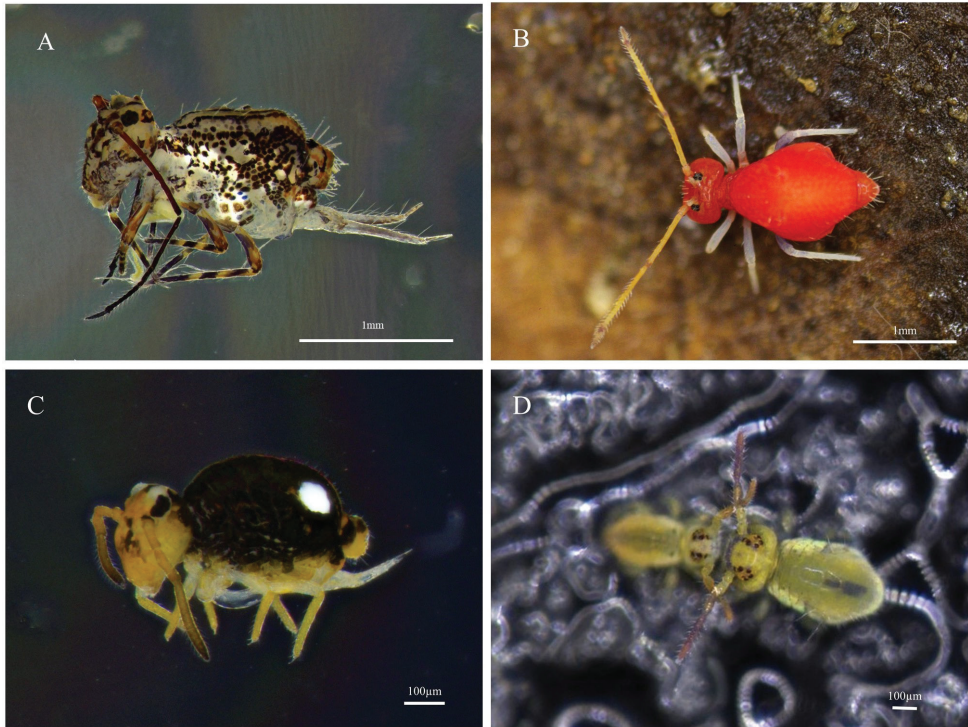


Figure 4. Photos of Collembola in Taiwan **A** *Ptenothrix denticulata* (Folsom, 1899) **B** *Ptenothrix monochroma* Yosii & Lee, 1963 **C** *Sminthurinus trinotatus* Axelson, 1905 **D** *Sminthurides penicillifer* (Schäffer, 1896).

57. *Szeptyckitheca formosana* (Yosii, 1965)

Sphyrotheca formosana Yosii, 1965: Chi 1981.

Remarks. Wulai, New Taipei City (Yosii 1965).

Family Sminthurididae Börner, 1906

***58. *Sminthurides penicillifer* (Schäffer, 1896)**

Sminthurus penicillifer Schäffer, 1896.

Fig. 4D

Remarks. New record. Collected in National Taiwan University, Taipei City (25°1'12.69"N, 121°32'37.25"E) on 11 November 2021.

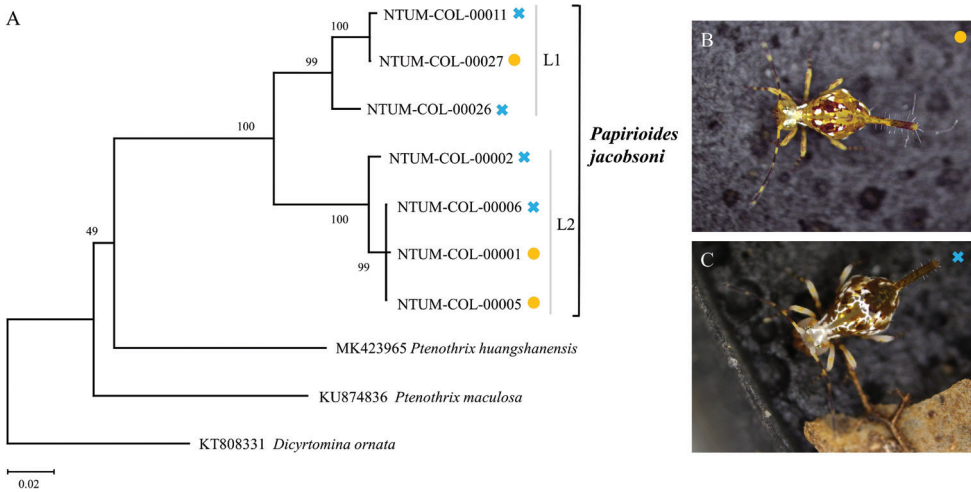


Figure 5. DNA barcode tree of *Papirioides jacobsoni* in Taiwan based on neighbor-joining analysis and Kimura's two-parameter model. The specimens analyzed form two genetically distinct lineages, L1 and L2 (A), corresponding to populations in northern and central Taiwan, respectively. Two color-morphs, "spotty" (B) and "milky" (C), can be found in both lineages. Specimens are labels with their NTUM catalog numbers followed by a symbol denoting their color-morphs. Numbers around nodes are bootstrap values.

Discussion

This study is the first update of Collembola in Taiwan in more than 40 years since Chi (1981) listed 26 species in his comprehensive review. The revised checklist comprises 58 species belonging to 31 genera and 12 families, including 13 newly-recorded species, and has been used to update the Catalog of Life in Taiwan database (TaiCoL; taibnet.sinica.edu.tw). Compared to the previous checklist by Chi (1981), this list recognises four more families, including Paronellidae, Dicyrtomidae, Katiannidae and Sminthurididae and follows the most updated taxonomy for genus assignment. This comprehensive checklist serves as an overview of our most up-to-date understanding on the status of collembolan diversity and ecology in Taiwan, fills a knowledge gap resulting from the lack of taxonomic expertise for more than 40 years and provides a foundation for future collembolan studies.

Our results rejected the hypothesis that the "spotty" and "milky" colour-morphs of *Papirioides jacobsoni* represent two distinct species and concluded that these morphological variations are intraspecific. A possible explanation for the distinct colour-morphs is sexual dimorphism. However, because the voucher specimens used for DNA extraction have become unsuitable for proper morphological examination, we are unable to test this hypothesis. In our phylogenetic results, the species consists of two genetically distinct lineages that are also geographically separated. The mean p -distance between the two lineages is smaller than the interspecific distances between

sister species (Porco et al. 2012; Katz et al. 2015). Thus, we consider the genetic variations observed in our samples as intraspecific. Further research with additional samples is needed to understand the morphological polymorphism, genetic structure and phylogeography of this species in Taiwan.

Our field sampling was not conducted systematically. The samples we collected are mostly from the northern part of Taiwan. We also did not attempt to revisit documented locations from which the recorded species were collected in the past. Thus, we were unable to make any specific inference regarding temporal changes based on our study and previous reports. However, we can safely assume that land-use changes in the last several decades have dramatically changed the landscapes and it is likely that habitats in most documented locations have been dramatically altered. It is unclear whether any of the specimens Chi (1981) examined still exist; if they do, the specimens need to be re-examined to confirm their species identity.

The majority of the 13 species newly recorded in this study are large-bodied, atmobiotic (surface-active) species (Potapov et al. 2016), which are relatively easy to find in the field with the naked eye during a targeted search, to collect using an aspirator and to examine and store in the laboratory. Other than the 13 species, many specimens we collected and examined so far could be assigned only to a subfamily or a genus. These putative species are in the families Neanuridae, Onychiuridae, Neelidae, Tomoceridae, Isotomidae, Orchesellidae, Paronellidae, Entomobryidae, Sminthurididae, Arrhopalitidae, Sminthuridae, Bourletiellidae and Dicyrtomidae and their image records are accessible on the lead author's Flickr page (<https://flic.kr/ps/3UjMUB>). Many of these presumptive species have voucher specimens archived at the NTU Museum of Zoology (preserved in 85% ethanol and stored at 4 °C). These specimens need to be further examined and barcoded to provide a more robust picture of the diversity of Collembola in Taiwan. In fact, the number of species in Taiwan, 58, is relatively low compared to those in neighbouring countries (e.g. 407 in Japan (Hishi et al. 2019)). This low number of species recorded has apparently resulted from the lack of research, as demonstrated by the 40-plus-year gap between Chi's (1981) review and this study.

Using digital photographs for collembolan species identification, albeit unconventional, is an overlooked and under-appreciated avenue that, when used properly, can accelerate the discovery of local species diversity and improve our understanding on the global distribution of widespread species. The combination of digital photography, community science and social media platform (e.g. Collembola of Taiwan Facebook group) has become instrumental in helping us locate certain species in Taiwan and uncover morphological polymorphism in *Papirioides jacobsoni*. We acknowledge that this approach, in general, has lower accuracy in species-level identification than conventional methods, even for large-bodied species and needs to be used with caution to avoid misidentification. Additionally, its use is likely limited to large-bodied and surface-active species, as smaller species and species living in the soil are less noticeable to the general public, harder to photograph and impossible to identify without examining detailed morphological characters (e.g. chaetotaxy) under a microscope.

Conclusions

Fifty-eight species of Collembola belonging to 31 genera and 12 families have been reported in Taiwan, including 13 species newly recorded in this study. These numbers mark a 123% increase in species richness from the previous comprehensive review. The results of this study have been used to update the “Catalog of Life in Taiwan” (taibnet.sinica.edu.tw) and the species information in the “Checklist of the Collembola of the World” (collembola.org). Additionally, although the dicyrtomid species *Papirioides jacobsoni* was shown to comprise two divergent mitochondrial lineages, these lineages are not concordant with morphological differences in colour morphs. Finally, we highlighted the potential and limitation of using macro photographs to reach species-level identification in Collembola.

Acknowledgements

We are grateful to Wanda M. Weiner, Diego Silva and Felipe N. Soto-Adames for their helpful and constructive comments on an earlier version of this article, to Katalin Szlavetz (Johns Hopkins University) and Chuan-Chin Huang (Harvard University) for helping with literature and to Zhi-Xiang Pan (Taizhou University) for sharing literature and comments on species identification. Funding for this study was supported by the National Science and Technology Council/Ministry of Science and Technology, Taiwan (MOST 108-2621-B-002-001-MY3 and MOST 111-2621-B-002-005-MY3) and by the Ministry of Education, Taiwan (Yushan Fellow Program) to Chih-Han Chang.

References

- Aoki JI (2015) Pictorial keys to soil animals of Japan. Tokai University Press 2: 1386–1387.
- Asahina S, Yasumatsu K, Ishihara T (1965) Iconographia Insectorum Japonicorum Colore Naturali Edita. Vol. 3. Hokuryukan, Tokyo, 358 pp. [In Japanese]
- Axelsson WM (1905) Einige neue Collembolen aus Finnland. Zoologischer Anzeiger 28: 788–794.
- Bellinger PF, Christiansen KA, Janssens F (1996–2022) Checklist of the Collembola of the world. <http://www.collembola.org>
- Bonet F (1930) Sur quelques Collemboles de l'Inde. Junta para la Ampliación de Estudios e Investigaciones Científicas 6(3): 249–273.
- Börner C (1901) Voläufige Mitteilung über einige neue Aphorurinen und zur Systematik der Collembola. Zoologischer Anzeiger 24(633): 1–15.
- Börner C (1906) Das System der Collembolen nebst Beschreibung neuer Collembolen des Hamburger Naturhistorischen Museums. Mitteilungen aus den Naturhistorischen Museum in Hamburg 23: 147–188.

- Börner C (1909) Japans Collembolenfauna. (Vorläufige Mitteilung). Sitzungsberichte der Gesellschaft Naturforschender Freunde zu Berlin 2: 99–135.
- Börner C (1913) Die Familien der Collembolen. Zoologischer Anzeiger 41: 315–322.
- Bretfeld G (1999) Symphypleona. In: Dunger W (Ed.) Synopses on Palaearctic Collembola, vol. 2. Abhandlungen und Berichte des Naturkundemuseum Görlitz 71: 1–318.
- Brook G (1882) On a new genus of Collembola (*Sinella*) allied to *Degeeria*, Nicolet. Zoological Journal of the Linnean Society 16(95): 541–545. <https://doi.org/10.1111/j.1096-3642.1882.tb02398.x>
- Chen JX, Christiansen K (1996) A new species of *Ptenothrix* from China (Collembola: Dicyrtomidae). The Florida Entomologist 79(4): 586–591. <https://doi.org/10.2307/3496072>
- Chen YF, Chung FY, Hsu PC, Lin CH, Chen YC (2020) A preliminary study on soil arthropods of different forest types in Xitou, Taiwan. Journal of the Experimental Forest of National Taiwan University 34(3): 213–226. [https://doi.org/10.6542/2fEFN.TU.202009_34\(3\).0003](https://doi.org/10.6542/2fEFN.TU.202009_34(3).0003)
- Chi H (1981) Literature review of Collembola in Taiwan. Annual of Taiwan Museum 24: 105–112.
- Denis J (1929) Collemboles d'Extrême-Orient. Notes sur les Collemboles récoltés dans ses voyages par le Prof. F. Silvestri (I). Bolletino del Laboratorio di Zoologia Portici 22: 166–171.
- Denis JMR (1934) Collemboles d'Indochine récoltés par CN Dawydoff (1^{re} note préliminaire) [Achorutini]. Bulletin de la Société Entomologique de France 39(8): 117–122. <https://doi.org/10.3406/bsef.1934.14714>
- Denis J (1948) Collemboles d'Indochine. Notes d'Entomologie Chinoise 12: 183–311.
- Folmer O, Black M, Hoeh W, Lutz R, Vrijenhoek R (1994) DNA primers for amplification of mitochondrial cytochrome *c* oxidase subunit I from diverse metazoan invertebrates. Molecular Marine Biology and Biotechnology 3: 294–299.
- Folsom JW (1898) Japanese Collembola (Part I). The Bulletin of the Essex Institute 24: 51–57. <https://doi.org/10.5962/bhl.part.14789>
- Folsom JW (1899) Japanese Collembola (Part II). Proceedings of the American Academy of Arts and Sciences 34(9): 261–274. <https://doi.org/10.2307/20020884>
- Folsom JW (1924) East Indian Collembola. Bulletin of the Museum of Comparative Zoology 65: 505–517.
- Gervais MP (1842) Communiqué une quinzaine d'espèces. Annales de la Société Entomologique de France 11: 45–49. <https://gallica.bnf.fr/ark:/12148/bpt6k63364141/>
- Gisin H (1950) Notes sur les Collemboles avec une espèce, un nom et trois synonymes nouveaux. Mitteilungen der Schweizerische Entomologische Gesellschaft 23(4): 411–416.
- Handschin E (1929) Beiträge zur Collembolenfauna von Süd-Indien. Revue Suisse de Zoologie 36: 229–262. <https://doi.org/10.5962/bhl.part.117939>
- Hishi T, Fujii S, Saitoh S, Yoshida T, Hasegawa M (2019) Taxonomy, distribution and trait data sets of Japanese Collembola. Ecological Research 34(4): 444–445. <https://doi.org/10.1111/1440-1703.12022>
- Hopkin SP (1997) Biology of the springtails (Insecta: Collembola). Oxford University Press, Oxford, 330 pp.

- Huang C-Y, Wu W-Y, Chang C-P, Tsao S, Yuan PB, Lin C-W, Xia KY (1997) Tectonic evolution of accretionary prism in the arc-continent collision terrane of Taiwan. *Tectonophysics* 281(1–2): 31–51. [https://doi.org/10.1016/S0040-1951\(97\)00157-1](https://doi.org/10.1016/S0040-1951(97)00157-1)
- Huang C-Y, Yuan PB, Lin C-W, Wang TK, Chang C-P (2000) Geodynamic processes of Taiwan arc-continent collision and comparison with analogs in Timor, Papua New Guinea, Urals and Corsica. *Tectonophysics* 325(1–2): 1–21. [https://doi.org/10.1016/S0040-1951\(00\)00128-1](https://doi.org/10.1016/S0040-1951(00)00128-1)
- Jordana R (2012) Capbryinae and Entomobryini. In: Dunger W, Bukhardt U (Eds) *Synopses on Palaearctic Collembola*, Volume 7/1. *Soil Organisms* 84(1): 1–390.
- Katz AD, Giordano R, Soto-Adames FN (2015) Operational criteria for cryptic species delimitation when evidence is limited, as exemplified by North American Entomobrya (Collembola: Entomobryidae). *Zoological Journal of the Linnean Society* 173(4): 818–840. <https://doi.org/10.1111/zoj.12220>
- Kimura M (1980) A simple method for estimating evolutionary rates of base substitutions through comparative studies of nucleotide sequences. *Journal of Molecular Evolution* 16(2): 111–120. <https://doi.org/10.1007/BF01731581>
- Kinoshita S (1917) Two new species of Collembola from Japan. *Zoological Magazine Tokyo* 29: 40.
- Kumar S, Stecher G, Li M, Knyaz C, Tamura K (2018) MEGA X: Molecular Evolutionary Genetics Analysis across computing platforms. *Molecular Biology and Evolution* 35(6): 1547–1549. <https://doi.org/10.1093/molbev/msy096>
- Larkin MA, Blackshields G, Brown NP, Chenna R, McGettigan PA, McWilliam H, Valentin F, Wallace IM, Wilm A, Lopez R, Thompson JD, Gibson TJ, Higgins DG (2007) Clustal W and Clustal X version 2.0. *Bioinformatics* 23(21): 2947–2948. <https://doi.org/10.1093/bioinformatics/btm404>
- Latreille (1804) *Histoire naturelle, générale et particulière des crustacés et des insectes*. Vol.3. F. Dufart, Paris, 467 pp.
- Lee BH, Kim JT (1990) Systematic studies on Chinese Collembola (Insecta): II. Five new species and two new records from Taiwan in the family Neanuridae. *Animal Systematics, Evolution and Diversity* 6(2): 235–249. <https://www.koreascience.or.kr/article/JAKO199011920826894.page?&lang=en>
- Lee BH, Park KH (1989) Systematic studies on Chinese Collembola (Insecta), I. Four new species and three new records of Entomobryidae from Taiwan. *Formosan Entomologist* 9: 263–282. <https://doi.org/10.6660%2fTESFE.1989025>
- Linnaeus C (1758) *Systema naturae*. Laurentii Salvii, Holmiae, 824 pp.
- Lubbock J (1862) Notes on the Thysanura. – Part I. Smythuridae. *Transactions of the Linnean Society of London* 23(3): 429–448. <https://doi.org/10.1111/j.1096-3642.1860.tb00141.x>
- Lubbock J (1867) Notes on the Thysanura Part III. *Transactions of the Linnean Society* 26(1): 295–304. <https://doi.org/10.1111/j.1096-3642.1968.tb00508.x>
- Lubbock J (1870) Notes on the Thysanura. – Part IV. *Transactions of the Linnean Society of London* 27(2): 277–297. <https://doi.org/10.1111/j.1096-3642.1870.tb00214.x>
- Nicolet H (1842) *Recherches pour Servir à l'Histoire des Podurelles*. *Nouveaux Mémoires de la Société Helvétique des Sciences Naturelles* 6: 1–88.

- Ono Y, Aoki T, Hasegawa H, Dali L (2005) Mountain glaciation in Japan and Taiwan at the global Last Glacial Maximum. *Quaternary International* 138: 79–92. <https://doi.org/10.1016/j.quaint.2005.02.007>
- Orgiazzi A, Bardgett RD, Barrios E (2016) *Global Soil Biodiversity Atlas*. European Commission, Luxembourg, 176 pp. <https://doi.org/10.1093/oso/9780199668564.003.0007>
- Oudemans JT (1890) Apterygota des Indischen Archipels. *Zoologische Ergebnisse* 1: 73–91.
- Porco D, Potapov M, Bedos A, Busmachiu G, Weiner WM, Hamra-Kroua S, Deharveng L (2012) Cryptic diversity in the ubiquitous species *Parisotoma notabilis* (Collembola, Isotomidae): A long-used chimeric species? *PLoS ONE* 7(9): e46056. <https://doi.org/10.1371/journal.pone.0046056>
- Potapov M (2001) Isotomidae. In: Dunger W (Ed.) *Synopses on Palaearctic Collembola: Vol. 3. Abhandlungen und Berichte des Naturkundemuseums Gorlitz* 73: 1–603.
- Potapov AA, Semenina EE, Korotkevich AY, Kuznetsova NA, Tiunov V (2016) Connecting taxonomy and ecology: Trophic niches of collembolans as related to taxonomic identity and life forms. *Soil Biology & Biochemistry* 10: 20–31. <https://doi.org/10.1016/j.soilbio.2016.07.002>
- Potapov A, Bellini B, Chown S, Deharveng L, Janssens F, Kováč L, Kuznetsova N, Ponge JF, Potapov M, Querner P (2020) Towards a global synthesis of Collembola knowledge: Challenges and potential solutions. *Soil Organisms* 92(3): 161–188.
- Ritter W (1911) Neue Thysanuren und Collembolen aus Ceylon and Bombay, gesammelt von Dr Uzel. *Annalen des Naturhistorischen Museums in Wien* 24: 379–398.
- Salmon JT (1964) An index to the Collembola. *Royal Society of New Zealand Bulletin* 7: 145–644.
- Schäffer C (1896) Die Collembolen der Umgebung von Hamburg und benachbarter Gebiete. *Mitteilungen aus dem Naturhistorischen Museum in Hamburg* 13: 149–216.
- Schäffer C (1898) Die Collembola des Bismarck-Archipels nach der Ausbeute von Prof. Dr. F. Dahl. *Archiv für Naturgeschichte* 64: 393–425.
- Schött H (1891) Beiträge zur Kenntniss Kalifornischer Collembola. *Bihang Till Kungliga Svenska vetenskapsakademiens Handlingar*, 26 pp.
- Shi SD, Pan ZX, Qi X (2009) A new species of the genus *Homidia* Börner, 1906 (Collembola: Entomobryidae) from East China. *Zootaxa* 2020(1): 63–68. <https://doi.org/10.11646/zootaxa.2020.1.4>
- Shi SD, Pan ZX, Zhang F (2010) A new species and a new record of the genus *Homidia* Börner, 1906 from East China (Collembola: Entomobryidae). *Zootaxa* 2351(1): 29–38. <https://doi.org/10.11646/zootaxa.2351.1.3>
- Shiraki T (1932) Collembola. In: *Pictorial handbook on Japanese insects*. Hokuryukan, Tokyo, 2115–2126. [In Japanese]
- Shiraki T (1954) Collembola. In: *Taxonomy of insects*. Hokuryukan, Tokyo, 7–21. [In Japanese]
- Takano S, Yanagihara M (1939) *Pests and beneficial insects of sugar cane in Taiwan*. Taiwan sugar cane society, 294 pp.
- Tullberg T (1871) Forteckning ofver Svenska Podurider. *Öfvers K Vetens Akad Förh* 28: 143–152.
- Uchida H (1943) On some Collembola-arthroleona from Nippon. *Bulletin of the National Science Museum* 8: 1–18.

- Uchida H (1955) Synopsis of the Apterygota of Japan and its vicinity. Historical reviews of the study on the Apterygota of the Far East and remarks on the geographical distribution of the Far Eastern Collembola. *Nihon Seibutsu Chiri Gakkai Kaiho* 16–19: 197–203.
- Uchida H (1956) Synopsis of the Apterygota of Japan and its vicinity. (III). Ordo Collembola, genus *Podura* to genus *Anurida*. *Papers in Science Reports. Hirosaki University* 3(1): 25–29.
- Uchida H (1957a) Synopsis of the Apterygota of Japan and its vicinity. (IV). Ordo Collembola, genus *Lobella* to genus *Ballistura*. *Papers in Science Reports. Hirosaki University* 4(1): 18–25.
- Uchida H (1957b) Synopsis of the Apterygota of Japan and its vicinity. (V). ordo Collembola, genus *Ballistura* to genus *Homidia*. *Papers in Science Reports. Hirosaki University* 4(2): 38–45.
- Uchida H (1958a) Synopsis of the Apterygota of Japan and its vicinity. (VI). Ordo Collembola, genus *Sira* to genus *Cyphoderus*. *Papers in Science Reports. Hirosaki University* 5(1): 13–20.
- Uchida H (1958b) Synopsis of the Apterygota of Japan and its vicinity. (VII). Ordo Collembola, genus *Megalothorax* to genus *Deuterosminthurus*. *Papers in Science Reports. Hirosaki University* 5(2): 33–35.
- Uchida H (1959a) Synopsis of the Apterygota of Japan and its vicinity. (IX). Bibliography. 1. *Papers in Science Reports. Hirosaki University* 6(2): 44–50.
- Uchida H (1959b) Synopsis of the Apterygota of Japan and its vicinity. (VIII). Ordo Collembola, genus *Sminthurus* to genus *Ptenothrix*. *Papers in Science Reports. Hirosaki University* 6(1): 22–26.
- Uchida H (1960) Synopsis of the Apterygota of Japan and its vicinity. (X). Bibliography. 2. *Papers in Science Reports. Hirosaki University* 7(1): 10–16.
- Usinger RL (1956) Aquatic insects of California: with keys to North American genera and California species. University of California Press, 507 pp. <https://doi.org/10.5962/bhl.title.61952>
- Willem V (1902) Note préliminaire sur les Collemboles des Grottes de Han et de Rochefort. *Annales de la Société Entomologique de Belgique* 46: 275–283.
- Wu M, Chen J (1996) A new species of the subgenus *Papirioides* from China (Collembola: Dicyrtomidae). *Insect Science* 3(2): 138–144. <https://doi.org/10.1111/j.1744-7917.1996.tb00219.x>
- Yoshii R (1995) Identity of some Japanese Collembola III. *Acta Zoologica Asiae Orientalis* 3: 51–68.
- Yoshii R (1940) On some Collembola from Formosa. *Annotationes Zoologicae Japonenses* 19(2): 114–118. <https://ci.nii.ac.jp/naid/110003352432>
- Yoshii R (1954) Höhlencollembolen Japans I. *Kontyû* 20(3–4): 62–70.
- Yoshii R (1956) Monographie zur Höhlencollembolen Japans. *Contributions from the Biological Laboratory, Kyoto University* 3: 1–109.
- Yoshii R (1959) Studies on the collembolan fauna of Malay and Singapore with special reference to the Genera: *Lobella*, *Lepidocyrtus* and *Callyntrura*. *Contributions from the Biological Laboratory Kyoto University* 10: 1–65. <https://ci.nii.ac.jp/naid/110003352432>

- Yosii R (1963) On some Collembola of Hindukush, with notes on *Isotoma* Bourlet and its allies. Results of the Kyoto University Scientific Expedition to the Karakoram and Hindukush 1955(4): 3–42.
- Yosii R (1965) On some Collembola of Japan and adjacent countries. Contributions from the Biological Laboratory, Kyoto University 19: 1–71. <http://hdl.handle.net/2433/155937>
- Yosii R (1966) On some Collembola of Afghanistan, India and Ceylon, collected by the Kuphe-Expedition, 1960. Results of the Kyoto University Scientific Expedition to the Karakoram and Hindukush 3: 333–405.
- Yosii R (1976) On some Neanurid Collembola of Southeast Asia. Nature and Life in Southeast Asia. Japan Society for the Promotion of Science 7: 291–298.
- Yosii R (1977) Critical check list of the Japanese species of Collembola. Contributions from the Biological Laboratory, Kyoto University 25(2): 141–170. <http://hdl.handle.net/2433/156007>
- Yosii R (1982) Lepidocyrtid Collembola of Sabah. Entomological Report from the Sabah Forest Research Center 5: 1–47.
- Yosii R, Lee CE (1963) On some Collembola of Korea, with notes on the genus *Ptenothrix*. Contributions from the Biological Laboratory Kyoto University 15: 1–37.
- Yuan X, Pan ZX (2013) Two new species of Entomobryidae (Collembola) of Taibai Mountain from China. ZooKeys 338: 67–81. <https://doi.org/10.3897/zookeys.338.5723>
- Zhao L, Tamura H, Ke X (1997) Tentative checklist of Collembolan species from China (Insecta). Publications of Itako Hydrobiological Station 9: 15–40. https://jglobal.jst.go.jp/en/detail?JGLOBAL_ID=200902180307909383

A DNA barcode library for katydids, cave crickets, and leaf-rolling crickets (Tettigoniidae, Rhaphidophoridae and Gryllacrididae) from Zhejiang Province, China

Yizheng Zhao¹, Hui Wang¹, Huimin Huang¹, Zhijun Zhou^{1,2}

1 Key Laboratory of Zoological Systematics and Application of Hebei Province, College of Life Sciences, Hebei University, Baoding, Hebei 071002, China **2** Institute of Life Science and Green Development, Hebei University, Baoding, Hebei 071002, China

Corresponding author: Zhijun Zhou (zhijunzhou@163.com, zhijunzhou@hbu.edu.cn)

Academic editor: Zhu-Qing He | Received 19 May 2022 | Accepted 6 September 2022 | Published 5 October 2022

<https://zoobank.org/005A1964-31AD-414A-8B32-209749AFFF5>

Citation: Zhao Y, Wang H, Huang H, Zhou Z (2022) A DNA barcode library for katydids, cave crickets, and leaf-rolling crickets (Tettigoniidae, Rhaphidophoridae and Gryllacrididae) from Zhejiang Province, China. ZooKeys 1123: 147–171. <https://doi.org/10.3897/zookeys.1123.86704>

Abstract

Barcode libraries are generally assembled with two main objectives in mind: specimen identification and species discovery/delimitation. In this study, the standard COI barcode region was sequenced from 681 specimens belonging to katydids (Tettigoniidae), cave crickets (Rhaphidophoridae), and leaf-rolling crickets (Gryllacrididae) from Zhejiang Province, China. Of these, four COI-5P sequences were excluded from subsequent analyses because they were likely NUMTs (nuclear mitochondrial pseudogenes). The final dataset consisted of 677 barcode sequences representing 90 putative species-level taxa. Automated cluster delineation using the Barcode of Life Data System (BOLD) revealed 118 BINs (Barcodes Index Numbers). Among these 90 species-level taxa, 68 corresponded with morphospecies, while the remaining 22 were identified based on reverse taxonomy using BIN assignment. Thirteen of these morphospecies were represented by a single barcode (so-called singletons), and each of 19 morphospecies were split into more than one BIN. The consensus delimitation scheme yielded 55 Molecular Operational Taxonomic Units (MOTUs). Only four morphospecies ($I_{\max} > \text{DNN}$) failed to be recovered as monophyletic clades (i.e., *Elimaea terminalis*, *Phyllomimus klapperichi*, *Sinochlora szechwanensis* and *Xizicus howardi*), so it is speculated that these may be species complexes. Therefore, the diversity of katydids, cave crickets, and leaf-rolling crickets in Zhejiang Province is probably slightly higher than what current taxonomy would suggest.

Keywords

Barcode Index Number, cryptic species, Ensifera, Orthoptera, species delimitation

Introduction

Accurate specimen identification and species discovery are fundamental to taxonomic research and essential prerequisite for many fields of research such as ecology, biogeography, and conservation biology (Agapow et al. 2004; Collins and Cruickshank 2013). DNA barcoding using a standardized gene region (5' region of the mitochondrial gene Cytochrome *c* oxidase subunit I, COI-5P) provide a powerful tool for specimen delimitation (Hebert et al. 2003). It can quickly distinguish species even with high morphological similarity, and it identifies cryptic genetic lineages within species, but it can fail if lineage sorting is incomplete (Yassin et al. 2009; Asis et al. 2016; Anderson et al. 2020). Specimen identification based on DNA barcodes does not rely on taxonomic expertise and can exclude the influence of human subjectivity in traditional morphological taxonomy. In recent years, increasing taxonomic practices have involved both morphological traits and DNA barcodes (DeSalle et al. 2005; Collado et al. 2021; Sabatelli et al. 2021). DNA barcodes have gained wide adoption for animal cryptic species recognition, species discovery, taxonomic revisions, and faunal assessments (Hebert et al. 2004, Tembe et al. 2014, Lone et al. 2020).

Cryptic species generally refer to highly genetically differentiated, but morphologically indistinguishable species (Van Campenhout et al. 2015). The discovery of cryptic species was critical for assessing biodiversity (Kundu et al. 2019). In the last 20 years, numerous studies using DNA barcoding have revealed cryptic species in several insect groups, such as Lepidoptera (Schonrogge et al. 2002; Burns et al. 2008), Thysanoptera (Tyagi et al. 2017), Diptera (Gajapathy et al. 2016; Chan-Chable et al. 2019). In morphological stasis, cryptic species within a complex or sister group remain highly morphologically similar for long periods of time, even tens of millions of years (Struck et al. 2017). Cryptic species may represent morphological stasis among related species experiencing similar environment conditions, but it may also reflect frequent, recent and/ or rapid speciation (Cerca et al. 2020).

Effective identification of a query specimen through DNA barcode sequence requires reliable reference libraries of known taxa. The process of assembling comprehensive and high-quality reference libraries of DNA barcodes allows the identification of newly collected specimens and accelerates taxonomic progress. The use of DNA barcoding for specimen identification and species discovery is greatly facilitated by the Barcode of Life Data System (BOLD, <http://www.boldsystems.org>).

Members of the suborder Ensifera diverged into grylloid (crickets) and non-grylloid (katydids) clades at the Triassic/Jurassic boundary (Zhou et al. 2017). Katydid (Tettigoniidae), cave crickets (Rhopidophoridae), and leaf-rolling crickets (Gryllacrididae) of non-grylloid (katydids) clades constitute a nearly cosmopolitan group with up to 10,000

valid species (Cigliano et al. 2021). DNA barcoding studies on katydid and related ensiferan groups have increased recently (Guo et al. 2016; Hawlitschek et al. 2017; Zhou et al. 2019; Kim et al. 2020), which has led to about 15% (1449 species) having been barcoded (www.boldsystems.org), including 7841 public records belonging to 1058 Barcode Index Numbers (BINs) or 871 species from Tettigoniidae, 145 public records belonging to 41 BINs or 13 species from Gryllacrididae, 1493 public records belonging to 150 BINs or 656 species from Rhaphidophoridae (accessed on 1 Dec., 2021).

Much research has been done on Zhejiang katydid and related ensiferan groups (Wang and Tong 2014; Wu et al. 2014; Liu et al. 2018). Currently, 115 species of Tettigoniidae, 12 species of Gryllacrididae, and 18 species of Rhaphidophoridae have been recorded from Zhejiang Province, China (see Suppl. material 1). Here, we present the next step in building-up a DNA barcode reference library for the katydids, cave crickets, and leaf-rolling crickets from Zhejiang Province, China. These DNA barcodes can help greatly in flagging unusual specimens that merit more careful revision using morphological characters.

Materials and methods

Sampling of specimens

Collections were performed throughout Zhejiang Province, China in the period of 2011–2019. Collection information (Fig. 1) can be found in the BOLD system under the public dataset DS-ZJCK. All specimens were preserved in absolute ethanol and identified by Yizheng Zhao using morphological traits, i.e., body shape, pronotum, and genitalia (Gorochov and Le 2002; Liu and Kang 2007; Guo and Shi 2012; Di et al. 2014; Jiao et al. 2014; Shi and Wang 2015; Bian and Shi 2016; Feng et al. 2016; Qin et al. 2016; Shi et al. 2016; Qin et al. 2017; Zhu and Shi 2018; Liu et al. 2019, 2021).

DNA extraction and COI barcode region sequencing

Total genomic DNA was extracted from hind legs of adults ($N = 676$) and nymphs ($N = 5$) using the Dneasy Blood and Tissue Kit (Tiagen Biotech, Beijing, China) according to the manufacturer's specifications. The remainder of the specimen was retained as a voucher stored at the Katydid Lab of Hebei University, China. The COI barcode region was amplified with primers COBU (5'-TYT CAA CAA AYC AYA ARG ATA TTG G-3') and COBL (5'-TAA ACT TCW GGR TGW CCA AAR AAT CA-3') (Pan et al. 2006). PCR amplification reactions were performed as follows. The 50 μ L of PCR mix contained 25 μ L of Premix Taq (TaKaRa), 5 μ L of each primer, 3 μ L of templated DNA and 12 μ L of ddH₂O. The PCR cycling protocol included an initial denaturation at 94 °C for 3 min, followed by 35 cycles of denaturation at 94 °C for 30 s, annealing at 49 °C for 30 s, extension at 72 °C for 1 min, with a final extension at 72 °C for 8 min. All amplicons were sent to GENEWIZ (Tianjin, China) for bidirectional sequencing using ABI 3730XL DNA sequencers.

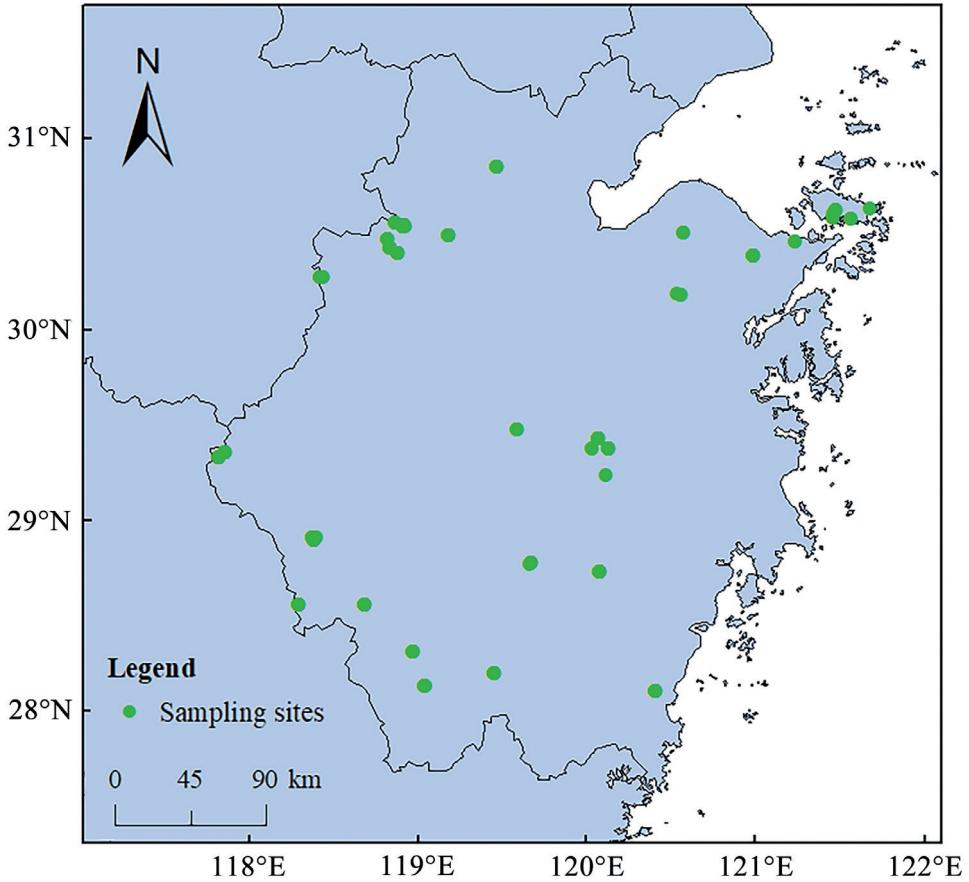


Figure 1. Sampling coverage of katydids, cave crickets, and leaf-rolling crickets in Zhejiang Province, China.

Data analyses

Forward and reverse sequences were trimmed, edited, and assembled to produce a consensus barcode sequence using SeqMan Pro (DNA star, Inc., Madison, Wisconsin, USA) for each specimen. All COI-5P barcode sequences were examined for potential stop codons using Editseq (DNA star, Inc., Madison, Wisconsin, USA). All sequences were aligned by employing MUSCLE (codons) algorithm (Edgar, 2004) with default parameters in MEGA ver. 7.0 (Kumar et al. 2016). The resulting alignments were cropped to a length of 658 bp. The COI-5P barcode sequences, trace files, and voucher information (i.e., collection data, photograph, taxonomic assignment) for each specimen are available in the BOLD dataset DS-ZJCK. All sequences meeting required quality criteria (> 500 bp, < 1% Ns, no stop codon or contamination flag) were assigned to a BIN by the BOLD system (Ratnasingham and Hebert 2013). Taxon ID Tree, BIN discordance, genetic distance analysis, and Barcode Gap Analysis were performed using analytical tools in BOLD ver.4 on 1 Dec., 2021.

The NJ tree was generated on BOLD with the Taxon ID tree tool using a Kimura-2-Parameter model, which is the mostly applied model in DNA barcoding studies (Hebert et al. 2003). The NJ tree was visualized using FigTree ver.1.4.4 (Rambaut 2018). BIN Discordance analysis on BOLD employs the Refined Single Linkage (RESL) algorithm for assigning barcode sequences to MOTUs independent of the BIN registry (Ratnasingham and Hebert 2013). There were four possible patterns of association between Linnaean species and Barcode Index Numbers (BINs), e.g., MATCH, SPLIT, MERGE, and MIXTURE. It should be noted that the BIN system is dynamic and dependent on the underlying data. Intraspecific distances and Barcode Gap Analysis could only be calculated for the 55 non-singleton species. The Barcode Gap Analysis provides mean and maximum intraspecific variations and a minimum genetic distance to the nearest-neighbour species (i.e., minimum interspecific distance).

In addition to BIN Discordance analysis, we also used other molecular delineation methods to delineate MOTUs. To minimize the risk of oversplitting (Talavera et al. 2013), the dataset was collapsed to retain only unique haplotypes. Four species delimitation approaches were employed: Assemble Species by Automatic Partitioning (ASAP) (Puillandre et al. 2021), jMOTU (Jones et al. 2011), General Mixed Yule Coalescent (GMYC) (Fujisawa and Barraclough 2013), and bPTP (Zhang et al. 2013). ASAP analysis was performed on the Web interface (<https://bioinfo.mnhn.fr/abi/public/asap/asapweb.html>) applying the K2P model, using default parameters (Puillandre et al. 2021). The jMOTU analysis was performed at cutoffs from 1 to 40 bp, covering a range between 0.15% and 6.08% divergence across the 658 bp COI-5P barcode. The General Mixed Yule Coalescent (GMYC) is a likelihood method for delimiting species, which tries to find the threshold between divergence events at the species level (modelled by a Yule process) and coalescent events between lineages within species (modelled by the coalescent). Both single-threshold GMYC (sGMYC) (Pons et al. 2006) and multi-threshold GMYC (mGMYC) (Monaghan et al. 2009) were computed. The best-fit nucleotide evolution model GTR+F+G4 was chosen by ModelFinder (Kalyaanamoorthy et al. 2017) under the Bayesian Information Criterion (BIC). The Bayesian Inference (BI) tree used for GMYC analysis was constructed using BEAST (Drummond and Rambaut 2007) using the Yule model and a constant clock. We checked runs for convergence and proper sampling of parameters [effective sample size (ESS) >200] using Tracer ver.1.7.1 (Rambaut et al. 2018). The BI tree was converted to the Newick format using FigTree ver.1.4.4 (Andrew 2016). The R package SPLITS (Ezard et al. 2009) was used for sGMYC and mGMYC analyses. The bPTP analysis models species formation events based on the number of substitutions in a given branch (Zhang et al. 2013). We used the BEAST tree created above to compare the generated outputs. The bPTP analysis was run using an online web server (<https://species.h-its.org/ptp/>) with default parameters except setting root tree, removing out-group and MCMC generation = 500,000.

The results of different species delimitation methods were pairwise compared. Firstly, match ratio $[2 \times N_{\text{match}} / (N_A + N_B)]$ (Ahrens et al. 2016), where N_{match} is the num-

ber of molecularly delimited species using two different methods exactly matching, N_A and N_B is the number of delimited species by methods A and B, respectively. Secondly, taxonomic index of congruence [$R_{\text{tax}}(AB) = n(A \cap B) / n(A \cup B)$] (Miralles and Vences 2013), where $A \cap B$ represents the number of speciation events shared by methods A and B, and $A \cup B$ represents the total number of speciation events inferred by method A and/or B. Thirdly, relative taxonomic resolving power index [$R_{\text{tax}}^A = nA / n(A \cup B \cup C \cup D \cup E)$] (Miralles and Vences 2013), where A, B, C, D, E represent the five species delimitation methods tested, nA represents the number of speciation events inferred by method A, and the denominator represents the cumulative number of speciation events inferred by all methods. Although large R_{tax} implies small type II error, it does not necessarily imply correct delimitations (i.e., can lead to over splitting) (Blair and Bryson 2017).

Results

The COI-5P of 681 specimens of katydid, cave crickets, and leaf-rolling crickets were sequenced. Among these specimens, 601 (88.25%) specimens were identified to 69 morphospecies (formally described species that are typically defined by distinct morphological characters) and the remaining 80 specimens were only identified at genus level (Tables 1, 2 and 3). The number of specimens per species ranged from one (14 singletons) to 58 in *Gampsocleis sinensis* Walker, 1869. Approximately half of these 69 morphospecies have five or more DNA barcodes. All sequences met the quality criteria (< 1% N and length > 500 bp) for BIN assignment. No insertions or deletions were observed.

Removal of problematic specimens

The preliminary “BIN Discordance” analysis (using BOLD ver.4 on 28 Dec., 2021) revealed five cases of merging, where each of the five BINs included two species from different genera or higher taxonomic taxa (Table 1). Species pairs in these five cases were distinctly morphologically different (Fig. 2). Five sequences located in apparently wrong positions on the NJ tree. To exclude contamination, DNA extraction from different leg and sequencing of these samples were repeated. Repeated experiments revealed that *Conocephalus gladius* Redtenbacher, 1891 DBTZC033-21 appeared

Table 1. Results of the internal BIN discordance report for the five BINs of 83 specimens. # sequences have been resubmitted, * possibly NUMT coamplification.

BIN	Conflicting species	Taxonomic rank
ADE4649	<i>Diestramima austrosinensis</i> (6) <i>Conocephalus gladius</i> DBTZC033-21#	family
ACD8581	<i>Conocephalus gladius</i> (17) <i>Tégra novaehollandiae</i> DBTZC057-21*	subfamily
ACD7803	<i>Isopsera sulcate</i> (4) <i>Orophyllus montanus</i> RBTC2009-18*	subfamily
ACD7324	<i>Ducetia japonica</i> (47) <i>Sinochlora szechwanensis</i> RBTC2050-18*	genus
ADF2961	<i>Melaneremus laticeps</i> (4) <i>Phryganogryllacris</i> DBTZC097-21*	genus

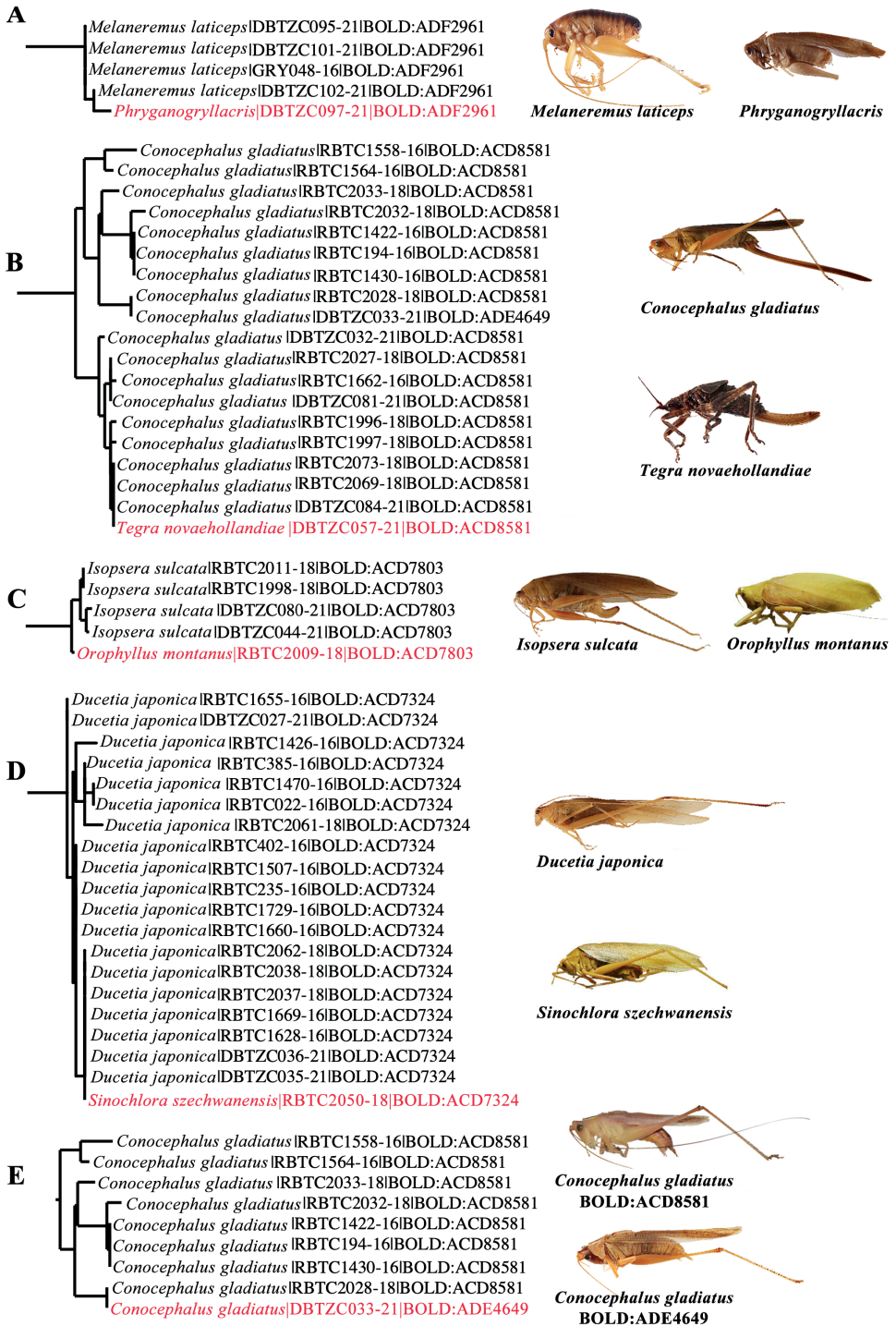


Figure 2. BIN discordance and the problems of interpreting potential NUMTs **A–E** represent the five cases of BIN discordance and individuals in red font represent individuals with potential NUMTs.

to have resulted from experimental operation errors, and the remaining four cases could not be explained by contamination or lab errors. We had updated the sequences of *C. gladiatus* DBTZC033-21 prior to our analysis, and it clustered with other *C. gladiatus* specimens on the NJ tree. It sharing ADE4649 with *Diastramima austrosinensis* Gorochoy, 1998 was the result of initial BIN assignment based on the previous incorrect sequence. Four records (*Orophyllus montanus* Beier, 1954 RBTC2009-18, *Phryganogryllacris* DBTZC097-21, *Sinochlorella szechwanensis* Tinkham, 1945 RBTC2050-18, and *Tegra novaehollandiae* Haan, 1843 DBTZC057-21) were highly likely COI-5P nuclear mitochondrial pseudogene (NUMT) intrusions and were excluded from our final dataset, since they each grouped separately from other individuals of the same species in the NJ tree (Fig. 5). Subsequent analyses focused on 677 barcode sequences, which were collapsed into 360 unique haplotypes. These records belong to three families, including Gryllacrididae ($N = 35$), Rhaphidophoridae ($N = 23$), and Tettigoniidae ($N = 619$).

Genetic divergence

Genetic distances for the resulting sequences were calculated in the BOLD System Distance Summary and Barcode Gap Analysis tools based on the K2P model. Table 4 provides sequence divergences (K2P) for differing levels of taxonomic affinity. The maximum intraspecific genetic distances (I_{\max}) of the 55 non-singleton species averaged 3.17% (range 0–21.64%), in which 24 species were above 2% (Table 2). Fourteen species are represented by only a single record, not allowing us to estimate intraspecific divergence. The genetic distance to the nearest neighbour (DNN) averaged 13.14% (ranging 3.31–19.38%), with the minimum nearest-neighbour distance occurring between *Xizicus laminatus* Shi, 2013 and *Xizicus howardi* Tinkham, 1956 (Table 2). Not a single haplotype was shared between species within our DNA barcode library. A barcode gap was present in 51 of 55 (92.73%) non-singleton species. Intraspecific distances were inflated by the presence of very high variation within some taxa, resulting in no significant barcode gaps (Fig. 3). The maximum intraspecific distance was higher than its nearest-neighbour distance in four species, including *Elimaea terminalis* Liu, 1993, *Melaneremus fuscoterminalis* Brunner von Wattenwyl, 1888, *Sinochlorella szechwanensis*, and *Xizicus howardi* (Table 1, Fig. 3). Eighteen of 24 species with deep intraspecific divergence (K2P model, $I_{\max} > 2\%$) were split into two or more BINs (Table 2). Interestingly, *Ruspolia dubia* Redtenbacher, 1891 were also split into two BINs, although the intraspecific divergence was relatively low ($I_{\max} = 1.55\%$).

Barcode index numbers (BINs) assignment and species delimitation

For the final dataset, 677 COI-5P records were assigned to 118 BINs that belong to 90 putative taxa. Among these, 68 corresponded to morphospecies, while another 22 belonged to a unique BIN that was currently only identified at genus level and highly likely to represent an unrecognized species. Of 68 morphospecies defined by morphology, a total of 49 contained only a single BIN, while 19 were represented by multiple BINs

Table 2. BIN assignments and genetic divergence of 68 morphospecies. BIN, Barcode Index Number; N , number of barcodes per BIN; I_{mean} , mean intraspecific distance; I_{max} , maximum intraspecific distance; DNN, distance to nearest neighbour; species in bold and labelled* $I_{\text{max}} > \text{DNN}$. Singletons are labeled as N/A and could not be evaluated.

Species	BIN (N)	I_{mean}	I_{max}	Nearest Neighbour	DNN
Gryllacrididae					
<i>Apotrechus bilobus</i>	ADF4059 (3)	0.31	0.46	<i>Eugryllacris elongata</i> DBTZC100-21	14.88
<i>Capnogryllacris melanocrania</i>	ADF2751 (1)	3.21	5.01	<i>Eugryllacris elongata</i> GRY018-16	16.4
	AEJ4972 (1)				
	ADF2750 (2)				
	AEJ9445 (2)				
<i>Eugryllacris elongata</i>	AEK0366 (1)	3.63	10.84	<i>Apotrechus bilobus</i> DBTZC103-21	14.88
	ADF4811 (5)				
<i>Homogryllacris anelytra</i>	ADF3866 (3)	0.83	1.09	<i>Phryganogryllacris xiaii</i> GRY040-16	17.42
<i>Melaneremus fuscoterminatus</i>*	ADF2959 (1)	14.73	14.73	<i>Melaneremus laticeps</i> DBTZC101-21	3.78
	ADF2960 (1)				
<i>Melaneremus laticeps</i>	ADF2961 (4)	0.08	0.15	<i>Melaneremus fuscoterminatus</i> GRY049-16	3.78
<i>Metriogryllacris permодesta</i>	ADF4959 (1)	N/A	0	<i>Phryganogryllacris xiaii</i> GRY040-16	18.4
<i>Phryganogryllacris superangulata</i>	ADF3568 (5)	0.15	0.31	<i>Capnogryllacris melanocrania</i> DBTZC078-21	18.92
<i>Phryganogryllacris xiaii</i>	ADF3457 (1)	N/A	0	<i>Homogryllacris anelytra</i> DBTZC096-21	17.42
Rhaphidophoridae					
<i>Diastramima austrosinensis</i>	ADE4649 (6)	0.3	0.61	<i>Diastramima brevis</i> DBTZC116-21	5.39
<i>Diastramima brevis</i>	AEJ2460 (5)	0.37	0.93	<i>Diastramima austrosinensis</i> DBTZC054-21	5.39
<i>Gymnaetoides testaceus</i>	AEJ5191 (3)	1.45	2.18	<i>Tachycines meditationis</i> DBTZC126-21	11.39
<i>Microtachycines elongatus</i>	AEJ2738 (2)	0.62	0.62	<i>Tachycines meditationis</i> DBTZC130-21	11.75
<i>Tachycines meditationis</i>	AEJ6894 (1)	1.77	3.31	<i>Gymnaetoides testaceus</i> DBTZC123-21	11.39
	AEK0279 (2)				
	AEJ9615 (4)				
Tettigoniidae					
<i>Atlanticus interval</i>	ADE2184 (3)	0.72	1.08	<i>Holochlora venusta</i> RBTC2022-18	19.38
<i>Conocephalus bidentatus</i>	ADB6577 (1)	N/A	0	<i>Conocephalus maculatus</i> RBTC1645-16	18.31
<i>Conocephalus gladius</i>	ADE4649 (1)	1.06	2.18	<i>Conocephalus maculatus</i> RBTC1645-16	16.97
	ACD8581 (17)				
<i>Conocephalus maculatus</i>	ACD2116 (1)	3.62	5.43	<i>Conocephalus gladius</i> DBTZC032-21	16.97
	ADB5579 (2)				
<i>Conocephalus melaenus</i>	ACD4634 (20)	0.1	0.31	<i>Conocephalus gladius</i> DBTZC032-21	17.65
<i>Deflorita deflorita</i>	ADB3725 (14)	0.79	2.67	<i>Hemielimaea chinensis</i> RBTC2067-18	16.35
<i>Ducetia japonica</i>	ACD7324 (47)	1.23	2.67	<i>Kuwayamaea brachyptera</i> DBTZC001-21	14.3
<i>Elimaea annamensis</i>	ADE1944 (9)	0.46	1.55	<i>Elimaea terminalis</i> RBTC2046-18	6.98
<i>Elimaea cheni</i>	ADB3480 (13)	0.09	0.46	<i>Elimaea nanpingensis</i> DBTZC006-21	9.69
<i>Elimaea nanpingensis</i>	ADB3475 (12)	0.06	0.17	<i>Elimaea cheni</i> DBTZC026-21	9.69
<i>Elimaea terminalis</i>*	ADB3392 (3)	6.35	10.68	<i>Elimaea annamensis</i> RBTC1668-16	6.98
	ADB3394 (3)				
<i>Euconocephalus nasutus</i>	ACD6726 (2)	1.39	1.39	<i>Ruspolia dubia</i> RBTC1561-16	14.22
<i>Euxiphidiopsis capricercus</i>	ADE2467 (1)	N/A	0	<i>Gampsocleis sinensis</i> RBTC1223-16	18.21
<i>Gampsocleis sinensis</i>	AAJ1322 (58)	0.87	2.03	<i>Euxiphidiopsis capricercus</i> HLXX121-16	18.21
<i>Grigoriona cheni</i>	ADE0541 (7)	0.79	1.39	<i>Sinocyrtaspis brachycerca</i> PSM013-19	13.2
<i>Hemielimaea chinensis</i>	ADB3478 (16)	1.51	3.63	<i>Elimaea nanpingensis</i> DBTZC006-21	14.64
	AEJ5565 (2)				
	ADE2233 (4)				
<i>Hexacentrus japonicus</i>	ACD8277 (4)	1.53	2.66	<i>Hexacentrus unicolor</i> BHC097-18	12.42
	ADM2486 (4)				
<i>Hexacentrus unicolor</i>	ACD7247 (36)	0.65	2.03	<i>Hexacentrus japonicus</i> BHC079-15	12.42
<i>Holochlora japonica</i>	ADE1373 (6)	0.16	0.31	<i>Holochlora venusta</i> RBTC2063-18	9.45
<i>Holochlora venusta</i>	ADB6143 (12)	0.05	0.31	<i>Holochlora japonica</i> RBTC1717-16	9.45
<i>Isopsera denticulata</i>	AEJ6400 (1)	5.96	9.72	<i>Deflorita deflorita</i> RBTC216-16	17.88
	ADE1596 (5)				
	ADB3788 (7)				
	ACD5193 (9)				

Species	BIN (M)	I_{min}	I_{max}	Nearest Neighbour	DNN
<i>Isoptera furcocerca</i>	ADB4481 (5)	0	0	<i>Paraxantia huangshanensis</i> RBTC1295-16	17.96
<i>Isoptera sulcate</i>	ACD7803 (4)	0.18	0.31	<i>Isoptera furcocerca</i> RBTC196-16	19.17
<i>Kuwayamaea brachyptera</i>	AEJ7401 (1)	1.81	2.82	<i>Ducetia japonica</i> DBTZC015-21	14.3
	AEK2062 (1)				
	AEK1896 (3)				
<i>Mecopoda niponensis</i>	AAF0977 (1)	1.09	7.53	<i>Diastramima austrosinensis</i> DBTZC054-21	15.02
	ACD8152 (18)				
<i>Mirollia bispina</i>	ADB4146 (3)	0.61	0.77	<i>Mirollia bispinosa</i> RBTC406-16	4.61
<i>Mirollia bispinosa</i>	ADB4148 (3)	0.1	0.15	<i>Mirollia bispina</i> RBTC237-16	4.61
<i>Nigrimacula paraquadrinotata</i>	ACD6675 (1)	N/A	0	<i>Grigoriora cheni</i> HLXX071-16	15.82
<i>Palaeoagraecia ascenda</i>	ACD8365 (4)	0	0	<i>Mecopoda niponensis</i> RBTC2086-18	16.8
<i>Paraxantia huangshanensis</i>	ADB6578 (1)	N/A	0	<i>Nigrimacula paraquadrinotata</i> HLXX059-16	16.76
<i>Phaneroptera falcata</i>	AAL2811 (2)	0.31	0.31	<i>Kuwayamaea brachyptera</i> DBTZC012-21	15.98
<i>Phaneroptera nigroantennata</i>	ACD4406 (2)	0.77	0.77	<i>Ducetia japonica</i> RBTC397-16	14.49
<i>Phyllomimus klapperichi</i>	ADM7559 (1)	10.3	17.47	<i>Ducetia japonica</i> RBTC397-16	18.08
	ADB9999 (4)				
	ADB4775 (6)				
<i>Pseudocosmetura fengyangshanensis</i>	ADW0286 (1)	N/A	0	<i>Sinocyrtaspis brachycerca</i> PSM014-19	11.19
<i>Pseudokuzicus pieli</i>	ACD4648 (1)	N/A	0	<i>Teratura megafurcula</i> HLXX099-16	13.71
<i>Pseudorhynchus concisus</i>	ADB6233 (7)	0.37	1.08	<i>Pyrgocorypha parva</i> BOCON142-16	16.24
<i>Pyrgocorypha parva</i>	ADC0410 (3)	0.51	0.77	<i>Pseudorhynchus concisus</i> DBTZC059-21	16.24
<i>Qinlingea brachystylata</i>	ADB4056 (1)	N/A	0	<i>Ruidocollaris truncatolobata</i> RBTC1677-16	18.9
<i>Ruidocollaris truncatolobata</i>	ACD6433 (15)	2.2	5.85	<i>Ducetia japonica</i> DBTZC015-21	16.25
	ADB6075 (5)				
<i>Ruspolia dubia</i>	ACD5503 (1)	1.09	1.55	<i>Euconocephalus nasutus</i> RBTC1705-16	14.22
	ADE5391 (3)				
<i>Ruspolia lineosa</i>	ACD5257 (26)	0.79	2.03	<i>Ruspolia dubia</i> RBTC1649-16	15.55
<i>Sinochlora longifissa</i>	AEJ1447 (1)	1.1	3.81	<i>Sinochlora szechwanensis</i> DBTZC067-21	5.68
	ADB3789 (34)				
<i>Sinochlora sinensis</i>	ACD4415 (1)	N/A	0	<i>Sinochlora szechwanensis</i> DBTZC038-21	5.93
<i>Sinochlora szechwanensis</i>*	ACI0121 (2)	4.61	8.71	<i>Sinochlora longifissa</i> DBTZC039-21	5.68
	ADB3463 (4)				
<i>Sinocyrtaspis brachycerca</i>	ADX3437 (4)	0.41	0.61	<i>Pseudocosmetura fengyangshanensis</i> PSM017-19	11.19
<i>Tegra novaehollandiae</i>	ADB5353 (10)	0.39	1.08	<i>Ducetia japonica</i> RBTC249-16	17.85
<i>Teratura megafurcula</i>	ACD5306 (1)	N/A	0	<i>Pseudokuzicus pieli</i> RBTC411-16	13.71
<i>Tettigonia chinensis</i>	ACD6622 (8)	0.32	0.77	<i>Hemielimaea chinensis</i> DBTZC092-21	16.74
<i>Xiphidiopsis gurneyi</i>	ADE1670 (2)	0	0	<i>Grigoriora cheni</i> HLXX074-16	16.27
<i>Xizicus biprocerus</i>	ADE1374 (1)	N/A	0	<i>Pseudokuzicus pieli</i> RBTC411-16	14.68
<i>Xizicus concavilaminus</i>	ADB3332 (3)	0.31	0.46	<i>Xizicus laminatus</i> HLXX037-16	3.63
<i>Xizicus howardi</i>*	AEJ3139 (1)	6.13	21.64	<i>Xizicus laminatus</i> HLXX037-16	3.31
	ADB5688 (10)				
	ACD5539 (3)				
	ADE3141 (4)				
<i>Xizicus laminatus</i>	ADB5868 (1)	N/A	0	<i>Xizicus howardi</i> RBTC1648-16	3.31
<i>Xizicus szechwanensis</i>	ADE0823 (2)	1.55	4.8	<i>Xizicus howardi</i> DBTZC013-21	15.37
	ADB3348 (9)				

(Table 2). The average number of BINs per species in “split” cases was 2.53, ranging from 2 to 4. Two BINs were found in each of 12 species: *Eugryllacris elongata* Bian & Shi, 2016 (AEK0366, ADF4811), *Melaneremus fuscoterminatus* (ADF2959, ADF2960), *Conocephalus gladius* (ADE4649, ACD8581), *Conocephalus maculatus* Le Guillou, 1841 (ACD2116, ADB5579), *Elimaea terminalis* (ADB3392, ADB3394), *Hexacentrus japonicus* Karny, 1907 (ACD8277, ADM2486), *Mecopoda niponensis* Haan, 1843

(AAF0977, ACD8152), *Ruidocollaris truncatolobata* Brunner von Wattenwyl, 1878 (ACD6433, ADB6075), *Ruspolia dubia* (ACD5503, ADE5391), *Sinochlora longifissa* Matsumura & Shiraki, 1908 (AEJ1447, ADB3789), *Sinochlora szechwanensis* (ACI0121, ADB3463), and *Xizicus szechwanensis* Tinkham, 1944 (ADE0823, ADB3348). Three BINs were found in each of four species: *Tachycines meditationis* Würlmli, 1973 (AEJ6894, AEK0279, AEJ9615), *Hemielimaea chinensis* Brunner von Wattenwyl, 1878 (ADB3478, AEJ5565, ADE2233), *Kuwayamaea brachyptera* Gorochoff & Kang, 2002 (AEJ7401, AEK2062, AEK1896), and *Phyllomimus klapperichi* Beier, 1954 (ADM7559, ADB9999, ADB4775). Four BINs were found in each of three species: *Capnogryllacris melanocrania* Karny, 1929 (ADF2751, AEJ4972, ADF2750, AEJ9445), *Isopsera denticulata* Ebner, 1939 (AEJ6400, ADE1596, ADB3788, ACD5193), and *Xizicus howardi* (AEJ3139, ADB5688, ACD5539, ADE3141) (Table 1). Furthermore, 79 sequenced specimens that only identified at genus level were allocated to 22 BINs. The interim species names of these unidentified specimens consisted of the genus name plus a corresponding BIN ID, such as *Bulbistridulous* BOLD:ADB3431. Specimens of five genera were each assigned to a unique BIN: *Bulbistridulous* BOLD:ADB3431, *Conanalus* BOLD:ADB5687, *Hexacentrus* BOLD:ADB5446, *Phryganogryllacris* BOLD:ADF3837, and *Prohimerta* BOLD:ADB4147, suggesting that each belongs to a single species. In contrast, specimens of the remaining three genera were heterogeneous and split into two or more BINs: *Elimaea* BOLD:ADE1399, ADM8940, and ADB3477; *Atlanticus* BOLD:ADB5602, ADB6974, ADR7192, ADE2402, ADB3445, ADE1821, and ADB3462; *Kuwayamaea* BOLD:ADB4962, ADE2183, ADE1620, ADB6899, ADB4961, ADB5240, and ADB4960.

The NJ tree was employed to assess support for detected BINs, not to reconstruct the phylogenetic relationships. The NJ tree showed the majority of non-singleton species and BINs were recovered as monophyletic (Fig. 5). All BIN species represented by two or more specimens, except ADE4649, formed a monophyletic lineage. High intraspecific divergence values also reflected deep splits in the NJ tree. All non-singleton morphospecies are clearly distinguishable through COI-5P, forming non-overlapping clades except for several species with deep intraspecific divergence exceeding DNN, namely *Elimaea terminalis* ($I_{\max} = 10.68\%$, DNN = 6.98), *Melaneremus fuscoterminalis* ($I_{\max} = 14.73\%$, DNN = 3.78%), *Sinochlora szechwanensis* ($I_{\max} = 8.71\%$, DNN = 5.68%) and *Xizicus howardi* ($I_{\max} = 21.64\%$, DNN = 3.31%) (Fig. 5, Table 2).

ASAP analysis identified 99 MOTUs with an asapscore of 9.00 (Fig. 5). jMOTU analysis delimited 101 at a 20 bp (3%) cut-off divergence (Fig. 5). The GMYC single-threshold method estimated 105 MOTUs, while the GMYC method with multiple thresholds delimited 132 MOTUs (Fig. 5). The bPTP analysis delimited 119 and 120 MOTUs based on the maximum likelihood and highest Bayesian supported analyses, respectively (Fig. 5).

Capnogryllacris melanocrania showed deep intraspecific divergence ($I_{\max} = 5.01\%$), and was split into four BINs (ADF2751, AEJ4972, ADF2750, AEJ9445), and these four BINs formed nearest-neighbour clusters. All species delimitation methods treated *C. melanocrania* as three MOTUs (ADF2750 and AEJ9445 were placed in a single MOTU, while ADF2751 and AEJ4972 were each placed in their own MOTU),

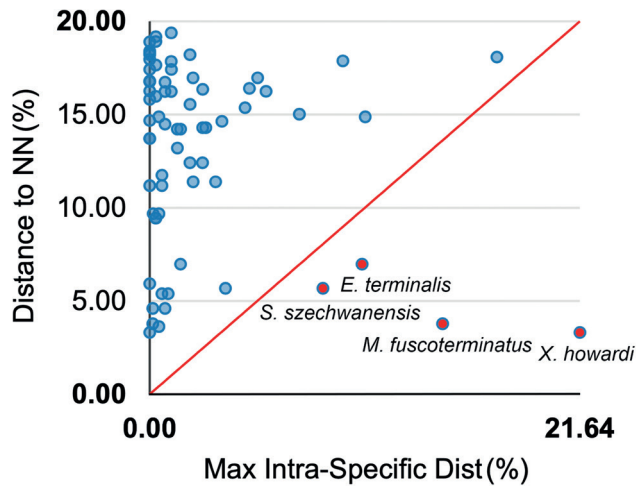


Figure 3. Scatter plot of maximum intraspecific distance and distance to nearest neighbour (NN). The four species to the right of the line represent a large intraspecific genetic distance.

Table 3. BIN assignments of 79 specimens identified only to genus level. BIN, Barcode Index Number; *N*, number of barcodes per BIN.

Taxon	BIN (<i>N</i>)
<i>Atlantiscus</i>	ADB5602 (1), ADB6974 (1), ADR7192 (1), ADE2402 (1), ADB3445 (2), ADE1821 (2), ADB3462 (3)
<i>Bulbistridulous</i>	ADB3431 (1)
<i>Conanalis</i>	ADB5687 (1)
<i>Elimaea</i>	ADE1399 (1), ADM8940 (1), ADB3477 (1)
<i>Hexacentrus</i>	ADB5446 (2)
<i>Kuwayamaea</i>	ADB4962 (1), ADE2183 (1), ADE1620 (13), ADB6899 (27), ADB4961 (4), ADB5240 (4), ADB4960 (6)
<i>Phryganogryllacris</i>	ADF3837 (4)
<i>Prohimerta</i>	ADB4147 (1)

Tables 4. Kimura 2 Parameter sequence divergence at each taxonomical level.

Distance class	n	Taxa	Comparisons	Min Dist (%)	Mean Dist (%)	Max Dist (%)
Intraspecific	585	55	6407	0.00	1.44	21.49
Congeners	314	13	2439	3.29	15.19	24.30
Confamilial	598	3	139568	11.12	22.66	34.59

except for ASAP which placed all specimens of *C. melanocrania* in two MOTUs. *Eugryllacris elongata* showed deep intraspecific divergence (Max Intra-Sp = 10.68%), and was split into two BINs (AEK0366, ADF4811). All species delimitation methods treated *E. elongata* AEK0366 and ADF4811 as two separate MOTUs. *Melaneremus fuscoterminatus* showed deep intraspecific divergence ($I_{\max} = 14.73\%$) and was split into two BINs (ADF2959 and ADF2960). The nearest neighbour of the *M. laticeps* ADF4959 clade was *M. fuscoterminatus* ADF2959, followed by *M. fuscoterminatus* ADF2960. All species delimitation methods suggested *M. fuscoterminatus* ADF2959

should be treated as a separate MOTUs. ASAP treated *M. fuscoterminatus* ADF2959 and *M. laticeps* ADF4959 as one MOTU. *Conocephalus maculatus* showed deep intraspecific divergence (Max Intra-Sp = 5.43%), and was split into two BINs (ACD2116, ADB5579). All species delimitation methods treated *E. elongata* ACD2116 and ADB5579 as two separate MOTUs. *Sinochlora szechwanensis* showed deep intraspecific divergence ($I_{\max} = 8.71\%$), while no barcode gap was present in *S. szechwanensis* and *S. longifissa* (Table 2). Three *Sinochlora* species formed two clades: one was composed of specimens identified as *S. szechwanensis* (ADB3463) and *S. sinensis*, and the other was composed of *S. szechwanensis* (ACI0121) and *S. longifissa* (Fig. 4). *Phyllomimus klapperichi* showed deep intraspecific divergence ($I_{\max} = 17.47\%$), and was split into three BINs (ADM7559, ADB9999, and ADB4775) (Fig. 4), reflecting three distinctly different subclusters of the *P. klapperichi* cluster on the NJ tree. All species delimitation methods split *P. klapperichi* into three MOTUs, except for mGMYC that split *P. klapperichi* into four MOTUs. *Elimaea terminalis* showed deep intraspecific divergence ($I_{\max} = 10.68\%$) and was split into two BINs (ADB3392 and ADB3394). Two *E. terminalis* BINs corresponded to two clades in the NJ tree: one contained three *E. terminalis* ADB3392 specimens and was sister to *Elimaea* ADM8940, whereas the other contained three *E. terminalis* ADB3394 specimens, which was sister to *Elimaea* ADB3477 and *Elimaea annamensis* Hebard, 1922 (Fig. 4). All species delimitation methods treated two *E. terminalis* BINs as separate MOTUs. Both *Xizicus howardi* ($I_{\max} = 21.64\%$) and *X. szechwanensis* (Max Intra-Sp = 4.8%) showed deep intraspecific divergence, and were split into four BINs (ACD5539, ADE3141, ADB5688, and AEJ3139) and two BINs (ADB3348 and ADE0823), respectively. Five *Xizicus* species formed three clades on the NJ tree: the first composed by specimens identified as *X. concavilaminus*, *X. laminatus*, and three *X. howardi* BINs (ACD5539, ADE3141, ADB5688); the second composed of all *X. szechwanensis* specimens and *X. howardi* AEJ3139, and the third composed of only a single *X. biprocerus*. All species delimitation methods except mGMYC revealed consistent results with BIN assignments. mGMYC split *X. howardi* ADB5688 as two MOTUs (Figs 4, 5). Therefore, *X. howardi* in Zhejiang might be a species complex of at least four species. Detailed comparative analyses of additional specimens was needed to evaluate the taxonomic status of *X. howardi*. Although *Ruspolia dubia* ($I_{\max} = 1.55\%$) was split into two BINs (ACD5503, ADE5391), all species delimitation methods treated *R. dubia* as a single MOTU. *Tachycines meditationis* ($I_{\max} = 3.31\%$) was split into three BINs (AEJ6894, AEK0279, AEJ9615). mGMYC, bPTP-ML, bPTP-BI approaches agreed on the subdivision of *T. meditationis* BINs while ASAP, jMOTU, and sGMYC analyses treated *T. meditationis* as a single MOTU. A BIN was assigned to the Match category when all of its specimens were assigned to single MOTU. Fifty-five out of 90 species-level taxa were recovered by all species delineation methods, suggesting that they may be a single species. R_{tax} values ranged from 0.71 for ASAP to 0.94 for mGMYC (Table 5), suggesting that mGMYC may overestimate the number of species. C_{tax} values between different species delimitation methods ranged from 0.75 (ASAP vs. mGMYC) to 0.99 (bPTP-ML vs. bPTP-BI), whereas, match ratios ranged from 0.65 (ASAP vs. mGMYC) to 0.99 (bPTP-ML vs. bPTP-BI) (Table 5).

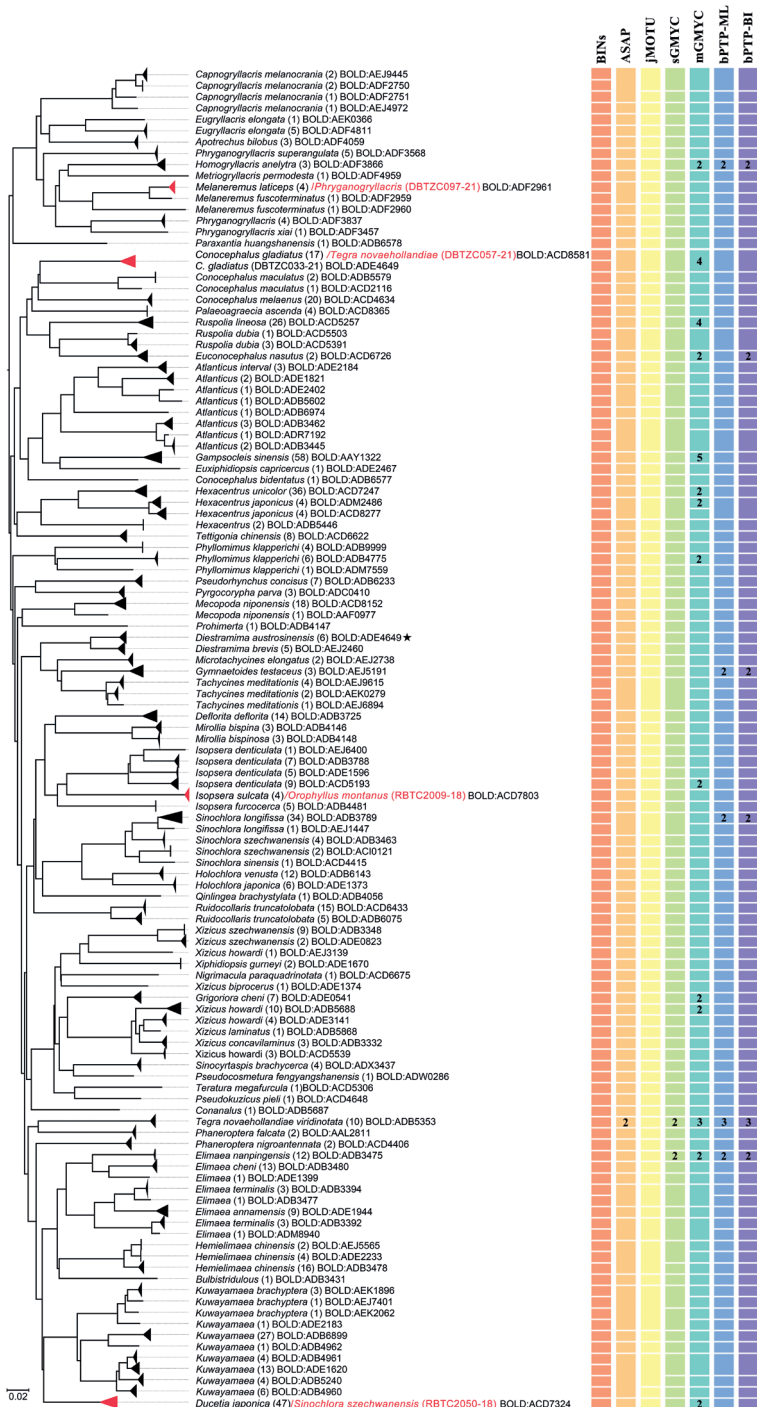


Figure 5. BOLD TaxonID Tree based on K2P distances and species delimitation results based on COI-5P sequences. The four barcode sequences marked by red are highly likely NUMTs and excluded from the species delimitation analyses. The MOTUs created by each delimitation algorithm are represented as squares on the right. The number within the rectangles indicates the number of MOTUs; no number indicates a single MOTU.

Discussion

In the past several hundred years, species diagnostics have been traditionally based on morphological characterizations. Morphology-based specimen identification is time consuming and requires high levels of taxonomic expertise. Compared with traditional taxonomy, DNA barcoding is a fast and inexpensive method for species identification. Numerous studies have revealed cryptic species using DNA barcodes (Kondo et al. 2016; Lassance et al. 2019; Farkas et al. 2020). However, using only DNA barcodes may lead to classification errors, and it is important to combine morphology and barcodes.

The utility of DNA barcoding heavily depends on the taxonomic coverage of an associated DNA barcode reference library. Barcode libraries are generally assembled with two main objectives in mind: specimen identification and aiding species discovery/delimitation (Knebelberger et al. 2014; Blagoev et al. 2016; Khamis et al. 2017; Ashfaq et al. 2019; Delrieu-Trottin et al. 2019; D’Ercole et al. 2021). The significant increase in studies of specific insect taxa using DNA barcodes in recent years, especially in some regions, has laid the foundations for building a comprehensive library of DNA barcodes at the continental-scale (D’Ercole et al. 2021; Dincă et al. 2021; Pesic et al. 2021). Only a few barcode studies of katydids and related ensiferan groups have been conducted in China, South Korea, Central Europe (Guo et al. 2016; Hawlitschek et al. 2017; Zhou et al. 2019; Kim et al. 2020). Our study provided 677 COI-5P barcode sequences, including 68 morphospecies and 80 specimens only identified to genus level.

BIN sharing between different species might be explained by mitochondrial introgression following hybridization, recent divergence with or without incomplete lineage sorting, inadequate taxonomy, misidentification (Geiger et al. 2021). One large-scale study for European Lepidoptera showed that more than half (58.6%) of the detected cases of non-monophyletic species are likely to be due to operational factors such as misidentification, oversplitting of species, overlooked synonymies or potential cryptic species (Mutanen et al. 2016). For the DNA barcode library of Central and Northern European Odonata, six of 31 BINs containing records of mixed taxonomic annotations conflict at generic levels, which is most likely due to misidentification, sample mix-up in the laboratory, sample number mix-up of specimens, or nomenclatural changes not applied to all affected datasets in BOLD (Geiger et al. 2021). Our previously mentioned example of BIN sharing between *Conocephalus gladius* DBTZC033-21 and *Diestramima austrosinensis* was caused by a sample confusion. The accuracy of DNA barcoding can be severely impacted when there are atypical NUMTs that lack the characteristic mutations (including in-frame stop codons and indels), which were difficult to identify and remove from the barcode dataset. NUMTs are rarely reported in DNA barcoding studies, despite a fairly frequent abundance across various insect groups (Hausberger et al. 2011; Jordal and Kambestad 2014; Hawlitschek et al. 2017). Our study also revealed four records shared with other species, which were highly likely the erroneous amplification of nonfunctional nuclear copies of COI-5P. The specimens of different species were admixed in a single cluster on the NJ tree, which often arises as the result of misidentification, contamination, or NUMTs (Mutanen et al. 2016). Previous studies found that NUMTs are coamplified using universal primers LCO1490/HCO2198, even across families: *Anabrus simplex*

(Tettigoniidae) vs. *Schistocerca americana* (Acrididae) (Moulton et al. 2010). Many NUMTs not having stop codons or indels may represent mitochondrial heteroplasmy, but this is a highly unusual phenomenon in insects (Jordal and Kambestad 2014).

Our analyses revealed 19 of 55 non-singleton morphospecies (34.55%) with multiple BINs. Most of these intraspecific BINs formed nearest-neighbour clusters to each other, reflecting the discrimination of geographical subclades within a currently recognized species. Previous studies have shown that BINs provide a very good reflection of classical taxonomy (Hausmann et al. 2013). For example, our prior study has shown a three-quarter species-BIN correspondence in katydids from China (Zhou et al. 2019). Species with BIN splits and high divergences are likely to represent a cryptic species complex (Ashfaq et al. 2019). Likewise, high levels of ‘intraspecific’ barcode variation also reflect overlooked species, but there is no fixed level of divergence that indicates species status (Huemer et al. 2020). Although the presence of a barcoding gap, intraspecific variation threshold, or monophyly of each putative species are sufficient conditions to ensure specimen correct identification, these are not essential criteria (Meyer and Paulay 2005; Yang and Rannala 2017).

Applying multiple species delimitation methods to the same dataset can provide a more reliable picture of species-level clustering. We obtained more MOTUs based on both the distance-based species-delimitation (ASAP, jMOTU) and the phylogeny-based methods (GMYC and bPTP) than the number of morphospecies. Several species with deep intraspecific divergence were split into more than one MOTU, and most of these additional BINs formed nearest-neighbour subclusters on the NJ tree. It was worth exploring the large intraspecific genetic distances for the same species although they were clustered together. Inconsistencies in delimitation results occur frequently as the result of different species delimitation methods. The mGMYC analysis produced a considerably higher number of MOTUs than other methods. R_{tax} values ranged from 0.71 for ASAP to 0.94 for mGMYC (Table 5), suggesting that mGMYC may overestimate the number of species. The performance of phylogeny-based methods is sensitive to multiple factors, such as general phylogenetic history, sampling intensity, DNA sequence length, speciation rate, and differences of effective population size among species (Esselstyn et al. 2012). The number of species can be underestimate or overestimate with ancestral polymorphism (Esselstyn et al. 2012), but previous studies showed that the sGMYC performs better than mGMYC (Talavera et al. 2013). Three indicators (Match ratio, C_{tax} , and R_{tax}) suggest that different species definition methods also diverge in terms of the location of species boundaries (Miralles and Vences 2013). Concordance among results of different species delimitation methods revealed that both *P. klapperichi* and *E. annamensis* may contain undocumented cryptic species. At present, we speculate that this is due to allopatric isolation due to the mountainous barriers between the samples. Despite the lack of clear morphological differentiation, the geographically and genetically distinct clusters suggest the existence of cryptic diversity. Therefore, our study indicates that the diversity of katydids, cave crickets, and leaf-rolling crickets in Zhejiang Province is slightly higher than the currently accepted taxonomy would suggest. The concordance among different species delimitation methods often implies higher reliability and should be used as primary taxonomic hypotheses that are subsequently tested with other types of data as part of an integrative taxonomic framework (Fujita et al. 2012; Blair and Bryson 2017).

Conclusions

Our DNA barcode library represents an important step for the molecular characterization of katydids, cave crickets, and leaf-rolling crickets in Zhejiang, China. Although some specimens still lack a Linnean name, their BIN assignments are treated as putative species in ecology, conservation biology and other biodiversity research (Sharkey et al. 2021). The number of detected BINs higher than traditionally accepted species suggests that DNA barcoding will complement morphology-based taxonomic system by revealing overlooked species complexes (Schmidt et al. 2015). The consensus delimitation scheme yielded 55 MOTUs, each of which may be a single species. Only three species ($I_{\max} > \text{DNN}$) failed to be identified as monophyletic (e.g., *Elimaea terminalis*, *Sinochlora szechwanensis*, and *Xizicus howardi*), so we speculate that these may be species complexes. If a species is split into two or more MOTUs implying cryptic diversity, then the number of katydid species in Zhejiang may be more than what is currently identified. However, prior to formal taxonomic changes, results should be subsequently tested using an integrative approach. This Barcode library was effective in assigning newly encountered specimens to either one or a few closely allied species. We expect it to be useful for future katydid taxonomic and conservation work.

Acknowledgements

The work of ZZ was supported by a grant of the Natural Science Foundation of Hebei Province (C2021201002).

References

- Agapow PM, Bininda-Emonds ORP, Crandall KA, Gittleman JL, Mace GM, Marshall JC, Purvis A (2004) The impact of species concept on biodiversity studies. *Quarterly Review of Biology* 79(2): 161–179. <https://doi.org/10.1086/383542>
- Ahrens D, Fujisawa T, Krammer HJ, Eberle J, Fabrizi S, Vogler AP (2016) Rarity and incomplete sampling in DNA-based species delimitation. *Systematic Biology* 65(3): 478–494. <http://10.1093/sysbio/syw002>
- Anderson K, Braoudakis G, Kvist S (2020) Genetic variation, pseudocryptic diversity, and phylogeny of *Erpobdella* (Annelida: Hirudinida: Erpobdelliformes), with emphasis on Canadian species. *Molecular Phylogenetics and Evolution* 143: 106688. <https://doi.org/10.1016/j.ympev.2019.106688>
- Andrew R (2016) FigTree: Tree figure drawing tool Version 1.4.3. Institute of Evolutionary Biology, United Kingdom, University of Edinburgh. <http://tree.bio.ed.ac.uk/software/figtree/>
- Ashfaq M, Blagojev G, Tahir HM, Khan AM, Mukhtar MK, Akhtar S, Butt A, Mansoor S, Herbert PDN (2019) Assembling a DNA barcode reference library for the spiders (Arachnida:

- Araneae) of Pakistan. PLoS ONE 14(5): e0217086. <https://doi.org/10.1371/journal.pone.0217086>
- Asis AM, Lacsamana JK, Santos MD (2016) Illegal trade of regulated and protected aquatic species in the Philippines detected by DNA barcoding. Mitochondrial DNA Part A 27(1): 659–666. <https://doi.org/10.3109/19401736.2014.913138>
- Bian X, Shi F (2016) Review of the genus *Eugryllacris* Karny, 1937 (Orthoptera: Gryllacridinae) from China. Zootaxa 4066(4): 438–450. <https://doi.org/10.11646/zootaxa.4066.4.5>
- Blagoev GA, deWaard JR, Ratnasingham S, deWaard SL, Lu LQ, Robertson J, Telfer AC, Hebert PDN (2016) Untangling taxonomy: a DNA barcode reference library for Canadian spiders. Molecular Ecology Resources 16(1): 325–341. <https://doi.org/10.1111/1755-0998.12444>
- Blair C, Bryson Jr RW (2017) Cryptic diversity and discordance in single-locus species delimitation methods within horned lizards (Phrynosomatidae: Phrynosoma). Molecular Ecology Resources 16(6): 1168–1182. <https://doi.org/10.1111/1755-0998.12658>
- Burns JM, Janzen DH, Hajibabaei M, Hallwachs W, Hebert PDN (2008) DNA barcodes and cryptic species of skipper butterflies in the genus *Perichares* in Area de Conservacion Guanacaste, Costa Rica. Proceedings of the National Academy of Sciences, USA 105(17): 6350–6355. <https://doi.org/10.1073/pnas.0712181105>
- Cerca J, Meyer C, Stateczny D, Siemon D, Wegbrod J, Purschke G, Dimitrov D, Struck TH (2020) Deceleration of morphological evolution in a cryptic species complex and its link to paleontological stasis. Evolution 74(1): 116–131. <https://doi.org/10.1111/evo.13884>
- Chan-Chable RJ, Martinez-Arce A, Mis-Avila PC, Ortega-Morales AI (2019) DNA barcodes and evidence of cryptic diversity of anthropophilous mosquitoes in Quintana Roo, Mexico. Ecology and Evolution 9(8): 4692–4705. <https://doi.org/10.1002/ece3.5073>
- Cigliano MM, Braun H, Eades DC, Otte D (2021) Orthoptera Species File (Version 5.0/5.0). [1-1-2022] <http://Orthoptera.SpeciesFile.org>
- Collado GA, Torres-Diaz C, Valladares MA (2021) Phylogeography and molecular species delimitation reveal cryptic diversity in *Potamolithus* (Caenogastropoda: Tateidae) of the southwest basin of the Andes. Scientific Reports 11(1): e15735. [10 pp] <https://doi.org/10.1038/s41598-021-94900-3>
- Collins RA, Cruickshank RH (2013) The seven deadly sins of DNA barcoding. Molecular Ecology Resources 13(6):969–975. <https://doi.org/10.1111/1755-0998.12046>
- D'Ercole J, Dinca V, Opler PA, Kondla N, Schmidt C, Phillips JD, Robbins R, Burns JM, Miller SE, Grishin N, Zakharov EV, DeWaard JR, Ratnasingham S, Hebert PDN (2021) A DNA barcode library for the butterflies of North America. PeerJ 9: e11157. <https://doi.org/10.7717/peerj.11157>
- Delrieu-Trottin E, Williams JT, Pitassy D, Driskell A, Hubert N, Viviani J, Cribb TH, Espiau B, Galzin R, Kulbicki M, de Loma TL, Meyer C, Mourier J, Mou-Tham G, Parravicini V, Plantard P, Salas P, Siu G, Tolou N, Veuille M, Weigt L, Planes S (2019) A DNA barcode reference library of French Polynesian shore fishes. Scientific Data 6: e114. <https://doi.org/10.1038/s41597-019-0123-5>
- DeSalle R, Egan MG, Siddall M (2005) The unholy trinity: taxonomy, species delimitation and DNA barcoding. Philosophical Transactions of the Royal Society B: Biological Sciences 360(1462): 1905–1916. <https://doi.org/10.1098/rstb.2005.1722>

- Di J, Bian X, Shi F, Chang Y (2014) Notes on the genus *Pseudokuzicus* Gorochov, 1993 (Orthoptera: Tettigoniidae: Meconematinae: Meconematini) from China. *Zootaxa* 3872(2): 154–166. <https://doi.org/10.11646/zootaxa.3872.2.2>
- Dincă V, Dapporto L, Somervuo P, Vodă R, Cuvelier S, Gascoigne-Pees M, Huemer P, Mutanen M, Hebert PDN, Vila R (2021) High resolution DNA barcode library for European butterflies reveals continental patterns of mitochondrial genetic diversity. *Communications Biology* 4: e315. <https://doi.org/10.1038/s42003-021-01834-7>
- Drummond AJ, Rambaut A (2007) BEAST: Bayesian evolutionary analysis by sampling trees. *BMC Evolutionary Biology* 7: e214. <https://doi.org/10.1186/1471-2148-7-214>
- Edgar RC (2004) MUSCLE: a multiple sequence alignment method with reduced time and space complexity. *BMC Bioinformatics* 5: e113. <https://doi.org/10.1186/1471-2105-5-113>
- Esselstyn JA, Evans BJ, Sedlock JL, Anwarali Khan FA, Heaney LR (2012) Single-locus species delimitation: a test of the mixed Yule-coalescent model, with an empirical application to Philippine round-leaf bats. *Proceedings of the Royal Society B: Biological Sciences* 279(1743): 3678–3686. <https://doi.org/10.1098/rspb.2012.0705>
- Ezard T, Fujisawa T, Barraclough TG (2009) SPLITS: SPecies' Limits by Threshold Statistics. R Package Version 1.0-18/R45. <http://R-Forge.R-project.org/projects/splits/> [Accessed 17 March 2021]
- Farkas P, Gyorgy Z, Toth A, Sojnoczki A, Fail J (2020) A simple molecular identification method of the *Thrips tabaci* (Thysanoptera: Thripidae) cryptic species complex. *Bulletin of Entomological Research* 110(3): 397–405. <https://doi.org/10.1017/S0007485319000762>
- Feng J, Chang Y, Shi F (2016) A revision of the subgenus *Xizicus* (Paraxizicus) Liu, 2004 (Orthoptera: Tettigoniidae: Meconematinae). *Zootaxa* 4138(3): 570–576. <https://doi.org/10.11646/zootaxa.4138.3.10>
- Fujisawa T, Barraclough TG (2013) Delimiting species using single-locus data and the Generalized Mixed Yule Coalescent approach: a revised method and evaluation on simulated data sets. *Systematic Biology* 62(5): 707–724. <https://doi.org/10.1093/sysbio/syt033>
- Fujita MK, Leache AD, Burbrink FT, McGuire JA, Moritz C (2012) Coalescent-based species delimitation in an integrative taxonomy. *Trends in Ecology & Evolution* 27(9): 480–488. <https://doi.org/10.1016/j.tree.2012.04.012>
- Gajapathy K, Tharmasegaram T, Eswaramohan T, Peries LB, Jayanetti R, Surendran SN (2016) DNA barcoding of Sri Lankan phlebotomine sand flies using cytochrome c oxidase subunit I reveals the presence of cryptic species. *Acta tropica* 161: 1–7. <https://doi.org/10.1016/j.actatropica.2016.05.001>
- Geiger M, Koblmüller S, Assandri G, Chovanec A, Ekrem T, Fischer I, Galimberti A, Grabowski M, Haring E, Hausmann A, Hendrich L, Koch S, Mamos T, Rothe U, Rulik B, Rewicz T, Sittenthaler M, Stur E, Tönczyk G, Zangl L, Moriniere J (2021) Coverage and quality of DNA barcode references for Central and Northern European Odonata. *PeerJ* 9: e11192. <https://doi.org/10.7717/peerj.11192>
- Gorochov AV, Le K (2002) Review of the Chinese species of *Ducetiini* (Orthoptera: Tettigoniidae: Phaneropterinae). *Insect Systematics and Evolution* 33(3): 337–360. <https://doi.org/10.1163/187631202X00190>

- Guo L, Shi F (2012) Notes on the Genus *Apotrechus* (Orthoptera: Gryllacrididae: Gryllacridinae) from China. *Zootaxa* 3177(3177): 52–58. <https://doi.org/10.11646/zootaxa.3177.1.5>
- Guo HF, Guan B, Shi FM, Zhou ZJ (2016) DNA Barcoding of genus *Hexacentrus* in China reveals cryptic diversity within *Hexacentrus japonicus* (Orthoptera, Tettigoniidae). *Zookeys* 596: 53–63. <https://doi.org/10.3897/zookeys.596.8669>
- Hausberger B, Kimpel D, van Neer A, Korb J (2011) Uncovering cryptic species diversity of a termite community in a West African savanna. *Molecular Phylogenetics and Evolution* 61(3): 964–969. <https://doi.org/10.1016/j.ympev.2011.08.015>
- Hausmann A, Godfray HC, Huemer P, Mutanen M, Rougerie R, van Nieuwerkerken EJ, Ratnasingham S, Hebert PDN (2013) Genetic patterns in European geometrid moths revealed by the Barcode Index Number (BIN) system. *PLoS ONE* 8(12): e84518. <https://doi.org/10.1371/journal.pone.0084518>
- Hawlotschek O, Moriniere J, Lehmann GUC, Lehmann AW, Kropf M, Dunz A, Glaw F, Detcharoen M, Schmidt S, Hausmann A, Szucsich NU, Caetano-Wyler SA, Haszprunar G (2017) DNA barcoding of crickets, katydids and grasshoppers (Orthoptera) from Central Europe with focus on Austria, Germany and Switzerland. *Molecular Ecology Resources* 17(5): 1037–1053. <https://doi.org/10.1111/1755-0998.12638>
- Hebert PDN, Cywinska A, Ball SL, deWaard JR (2003) Biological identifications through DNA barcodes. *Proceedings of the Royal Society B: Biological Sciences* 270(1512):313–321. <https://doi.org/10.1098/rspb.2002.2218>
- Hebert PDN, Penton EH, Burns JM, Janzen DH, Hallwachs W (2004) Ten species in one: DNA barcoding reveals cryptic species in the neotropical skipper butterfly *Astraptes fulgerator*. *Proceedings of the National Academy of Sciences, USA* 101(41): 14812–14817. <https://doi.org/10.1073/pnas.0406166101>
- Huemer P, Karsholt O, Aarvik L, Berggren K, Bidzilya O, Junnilainen J, Landry JF, Mutanen M, Nupponen K, Segerer A, Sumpich J, Wieser C, Wiesmair B, Hebert PDN (2020) DNA barcode library for European Gelechiidae (Lepidoptera) suggests greatly underestimated species diversity. *Zookeys* 921: 141–157. <https://doi.org/10.3897/zookeys.921.49199>
- Jiao J, Chang Y, Shi F (2014) Notes on a collection of the tribe Meconematini (Orthoptera: Tettigoniidae) from Hainan, China. *Zootaxa* 3836(5) 548–556. <https://doi.org/10.11646/zootaxa.3836.5.4>
- Jones M, Ghoorah A, Blaxter M (2011) jMOTU and Taxonator: turning DNA Barcode sequences into annotated operational taxonomic units. *PLoS ONE* 6(4): e19259. <https://doi.org/10.1371/journal.pone.0019259>
- Jordal BH, Kambestad M (2014) DNA barcoding of bark and ambrosia beetles reveals excessive NUMTs and consistent east-west divergence across Palearctic forests. *Molecular Ecology Resources* 14(1): 7–17. <https://doi.org/10.1111/1755-0998.12150>
- Kalyaanamoorthy S, Minh BQ, Wong TKF, von Haeseler A, Jermiin LS (2017) ModelFinder: fast model selection for accurate phylogenetic estimates. *Nature Methods* 14(6): 587–589. <https://doi.org/10.1038/Nmeth.4285>
- Khamis FM, Rwomushana I, Ombura LO, Cook G, Mohamed SA, Tanga CM, Nderitu PW, Borgemeister C, Setamou M, Grout TG, Ekesi S (2017) DNA Barcode Reference Library for the African Citrus Triozid, Trioza erytrae (Hemiptera: Triozidae): Vector of African

- Citrus Greening. *Journal of Economic Entomology* 110(6): 2637–2646. <https://doi.org/10.1093/jee/tox283>
- Kim SY, Kang TH, Kim TW, Seo HY (2020) DNA barcoding of the South Korean Tettigoniidae (Orthoptera) using collection specimens reveals three potential species complexes. *Entomological Research* 50(6): 267–281. <https://doi.org/10.1111/1748-5967.12433>
- Knebelberger T, Landi M, Neumann H, Kloppmann M, Sell AF, Campbell PD, Laakmann S, Raupach MJ, Carvalho GR, Costa FO (2014) A reliable DNA barcode reference library for the identification of the North European shelf fish fauna. *Molecular Ecology Resources* 14(5): 1060–1071. <https://doi.org/10.1111/1755-0998.12238>
- Kondo NI, Ueno R, Ohbayashi K, Golygina VV, Takamura K (2016) DNA barcoding supports reclassification of Japanese *Chironomus* species (Diptera: Chironomidae). *Entomological Science* 19(4): 337–350. <https://doi.org/10.1111/ens.12212>
- Kumar S, Stecher G, Tamura K (2016) MEGA7: molecular evolutionary genetics analysis Version 7.0 for bigger datasets. *Molecular Biology and Evolution* 33(7): 1870–1874. <https://doi.org/10.1093/molbev/msw054>
- Kundu S, Kumar V, Tyagi K, Rath S, Pakrashi A, Saren PC, Laishram K, Chandra K (2019) Mitochondrial DNA identified bat species in northeast India: electrocution mortality and biodiversity loss. *Mitochondrial DNA Part B-Resources* 4(2): 2454–2458. <https://doi.org/10.1080/23802359.2019.1638320>
- Lassance JM, Svensson GP, Kozlov MV, Francke W, Lofstedt C (2019) Pheromones and barcoding delimit boundaries between cryptic species in the primitive moth genus *Eriocrania* (Lepidoptera: Eriocraniidae). *Journal of Chemical Ecology* 45(5–6): 429–439. <https://doi.org/10.1007/s10886-019-01076-2>
- Liu C, Kang L (2007) Revision of the genus *Sinochlora* tinkham (Orthoptera: Tettigoniidae, Phaneropterinae). *Journal of Natural History: An International Journal of Systematics and General Biology* 41(21–24): 1313–1341. <https://doi.org/10.1080/00222930701437667>
- Liu X, Chen G, Sun B, Qiu X, He Z (2018) A systematic study of the genus *Atlanticus* Scudder, 1894 from Zhejiang, China (Orthoptera: Tettigoniidae: Tettigoniinae). *Zootaxa* 4399(2): 170–180. <https://doi.org/10.11646/zootaxa.4399.2.2>
- Liu Y, Shen C, Gong P, Zhang L, He Z (2019) Three new species of genus *Mecopoda* Serville, 1831 from China (Orthoptera: Tettigoniidae: Mecopodinae). *Zootaxa* 4585(3): 561. <https://doi.org/10.11646/zootaxa.4585.3.10>
- Liu J, Bin W, Bian X (2021) Contribution to the knowledge of Chinese Gryllacrididae (Orthoptera) III: New additions of *Metriogryllacris* Karny, 1937. *Zootaxa* 5068(1): 142–148. <https://doi.org/10.11646/zootaxa.5068.1.8>
- Lone AR, Tiwari N, Thakur SS, Pearlson O, Pavlicek T, Yadav S (2020) Exploration of four new *Kanchuria* sp. of earthworms (Oligochaeta: Megascolecidae) from the North Eastern Region of India using DNA barcoding approach. *Journal of Asia-Pacific Biodiversity* 13(2): 268–281. <https://doi.org/10.1016/j.japb.2020.02.004>
- Meyer CP, Paulay G (2005) DNA barcoding: Error rates based on comprehensive sampling. *PLoS Biology* 3(12): e422. <https://doi.org/10.1371/journal.pbio.0030422>
- Miralles A, Vences M (2013) New metrics for comparison of taxonomies reveal striking discrepancies among species delimitation methods in *Madascincus* lizards. *PLoS ONE* 8(7): e68242. <https://doi.org/10.1371/journal.pone.0068242>

- Monaghan MT, Wild R, Elliot M, Fujisawa T, Balke M, Inward DJ, Lees DC, Ranivosolo R, Eggleton P, Barraclough TG, Vogler AP (2009) Accelerated species inventory on Madagascar using coalescent-based models of species delineation. *Systematic Biology* 58(3): 298–311. <https://doi.org/10.1093/sysbio/syp027>
- Moulton MJ, Song H, Whiting MF (2010) Assessing the effects of primer specificity on eliminating numt coamplification in DNA barcoding: a case study from Orthoptera (Arthropoda: Insecta). *Molecular Ecology Resources* 10(4): 615–627. <https://doi.org/10.1111/j.1755-0998.2009.02823.x>
- Mutanen M, Kivela SM, Vos RA, Doorenweerd C, Ratnasingham S, Hausmann A, Huemer P, Dinca V, van Nieuwerkerken EJ, Lopez-Vaamonde C, Vila R, Aarvik L, Decaens T, Efetov KA, Hebert PDN, Johnsen A, Karsholt O, Pentinsaari M, Rougerie R, Segerer A, Tarmann G, Zahiri R, Godfray HC (2016) Species-level para- and polyphyly in DNA barcode gene trees: Strong operational bias in European Lepidoptera. *Systematic Biology* 65(6): 1024–1040. <https://doi.org/10.1093/sysbio/syw044>
- Pan C, Hu J, Zhang X, Huang Y (2006) The DNA Barcoding application of mtDNA COI genes in seven species of Catantopidae (Orthoptera). *Entomotaxonomia* 28(2): 103–110. <http://10.3969/j.issn.1000-7482.2006.02.004>
- Pesic V, Zawal A, Manovic A, Bankowska A, Jovanovic M (2021) A DNA barcode library for the water mites of Montenegro. *Biodiversity Data Journal* 9: e78311. <https://doi.org/10.3897/BDJ.9.e78311>
- Pons J, Barraclough TG, Gomez-Zurita J, Cardoso A, Duran DP, Hazell S, Kamoun S, Sumlin WD, Vogler AP (2006) Sequence-based species delimitation for the DNA taxonomy of undescribed insects. *Systematic Biology* 55(4): 595–609. <https://doi.org/10.1080/10635150600852011>
- Puillandre N, Brouillet S, Achaz G (2021) ASAP: Assemble Species by Automatic Partitioning. *Molecular Ecology Resources* 21(2): 609–620. <https://doi.org/10.1111/1755-0998.13281>
- Qin Y, Wang H, Liu X, Li K (2016) A taxonomic study on the species of the genus *Diestramima* Storozhenko (Orthoptera: Rhaphidophoridae; Aemodogryllinae). *Zootaxa* 4126(4): 514–532. <https://doi.org/10.11646/zootaxa.4126.4.4>
- Qin Y, Liu X, Li K (2017) A new genus of the tribe Aemodogryllini (Orthoptera, Rhaphidophoridae, Aemodogryllinae) from China. *Zootaxa* 4250(2): 186–190. <https://doi.org/10.11646/zootaxa.4250.2.4>
- Rambaut A (2018) FigTree v1.4.4. Computer program and documentation distributed by the author. <http://tree.bio.ed.ac.uk/software/figtree> [accessed 2018-11-25]
- Rambaut A, Drummond AJ, Xie D, Baele G, Suchard MA (2018) Posterior summarization in Bayesian phylogenetics using Tracer 1.7. *Systematic Biology* 67(5): 901–904. <https://doi.org/10.1093/sysbio/syy032>
- Ratnasingham S, Hebert PDN (2013) A DNA-based registry for all animal species: the barcode index number (BIN) system. *PLoS ONE* 8(7): e66213. <https://doi.org/10.1371/journal.pone.0066213>
- Sabatelli S, Ruspantini P, Cardoli P, Audisio P (2021) Underestimated diversity: Cryptic species and phylogenetic relationships in the subgenus *Cobalius* (Coleoptera: Hydraenidae) from marine rockpools. *Molecular Phylogenetics and Evolution* 163: 107243. <https://doi.org/10.1016/j.ympev.2021.107243>

- Schmidt S, Schmid-Egger C, Moriniere J, Haszprunar G, Hebert PDN (2015) DNA barcoding largely supports 250 years of classical taxonomy: identifications for Central European bees (Hymenoptera, Apoidea *partim*). *Molecular Ecology Resources* 15(4): 985–1000. <https://doi.org/10.1111/1755-0998.12363>
- Schonrogge K, Barr B, Wardlaw J, Napper E, Gardner M, Breen J, Elmes G, Thomas J (2002) When rare species become endangered: cryptic speciation in myrmecophilous hoverflies. *Biological Journal of the Linnean Society* 75(3): 291–300. <https://doi.org/10.1046/j.1095-8312.2002.00019.x>
- Sharkey MJ, Janzen DH, Hallwachs W, Chapman EG, Smith MA, Dapkey T, Brown A, Ratnasingham S, Naik S, Manjunath R, Perez K, Milton M, Hebert P, Shaw SR, Kittel RN, Solis MA, Metz MA, Goldstein PZ, Brown JW, Quicke DLJ, van Achterberg C, Brown BV, Burns JM (2021) Minimalist revision and description of 403 new species in 11 sub-families of Costa Rican braconid parasitoid wasps, including host records for 219 species. *Zookeys* 1013: 1–665. <https://doi.org/10.3897/zookeys.1013.55600>
- Shi F-M, Wang P (2015) The genus *Conocephalus* Thunberg (Orthoptera: Tettigoniidae: Conocephalinae) in Hainan, China with description of one new species. *Zootaxa* 3994(1): 142–144. <https://doi.org/10.11646/zootaxa.3994.1.8>
- Shi F, Zhou Z, Bian X (2016) Comments on the status of *Xiphidiopsis quadrinotata* bey-bienko, 1971 and related species with one new genus and species (orthoptera: tettigoniidae: meconematinae). *Zootaxa* 4105(4): 353–367. <https://doi.org/10.11646/zootaxa.4105.4.4>
- Struck TH, Koczula J, Stateczny D, Meyer C, Purschke G (2017) Two new species in the annelid genus *Stygocapitella* (Orbiniida, Parergodrilidae) with comments on their biogeography. *Zootaxa* 4286(3): 301–332. <https://doi.org/10.11646/zootaxa.4286.3.1>
- Talavera G, Dincă V, Vila R (2013) Factors affecting species delimitations with the GMYC model: insights from a butterfly survey. *Methods in Ecology and Evolution* 4:1101–1110. <https://doi.org/10.1111/2041-210X.12107>
- Tembe S, Shouche Y, Ghate HV (2014) DNA barcoding of Pentatomomorpha bugs (Hemiptera: Heteroptera) from Western Ghats of India. *Meta Gene* 2: 737–745. <https://doi.org/10.1016/j.mgene.2014.09.006>
- Tyagi K, Kumar V, Singha D, Chandra K, Laskar BA, Kundu S, Chakraborty R, Chatterjee S (2017) DNA Barcoding studies on Thrips in India: Cryptic species and Species complexes. *Scientific Reports* 7: e4898. <https://doi.org/10.1038/s41598-017-05112-7>
- Van Campenhout J, Vanreusel A, Van Belleghem S, Derycke S (2015) Transcription, signaling receptor activity, oxidative phosphorylation, and fatty acid metabolism mediate the presence of closely related species in distinct intertidal and cold-seep habitats. *Genome Biology & Evolution* 8(1): 51–69. <https://doi.org/10.1093/gbe/evv242>
- Wang YP, Tong CL (2014) *Insect in Qingliangfeng Zhejiang Province*. China Forestry Press.
- Wu H, Wang Y, Yang X, Yang S, Yin WY, Pan WB, Shi FM (2014) *Fauna of Tianmu Mountain III*. Zhejiang University Press.
- Yang ZH, Rannala B (2017) Bayesian species identification under the multispecies coalescent provides significant improvements to DNA barcoding analyses. *Molecular Ecology* 26(11): 3028–3036. <https://doi.org/10.1111/mec.14093>

- Yassin A, Amedegnato C, Cruaud C, Veuille M (2009) Molecular taxonomy and species delimitation in Andean *Schistocerca* (Orthoptera: Acrididae). *Molecular Phylogenetics and Evolution* 53(2): 404–411. <https://doi.org/10.1016/j.ympev.2009.06.012>
- Zhang J, Kapli P, Pavlidis P, Stamatakis A (2013) A general species delimitation method with applications to phylogenetic placements. *Bioinformatics* 29(22): 2869–2876. <https://doi.org/10.1093/bioinformatics/btt499>
- Zhou Z, Zhao L, Liu N, Guo H, Guan B, Di J, Shi F (2017) Towards a higher-level Ensifera phylogeny inferred from mitogenome sequences. *Molecular Phylogenetics and Evolution* 108: 22–33. <https://doi.org/10.1016/j.ympev.2017.01.014>
- Zhou Z, Guo H, Han L, Chai J, Che X, Shi F (2019) Singleton molecular species delimitation based on COI-5P barcode sequences revealed high cryptic/undescribed diversity for Chinese katydids (Orthoptera: Tettigoniidae). *BMC Evolutionary Biology* 19(1): e79. <https://doi.org/10.1186/s12862-019-1404-5>
- Zhu Q, Shi F (2018) Review of the genus *Diestramima* Storozhenko, 1990 (Orthoptera: Rhaphidophoridae: Aemodogryllinae) from China. *Zootaxa* 4450(2): 249–274. <https://doi.org/10.11646/zootaxa.4450.2.5>

Supplementary material I

List of species of the family Tettigoniidae, Rhaphidophoridae, and Gryllacrididae in Zhejiang Province, China

Authors: Yizheng Zhao, Hui Wang, Huimin Huang, Zhijun Zhou

Data type: species data

Copyright notice: This dataset is made available under the Open Database License (<http://opendatacommons.org/licenses/odbl/1.0/>). The Open Database License (ODbL) is a license agreement intended to allow users to freely share, modify, and use this Dataset while maintaining this same freedom for others, provided that the original source and author(s) are credited.

Link: <https://doi.org/10.3897/zookeys.1123.86704.suppl1>

A new species of *Austrocypraea* (Mollusca, Gastropoda, Cypraeidae) from the Pliocene of Flinders Island, Tasmania

Paul C. Southgate^{1,2}, Mike Roberts³

1 School of Science, Technology and Engineering, University of the Sunshine Coast, Maroochydore, Queensland 4558, Australia **2** Australian Centre for Pacific Islands Research, University of the Sunshine Coast, Maroochydore, Queensland 4558, Australia **3** Post Office, Lady Barron, Flinders Island, Tasmania 7255, Australia

Corresponding author: Paul C. Southgate (psouthgate@usc.edu.au)

Academic editor: Thomas A. Neubauer | Received 27 July 2022 | Accepted 26 August 2022 | Published 7 October 2022

<https://zoobank.org/E585BF11-44FE-4B57-A12C-AE7EB04BCD41>

Citation: Southgate PC, Roberts M (2022) A new species of *Austrocypraea* (Mollusca, Gastropoda, Cypraeidae) from the Pliocene of Flinders Island, Tasmania. ZooKeys 1123: 173–185. <https://doi.org/10.3897/zookeys.1123.90917>

Abstract

A new morphologically distinct species of cowry (family Cypraeidae Rafinesque, 1815) is described from the Pliocene of Flinders Island, Tasmania. *Austrocypraea jimgracei* sp. nov. differs morphologically from other members of the genus and is particularly characterised by the development of a heavily callused labral margin, with a distinct marginal edge that bends up towards the dorsum centrally. This feature is unique within the genus. The new taxon is only the second known *Austrocypraea* from the Pliocene. A revised key to the known *Austrocypraea* fossil species is presented.

Keywords

Cameron Inlet Formation, cowrie, cowry, fossil, taxonomy

Introduction

The marine gastropod genus *Austrocypraea* Cossmann, 1903 (Gastropoda, Cypraeidae) is endemic to southern Australia where it has an extensive fossil record from the Oligocene (Yates 2009). Ten of the 12 currently known *Austrocypraea* fossil species are from the Miocene: *A. archeri* (Tenison-Woods, 1876), from the Early Miocene (Longfordian)

of Tasmania; *A. contusa* (McCoy, 1877), *A. scalena* (Tate, 1890), *A. subsidua* (Tate, 1890), *A. ampullacea* (Tate, 1890), *A. parallela* (Tate, 1890), *A. constricta* Schilder, 1935, *A. subcontusa* Schilder, 1935, and *A. goudeyana* Fehse, 2013, from the Middle Miocene (Balcombian) of Victoria; and *A. rumballi* Fehse, 2003 from the Middle Miocene (Balcombian) of South Australia. The youngest member of the genus, *A. amae* Fehse and Kendrick, 2000, is the only known Pliocene species. *Austrocypraea amae* is generally acknowledged to be ancestral to the only extant member of the genus, *A. reevei* (Sowerby II, 1832), which lives on reefs associated with sponges, from central Western Australia to South Australia (Wilson 1993; Lorenz 2017).

The geology and fossil molluscan fauna of Flinders Island, in the Bass Strait off the north-eastern coast of Tasmania, were described by Sutherland and Kershaw (1970). The Pliocene Cameron Inlet Formation of Flinders Island is relatively rich in mollusc fossils, and was recognised by Darragh (1985) (as ‘Molluscan Assemblage XVII - Flinders Island’) as one of 18 informal assemblages characterising molluscan biogeography and biostratigraphy of the Tertiary of south-eastern Australia. Mollusc fossils from the Cameron Inlet Formation are generally obtained from spoil material excavated for drainage channels and farm dams, and four members of the Cypraeidae (cowries) have so far been reported: *Umbilia hestitata* (Iredale, 1916), *U. furneauxensis* Southgate, Militz & Roberts, 2021, *Notocypraea jonesiana* (Tate, 1890), and *N. angustata* (Gmelin, 1791) (Sutherland and Kershaw 1970; Darragh 1985; Goudey 2015; Southgate et al. 2021). A number of specimens of an apparently undescribed species of fossil cowry were recently recovered from excavated material in the Lackrana area of Flinders Island. Described here as *Austrocypraea jimgracei* sp. nov., it is the second representative of the genus from the Pliocene.

Materials and methods

Examined material

All examined specimens were recovered from material excavated for farm dams in the Lackrana area of Flinders Island, Tasmania. Assignment of specimens to the late Pliocene Cameron Inlet Formation was confirmed by reference to molluscan assemblages previously described for the Cameron Inlet Formation and the Pleistocene Memana Formation that disconformably overlies the Cameron Inlet Formation (Sutherland and Kershaw 1970; Darragh 1985).

Morphological methods

Shell length (**L**), width (**W**), and height (**H**) were measured as described by Lorenz (2017) using a vernier calliper. Counts of columellar teeth (**CT**) excluded the terminal ridge bordering the anterior canal but included the posterior-most denticle that merges with the anterior edge of the columella callus bordering the posterior canal. All labral

teeth (**LT**) were counted. Quantitative comparisons used the shell formula [L (W/L-H/L-H/W) nLT: nCT], where L = average shell length (mm), W/L = average width/length ratio (%), H/L = average height/length ratio (%), H/W = average height/width ratio (%), and nLT and nCT are normalised labral and columellar tooth counts, respectively, for a hypothetical shell length of 25 mm (Schilder 1935), calculated as described by Lorenz (2017). Descriptive terminology generally follows that of Lorenz (2002, 2017).

Abbreviations

TMAG	Tasmanian Museum and Art Gallery, Hobart, Australia;
AM	Australian Museum, Sydney, Australia;
MR	Mike Roberts collection, Flinders Island, Tasmania, Australia;
PS	Paul Southgate collection, Brisbane, Australia.

Results

Systematics

Class Gastropoda Cuvier, 1795

Order Littorinimorpha Golikov & Starobogatov, 1975

Superfamily Cypraeoidea Rafinesque, 1815

Family Cypraeidae Rafinesque, 1815

Genus *Austrocypraea* Cossmann, 1903

Type species. *Cypraea contusa* McCoy, 1877, by original designation. Balcombian, Middle Miocene, Fossil Beach, Victoria, Australia.

***Austrocypraea jimgracei* sp. nov.**

<https://zoobank.org/C1F042E5-6E4B-4038-A757-53B289C377CD>

Figs 1, 2, 3, Table 1

Material examined. Holotype. AUSTRALIA, Lackrana, Flinders Island, Tasmania; 40°06'37"S, 148°10'18"E; May, 2012; P.C. Southgate and M. Roberts leg.; dry specimen (fossil); among spoil material excavated for farm dam; TMAGZ10628.

Paratypes. AUSTRALIA; same location as holotype; May, 2012-Feb, 2021; P.C. Southgate and M. Roberts leg.; dry specimens (fossils); among spoil material excavated for farm dam; TMAGZ10629 (1 specimen); AM F.156043 (1 specimen); AM F.156044 (1 specimen); MR 635 (1 specimen); PS CF.174/175 (2 specimens).

Other material. AUSTRALIA; same location as holotype; May, 2012-Feb, 2021; P.C. Southgate and M. Roberts leg.; dry specimens (fossils); among spoil material

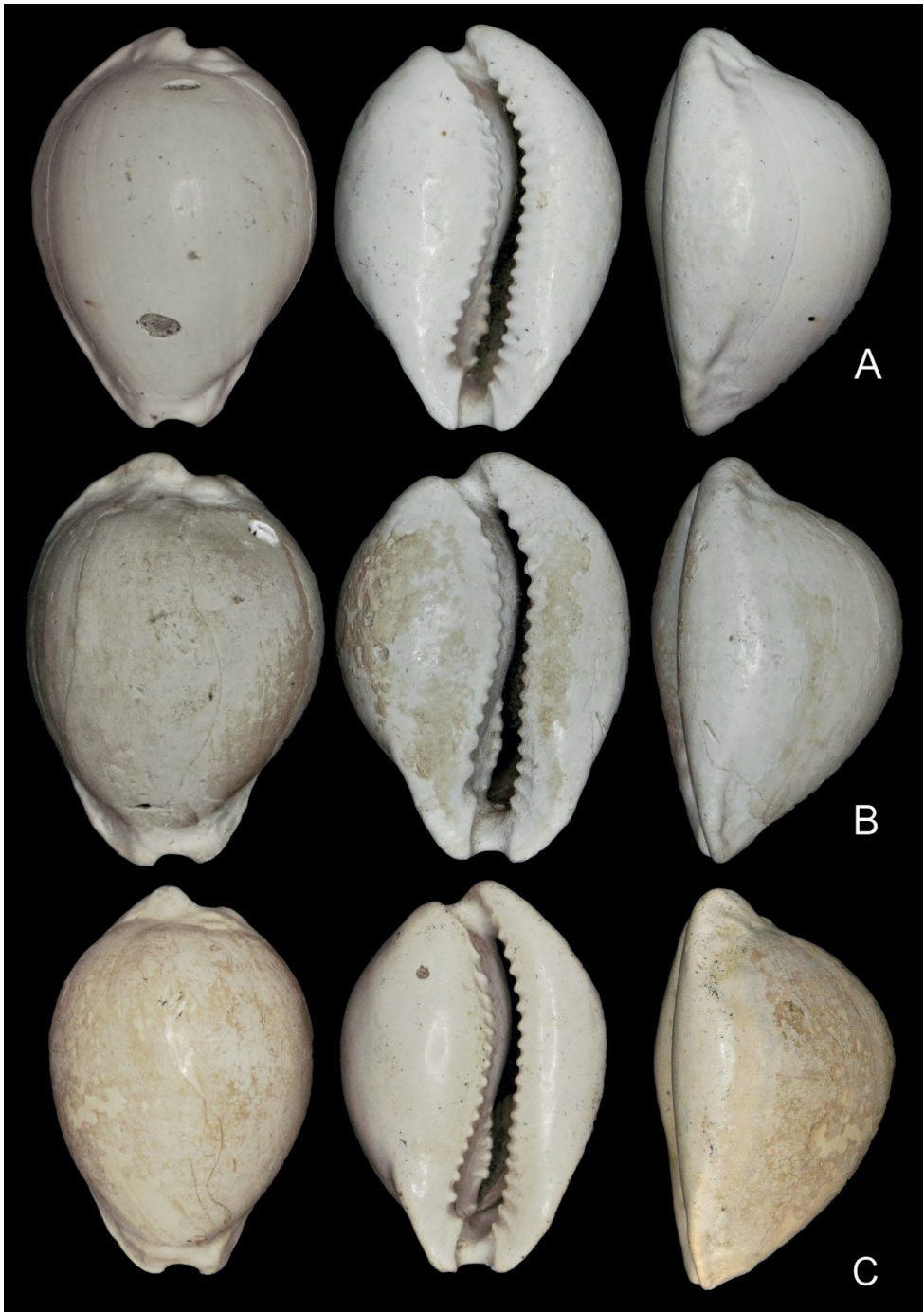


Figure 1. *Austrocypraea jimgracei* sp. nov.; dorsal, ventral and marginal (labral) aspects **A** holotype, TMAGZ10628 **B** paratype 1, TMAG Z10629 **C** paratype 5, senior author collection (PS CF.174)

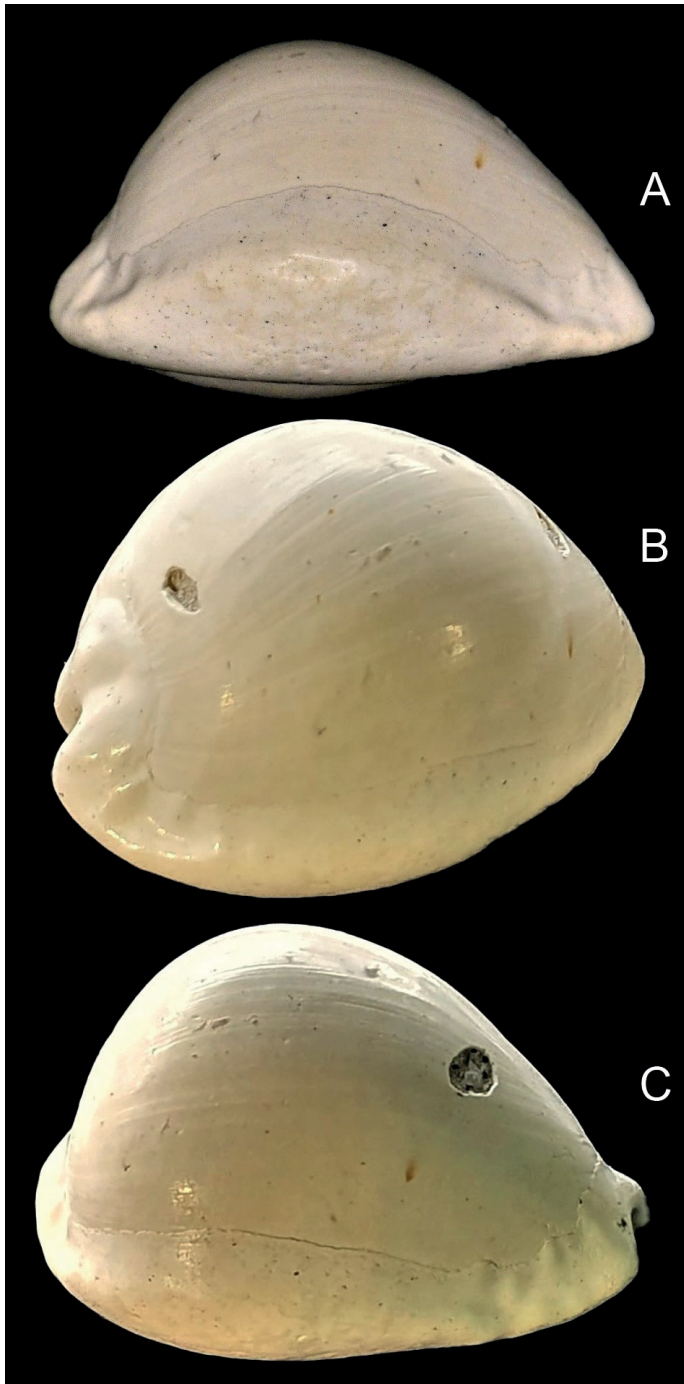


Figure 2. Detail of labral margin of the holotype of *Austrocypraea jimgracei* sp. nov. (TMAGZ10628) showing labral margin (**A**), posterior labral groove (**B**) and anterior labral groove (**C**).

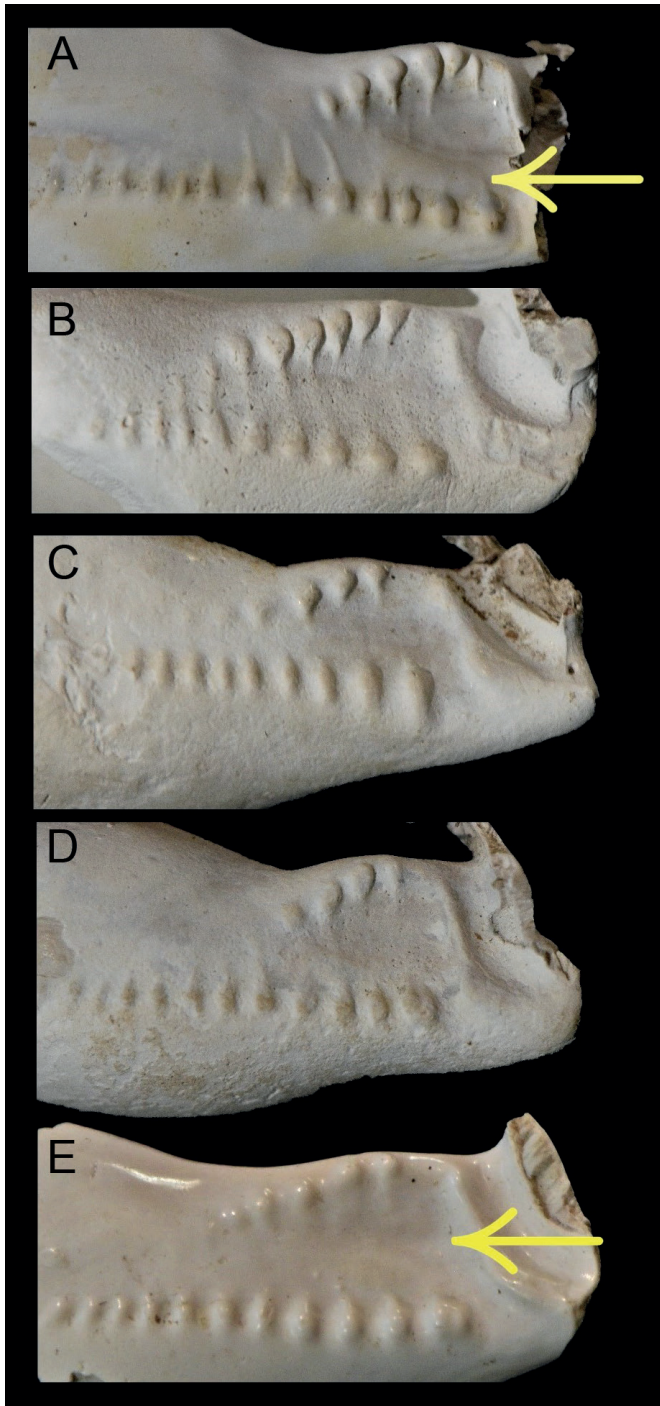


Figure 3. Detail of the fossula of sectioned shells of *Austrocypraea jimgracei* sp. nov., showing variation amongst specimens (TMAGZ10630). Arrows indicate a slightly raised ridge (**A**) and shallow longitudinal depression (**E**) sometimes present on the fossula.

excavated for farm dam; PS CF.305/306 (2 specimens); MR 657/658 (2 specimens); TMAGZ10630 (five partial specimens).

Diagnosis. *Austrocypraea jimgracei* sp. nov. can be separated from all other members of the genus, fossil and extant, by a combination of the following characteristics: shell ovate to sub-pyriform, humped, highest point towards posterior, shell height around 71% length, shell width around 59% length; anterior extremity subtruncate, not extended in lateral profile, supported by well-defined anterior lateral flanges; protoconch paucispiral, spire projecting, overlain by callus. Aperture gently curved to the left posteriorly, widening slightly towards anterior; evenly spaced, relatively strong dentition; 13–17 columellar teeth, restricted to aperture, larger towards anterior; 17–21 labral teeth are longer, incised, and restricted to aperture margin. Fossula is broad, concave and smooth centrally, with shallow, barely discernible longitudinal depression or slightly raised ridge sometimes present; fossular margin with 4–6 denticles, visible in ventral view; anterior denticles not linked to adjacent columellar teeth by transverse ridges, but fine ridges may link posterior fossular denticles to adjacent columellar teeth. Columella smooth posterior to the fossula, lacking a defined columella ridge. Labral margin heavily callused, forming a distinct marginal edge, bent up towards the dorsum centrally; shallow anterior and posterior labral grooves may accommodate small, irregular, often elongate, pustules dorsal to the labral marginal edge; marginal edge may be weakly crenulate where marginal pustules intersect.

Description. Average size for the genus (Table 1); shell length 23.1–25.5 mm (mean 24.5), W/L = 69–73% (mean 71%), H/L = 58–61% (mean 59%), H/W = 82–85% (mean 84%); ovoid to sub-pyriform, maximum shell height towards posterior; protoconch paucispiral, rounded; spire projecting, overlain by callus (Fig. 1). Shell formula: [24 (71-59-84) 19:15]. Dorsal surface smooth except for weak longitudinal growth lines. Basal callus strongly developed; base rounded. Shell margins callused; left margin rounded, smooth; labral marginal callus well developed, with distinct marginal edge, bent up towards the dorsum centrally (Fig. 2A); more sharply margined anteriorly and posteriorly, forming shallow labral grooves that may accommodate pustules or small tubercles, often elongate, dorsal to the marginal edge (Fig. 2B, C). The right marginal edge may be slightly crenulate where pustules intersect. Anterior and posterior canals are deep and bordered by strong projecting callus; anterior canal with dorsoventral orientation, not angled; anterior terminal subtruncate, hardly extended, supported by anterior lateral flanges; anterior tips moderately pointed. Posterior canal short, bent to the left; bordered on the left by well-developed columellar callus, not extending as far as the posterior end of the labrum. Aperture gently curved to the left posteriorly, widening anteriorly. Fossula broad (Fig. 3), concave and constricted posteriorly; bordered anteriorly by a well-defined terminal pleat, thickening where it joins the terminal ridge. Fossula margin with 4–6 denticles becoming weaker posteriorly; anterior denticles not linked to adjacent columellar teeth by transverse ridges; poorly developed ribs may link the smaller denticles at the posterior end of the fossula with columellar teeth, where the fossula merges with the columella (Fig. 3B). Very weak ridges may extend onto the fossula from the marginal denticles and from

the anterior-most columellar teeth, but they do not join; central fossula smooth, with shallow, longitudinal depression (Fig. 3E) or slightly raised ridge on the central fossula sometimes evident (Fig. 3A). A well-defined fossular gap is present at the anterior end of the fossula margin, between the anterior-most marginal denticle and the dorsal extremity of the terminal pleat. Columella lacks a defined columellar ridge and is smooth posterior to the fossula. Columellar teeth (13–17, Table 1) spaced about one tooth width apart; present along the length of the columella, terminating at the anterior edge of columella callus bordering the posterior canal; anterior columella teeth stronger, first tooth generally stronger than those posterior to it, and separated from the terminal ridge by a prominent anterior gap. Labral teeth (17–21, Table 1) restricted to aperture, longer anteriorly, more elongate and more numerous than columella teeth.

Variation. Available specimens show variation in the angle of slope of the fossula, the number and form of fossular marginal denticles, and the presence, or otherwise, of a shallow depression or a slightly raised ridge on the central part of the fossula (Fig. 3). Pustules dorsal to the anterior and posterior labral margins may or may not be present or visible, and this probably relates to specimen maturity and the degree of preservation. Pustules may produce a weakly crenulate marginal edge in some specimens where (and if) they intersect. This feature is present in the holotype and its development is likely related to specimen maturity and the degree of callus development.

Differential diagnosis. Shell shape in cowries is commonly expressed using a ‘shell formula’ which reports linear shell measurements, and their ratios, as well as normalised tooth counts (Bridges and Lorenz 2013). The shell formula of *Austrocypraea jimgracei* sp. nov. is compared with those of all other *Austrocypraea* fossil species, for which morphometric data are available, in Table 2. In terms of shell shape (i.e., W/L, H/L and H/W), *A. jimgracei* sp. nov. is closest to *A. amae* and *A. rumballi* (Table 2) and a broader range of shell characteristics is compared for these three species in Table 3. The new species is similar in size and dimensions to *A. amae*, where shell width relative to length (71%), height relative to length (60%), and height relative to width (84%) are very similar to values of 71%, 59% and 84%, respectively, for the same parameters in *A. jimgracei* sp. nov. (Table 2). The anterior extremity of *A. amae* is shorter and less produced, and the anterior canal is wider, deeper and more angled than in *A. jimgracei* sp. nov. The anterior lateral flanges supporting the anterior extremity of *A. jimgracei* sp. nov. are more developed than in *A. amae*. The posterior extremity is more produced in *A. jimgracei* sp. nov. than in *A. amae*, particularly on the right side. The new species can be easily separated from *A. rumballi* by its much larger size.

Clear differences in fossula structure also separate *A. jimgracei* sp. nov. from *A. amae* and *A. rumballi*. The fossula of *A. amae* is crossed by ribs which are continuous with the anterior columellar teeth and extend to the inner margin of the fossula (Table 3). Denticles on the inner fossular margin of *A. jimgracei* sp. nov. are separated from adjacent

anterior columellar teeth by a smooth central area of the fossula. The fossula of *A. rumballi* is similar to that of *A. jimgracei* sp. nov. but differs by protruding further into the aperture, having a greater number of denticles on the inner margin (generally 6–7), and transverse ridges that link the denticles to columellar teeth, at least posteriorly (Yates 2008). An interesting feature of the fossula of *A. rumballi* is an indistinct tubercle or longitudinal ridge in the middle of the fossula between the terminal ridge and the first or second transverse ridge of the fossula (Yates 2008). A shallow longitudinal depression or slightly raised ridge is sometimes present in the middle of the fossula of *A. jimgracei* sp. nov. (Fig. 3); however, the form of this feature varies and it is absent in some specimens.

The Miocene species *A. contusa* and *A. goudeyana* have similar size and proportions to *A. jimgracei* sp. nov., and the form of the anterior extremity, supported by distinct anterior lateral flanges, may also be similar for these species. However, *A. contusa* and *A. goudeyana* are readily separated from *A. jimgracei* sp. nov. because of their more produced anterior extremity, narrower aperture, which has consistent width throughout, and stronger dentition that may extend onto the columella. The form of the heavily callused labral margin of *A. jimgracei* sp. nov., that is bent up towards the dorsum centrally, is unique within the genus. Other species within the genus, such as *A. contusa*, *A. goudeyana* and *A. subcontusa*, may also develop a well-defined thickened labral margin, but unlike that of *A. jimgracei* sp. nov., when present, it generally forms a thin step-like rim to the shell margin that does not bend up towards the dorsum. The shells of a number of *Austrocypraea* species, including the extant *A. reevei*, have shallow contusions or ‘malleation’ on the dorsal surface of the shell, but this is not a ubiquitous feature of the genus. For example, malleation is prominent on the shells of *A. contusa* and *A. goudeyana*, less prominent and generally restricted to the posterior half of the body whorl in *A. rumballi* and *A. amae*, obscure or absent in *A. scalena*, but totally lacking in *A. onkastoma*, *A. archeri*, *A. subsidua* and *A. parallela*, and in all examined specimens of *A. jimgracei* sp. nov.

Etymology. Named in honour and in memory of the late Jim Grace of Lackrana, Flinders Island, on whose property all specimens of the new species were recovered.

Distribution. Known only from the Cameron Inlet Formation, Lackrana area, Flinders Island, Tasmania.

Table 1. Descriptions and repositories of the type series of *Austrocypraea jimgracei* sp. nov.

Specimens (repository)	Length (mm)	Width (mm)	Height (mm)	Columellar teeth	Labral Teeth
Holotype (TMAGZ10628)	24.2	17.5	14.5	16	21
Paratype 1 (TMAG Z10629)	25.4	18.5	15.4	13	17
Paratype 2 (AM F.156043)	23.1	16.4	13.8	16	20
Paratype 3 (AM F.156044)	25.2	18.2	14.9	16	18
Paratype 4 (MR 635)	23.6	16.4	13.9	14	18
Paratype 5 (PS CF.174)	24.4	16.9	14.4	15	20
Paratype 6 (PS CF.175)	25.5	17.7	14.9	17	20
Mean (\pm SD)	24.5 (\pm 0.9)	17.4 (\pm 0.8)	14.5 (\pm 0.6)	15.3 (\pm 1.4)	19.0 (\pm 1.5)

Table 2. Shell formulae [L (W/L – H/L – H/W) nLT: nCT] for known *Austrocypraea* fossil species for which complete morphometric data are available.

Species	Shell formula	Data source(s)
<i>Austrocypraea constricta</i>	14 (59-48-81) 26:14	Schilder (1935)
<i>A. archeri</i>	21 (61-50-86) 22:17	PS collection
<i>A. subsidua</i>	22 (65-52-80) 25:18	Schilder (1935)
<i>A. scalena</i>	30 (64-57-89) 24:16	Schilder (1935)
<i>A. subcontusa</i>	15 (67-55-82) 18:15	Schilder (1935)
<i>A. contusa</i>	26 (74-66-89) 21:17	Schilder (1935)
<i>A. ampullacea</i>	34 (56-53-94) 27:22	Schilder (1935)
<i>A. parallela</i>	18 (53-46-86) 32:20	Schilder (1935)
<i>A. amae</i>	28 (71-60-84) 22:16	Fehse and Kendrick (2000)
<i>A. rumballi</i>	16 (73-63-85) 16:14	Fehse (2003); Yates (2008)
<i>A. goudeyana</i>	22 (68-58-86) 17:16	Fehse (2013)
<i>A. jimgracei</i> sp. nov.	24 (71-59-84) 19:15	This study

Table 3. Comparison of shell characters of *Austrocypraea amae* Fehse & Kendrick, 2000, *A. rumballi* Fehse, 2003 and *A. jimgracei* sp. nov.

Character	Species		
	<i>Austrocypraea amae</i>	<i>A. rumballi</i>	<i>A. jimgracei</i> sp. nov.
Length (mm):	20.7–38.9	11.0–22.1	23.1–25.5
Shape:	ovate, sub-pyriform to sub-cylindrical; highest point in posterior third. Short anterior extremity not extended in lateral profile.	broadly ovoid; inflated specimens globular. Anterior extremity short but extended in lateral profile.	ovate to sub-pyriform; highest point towards posterior; short anterior extremity, not extended in lateral profile, supported by well-developed lateral flanges.
Sculpture:	moderately to weakly malleate, mainly posteriorly; base smooth.	malleation present on the left side of many specimens but absent in others; base smooth.	malleation absent; base smooth.
Fossula:	broad, impressed, traversed by 6 or 7 ribs continuous with columella teeth.	broad with projecting inner margin; fossula denticles (– 6) linked to columella teeth by transverse ridges becoming obsolete anteriorly. Indistinct tubercle or ridge centrally.	broad, inner margin with 4–6 denticles that do not connect to columella teeth; central fossula smooth. Shallow, longitudinal depression or raised area sometimes present centrally.
Labral margin:	rounded but not heavily thickened; generally rounded in posterior profile.	rounded but not heavily thickened; generally rounded in posterior profile.	heavily callused, forming a distinct marginal edge, bent up centrally; pustules or small tubercles often present dorsal to marginal edge.
Data source(s):	Fehse and Kendrick, 2000	Fehse, 2003; Yates (2008)	This study

Key to the known fossil species of *Austrocypraea*

The following key is based on shell morphology and is modified from Schilder (1935) to include subsequently described species.

- 1 Shell ovate, globular or pyriform; fossula abruptly constricted posteriorly...2
- Shell cylindrical; fossula scarcely constricted posteriorly, broad but rather shallow.....*A. parallela*

- 2 Fossula very broad, concave, projecting; dorsum smooth, small contusions more apparent posteriorly if present; columella smooth posteriorly.....3
- Fossula rather narrow, concave; dorsum with numerous, close small contusions throughout; columellar teeth often produced across the columella posteriorly.....5
- 3 Shell not exceeding 17 mm; aperture sinuous, inner lip rather constricted in the anterior third; shell subcylindrical.....*A. constricta*
- Shell exceeding 17 mm.....4
- 4 Base flattened; aperture rather wide; anterior top of outer lip rather rounded; fossula extremely broad, irregularly ribbed.....*A. subsidua*
- Base convex; aperture equally narrow but may widen slightly anteriorly.....5
- 5 Shell generally not exceeding 20 mm.....6
- Shell exceeding 20 mm.....7
- 6 Shell ovate, slightly depressed; dentition rather coarse, columella teeth often produced.....*A. subcontusa*
- Shell ovate to globose; columella teeth short, second tooth weakly developed; fossula greatly protruding, with central tubercle.....*A. rumballi*
- 7 Elongate; dentition extremely fine and numerous.....*A. ampullacea*
- Shell inflated, pyriform, ovate or globular.....8
- 8 Pyriform to globular, inflated, dorsum intensely malleate.....9
- Ovate to sub-pyriform, inflated, dorsal contusions reduced or absent.....10
- 9 Anterior terminal collar elongated, elevated in lateral profile...*A. goudeyana*
- Anterior terminal collar shorter and low in lateral profile.....*A. contusa*
- 10 Fossula ribbed, or marginal denticles present.....11
- Fossula smooth, without marginal denticles; columellar teeth developed posteriorly, no dorsal contusions.....*A. onkastoma*
- 11 Aperture equally narrow throughout.....12
- Aperture widening towards anterior.....13
- 12 Sub-pyriform; narrow, ribbed fossula; no dorsal contusions; rarely exceeding 27 mm.....*A. archeri*
- Ovate, mostly exceeding 27 mm; fossula regularly ribbed.....*A. scalena*
- 13 Ovate to sub-pyriform; fossula traversed by 6 or 7 ribs continuous with columellar teeth; contusions, if present, more apparent posteriorly.....*A. amae*
- Ovate to sub-pyriform; fossula smooth centrally, margin with 4–6 denticles; no dorsal contusions; well-developed labral margin.....*A. jimgracei* sp. nov.

Discussion

Austrocypraea jimgracei sp. nov. is only the second known member of the genus from the Pliocene and this description increases the number of known fossil species within *Austrocypraea* to thirteen. The new species has characteristics that are typical of the genus, including a well-produced denticulate fossula, a paucispiral protoconch indicating

intracapsular development, and a projecting spire. It also has some characteristics that are not present in any other *Austrocypraea* species, including a heavily callused labral margin and the presence of pustules or small tubercles within the labral grooves above (dorsal to) the marginal edge. Extensive molecular analysis within the family Cypraeidae (e.g., Meyers 2003, 2004) has shown that the closest living relatives to *Austrocypraea* are within the genus *Raybaudia* Lorenz, 2017, and that both genera evolved from *Lyncina* Troschel, 1863, shortly after it split from *Callistocypraea* Schilder, 1927 (Lorenz 2017). It is interesting to note that species with similar development of the labral shell margin, some of which may be tuberculate or pustulate, are present within these three genera most closely related to *Austrocypraea*. It is also interesting to note that despite the close phylogenetic relationship between these three Indo-West Pacific genera and *Austrocypraea*, they differ from *Austrocypraea* in undergoing pelagic not intracapsular development (Lorenz 2017).

Acknowledgements

We thank Betty and Jim Grace and their family for access to their property for specimen collection and Dawn and Naomi for support and technical assistance. We also thank Drs Felix Lorenz and Adam Yates, who provided constructive inputs to this paper. This study was supported by University of the Sunshine Coast Research Initiative funding to the first author.

References

- Bridges RJ, Lorenz F (2013) A revised morphometric formula for the characterisation of cowries (Gastropoda: Cypraeidae). *Conchylia* 43(1–4): 27–40.
- Darragh TA (1985) Molluscan biogeography and biostratigraphy of the Tertiary of south-eastern Australia. *Alcheringa* 9(2): 83–116. <https://doi.org/10.1080/03115518508618960>
- Fehse D (2003) Katalog der fossilen Cypraeoidea (Mollusca: Gastropoda) in der Sammlung Franz Alfred Schilder. III.I Die Gattung *Austrocypraea* Cossmann, 1903 (Mollusca: Gastropoda: Cypraeoidea) in Australien. *Club Conchylia Informationen* 35: 49–73.
- Fehse D (2013) A new fossil species of *Austrocypraea* (Mollusca: Gastropoda: Cypraeidae) from Red Bluff, Victoria of Australia. *Palaeontographica. Abteilung A* 299(1–6): 115–125. <https://doi.org/10.1127/pala/299/2013/115>
- Fehse D, Kendrick GW (2000) A new species of *Austrocypraea* (Gastropoda: Cypraeidae) from the Late Pliocene of the Eucla Basin, southern Australia. *Records of the Western Australian Museum* 20: 95–101.
- Goudey CJ (2015) A pictorial guide of Australian fossil cowries and their allies. C.J. Goudey, Avalon. 87 pp.
- Lorenz F (2002) New worldwide cowries. *ConchBooks*, Hackenheim, 292 pp.

- Lorenz F (2017) Cowries: A guide to the gastropod family Cypraeidae. Volume 1: Biology and systematics. Conchbooks, Harxheim, 644 pp.
- Meyers CP (2003) Molecular systematics of cowries (Gastropoda: Cypraeidae) and diversification patterns in the tropics. *Biological Journal of the Linnean Society* 79(3): 401–459. <https://doi.org/10.1046/j.1095-8312.2003.00197.x>
- Meyers CP (2004) Towards comprehensiveness: Increased molecular sampling within Cypraeidae and its phylogenetic implications. *Malacologia* 46(1): 127–156.
- Schilder FA (1935) Revision of the Tertiary Cypraeacea of Australia and Tasmania. *Proceedings of the Malacological Society of London* 21(6): 325–355.
- Southgate PC, Militz TA, Roberts M (2021) A new species of *Umbilia* Jousseume, 1884 (Mollusca: Cypraeidae) from the Australian Pliocene. *Molluscan Research* 41(3): 214–221. <https://doi.org/10.1080/13235818.2021.1962588>
- Sutherland FL, Kershaw RC (1970) The Cainozoic geology of Flinders Island, Bass Strait. *Papers and Proceedings of the Royal Society of Tasmania* 105: 151–176. <https://doi.org/10.26749/rstpp.105.151>
- Wilson B (1993) *Australian Marine Shells, Vol. 1*. Odyssey Publishing, Kallaroo, Western Australia, 408 pp.
- Yates AM (2008) Two new cowries (Gastropoda: Cypraeidae) from the middle Miocene of South Australia *Alcheringa* 32: 353–364. <https://doi.org/10.1080/03115510802417927>
- Yates AM (2009) The oldest South Australian cowries (Gastropoda: Cypraeidae) from the Paleogene of the St Vincent Basin. *Alcheringa* 33(1): 23–31. <https://doi.org/10.1080/03115510802618219>

Evidence of late root formation of molars in Anderson's red-backed vole, *Eothenomys andersoni* (Thomas, 1905) (Cricetidae, Rodentia), and arguments for its generic allocation

Masahiro A. Iwasa¹, Yukibumi Kaneko², Yoshiyuki Kimura³

1 College of Bioresource Sciences, Nihon University, Fujisawa, Kanagawa 252-8510, Japan **2** Takayacho 502-4, Sakaide, Kagawa 762-0017, Japan **3** Mitouchi 6-10, Houkida, Fukushima, Fukushima 960-8163, Japan

Corresponding author: Masahiro A. Iwasa (iwasa.masahiro@nihon-u.ac.jp)

Academic editor: R. López-Antoñanzas | Received 25 May 2022 | Accepted 15 September 2022 | Published 7 October 2022

<https://zoobank.org/E3F79476-248F-40B0-A02B-9B0A06103A28>

Citation: Iwasa MA, Kaneko Y, Kimura Y (2022) Evidence of late root formation of molars in Anderson's red-backed vole, *Eothenomys andersoni* (Thomas, 1905) (Cricetidae, Rodentia), and arguments for its generic allocation. ZooKeys 1123: 187–204. <https://doi.org/10.3897/zookeys.1123.86960>

Abstract

We evaluated the molars in Anderson's red-backed vole ($n = 114$) from the Kii Peninsula of Honshu, Japan. Two of the specimens are considered extremely old aged based on their dimensions and on the loss of alveolar capsules of M^2 , and a third one is also old based on its strongly worn left M^3 and M_1 . Of the former two individuals, one showed an incipient closure of re-entrant angles at its basal end, as estimated from the difference between the occlusal patterns of the occlusal and basal surfaces of the left M_2 . The latter individual also showed a complete closure of the basal end in the left M^3 . These patterns differ from incipient roots observed in other vole taxa but were similar to a previous example of incipient roots in Anderson's red-backed vole. Therefore, we suggest that molar roots in this species form at an extremely late age or by strong wear. Root formation in molars is considered an important diagnostic character, as *Eothenomys* molars lack roots, while *Craseomys* molars develop roots at a late age. However, this dental character may be particularly difficult to assess in voles under natural conditions. Considering previous phylogenetic findings based on molecular analyses, *Craseomys* is the most appropriate genus for Anderson's and other Asiatic red-backed voles.

Keywords

Craseomys, dental characteristics, taxonomy

Introduction

The taxonomic allocation of Anderson's red-backed vole, *Eothenomys andersoni* (Thomas, 1905) (Rodentia, Cricetidae, Arvicolinae), is still a matter of discussion, as is that of Smith's red-backed vole, *E. smithii* (Thomas, 1905) (Iwasa 2015a, 2015b). The distribution of Anderson's red-backed vole is restricted to north-eastern and central Honshu and the Kii Peninsula of western Honshu, Japan (Iwasa 2015a). Previous studies of this vole taxon have disclosed intraspecific morphological and genetical variations (Aimi 1967, 1980; Miyao 1981; Tsuchiya 1981; Kitahara 1995; Kitahara and Harada 1996; Suzuki et al. 1999; Iwasa and Tsuchiya 2000; Iwasa and Suzuki 2002a, b, 2003). Various authors have varying opinions on its specific allocation: one species for all of the geographical populations (Kitahara 1995; Iwasa 2015a), two species for the north-eastern to central Honshu and the Kii Peninsula populations (Musser and Carleton 2005), or three species for the north-eastern Honshu, the central Honshu, and the Kii Peninsula populations (Imaizumi 1998). *Evotomys* Coues, 1874, *Craseomys* Miller, 1900, *Aschizomys* Miller, 1899, *Clethrionomys* Tilesius, 1850, *Phaulomys* Thomas, 1905, *Eothenomys* Miller, 1900, and *Myodes* Pallas, 1811 has been used for the species (Miller 1896, 1898; Thomas 1905; Anderson 1909; Tokuda 1941; Imaizumi 1960; Jameson 1961; Corbet 1978; Aimi 1980; Kawamura 1988; Corbet and Hill 1991; Musser and Carleton 1993, 2005; Kaneko and Murakami 1996; Luo et al. 2004; Shenbrot and Krasnov 2005; Suzuki et al. 2014; Iwasa 2015a, b; Kryštufek and Shenbrot 2022). Recent opinions have allocated Anderson's red-backed vole to the genus *Craseomys* with other species having the *rufocanus* cytotype of the G-band patterns of chromosomes (Gamperl 1982; Modi and Gamperl 1989; Iwasa and Suzuki 2002b; Kohli et al. 2014; Tang et al. 2018; ASM (American Society of Mammalogists) Mammal Diversity Database, <https://mammaldiversity.org/>). In addition, according to Musser and Carleton (2005) and the ASM Mammal Diversity Database, a population of Anderson's red-backed vole from the Kii Peninsula received specific rank, as *Myodes* (= *Clethrionomys*) *imaizumii* or *Craseomys* *imaizumii*, based on an assumed phylogenetically independent position (Iwasa et al. 1999; Suzuki et al. 1999).

At present, the vole has been assigned either to *Eothenomys*, *Myodes* (= *Clethrionomys*; see Kryštufek et al. 2020 concerning the availability of these two names for the genus of red-backed voles), or *Craseomys* (Kaneko and Murakami 1996; Musser and Carleton 2005; Iwasa 2015a, b; ASM Mammal Diversity Database; Tang et al. 2018; Kryštufek et al. 2020; Kryštufek and Shenbrot 2022). The different allocations are based on the possession or lack of root in its molars: *Eothenomys* (as a subgenus of *Microtus* in Miller 1896: 29, 44–47) has rootless molars and *Clethrionomys* (= *Evotomys* in Miller 1896: 29, 42–44) rooted ones, and *Craseomys* has molars developing roots late in life (Miller 1900: 87–91). Aimi (1980) studied allometric cranial measurements and molars of Anderson's red-backed vole and referred it *Eothenomys* because of exclusively rootless molars in 416 individuals examined. Suzuki et al. (2014) also suggested that Anderson's red-backed vole should be allocated as *Eothenomys* based on cytogenetic criteria. However, Jameson (1961) and Kitahara (1995) already had reported some

teeth showing the beginnings of root formation: closed pulp cavities and incipient roots in one individual from a mountainous region of central Honshu (Jameson 1961: 599, 600); and signs of root closure, as in incipient roots, in the upper molars of one individual from the Kii Peninsula that had been kept in captivity (796 days old) (Kitahara 1995: 13). Consequently, Jameson (1961) allocated Anderson's red-backed vole to *Clethrionomys*, whereas Kitahara (1995) classified this vole as an *Eothenomys*, considering the abnormal condition of growth without free occlusion due to excessive growth of the incisors. The generic allocation of Anderson's red-backed vole has been discussed since its original description by Thomas (1905). The root condition of molars has been always an important argument for its generic status, even if it a bit ambiguous.

The purpose of the present study is to reconsider whether voles of this taxon have the potential to form roots in molars. We investigated signs of molar root formation, particularly in late-aged individuals in samples from the Kii Peninsula. On the basis of the current results, we re-evaluated the validity of the root condition of molars for generic determination in red-backed voles and tried to conclude the appropriate generic allocation of Anderson's and other Asiatic red-backed voles.

Materials and methods

Musser and Carleton (2005) distinguished two species within what has been known as Anderson's red-backed vole, *Myodes* (= *Clethrionomys*) *andersoni* for populations from north-eastern and central Honshu, and *M. imaizumii* for a population from the Kii Peninsula of Honshu. However, these taxa are now considered to be conspecific because it is possible to obtain fertile offspring for several generations from their crosses (Kitahara 1995) and because molecular analyses show substantial differentiations within and among the populations (Iwasa and Suzuki 2002a, b, 2003; Iwasa 2008). Therefore, in this study, we consider these taxa conspecific in accordance with Iwasa (2015a). In total, 114 individuals of Anderson's red-backed vole were collected using snap traps in the Wakayama Experimental Forest of Hokkaido University, Kozagawa, Wakayama Prefecture, Japan (33°39'N, 135°40'E), as shown in Appendix 1: Table A1. These individuals were collected in January to March, June, July, September, November, and December over 10 years (1986–1995) at the same sampling site, since collecting this species is difficult due to its low population density. For comparison, we also examined three individuals (HEG1-97, MAI-26, and MAI-347) of the grey red-backed vole, *M. rufocanus* (Sundevall, 1846) (Musser and Carleton 2005), from Hokkaido, Japan, that has rooted molars. These individuals are stored in the private collection in the laboratory of one of the authors.

Condylbasal length (CBL; the distance between the occipital condyle and the anterior point of the premaxillae) was measured to the nearest 0.1 mm using digital calipers. In addition, the height from the occlusal surface of the M² to the upper edge of the alveolar capsules of M² (HAC) was measured to the nearest 0.1 mm under a stereoscopic microscope using an objective micrometer (Kaneko 1988; Fig. 1; Appendix 1: Table A1). Moreover, from some skulls (HEG1-97, MAI-26, MAI-347, K6059, K7088, K7344, and

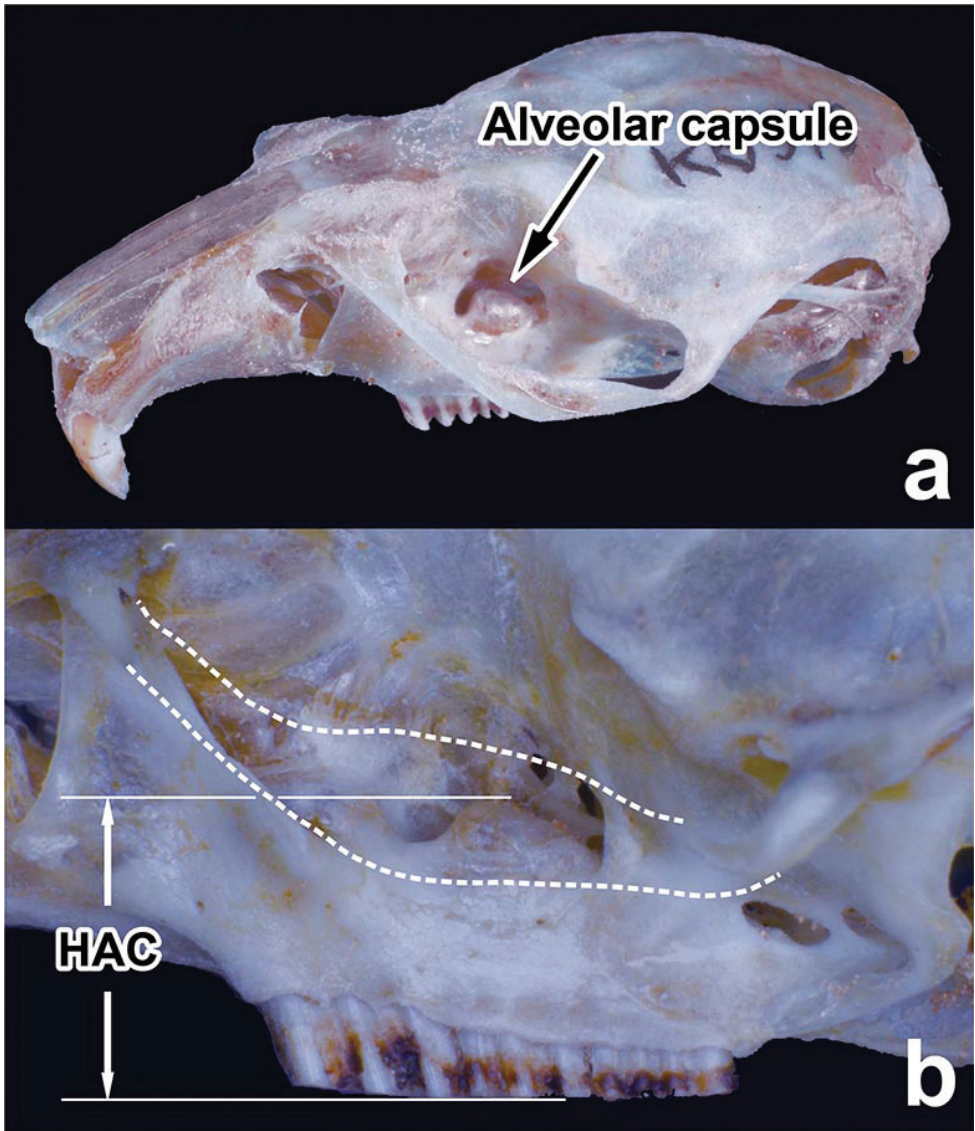


Figure 1. Position of the alveolar capsule **a** height from the occlusal surface of M^2 to the upper edge of the alveolar capsule (HAC) at the left lateral view **b** dotted lines indicate outlines of the zygomatic arch, after its removal, to explain how the measurements were made.

K7367), we removed the molars and checked the enamel patterns at the occlusal and basal ends to detect a possible closure of the basal end, which would infer a root formation.

We defined adults as individuals that had reached sexual maturation (Appendix 1: Table A1) by correspondence to any of the following genital conditions: appearance of the papilla mammae, opening of the pubic symphysis, pregnancy, and the presence of placental scars in females, and the presence of the ductus epididymis at the cauda epididymis and

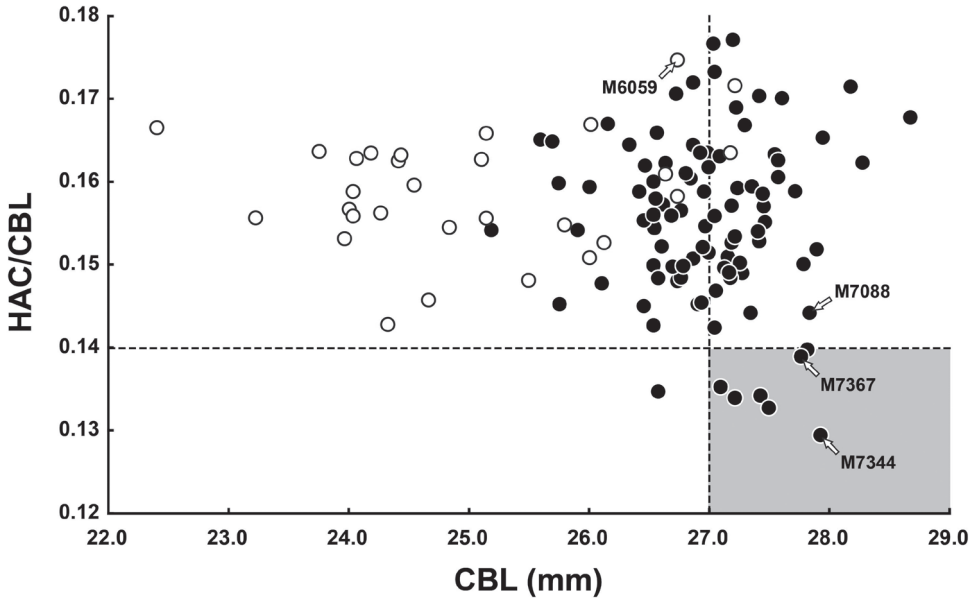


Figure 2. Scatter plots of a relationship between CBL and HAC/CBL. We recognized individuals showing quite lower HAC by the following definitions as old aged (greyish zone, see text): $HAC/CBL \leq 0.14$ and $CBL \geq 27.0$ mm. White and black circles indicate immature and mature individuals, respectively (Appendix 1: Table A1). Arrows indicate individuals showing incipient roots (see text and Appendix 1: Table A1).

testes larger than 7.5 mm in males. For references to the aging variation, external dimensions were measured and were described in Appendix 1: Table A1 as follows: body weight (BW), head and body length (HB), tail length (T), and hind foot length sine-unguis (HF).

Results

The studied individuals ($n = 114$) were determined as immature ($n = 30$) or mature ($n = 84$) ones based on their genital conditions (Appendix 1: Table A1). According to Kaneko (1990), the alveolar capsules of M^2 disappear in red-backed voles during root formation. Thus, we primarily analysed the relationship between HAC/CBL and CBL, displayed in a scatterplot (Fig. 2). This relationship indicated that sexually immature individuals showed a $HAC/CBL > 0.14$. In addition, we referred individuals with a $CBL \geq 27.0$ mm as mature because most immature individuals showed a $CBL \leq 27.0$ mm (Fig. 2). On the basis of these discriminations, individuals with both $HAC/CBL < 0.14$ and $CBL \geq 27.0$ mm were considered to be of extremely old age under natural condition, which probably correlates with an age of more than one year (Kitahara 1995). Namely, seven individuals included in the cluster with both $HAC/CBL < 0.14$ and $CBL \geq 27.0$ mm (greyish zone of Fig. 2; Appendix 1: Table A1) were studied for molar characteristics.

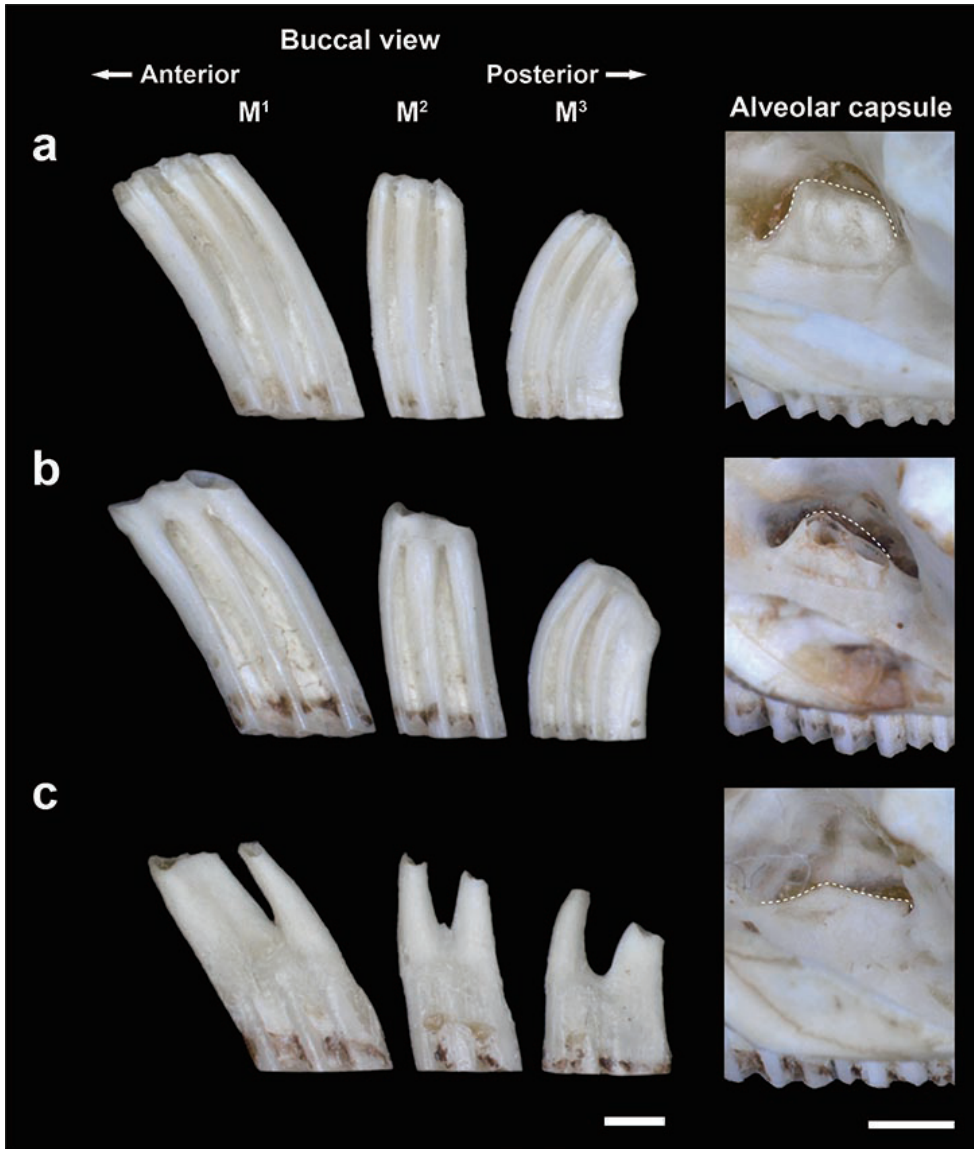


Figure 3. Typical buccal views of the left upper molars and alveolar capsule conditions of the grey red-backed vole showing a non-rooted type **a** MAI-26, an incipient rooted type (**b** HEG1-97 inverted image of a right capsule) and a completely rooted type **c** MAI-347. Dotted lines indicate outlines of alveolar capsules (partially broken in HEG1-97). Scale bars: 1 mm.

As a control group for the molar root condition, we documented three adult individuals of the grey red-backed vole with rooted molars as in Fig. 3 (Kaneko 1990; Nakata 2015). From these, the individuals MAI-26 and HEG1-97 were considered to be relatively younger, because one showed a higher alveolar capsule and no signs of root

formation and the other showed a moderately higher alveolar capsule and root formation, respectively, whereas the individual MAI-347 showed a completely formed root and the alveolar capsule was lost.

In the seven extremely old-aged individuals of Anderson's red-backed vole, we checked the condition of the basal ends of the molars. Of the seven individuals, two (K7344 and K7367) showed a loss of the alveolar capsules of M^2 . In addition, one individual (K7088) showed an extremely worn molar crown (Fig. 4a, b). Both buccal and lingual views of the left upper and lower molars and the alveolar capsule conditions of these individuals and of one with an apparent high alveolar capsule (K6059) are shown in Fig. 5. In K6059, all the basal ends of the tooth crown were open, and grooves occurred between the occlusal surfaces and the basal ends, in combination with a high alveolar capsule. In contrast, of the two individuals which lost their alveolar capsule, K7367 showed that the basal end tapered off (indicated by asterisks in Fig. 5) in M_2 . In addition, K7088 displayed that the basal end of M^3 showed a complete closure (indicated by white arrowheads in Figs 4, 5), irrespective of having a higher alveolar capsule of M^2 (Appendix 1: Table A1). Moreover, the occlusal surface of M_1 was cracked and split into two parts, and the basal end of the posterior part of M_1 was bent in the anterior direction and tapered off (indicated by black arrowheads in Figs 4, 5). Interestingly, the individual K7088 demonstrated that, as a rare example, the right M^3 was lacking and the right M^2 was elongated to the posterior part, and the left side of M_1 was extremely worn as compared with the right M_1 (Figs 4, 5).

Furthermore, we observed the enamel patterns of occlusal surfaces and the basal ends of the molars in detail with higher magnification, shown in Figs 6, 7. The enamel patterns of the basal ends corresponded completely to the enamel patterns of occlusal surfaces in individuals with apparent alveolar capsules and/or no sign of incipient closure of re-entrant angles at the basal ends, as in K6059 (Fig. 6), for example. On the other hand, in K7367, which lacked alveolar capsules, most molars showed the same situation as in K6059, but the basal ends of the left M_2 were dully tapered off as incipient closures of re-entrant angles (Figs 6, 7). Therefore, the enamel pattern of the occlusal surface of M_2 was apparently different from that of the basal ends of M_2 (Figs 6, 7). An incipient root formation of M_2 (HEG1-97) of the grey red-backed vole also showed that the enamel shape of the basal ends was completely different from that of its occlusal surface (Fig. 7).

Discussion

Thomas (1905) in his original description, allocated Anderson's red-backed vole to the genus *Evotomys*, which had been erected by Miller (1896), until the priority of *Clethrionomys* had been discovered by Palmer (1928), and later to *Eothenomys*, then a subgenus of *Microtus*, because roots in molars were considered being absent. Following Miller (1896), Jameson (1961) classified this vole as *Clethrionomys*. Also, Corbet (1978) and Corbet and Hill (1991) designated it as *Clethrionomys*, following Miller (1896) and

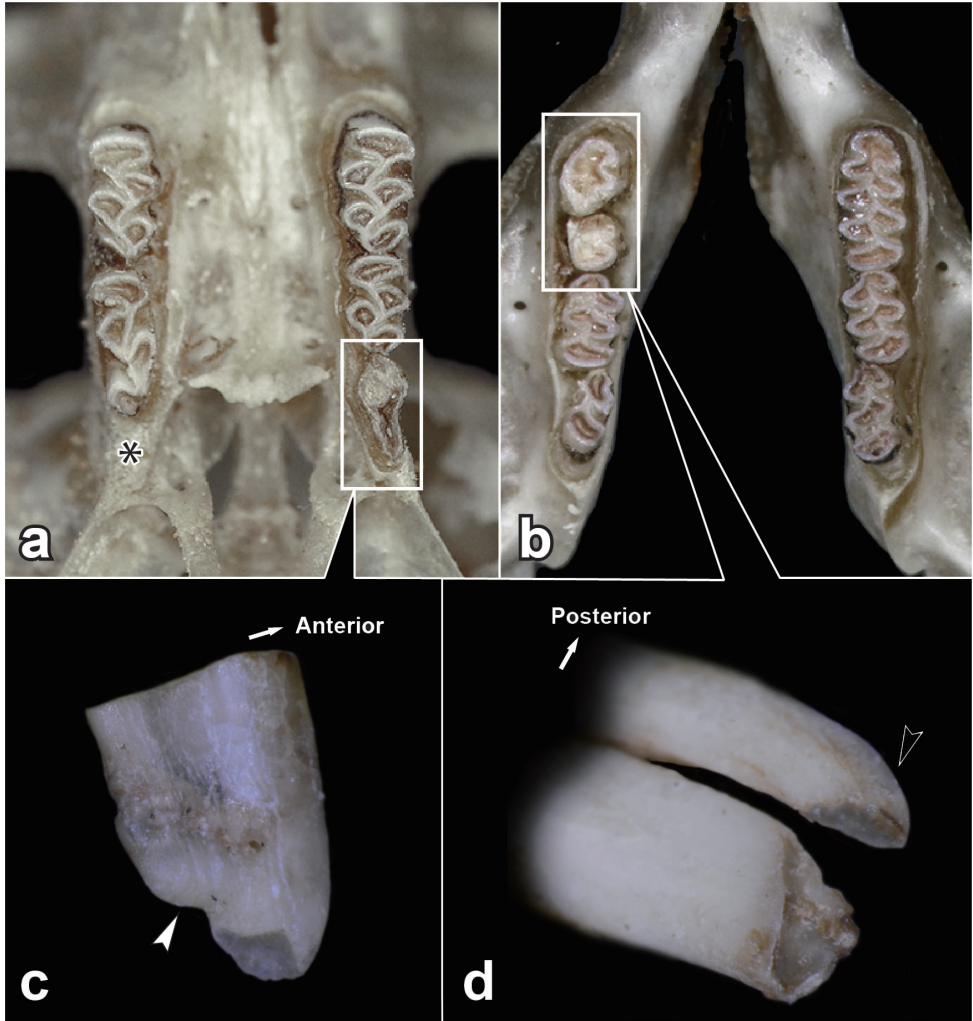


Figure 4. Occlusal views of the upper **a** and lower **b** tooth rows, buccal view of the left M³ **c** and antero-buccal view of the left M₁ **d** of individual K7088. Asterisk indicates an abnormal lack of the right upper third molar. Black and white arrowheads indicate a bent basal end and a complete closure of re-entrant angles at the basal end, respectively.

Jameson (1961). In addition, Musser and Carleton (2005) expanded the definition of *Myodes* (= *Clethrionomys*) to include species with and without rooted molars, allocating it to the genus *Myodes* based on molecular studies. On the other hand, some Japanese taxonomists have allocated Anderson's red-backed vole to the genus *Eothenomys* because it was believed that this taxon had rootless molars (Aimi 1980; Kitahara 1995; Kaneko and Murakami 1996; Iwasa 2015a, b), but the ASM Mammal Diversity Database recently assigned the Asian vole species *rufocanus*, *rex*, *andersoni*, *smithii*, *regulus*, and *shanseius* to the genus *Craseomys*, according to Abramson and Lissovsky (2012) and

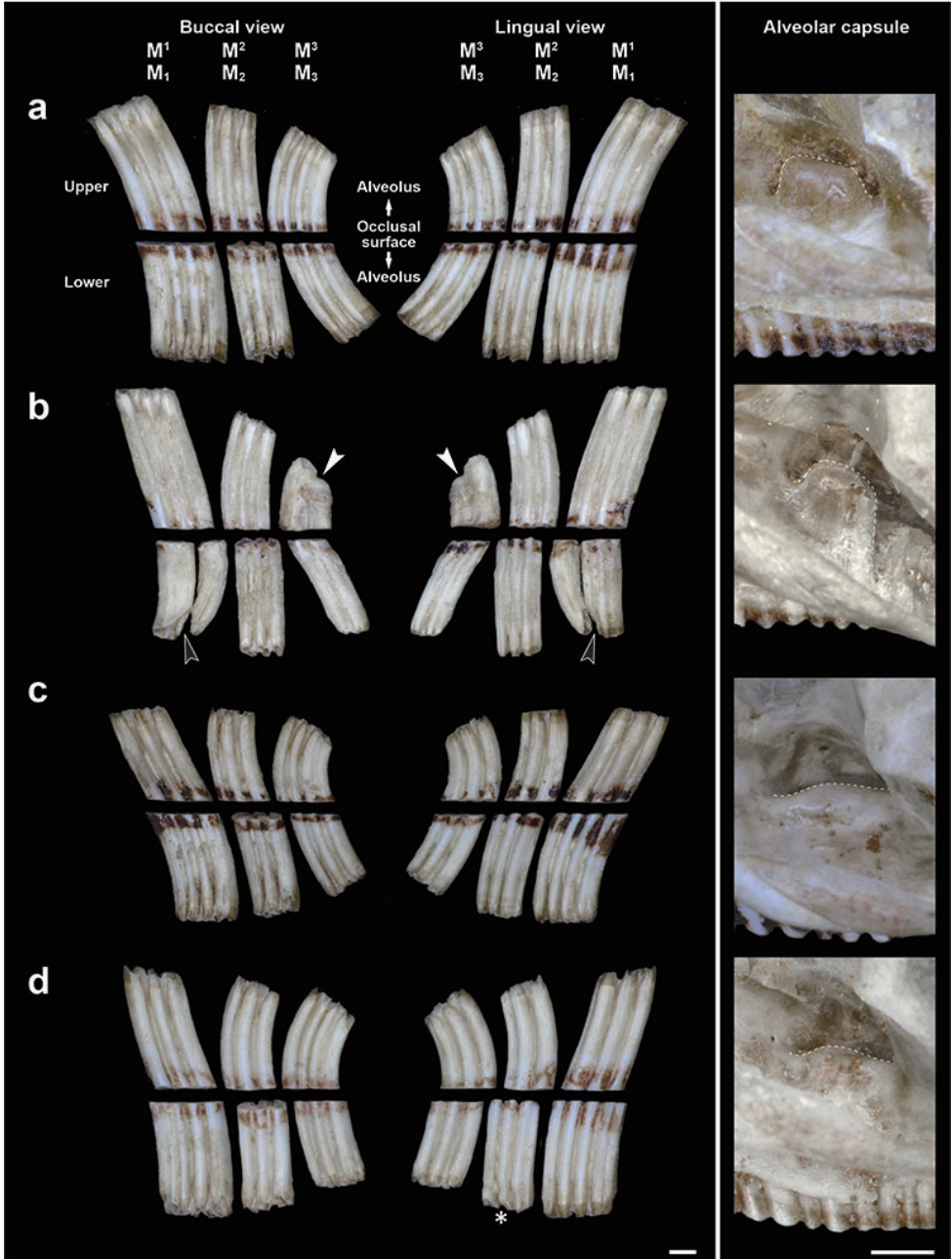


Figure 5. Typical buccal and lingual views of the left upper and lower molars and alveolar capsule conditions of four individuals of Anderson's red-backed vole **a** K6059 **b** K7088 **c** K7344 **d** K7367. Arrowheads indicate a root-like strong crevice caused by a crack. Basal ends indicated by white arrowheads and asterisks are considered to be complete closures of re-entrant angles as a root at the basal end and an incipient closure of re-entrant angles, leading to incipient root formation, respectively. Black arrowheads indicate abnormal cracks. Dotted lines indicate outlines of alveolar capsules. Scale bars: 1 mm.

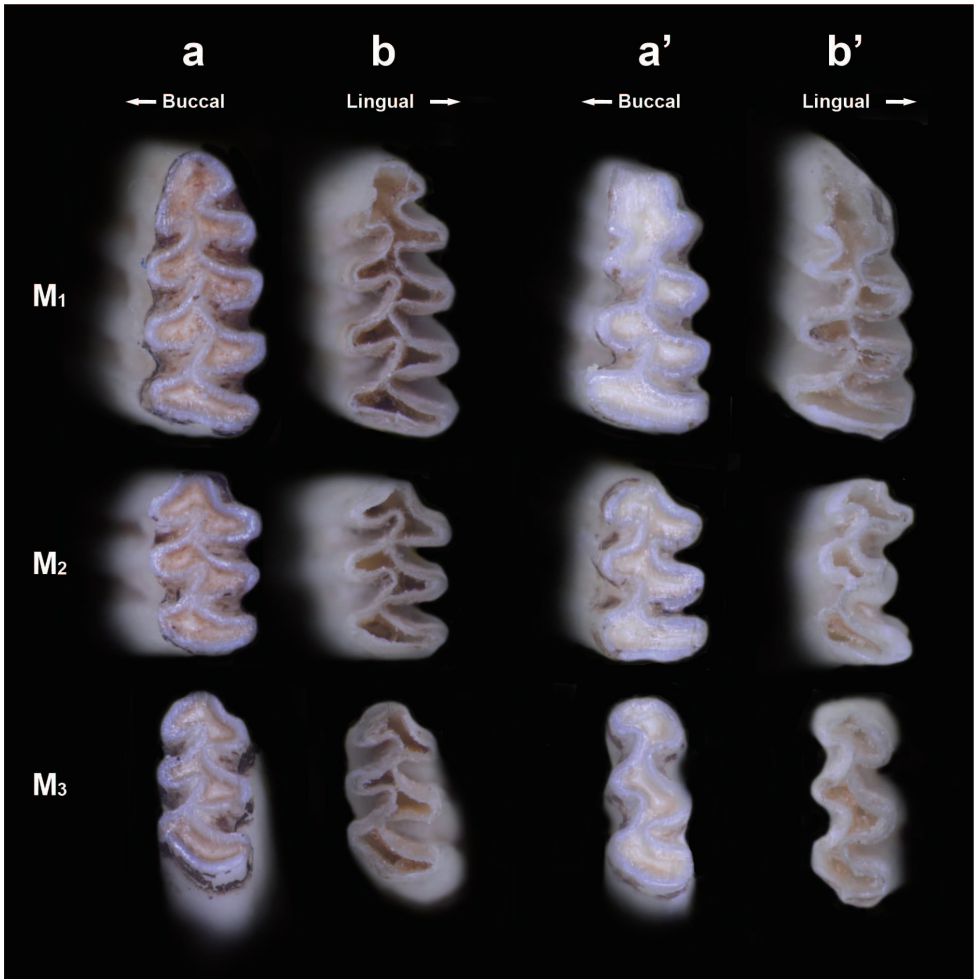


Figure 6. Typical views of occlusal surfaces **a, a'** and basal ends **b, b'** of the left lower molars of two typical individuals **a, b** K6059 with alveolar capsules **a', b'** K7367 without them of Anderson's red-backed voles. Inversed images indicate whether basal end views **b, b'** correspond to the enamel patterns of occlusal surfaces **a, a'**.

Kohli et al. (2014). This opinion is in good accordance with the karyological findings that red-backed voles are divided into two lineages, the *glareolus* cytotype group in the Holarctic and Nearctic realms and the *rufocanus* cytotype group in the Palearctic realm, based on the G-band patterns. At least all of above members of Asian red-backed voles show the *rufocanus* cytotype as a monophyly (Gamperl 1982; Modi and Gamperl 1989; Jiang and Ma 1991; Iwasa and Suzuki 2002b; Tang et al. 2018).

Jameson (1961) and Kitahara (1995) had previously studied the molar root formation of Anderson's red-backed vole, but little attention has been paid elsewhere. Jameson (1961: 599–600) mentioned the presence of incipient roots in one of the

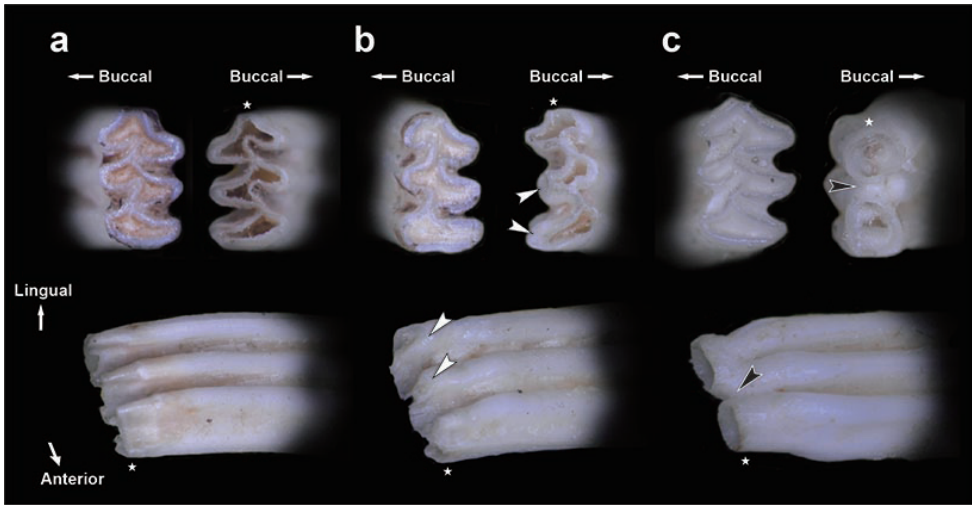


Figure 7. Typical views of occlusal surfaces (above left) and basal ends (above right), and antero-lingual views (below each) of M_2 of three typical individuals **a** K6059 with alveolar capsules **b** K7367 without them of Anderson's red-backed voles and the grey red-backed vole **c** HEG1-97 with the middle height of the alveolar capsule showing an incipient root. Black and white arrowheads indicate that the basal end was completely closed and that the basal ends were dully tapered off, showing incipient closures of re-entrant angles, respectively. Stars indicate correspondences of anterior points.

nine individuals of the vole from the central mountain region (Yatsugatake Mountains) of Honshu and allocated it as *Clethrionomys*. However, for the nine individuals likely investigated by Jameson (1961), one individual (USNM399102, preserved in the Smithsonian National Museum of Natural History) and four individuals (2565z, 2572z, 2777z, and 2778z, preserved in the Museum of Wildlife and Fish Biology of the University of California, Davis) were investigated by one of the present authors (Y. Kaneko) and the curator of the MWFB of UC Davis (A. Engilis Jr.) for the root conditions of molars. Contrary to Jameson's (1961) observation, it was confirmed that these individuals do not carry an incipient root condition. To date, unfortunately, another individual (M-184568, preserved in the American Museum of Natural History) has not been investigated, and the three other individuals are missing.

In the M_1 of an individual of *Ondatra zibethicus* (Linnaeus, 1766) in which the roots are not yet expressed, the re-entrant angles in the alveolar basal part are completely closed (Borodin 2009: fig. 11-2-d). Such a closed alveolar basal part has been confirmed in other voles (Gromov and Erbajeva 1995; Koenigswald and Kolfschoten 1996; Borodin 2009). In all of the molar samples showing these incipient root conditions, the enamel patterns of the occlusal surfaces do not commonly repeat those of the basal ends and both patterns do not correspond. Therefore, we consider that such discordance between the enamel patterns of the occlusal surface and the basal ends (Figs 4, 7) is a sign of an incipient closure of the re-entrant angles at the basal ends, reaching an incipient root formation. On the other hand, Kitahara (1995) regarded the signs for

root-closure in one individual kept in captive conditions (796 days old) collected from the Kii Peninsula as an abnormal condition of growth without free occlusion due to excessive growth of the incisors, therefore allocating the vole as *Eothenomys*. According to the photographs of these root-closure molars (Kitahara 1995: 13B), the basal ends of M_1 , M_2 , and M_3 were apparently tapered off from the occlusal surfaces, and the grooves were still clearly formed from the occlusal surface to the basal ends, particularly in M_3 . In addition, the middle portion of M_2 was abnormally bulged, and such bulging has not been confirmed in voles. These characteristics were apparently different from those of the so-called incipient roots and roots of molars in other arvicolines, such as the grey red-backed vole (Fig. 3b, c) and *O. zibethicus* (Borodin 2009). However, the features of the basal end of M_1 of Kitahara (1995) are similar to those of M^3 of K7088 as an incipient root, as caused by the abnormally strong wearing of M^3 in K7088 (Fig. 4). It is considered that the characteristics of the basal end of K7088 might be caused by an abnormal occlusion due to a lack of right M^3 (Fig. 4). In addition, those of the basal end of M_1 of Kitahara (1995) are also similar to those of M_2 of K7367 as an incipient closure of re-entrant angles (Figs 6, 7). The current observation does not correspond to previous findings by Gromov and Erbajeva (1995) and Borodin (2009), as to the typical incipient root status. However, we suggest that the current characteristics, the basal ends tapered off as in Kitahara (1995), the discordance of the enamel patterns between the occlusal surface and the basal ends, and the loss of alveolar capsule of M_2 (Figs 4, 5, 7) would be regarded as early stages reaching into molar root formation. Accordingly, the current characteristics of the basal ends of molars mentioned above suggest that molar root formation potentially appears at an extremely old-aged stage of life or by strong wearing in Anderson's red-backed vole, corresponding to the characteristic of *Craseomys*, with roots of molars that develop late in life (Miller 1900) rather than that of *Myodes*.

Considering the cytotype phylogenetic relationships and the dental characteristics of the root formation period in molars, ASM Mammal Diversity Database's allocation of Anderson's red-backed vole in *Craseomys* is acceptable. However, Anderson's red-backed vole has similarities with genus *Eothenomys* for by two reasons. First, incipient roots were present only in individuals of the Kii Peninsula, including one starving individual reared by Kitahara (1995), and it is unclear whether root formation is present in Anderson's red-backed voles collected from other localities of central and northern Honshu. Second, morphological and phylogenetic findings disclosed the close relationship between Anderson's red-backed vole and Smith's red-backed vole (Kaneko et al. 1992; Kimura et al. 1994, 1999; Suzuki et al. 1999; Iwasa and Tsuchiya 2000; Iwasa and Suzuki 2002a, b, 2003; Fujimoto and Iwasa 2010; Iwasa 2015b), and rooted molars have never been reported in Smith's red-backed vole to date (Imaizumi 1949, 1960; Tanaka 1971; Aimi 1980).

In our study, two individuals (K7088 and K7367) showed incipient root conditions and the incipient closure of the re-entrant angles in the molars among 114 individuals of Anderson's red-backed vole from the Kii Peninsula (Figs 4, 5, 7). These two were found among 114 individuals collected in all months except April, May, and October, suggesting that this molar condition is not specific but a normal phenomenon in the field. Our vole sampling was carried out in just a few days per year, as sampling of the vole is very difficult due to its low density and its specific habitat in rocky terrain, as compared to mice of the

genus *Apodemus* which are dominant in the Japanese Islands (Iwasa 2008, 2015a). Considering such limited sampling of the voles, the determination of the period of molar root formation is difficult using vole samples caught in natural conditions, whose true ages are unknown. Particularly, such difficulty would be expected in red-backed voles showing molar root formation at late age stages, as in the present results, because longevity in these animals in natural conditions is usually ecological rather than physiological. The difficulty of confirming molar root formation has probably caused the confusion in the genus allocation, and the dental feature may not be realistic for the generic classification of red-backed voles, particularly Anderson's and Smith's red-backed voles, which are apparently closely related. Therefore, we suggest that *Craseomys* is the most appropriate genus for Anderson's red-backed vole and other Asiatic red-backed voles, including Smith's red-backed vole. Our suggestion agrees with Kryštufek and Shenbrot (2022) and the ASM Mammal Diversity Database, and it considers the karyological and molecular phylogenetic relationships (Modi and Gamperl 1989; Iwasa and Suzuki 2002b; Tang et al. 2018).

Acknowledgements

We are grateful to M.D. Carleton for his kind cooperation to the observation of the storage specimens in Smithsonian National Museum of Natural History and A. Engilis Jr. for his kind cooperation to the observation of the specimens in MWFb of UC Davis. We also thank T. Aoi and staff of the Wakayama Experimental Forest of Hokkaido University. Special thanks are also due to T.A. Suzuki for his kind information about the specimens obtained by E.W. Jameson Jr. We wish to express our thanks to two reviewers, C. Laplana and L. Maul, for their invaluable comments.

References

- Abramson NI, Lissovsky AA (2012) Subfamily Arvicolinae. In: Pavlinov IY, Lissovsky AA (Eds) *The Mammals of Russia: a Taxonomic and Geographic Reference*. KMK Scientific Press, Moscow, 220–276.
- Aimi M (1967) Similarity between the voles of Kii Peninsula and of northern part of Honshu. *Zoological Magazine* 76(2): 44–49. [in Japanese with English summary] https://dl.ndl.go.jp/view/download/digidepo_10843054_po_ART0003793627.pdf?contentNo=1&alternativeNo=
- Aimi M (1980) A revised classification of the Japanese red-backed voles. *Memoirs of the Faculty of Science, Kyoto University, Series Biology* 8(1): 35–84. https://repository.kulib.kyoto-u.ac.jp/dspace/bitstream/2433/258844/1/mfsku-bn_08_1_35.pdf
- Anderson MP (1909) Description of a new Japanese vole. *The Annals and Magazine of Natural History (Series 8)* 4: 317–318. <https://doi.org/10.1080/00222930908692678>
- Borodin AV (2009) *A Diagnostic Guide to Teeth of Arvicolines of the Urals and Western Siberia (Late Pleistocene-modern time)*. Ural Branch of the Russian Academy of Sciences Publishing, Yekaterinburg, 100 pp. [In Russian]

- Corbet GB (1978) The Mammals of the Palaearctic Region: a Taxonomic Review. British Museum (Natural History), London, 314 pp.
- Corbet GB, Hill JE (1991) A World List of Mammalian Species. 3rd Edn. Oxford University Press, London, 243 pp.
- Fujimoto A, Iwasa MA (2010) Intra- and interspecific nuclear ribosomal gene variation in the two Japanese *Eothenomys* species, *E. andersoni* and *E. smithii*. Zoological Science 27(12): 907–911. <https://doi.org/10.2108/zsj.27.907>
- Gamperl R (1982) Chromosomal evolution in the genus *Clethrionomys*. Genetica 57(3): 193–197. <https://doi.org/10.1007/BF00056482>
- Gromov IM, Erbajeva MA (1995) The Mammals of Russia and Adjacent Territories. Zoological Institute, Russian Academy of Sciences, St. Petersburg, 520 pp. [in Russian]
- Imaizumi Y (1949) The Natural History of Japanese Mammals. Yoyo-Shobo, Tokyo, 348 pp. [In Japanese]
- Imaizumi Y (1960) Colored Illustrations of the Mammals of Japan. Hoikusha, Osaka, 196 pp. [In Japanese]
- Imaizumi Y (1998) Evolution Theory of Mammals – Species and Speciation of Mammals. Newton Press, Tokyo, 341 pp. [In Japanese]
- Iwasa MA (2008) Speciation of relic populations in red-backed voles. In: Motokawa M (Ed.) Mammalogy in Japan (1). University of Tokyo Press, Tokyo, 59–83. [In Japanese]
- Iwasa MA (2015a) *Eothenomys andersoni*. In: Ohdachi SD, Ishibashi Y, Iwasa MA, Fukui D, Saitoh T (Eds) The Wild Mammals of Japan, 2nd Edn. Shoukadoh, Kyoto, 158–159.
- Iwasa MA (2015b) *Eothenomys smithii*. In: Ohdachi SD, Ishibashi Y, Iwasa MA, Fukui D, Saitoh T (Eds) The Wild Mammals of Japan, 2nd Edn. Shoukadoh, Kyoto, 160–161.
- Iwasa MA, Suzuki H (2002a) Evolutionary networks of maternal and paternal gene lineages in voles (*Eothenomys*) endemic to Japan. Journal of Mammalogy 83(3): 852–865. [https://doi.org/10.1644/1545-1542\(2002\)083<0852:ENOMAP>2.0.CO;2](https://doi.org/10.1644/1545-1542(2002)083<0852:ENOMAP>2.0.CO;2)
- Iwasa MA, Suzuki H (2002b) Evolutionary significance of chromosome changes in northeastern Asiatic red-backed voles inferred from the aid of intron 1 sequences of the *G6pd* gene. Chromosome Research 10(5): 419–428. <https://doi.org/10.1023/A:1016809921433>
- Iwasa MA, Suzuki H (2003) Intra- and interspecific genetic complexities of two *Eothenomys* species in Honshu, Japan. Zoological Science 20(10): 1305–1313. <https://doi.org/10.2108/zsj.20.1305>
- Iwasa MA, Tsuchiya K (2000) Karyological analysis of the *Eothenomys* sp. from Nagano City, central Honshu, Japan. Chromosome Science 4(1): 31–38.
- Iwasa MA, Obara Y, Kitahara E, Kimura Y (1999) Synaptonemal complex analyses in the XY chromosomes of six taxa of *Clethrionomys* and *Eothenomys* from Japan. Mammal Study 24(2): 103–113. <https://doi.org/10.3106/mammalstudy.24.103>
- Jameson Jr EW (1961) Relationship of the red-backed vole of Japan. Pacific Science 15(4): 594–604. <https://scholarspace.manoa.hawaii.edu/server/api/core/bitstreams/bf1b1210-91b3-4ffc-862d-fe95e61f260d/content>
- Jiang JQ, Ma Y (1991) Study of taxonomic status of *Craseomys shanseius* Thomas in China. Scientific Treatise on Systematic and Evolutionary Zoology 1: 73–79. [in Chinese]
- Kaneko Y (1988) Relationship of skull dimensions with latitude in the Japanese field vole. Acta Theriologica 33(3): 35–46. <https://doi.org/10.4098/AT.arch.88-3>

- Kaneko Y (1990) Identification and some morphological characters of *Clethrionomys rufocanus* and *Eothenomys regulus* from USSR, northeast China and Korea in comparison with *C. rufocanus* from Finland. *Journal of the Mammalogical Society of Japan* 14(2): 129–148. <https://doi.org/10.11238/jmammsojapan1987.14.129>
- Kaneko Y, Murakami O (1996) The history of taxonomy in Japanese small rodents. *Mammalian Science* 36(1): 109–128. [in Japanese with English abstract] https://www.jstage.jst.go.jp/article/mammaliainscience/36/1/36_1_109/_pdf/-char/ja
- Kaneko Y, Nakashima T, Kimura Y (1992) Identification and vertical distribution of two species of *Eothenomys* on Ryo-Hakusan mountains, central Honshyu, Japan. *Bulletin of Gifu Prefectural Museum* 11: 23–34. [In Japanese with English abstract]
- Kawamura Y (1988) Quaternary rodent fauna in the Japanese Islands (Part. I). *Memoirs of the Faculty of Science, Kyoto University, Series of Geology and Mineralogy* 53(1–2): 31–348. https://repository.kulib.kyoto-u.ac.jp/dspace/bitstream/2433/186660/1/mfskugm%20053001_002_031.pdf
- Kimura Y, Kaneko Y, Yoshida T (1994) Small mammalian fauna in Adataro mountain regions with special reference to genus *Eothenomys*. *Fukushima Seibutsu* 37: 13–19. [In Japanese]
- Kimura Y, Kaneko Y, Iwasa MA (1999) Identification and vertical distribution of two species of *Eothenomys* in the Oze District, northeastern Honshu, Japan. *Mammalian Science* 39(2): 257–268. [in Japanese with English abstract] <https://doi.org/10.11238/mammaliainscience.39.257>
- Kitahara E (1995) Taxonomic status of Anderson's red-backed vole on the Kii Peninsula, Japan, based on skull and dental characters. *Journal of the Mammalogical Society of Japan* 20(1): 9–28. <https://doi.org/10.11238/jmammsojapan.20.9>
- Kitahara E, Harada M (1996) Karyological identity of Anderson's red-backed voles from the Kii Peninsula and central Honshu in Japan. *Bulletin of the Forestry and Forest Products Research Institute* 370: 21–30. https://dl.ndl.go.jp/view/download/digidepo_9366212_po_370-2.pdf?contentNo=1&alternativeNo=
- Koenigswald Wv, Kolschoten Tv (1996) The *Mimomys-Arvicola* boundary and the enamel thickness quotient (SDQ) of *Arvicola* as stratigraphic markers in the Middle Pleistocene. In: Turner C (Ed.) *The Early Middle Pleistocene in Europe*. Balkema, Rotterdam, 211–226. <https://doi.org/10.1201/9781003077879-15>
- Kohli BA, Speer KA, Kilpatrick CW, Batsaikhan N, Damdinbazar D, Cook JA (2014) Multilocus systematics and non-punctuated evolution of Holarctic Myodini (Rodentia: Arvicolinae). *Molecular Phylogenetics and Evolution* 76: 18–29. <https://doi.org/10.1016/j.ympev.2014.02.019>
- Kryštufek B, Shenbrot GI (2022) Voles and Lemmings (Arvicolinae) of the Palaearctic Region. University of Maribor, University Press, Maribor, 449 pp. <https://doi.org/10.18690/um.fnm.2.2022>
- Kryštufek B, Tesakov AS, Lebedev VS, Bannikova AA, Abramson NI, Shenbrot G (2020) Back to the future: The proper name for red-backed voles is *Clethrionomys Tilesius* and not *Myodes Pallas*. *Mammalia* 84(2): 214–217. <https://doi.org/10.1515/mammalia-2019-0067>
- Luo J, Yang D, Suzuki H, Wang Y, Chen WJ, Campbell KL, Zhang YP (2004) Molecular phylogeny and biogeography of Oriental voles: Genus *Eothenomys* (Muridae, Mammalia). *Molecular Phylogenetics and Evolution* 33(2): 349–362. <https://doi.org/10.1016/j.ympev.2004.06.005>
- Miller Jr GS (1896) Genera and subgenera of voles and lemmings. *North American Fauna* 12: 1–86. <https://doi.org/10.3996/nafa.12.0001>

- Miller Jr GS (1898) Description of a new genus and species of microtine rodent from Siberia. Proceedings. Academy of Natural Sciences of Philadelphia 50: 368–371. <https://hdl.handle.net/10088/34342>
- Miller Jr GS (1900) Preliminary revision of the European redbacked mice. Proceedings of the Washington Academy of Sciences 2: 83–109. <https://www.biodiversitylibrary.org/item/35745#page/121>
- Miyao T (1981) Geographic variation of *Apodemus speciosus* and *Eothenomys andersoni* in Japan proper. Mammalian Science 42(1): 35–49. [in Japanese] https://doi.org/10.11238/mammalian-science.21.1_35
- Modi WS, Gamperl R (1989) Chromosomal banding comparisons among American and European red-backed mice, genus *Clethrionomys*. Zeitschrift für Säugetierkunde 54: 141–152. https://www.zobodat.at/pdf/Zeitschrift-Saeugetierkunde_54_0141-0152.pdf
- Musser GG, Carleton MD (1993) Family Muridae. In: Wilson DE, Reeder DM (Eds) Mammal Species of the World, 2nd Edn. Smithsonian Institution Press, Washington DC, 501–806.
- Musser GG, Carleton MD (2005) Superfamily Muroidea. In: Wilson DE, Reeder DM (Eds) Mammal Species of the World: a Taxonomic and Geographic Reference, 3rd Edn. Johns Hopkins University Press, Baltimore, 894–1531.
- Nakata K (2015) Handbook for Vole Census Methods and Control, 3rd Edn. Hokkaido Forestry Conservation Association, Sapporo, 77 pp. [In Japanese]
- Palmer TS (1928) An earlier name for the genus *Evotomys*. Proceedings of the Biological Society of Washington 41: 87.
- Shenbrot GI, Krasnov BR (2005) An Atlas of the Geographic Distribution of the Arvicoline Rodents of the World (Rodentia, Muridae: Arvicolinae). Pensoft, Moscow, 336 pp.
- Suzuki H, Iwasa M, Harada M, Wakana S, Sakaizumi M, Han SH, Kitahara E, Kimura Y, Kartavtseva I, Tsuchiya K (1999) Molecular phylogeny of red-backed voles in Far East Asia based on variation in ribosomal and mitochondrial DNA. Journal of Mammalogy 80(2): 512–521. <https://doi.org/10.2307/1383297>
- Suzuki T, Obara Y, Tsuchiya K, Oshida T, Iwasa MA (2014) Ag-NORs analysis in three species of red-backed voles, with a consideration of generic allocation of Anderson's red-backed vole. Mammal Study 39(2): 91–97. <https://doi.org/10.3106/041.039.0204>
- Tanaka R (1971) A research into variation in molar and external features among a population of the Smith's red-backed vole for elucidation of its systematic rank. Japanese Journal of Zoology 16: 163–176.
- Tang MK, Jin W, Tang Y, Yan CC, Murphy RW, Sun ZY, Zhang XY, Zeng T, Liao R, Hou QF, Yue BS, Liu SY (2018) Reassessment of the taxonomic status of *Craseomys* and three controversial species of *Myodes* and *Altricola* (Rodentia: Arvicolinae). Zootaxa 4429(1): 1–52. <https://doi.org/10.11646/zootaxa.4429.1.1>
- Thomas O (1905) Abstract. Proceedings of the Zoological Society of London 23: 18–19.
- Tokuda M (1941) A revised monograph of the Japanese and Manchou-Korean Muridae. Transaction of the Biogeographical Society of Japan 4: 1–156.
- Tsuchiya K (1981) On the chromosome variations in Japanese cricetid and murid rodents. Mammalian Science 42(1): 51–58. [in Japanese] https://doi.org/10.11238/mammalian-science.21.1_51

Appendix I

Table A1. Anderson's red-backed vole individuals examined in this study.

No.	Sex	BW (g)	TL* (mm)	HBL (mm)	HFLsu (mm)	Testis length (mm)	C. e.*	P. m.*	P. sym.*	Pg.* s.*	C. e.*	P. m.*	P. sym.*	Pg.* s.*	CBL (mm)	HAC (mm)	Mat.*
K6519	m	26.5	55.7	104.5	19.7	3.5	-			25.1	3.91	Im			25.9	3.99	M
K5620	f	31.5	59.0	117.4	18.9			+	-	nd	4.44	M			26.8	3.97	M
K5646	f	24.2	61.5	105.7	19.6			-	+	24.5	3.92	Im			24.7	3.60	Im
K5647	f	37.5	71.9	112.3	19.3			+	nd	26.5	4.10	M			26.6	4.29	Im
K5648	m	37.5	62.5	118.2	20.2	5.6	-			27.2	4.67	Im			27.5	3.65	M
K6034	m	42.0	64.2	123.1	20.8	9.2	+			27.3	3.94	M			25.5	3.78	Im
K6035	f	36.5	66.9	112.8	20.4			+	-	27.0	4.17	M			26.0	4.15	M
K6036	m	38.0	62.3	122.2	19.5	8.4	+			27.3	4.07	M			27.2	4.04	M
K6037	m	40.4	62.7	118.2	20.5	9.6	+			27.7	4.40	M			27.4	4.22	M
K6038	f	37.0	71.7	116.0	20.4			+	-	26.5	3.98	M			26.5	4.25	M
K6039	m	38.9	65.6	123.5	20.1	8.5	+			26.6	4.41	M			26.7	4.23	Im
K6040	m	44.0	63.3	122.4	19.5	8.9	+			27.5	4.31	M			26.8	4.31	M
K6041	f	38.2	67.6	113.8	19.6			+	-	27.2	4.10	M			27.9	4.62	M
K6042	f	35.1	73.1	117.2	19.6			+	-	27.4	4.19	M			27.0	4.78	M
K6043	f	35.5	56.8	112.9	20.0			+	-	26.1	3.86	M			26.2	4.37	M
K6044	m	44.6	62.5	122.2	21.2	8.6	+			27.2	3.65	M			27.3	4.10	M
K6052	m	41.0	66.5	122.9	20.1	8.3	+			27.0	4.41	M			nd	nd	M
K6053	f	45.4	65.2	120.1	20.0			+	-	27.0	4.22	M			24.4	3.97	Im
K6054	m	37.0	58.8	117.8	20.0	9.2	+			27.0	3.85	M			23.8	3.89	Im
K6055	f	45.4	65.3	118.0	19.5			+	nd	27.1	3.97	M			27.9	4.24	M
K6056	f	34.3	60.5	113.5	20.4			+	+	26.6	4.19	M			27.8	4.02	M
K6057	f	40.8	57.8	118.8	19.1			+	-	27.0	4.09	M			24.4	3.99	Im
K6058	m	39.0	64.4	117.2	19.8	8.8	+			26.9	3.91	M			24.0	3.75	Im
K6059	m	31.5	61.3	111.2	19.8	6.0	-			26.7	4.67	Im			25.6	4.23	M
K6070	m	42.5	nd	121.9	20.2	10.0	+			27.8	3.89	M			22.4	3.73	Im
K6071	f	41.0	62.3	117.7	19.5			+	-	27.2	4.27	M			24.2	3.95	Im
K6072	f	42.8	50.2	123.4	19.2	9.2	+			27.4	3.68	M			27.1	4.06	M
K6073	f	36.5	64.9	112.5	20.2			+	-	26.9	4.42	M			24.0	3.82	Im
K6074	m	40.9	64.5	122.2	19.9	8.9	+			27.1	3.67	M			24.3	3.79	Im
K6075	f	31.0	71.9	110.2	20.3			+	+	nd	4.07	M			27.1	4.42	M
K6118	m	26.2	61.9	100.9	20.1	3.0	-			25.1	4.17	Im					

No.	Sex	BW (g)	TL* (mm)	HBL (mm)	HFLsu (mm)	Testis length (mm)	C. e.*	P. m.*	P. sym.*	No.	Sex	BW (g)	TL* (mm)	HBL (mm)	HFLsu (mm)	Testis length (mm)	C. e.*	P. m.*	P. sym.*	Pg.*	P. s.*	CBL (mm)	HAC (mm)	HAC Mac.*	
K6119	f	31.5	67.8	116.3	20.3						f	42.7	65.2	121.2	20.6							27.2	4.60	M	
K6442	m	34.4	59.9	114.8	20.8	9.6	+				m	43.1	64.3	118.2	19.4	8.6	+					27.2	4.05	M	
K6537	m	25.9	57.0	96.2	20.2	6.1	-				m	40.0	68.1	120.0	19.9	8.4	+					27.2	4.18	M	
K6538	f	31.1	59.0	111.1	20.0		-				f	44.6	70.4	123.8	19.9		+					28.7	4.81	M	
K6539	f	46.9	66.5	118.2	19.3		-				f	49.1	67.2	121.6	19.2		+					27.6	4.43	M	
K6540	f	31.8	62.2	111.7	20.0		+				f	38.6	69.5	111.2	20.7		+					26.6	4.32	M	
K6541	f	18.6	53.7	92.1	19.2		-				m	39.3	72.5	117.2	20.4	7.9	+					26.9	4.62	M	
K6542	f	25.5	61.5	100.4	20.5		-				m	39.0	67.7	116.7	19.8		+					26.7	4.56	M	
K6543	f	28.1	59.4	107.1	20.8		-				m	45.3	67.6	125.2	20.4	9.2	+					28.2	4.83	M	
K6559	f	46.4	69.0	120.3	20.0		+				m	43.2	63.3	119.6	19.7		+					26.9	4.10	M	
K6560	f	49.1	68.5	125.5	20.8		+				m	37.7	61.0	115.6	19.8		+					26.4	4.20	M	
K6561	f	40.1	67.6	119.5	20.4		+				m	42.7	70.0	122.1	20.6	9.2	+					27.4	4.36	M	
K6562	m	38.5	69.2	116.5	20.0	8.4	+				m	38.9	63.8	116.4	19.4		+					26.6	4.20	M	
K6563	m	25.5	63.5	98.0	19.6	6.2	-				m	43.7	64.6	121.3	21.0	10.0	+					27.5	4.50	M	
K6564	m	34.0	58.2	109.8	20.9	8.5	+				m	33.5	60.0	112.6	20.9	8.6	+					26.5	4.14	M	
K6565	m	33.5	57.2	111.8	19.3	8.5	+				m	35.1	58.2	119.2	19.2	9.5	+					26.5	3.84	M	
K6575	f	40.2	74.2	111.5	20.3		+	nd			f	48.2	63.0+	125.2	20.2		+					27.9	3.62	M	
K6576	f	25.9	60.3	97.1	20.2		-				m	45.7	63.8	118.2	20.5		+					26.7	4.00	M	
K6577	f	22.7	51.9	96.5	19.2		-				m	39.8	59.6	117.7	20.0	10.1	+					27.2	4.82	M	
K6781	m	31.0	70.0	115.2	20.5	8.5	+				m	44.2	66.1	121.6	20.0		+					27.8	4.17	M	
K6782	f	34.3	62.0	116.8	19.8		nd				m	32.7	65.1	112.6	20.2	7.2	-					26.0	3.92	Im	
K6783	f	36.6	73.0	125.6	20.2		+				m	38.3	59.0	115.6	19.2	10.1	+					26.8	4.32	M	
K6784	m	36.6	67.9	117.5	20.0	7.2	+				f	36.8	67.5	115.3	20.2		+					26.8	4.02	M	
K6785	f	31.0	64.3	113.2	20.0		-				f	40.4	71.0	128.5	19.8		+					27.8	3.85	M	
K6786	m	32.8	65.3	111.2	19.8	8.0	+				m	42.1	70.6	121.0	20.1		+					27.4	4.35	M	
K6787	f	32.4	66.2	113.6	19.4		+				m	34.3	64.3	112.9	19.2		+					25.8	3.74	M	
K6788	f	28.9	63.7	104.5	19.3		-				m	28.0	61.6	105.2	20.2	7.0	-					25.1	4.09	Im	
K6789	f	34.7	63.2	118.2	19.4		nd				m	44.3	68.2	125.3	20.3	10.5	+					27.6	4.48	M	
K6790	f	34.8	64.5	115.0	19.0		-	nd			m	32.9	65.9	113.5	20.2		+					25.7	4.24	M	
K6791	m	38.8	66.2	117.1	20.5	8.0	-				f	39.7	62.5	119.2	19.2		+					26.9	4.40	M	
K6792	m	41.0	63.2	118.1	19.9	8.8	+				m	40.4	63.2	122.3	20.0	9.4	+					26.9	3.92	M	
K6793	m	33.8	61.4	114.8	20.6	8.8	+				m	40.4	55.0+	122.0	20.2	9.6	+					27.0	4.69	M	
K6794	f	34.2	69.5	109.9	20.5		+				m	40.4	55.0+	122.0	20.2		+								M

*+ in TL, tail partially lost; C. e., cauda epididymidis appear, -; ductus epididymidis disappear; P. m., papilla mammae (+; appear, -; disappear); P. sym., pubic symphysis (+; close, -; open); Pg., Pregnancy; P. s., placental scars; Mat., sexually maturation (Im: immature, M: matured).
nd, no data.

Four new species and two newly recorded species of Limacodidae (Lepidoptera, Zygaenoidea) from China

Jun Wu¹, Alexey V. Solovyev², Hui-Lin Han^{1,3,4}

1 School of Forestry, Northeast Forestry University, Harbin, 150040, China **2** Department of Biology and Chemistry, Ulyanovsk State Pedagogical University, Ulyanovsk, 432071, Russia **3** Northeast Asia Biodiversity Research Center, Northeast Forestry University, Harbin, 150040, China **4** Key Laboratory of Sustainable Forest Ecosystem Management, Ministry of Education, Northeast Forestry University, Harbin, 150040, China

Corresponding author: Hui-Lin Han (hanhuilin@aliyun.com)

Academic editor: E.J. van Nieuwerkerken | Received 28 October 2021 | Accepted 17 September 2022 | Published 7 October 2022

<https://zoobank.org/C890909D-0AD5-4E5C-ADB4-1129BBECE4FF>

Citation: Wu J, Solovyev AV, Han H-L (2022) Four new species and two newly recorded species of Limacodidae (Lepidoptera, Zygaenoidea) from China. ZooKeys 1123: 205–219. <https://doi.org/10.3897/zookeys.1123.77217>

Abstract

Four new species, *Kitanola shilinensis* **sp. nov.**, *K. eleganta* **sp. nov.**, *Fignya ravalba* **sp. nov.**, and *Euphlyctinides pseudolaika* **sp. nov.**, are described from southwestern China. Two species are reported new to China, *Euphlyctinidis indi* Solovyev, 2009 and *Limacocera pachycera* (Hampson, 1897). The adults and genitalia of all the treated species are illustrated. A checklist for the species belonging to the treated genera is provided.

Keywords

Checklist, new record, slug caterpillar moth, southwest China, taxonomy, Xizang, Yunnan

Introduction

The family Limacodidae, more commonly known as slug caterpillar moths, contains 301 genera and 1672 species globally (van Nieuwerkerken et al. 2011). Wu et al. (2022) estimated the number of slug moths is nearly, or already more than, 1750 species to

date. The diversity of Chinese Limacodidae, especially in southern China, is rich but poorly studied. Wu (2010) reported 64 genera and 230 species in China, including 89 species with larval host plant records.

This study aims to describe four new species and to report two unrecorded species in the family Limacodidae from the Xizang Autonomous Region (= Tibet) and Yunnan Province, southwest China. These species belong to the genera *Fignya* Solovyev & Witt, 2009, *Kitanola* Matsumura, 1925, *Euphlyctinides* Hering, 1931, and *Limacocera* Hering, 1931. Brief introductions to these genera are given below.

Materials and methods

The specimens were collected in field, using a 220 V/450 W mercury light and a DC black light. Wingspan was measured from forewing apex to apex. Standard methods were used to dissect and prepare slides of the genitalia (Kononenko and Han 2007). The specimens were photographed using a Nikon D700 camera, and the genitalia slides were photographed using an Olympus photo microscope aided by Helicon Focus software and further processed using Adobe Photoshop CS6.

All the specimens examined, including the type specimens, were deposited in the collection of the Northeast Forestry University (NEFU), Harbin, China. The specimens for comparison were borrowed from the Museum Witt München/Zoologische Staatssammlung München, Munich, Germany (MWM/ZSM), the Zoological Institute of Russian Academy of Sciences, St. Petersburg, Russia (ZISP), and the collection of Alexey V. Solovyev, Ulyanovsk, Russia (CASU).

Taxonomic account

Genus *Kitanola* Matsumura, 1925

Kitanola Matsumura, 1925: 116. Type species: *Kitanola sachalinensis* Matsumura, 1925.

Microcampa Kawada, 1930: 256. Type species: *Heterogena uncula* Staudinger, 1887.

Mediocampa Inoue, 1982: 301. Type species: *Kitanola speciosa* Inoue, 1956.

Note. Members of the genus *Kitanola* Matsumura, 1925 are small in size. *Kitanola* species have up-curved labial palpi, filiform male antennae, and forewing veins R_3+R_4 stalked with R_5 . The tibial spurs are 0-2-4. The uncus and gnathos in the male genitalia are usually or slightly widened, and the transtilla usually bears a long process. The genus is mainly distributed in eastern Asia and contains 10 species to date, eight of which are recorded from China (Inoue 1956; Tshistjakov 1995; Sasaki 1998; Solovyev 2008; Wu and Fang 2008; Hirowatari et al. 2013).

***Kitanola shilinensis* sp. nov.**

<https://zoobank.org/464D8EB1-4EF1-4398-A096-494FA5AC4A06>

Figs 1, 15

Material examined. *Holotype*. ♂, CHINA, Prov. Yunnan, Kunming City, Shilin County, Changhu Town, Changhu wetland park, 23–28.VIII.2020, KL. Wu leg., genit. prep. WuJ-248-1 (NEFU). *Paratypes*. 2♂, CHINA, same data as for holotype, genit. prep. WuJ-247-1, WuJ-299-1 (NEFU).

Diagnosis. The new species *K. shilinensis* sp. nov. (Fig. 1) is hardly separable from *K. spina* Wu & Fang, 2008 (Fig. 2) and *K. spinula* Wu & Fang, 2008 (Fig. 3), but there are several distinguishing features in the male genitalia, as follows (the details of the latter two species are in parentheses): the serrated transtilla is small with only one single long finger-shaped process on its lateral side in *K. shilinensis* sp. nov. (Fig. 15), whereas in *K. spina* the smooth transtilla has a thick finger-shaped process (Fig. 16) and in *K. spinula* (Fig. 17) the serrated transtilla is larger and has two lateral processes (one long, the other short) compared to *K. shilinensis* sp. nov.; the terminal part of aedeagus with two groups of strongly sclerotized spines in *K. shilinensis* sp. nov. (the terminal part of aedeagus with a circle of strongly sclerotized spines in *K. spina*; the terminal part of aedeagus with a cluster of fine spines in *K. spinula*).

Description. Adult (Fig. 1). Forewing length 7.0–7.5 mm, wingspan 14.5–15.0 mm. Head yellowish white; labial palpus up-curved; antennae filiform, brown. Thorax yellowish white. Forewing ground colour yellowish white, covered with dense brown scales, with a large brown patch in medium part; M-area and inner margin area covered with black scales; outer margin with two distinct black dots near apex; fringe long, greyish white. Hindwing pale brown, with a distinct black dot near apex; fringe greyish white. Abdomen brown, dark brown terminally. Scales on legs greyish white, terminal of tarsus black.

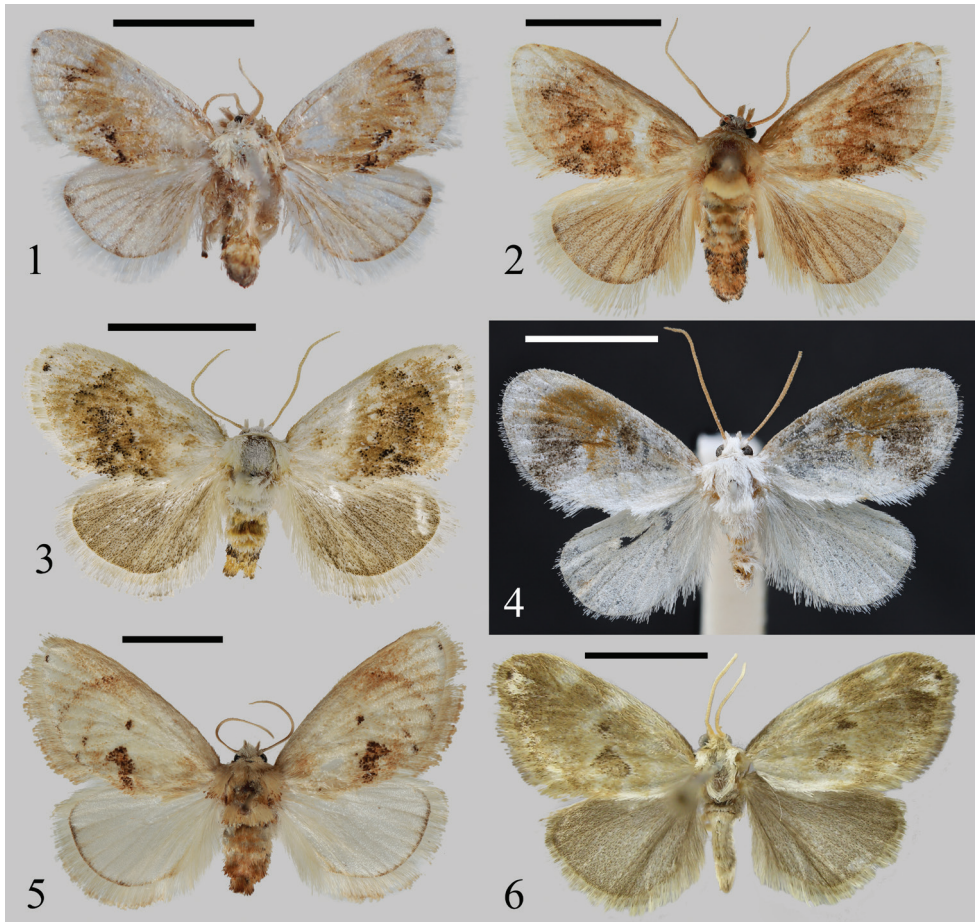
Male genitalia (Fig. 15). Both lateral processes of uncus broad, densely covered with short hairs, with a very small apical spur. Gnathos short, acute apically. Valva slender, narrow at base, medial part with a sclerotized region near the sacculus process; cucullus visibly narrowing at lower part; transtilla broad, strongly sclerotized, posterior margin serrated, with a long finger-shaped process on lateral side; sacculus narrow, slightly inflated at base; sacculus process strongly sclerotized, small triangular in shape. Aedeagus slender, usually with two groups (each with 1–3) strongly sclerotized, robust spines at the terminal.

Female. Unknown.

Bionomics. The specimens were collected in late August at altitudes of 1,850 m a.s.l. The collection site was a wetland park, surrounded mainly by planted pine (family Pinaceae) and camphor (family Lauraceae) trees and some landscaping vegetation, with a large number of grasses growing as a ground cover layer in the woods (Fig. 32).

Distribution (Fig. 29). China (Yunnan).

Etymology. The species is named *shilinensis* after its type locality in Shilin County, Yunnan Province, China.



Figures 1–6. Adults of *Kitanola* spp. **1** *K. shilinenensis* sp. nov., holotype, Yunnan, China (NEFU) **2** *K. spina* Wu & Fang, 2008, Chongqing, China (NEFU) **3** *K. spinula* Wu & Fang, 2008, Zhejiang, China (NEFU) **4** *K. eleganta* sp. nov., holotype, Xizang, China (NEFU) **5** *K. linea* Wu & Fang, 2008, Guangdong, China (NEFU) **6** *K. uncula* (Staudinger, 1887), Sakhalin, Russia (ZISP). Scale bars: 5 mm.

***Kitanola eleganta* sp. nov.**

<https://zoobank.org/E5445A39-A21F-41D5-89AD-F0778EE5D949>

Figs 4, 18

Material examined. *Holotype*. ♂, CHINA, Xizang Autonomous Region, Linzhi (= Nyingchi) City, Motuo (= Medog) County, Gedang Countryside, 25–30.V.2021, J. Wu and JJ. Fan legs (NEFU). *Paratypes*. 2♂, CHINA, same data as for holotype, genit. prep. WuJ-500-1, WuJ-501-1 (NEFU).

Diagnosis. The new species (Fig. 4) is somewhat similar in appearance to *K. shilinenensis* sp. nov. (Fig. 1), *K. spina* (Fig. 2), and *K. spinula* (Fig. 3), but it can be distinguished from these by the ground colour of the forewing and thorax, which is white; the forewing with a large patch, which is composed of brown and dark brown;

the hindwing is white; and the abdomen is brown alternating with white. In contrast, in the three similar species, the ground colour of the forewing and thorax is yellowish white; the forewing has a broad, dark yellowish-brown band; the hindwings are greyish brown to brown; and the abdomen is brown to dark brown.

It can be also separated from these three species by the following male genitalia characters. In *K. eleganta* sp. nov. (Fig. 18), the uncus is acute apically; the transtilla is lacking; the valva bears a conspicuous triangular basal spine on costa and a strongly sclerotized, eagle-claw-shaped process near middle of sacculus; the aedeagus is short, has an apically bifid, long spur. However, in *K. shilinensis* sp. nov. (Fig. 15), *K. spina* (Fig. 16), and *K. spinula* (Fig. 17), the uncus is broad; the transtilla is present (in *K. spina* the serrated transtilla is lacking a thick finger-shaped lateral process is present); the aedeagus is slender, with the various numbers of apical spines or spinules.

Kitanola eleganta sp. nov. differs markedly in appearance from *K. linea* Wu & Fang, 2008 (Fig. 5) and *K. uncula* (Staudinger, 1887) (Fig. 6) mainly in that the new species has a white ground colour and lacks a small black spot near the apex of the forewing, whereas the latter two are greyish white to ochreous in ground colour and usually have a small black spot near the apex. However, in the male genitalia, the new species has more similar to *K. linea* (Fig. 19) and *K. uncula* (Fig. 20), but it can be distinguished by the following characters: in *K. eleganta* sp. nov., the uncus is small, the sacculus bears an eagle-claw-shaped process, and the aedeagus is short, with a long bifid spur terminally; in *K. linea* and *K. uncula*, the uncus is large, the process located in the sacculus is straight, and the aedeagus is sinuous and with a large apical spine.

Description. Adult (Fig. 4). Forewing length 9.0–9.5 mm, wingspan 18–20 mm. Head white; labial palpus up-curved, brown; antennae filiform, brown. Thorax white. Forewing ground colour white, covered with sparse dark brown scales; smoothly curved subterminal line runs from the costal margin near apex to tornus, terminal area crescent-like, white, tinted slightly brown; inner margin area white; rest mainly with large irregular brown and dark brown patches; fringe white to dark brown. Hindwing ground colour white with M-area tinted pale brown. Abdomen brown alternating with white, terminal white.

Male genitalia (Fig. 18). Uncus and gnathos slender, pointed apically. Basal half of valva without setae, whereas upper half densely covered with setae; valva with a conspicuous triangular spine on the base of costa and a strongly sclerotized, eagle-claw-shaped process near middle of sacculus, with six or seven strongly sclerotized, slightly curved spines on the outer margin; cucullus narrow and rounded; sacculus slightly sclerotized at base; sacculus process not obvious, showing as a hairy rounded papula. Juxta flattened, nearly square. Saccus conspicuous, broadly tongue-shaped. Aedeagus short, caecum large, tapering towards apex; terminal part with a strongly sclerotized, bifid apically spur that almost same length as aedeagus.

Female. Unknown.

Bionomics. The specimens were collected in May at an altitude of 2,120 m a.s.l., near a subtropical evergreen broadleaf forest, with massive shrubs, ferns, and patches of grassland growing as the ground cover layer in the forest (Fig. 31).

Distribution (Fig. 29). China (Xizang).

Etymology. The species name, a noun in apposition, is derived from the Latin noun “elegans”, alluding to the fine, perfect, elegant wing features.

Genus *Euphlyctinides* Hering, 1931

Euphlyctinides Hering, 1931: 704. Type species (by original designation): *Euphlyctinides rava* Hering, 1931. Type locality: India, Darjeeling.

Note. The genus *Euphlyctinides* was erected by Hering (1931), with the type species, *E. rava* Hering, 1931. The moths in this genus are medium sized, with a yellowish-brown ground colour. The forewings are elongate, with two non-intersecting dark smooth fasciae. The forewing with R_5 stalked from discal vein near branch R_3+R_4 . The tibial spurs are 0-2-4. The genus contains four described species to date, two of which are recorded from China (Solovyev 2009; Solovyev and Witt 2009; Wu 2011; Irungbam et al. 2017; Ji 2018).

***Euphlyctinides pseudolaika* sp. nov.**

<https://zoobank.org/EAC31D21-0F9B-4E28-A702-F4B93A7A0084>

Figs 7, 8, 21, 22

Material examined. Holotype. ♂, CHINA, Prov. Yunnan, Pu'er City, Manxieba Village, 3.VIII.2018, HL. Han, J. Wu, and MR. Li legs., genit. prep. WuJ-177-1 (NEFU).

Paratype. 1♂, CHINA, Prov. Yunnan, Baoshan City, Mangkuan Village, 30.VII–2.VIII.2014, HL. Han leg., genit. prep. WuJ-702-1 (NEFU).

Diagnosis. The new species is similar in appearance to *E. laika* Solovyev & Witt, 2009 (Fig. 9), but can be separated from the latter by the almost invisible subterminal line, and the weakly sinuous outer margin of the hindwing.

It can also be easily distinguished from the latter by the characters of the male genitalia. In *E. pseudolaika* sp. nov. (Figs 21, 22), the basal flap of the costa in the valva is small, with distinct apical and subapical spines; the juxta is slightly forked apically; the apical process of aedeagus is short and blunt. However, in *E. laika* (Fig. 23), the basal flap of costa is elongate, from the medial part of the valva to its basal, with tiny teeth apically; the apex of juxta is divided into two slender finger-shaped processes; the apical spur of aedeagus is long and acute.

Description. Adult (Figs 7, 8). Forewing length 10.5–11.0 mm, wingspan 23.0–24.5 mm. Head brown; labial palpus brown; antennae filiform, brown. Thorax brown to pale brown. Forewing elongate, ground colour brown, covered with sparse dark scales; anterior basal patch distinct, dark brown; medial fascia sinuous, dark brown, running from ca 2/3 of the costal margin to ca 1/3 of the inner margin from wing base, with large patches on basal, median, and apical area; subterminal line almost invisible; fringe brown. Hindwing reddish brown, with weakly sinuous outer margin; venation distinctly dark brown; fringe brown. Scales on legs brown.



Figures 7–14. Male adults **7** *Euphyctinides pseudolaika* sp. nov., holotype, Yunnan, China (NEFU) **8** *E. pseudolaika* sp. nov., paratype, Yunnan, China (NEFU) **9** *E. laika* Solovyev & Witt, 2009, Nghe An, Vietnam **10** *E. indi* Solovyev, 2009, Xizang, China (NEFU) **11** *Fignya ravalba* sp. nov., holotype, Xizang, China (NEFU) **12** *F. melkaya* Solovyev & Witt, 2009, holotype, Lào Cai, Vietnam (MWM/ZSM) **13** *Limacocera pachycera* (Hampson, 1897), Xizang, China (NEFU) **14** *L. bel* Hering, 1931, Chongqing, China (NEFU). Scale bars: 5 mm.

Male genitalia (Figs 21, 22). Uncus elongate, with a strongly sclerotized, acute subapical spur. Gnathos slender, hooked. Valva elongate; base of costa with a distinct flap, which is covered with sparse short spines on the surface and bears a cluster of strongly sclerotized, various-sized, apically acute spines; sacculus slightly inflated at

base, lacking sacculus process; cucullus rounded. Juxta flattened, nearly oblong, slightly forked apically. Aedeagus slender, slightly curved near caecum, with a short, blunt apical process coiled in half a turn.

Female. Unknown.

Bionomics. The two specimens were collected in late July to early August using a light trap in a coniferous forest; the main vegetation around the collecting site of the holotype consisted of *Pinus yunnanensis* Franch. (Pinaceae) (Fig. 33).

Distribution (Fig. 29). China (Yunnan).

Etymology. The name, a noun in apposition, is a combination of the Greek adjective “pseudes” (= false) with the specific name “laika”, showing the similarity with *E. laika*.

Remarks. Although only two males have been collected, the appearance differs from other congeners, particularly in the male genitalia. Hence, in this study, we formally describe them as a new species.

***Euphlyctinidis indi* Solovyev, 2009**

Figs 10, 24

Euphlyctinidis indi Solovyev, 2009: 175. Type locality: Indien WB, Darjeeling Mangu-pu-road.

Material examined. 2♂, CHINA, Xizang Autonomous Region, Linzhi (= Nyingchi) City, Motuo (= Medog) County, Beibeng Countryside, Dergong village, 25.V–4.VI.2021, HL. Han leg., genit. prep. WuJ-552-1 (NEFU); 3♂, CHINA, Xizang Autonomous Region, Linzhi (= Nyingchi) City, Motuo (= Medog) County, Gedang Countryside, 25.V–5.VI.2021, J. Wu and JJ. Fan legs., genit. prep. WuJ-512-2, WuJ-565-1 (NEFU).

Diagnosis. *Euphlyctinidis indi* differs from its congeners by the darker coloration of the forewing, the postmedial line is without distinctive interruptions, the valva is broad in the distal part, and by the juxta without any processes.

Bionomics. The moth flies from May to June. The specimens were collected with a light trap at altitudes of 1,450–2,120 m a.s.l. in a subtropical evergreen broadleaf forest with massive shrubs, ferns, and patches of grassland as in the ground cover layer in the forest (Figs 30, 31).

Distribution. China (Xizang), India.

Genus *Fignya* Solovyev & Witt, 2009

Fignya Solovyev & Witt, 2009: 197. Type species (by original designation): *Fignya melkaya* Solovyev & Witt, 2009. Type locality: Vietnam, Mt. Fan-si-pan (West).

Note. *Fignya* was first described by Solovyev and Witt (2009). Previously, it contained only the type species *F. melkaya* Solovyev & Witt, 2009, known to be distributed in Vietnam and China. *Fignya* species are small in size, antennae are filiform in both sexes; the labial

palpi are slightly up-curved; the forewing has large white spot in the Cu-area with brown border, with sinusoidal vein R_1 , and the veins R_3+R_4 are branched from R_5 . The tibial spurs are 0-2-4. In the male genitalia, the gnathos is fishtail-shaped with a comb-like apex; the vesica bears large, strongly sclerotized cornuti (Solovyev and Witt 2009; Ji 2018). The second species of this genus, *F. ravalba* sp. nov., collected from Xizang, is described below.

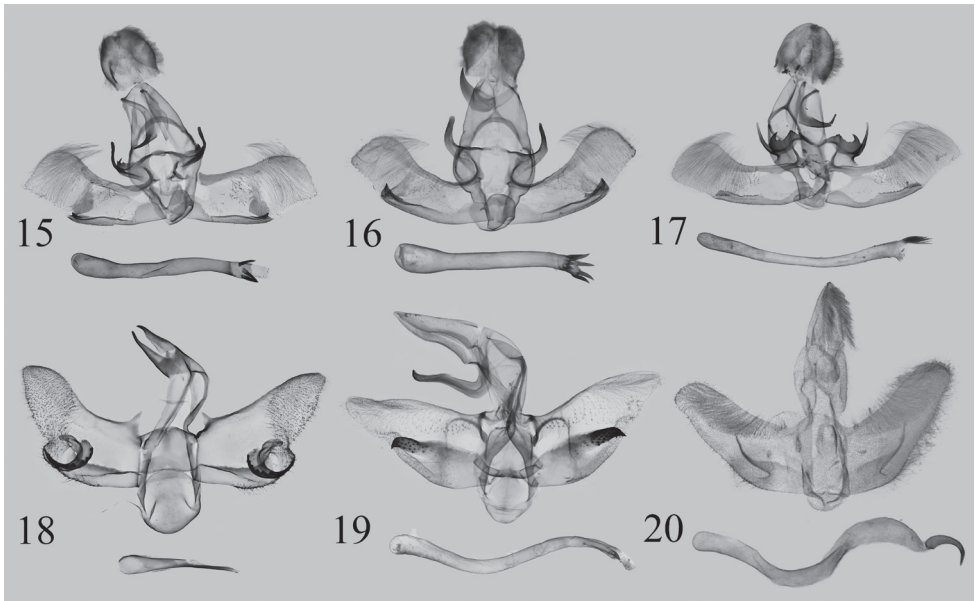
***Fignya ravalba* sp. nov.**

<https://zoobank.org/7357A6BD-A186-4503-B97A-1EA60C8C7978>

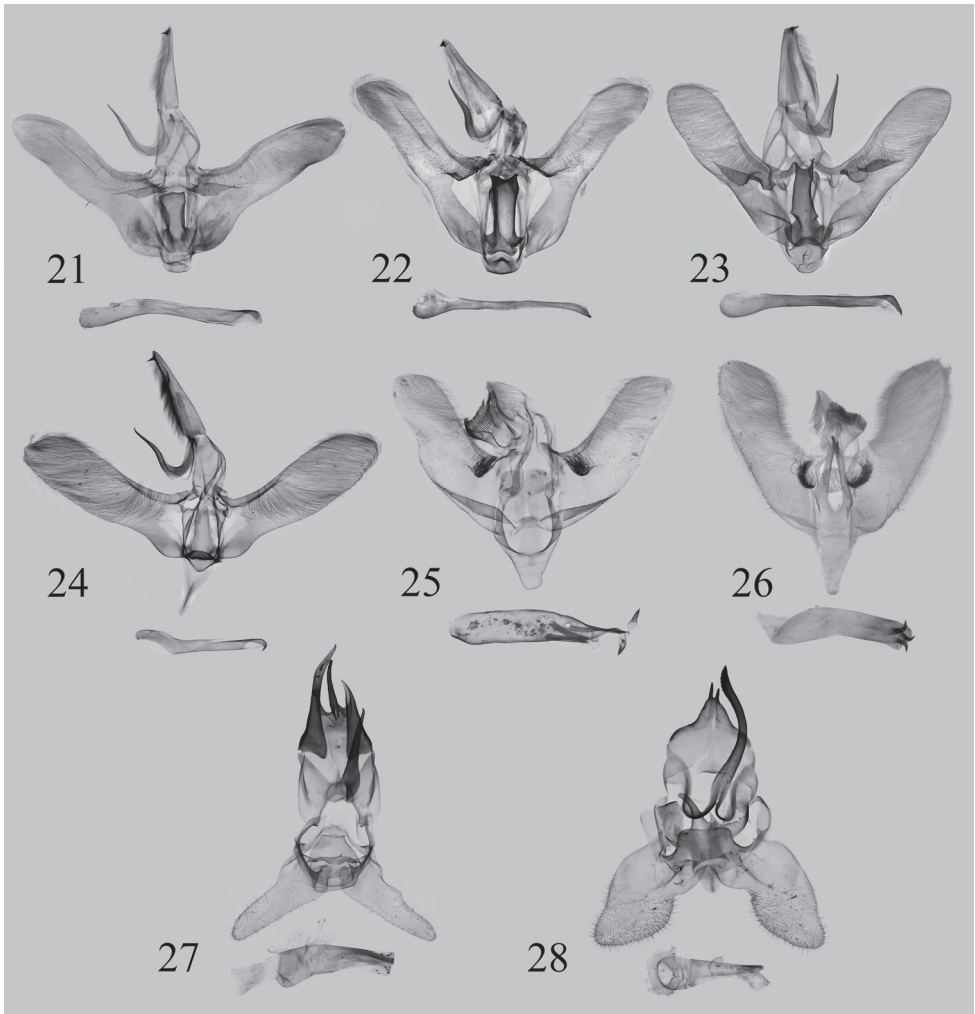
Figs 11, 25

Material examined. Holotype. ♂, CHINA, Xizang Autonomous Region, Linzhi (= Ny-yingchi) City, Motuo (= Medog) County, Beibeng Countryside, Dergong Village, 25.V–4.VI.2021, HL. Han leg., genit. prep. WuJ-572-1 (NEFU). **Paratypes.** 3♂, CHINA, same data as for holotype, genit. prep. WuJ-573-1, WuJ-556-1, WuJ-557-1 (NEFU).

Diagnosis. The new species is extremely similar to the type species *F. melkaya* (Fig. 12) in appearance, only the ground colour of the whole body is paler than the latter. It can be clearly distinguished from the latter by the male genitalia as follows. In *F. ravalba* sp. nov. (Fig. 25), the basal hairy papula on the valva is small, rounded; the



Figures 15–20. Male genitalia of *Kitanola* spp. **15** *K. shilimensis* sp. nov., holotype, Yunnan, China, genit. prep. WuJ-248-1 (NEFU) **16** *K. spina* Wu & Fang, 2008, Chongqing, China, genit. prep. WuJ-293-1 (NEFU) **17** *K. spinula* Wu & Fang, 2008, Zhejiang, China, genit. prep. WuJ-589-1 (NEFU) **18** *K. eleganta* sp. nov., paratype, Xizang, China, genit. prep. WuJ-501-1 (NEFU) **19** *K. linea* Wu & Fang, 2008, Guangdong, China, genit. prep. WuJ-610-1 (NEFU) **20** *K. uncula* (Staudinger, 1887), Sakhalin, Russia, genit. prep. SAV-10-02 (ZISP).



Figures 21–28. Male genitalia **21** *Euphlyctinides pseudolaika* sp. nov., holotype, Yunnan, China, genit. prep. WuJ-177-1 (NEFU) **22** *E. pseudolaika* sp. nov., paratype, Yunnan, China, genit. prep. WuJ-702-1 (NEFU) **23** *E. laika* Solovyev & Witt, 2009, paratype, Nghe An, Vietnam, genit. prep. 0061 (CASU) **24** *E. indi* Solovyev, 2009, Xizang, China, genit. prep. WuJ-552-1 (NEFU) **25** *Fignya ravalba* sp. nov., holotype, Xizang, China, genit. prep. WuJ-572-1 (NEFU) **26** *F. melkaya* Solovyev & Witt, 2009, holotype, Lào Cai, Vietnam, genit. prep. 14047 (MWM/ZSM) **27** *Limacocera pachycera* (Hampson, 1897), Xizang, China, genit. prep. WuJ-555-1 (NEFU) **28** *L. hel* Hering, 1931, Chongqing, China, genit. prep. WuJ-287-1 (NEFU).

juxta lacks a lateral process; the aedeagus bears several strongly sclerotized long spines at the apical part; the vesica contains two peg-like cornuti. However, in *F. melkaya* (Fig. 26), the basal hairy papula of the valva is larger than in the new species and transverse in shape; the juxta has a pair of slender lateral processes; the apical part of the aedeagus is without any spines; the vesica contains three large hooked cornuti.



Figure 29. Distribution map of four new Limacodidae species: circle = *Fignya ravalba* (China: Xizang); triangle = *Kitanola eleganta* (China: Xizang); star = *K. shilnensis* (China: Yunnan); square = *Euphlyctinides pseudolaika* (China: Yunnan).

Description. Adult (Fig. 11). Forewing length 7.0–7.5 mm, wingspan 16–17 mm. Head white; labial palpus white; antennae filiform, pale brown. Thorax with white scales above. Forewing ground colour greyish white, covered with sparse dark scales, a pair of large white spots in Cu-area with brown border; venation visible, brown; fringe dark brown. Hindwing greyish yellow. Abdomen brown to dark brown, mixed with white scales.

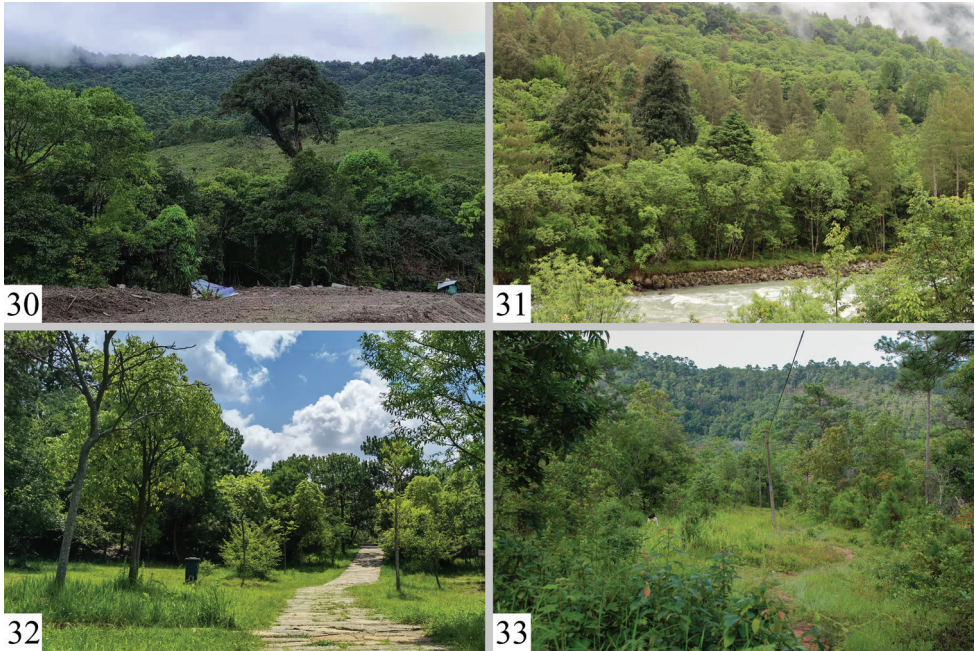
Male genitalia (Fig. 25). Uncus pointed apically, without any spur. Gnathos flattened, fishtail-shaped, comb-like apically. Valva elongate, with a basal papula with long bristles; base of sacculus slightly sclerotized; cucullus narrow and rounded. Juxta flattened, weakly sclerotized, without lateral process. Saccus long. Aedeagus short, tube-shaped, thinned proximally, bearing 3–5 strongly sclerotized long spines near apical part; vesica with a pair of strongly sclerotized, peg-like cornuti.

Female. Unknown.

Bionomics. The specimens were collected from late May to early June, at an altitude of 1,450 m a.s.l., in a subtropical forest (Fig. 30).

Distribution (Fig. 29). China (Xizang).

Etymology. The specific name *ravalba*, an adjective, is derived from the Latin “ravus” (= grey) and “albus” (= white), corresponding to the greyish-white ground colour of the forewing.



Figures 30–33. Biotopes of Limacodidae **30, 31** China, Xizang, Motuo County: **30** Beibeng Countryside, Dergong Village, biotope of *Fignya ravalba* sp. nov., *Euphlyctinidis indi* Solovyev, 2009 and *Limacocera pachycera* (Hampson, 1897), photo by HL. Han **31** Gedang Countryside, biotope of *Kitanola eleganta* sp. nov. and *E. indi*, photographs by J. Wu. **32, 33** China, Prov. Yunnan: **32** Kunming City, Shilin County, Changhu Town, Changhu wetland park, biotope of *K. shilinensis* sp. nov., photo by KL. Wu **33** Pu'er City, Manxieba Village, biotope of *E. pseudolaika* sp. nov., photographs by HL. Han.

Genus *Limacocera* Hering, 1931

Limacocera Hering, 1931: 674. Type species (by original designation): *Narosa pachycera* Hampson, 1897. Type locality: India, “Khásis” [Meghalaya, Khasi Hills].

Note. *Limacocera* is a small and rare genus, erected by Hering (1931), with the type species, “*Narosa pachycera* Hampson, 1897”. The forewings in this genus are grey, crossed by a characteristic broad, brown medial fascia. The labial palpi are up-curved, almost reaching to the vertex. The base of vein R_1 in the forewing is strongly curved toward the vein Sc; the vein R_2 is separate; the veins R_3+R_4 are stalked of R_5 . The tibial spurs are 0-2-4. The most obvious feature of this genus are the significantly extended antennae. The female antennae as long as the costal margin of the forewing, whereas the male antennae are longer than the costal margin and markedly enlarged (Hampson 1897; Hering 1931; Holloway 1990; Solovyev and Witt 2009). In China, there was until now only one species known, *L. hel* Hering, 1931, from the type locality in Guangdong Province.

***Limacocera pachycera* (Hampson, 1897)**

Figs 13, 27

Narosa pachycera Hampson, 1897: 294. Type locality: India, “Khásis” [Meghalaya, Khasi Hills].

Limacocera pachycera (Hampson): Hering 1931: 674.

Material examined. 1♂, CHINA, Xizang Autonomous Region, Linzhi (= Nyingchi) City, Motuo (= Medog) County, Beibeng Countryside, Dergong village, 25.V–4.VI.2021, HL. Han leg., genit. prep. WuJ-555-1 (NEFU).

Diagnosis. The differences between *L. pachycera* (Fig. 13) and its congener *L. hel* (Fig. 14) are that the former is larger than the latter; the dent of the postmedial line incurved above the cell, whereas the same dent in *L. hel* is deeper and incurved below the cell.

The male genitalia of *L. pachycera* (Fig. 27) bear a long, robust, strongly sclerotized uncus; the gnathos is straight and pointed apically; the valva is narrow. However, in *L. hel* (Fig. 28), the uncus is small and divided into two asymmetrical parts; the gnathos is slender, sinuous, and longer than *L. pachycera*; the valva is broad.

Bionomics. The single male specimen was collected in late May to early June at an altitude of 1,450 m a.s.l. in a subtropical forest (Fig. 30).

Distribution. China (Xizang), India.

Checklist of the treated genera with distribution data

Kitanola Matsumura, 1925

K. uncula (Staudinger, 1887) (China: Heilongjiang; Japan; Korean peninsula; Russia: south-eastern Siberia, Sakhalin)

= *K. sachalinensis* Matsumura, 1925

= *Microcampa suzukii* Matsumura, 1931

= *Microcampa corana* Matsumura, 1931

K. masayukii Sasaki, 1998 (Japan)

K. meridiana Sasaki, 1998 (Japan)

K. albigrisea Wu & Fang, 2008 (China: Shaanxi, Gansu, Henan, Sichuan)

K. brachygnatha Wu & Fang, 2008 (China: Yunnan)

K. caii Wu & Fang, 2008 (China: Anhui, Henan, Gansu; Japan)

K. eurygnatha Wu & Fang, 2008 (China: Zhejiang, Jiangxi, Hunan, Guangdong)

K. linea Wu & Fang, 2008 (China: Hubei, Sichuan, Guangxi)

K. spina Wu & Fang, 2008 (China: Shaanxi, Sichuan, Chongqing, Hubei, Guizhou)

K. spinula Wu & Fang, 2008 (China: Zhejiang, Anhui, Jiangxi, Hunan)

K. shilinensis sp. nov. (China: Yunnan)

K. eleganta sp. nov. (China: Xizang)

Euphlyctinides Hering, 1931

E. albifusum (Hampson, 1892) (China: Xizang; India; Bhutan; Nepal)

= *E. rava* Hering, 1931

- E. indi* Solovyev, 2009 (China: Xizang; India)
E. aeneola Solovyev, 2009 (China: Yunnan; Thailand)
E. laika Solovyev & Witt, 2009 (Vietnam)
E. pseudolaika sp. nov. (China: Yunnan)
Fignya Solovyev & Witt, 2009
F. melkaya Solovyev & Witt, 2009 (China: Sichuan; Vietnam)
F. navalba sp. nov. (China: Xizang)
Limacocera Hering, 1931
L. pachycera (Hampson, 1897) (China: Xizang; India)
L. hel Hering, 1931 (China: Guangdong, Chongqing, Hunan; Vietnam)

Acknowledgements

This study was supported by the National Nature Science Foundation of China (No. 31872261), the project of Northeast Asia Biodiversity Research Center (2572022DS09), and the Fundamental Research Funds for the Central Universities (No. 2572021DJ08, 2572019CP11). We also sincerely thank Mr. Pei Wang (The People's Government of Motuo County, China) for his help during collecting in Motuo County; to Mr. Kelun Wu, who collected and provided the material of *Kitanola shilinensis* sp. nov.; and to the colleagues from our laboratory for collecting some of the material examined in this study.

References

- Hampson GF (1897) The moths of India. Supplementary paper to the volumes in “the fauna of British India”. Part I. Journal of the Bombay Natural History Society 11: 277–297.
- Hering M (1931) Limacodidae (Cochliopodidae). In: Seitz A (Ed.) Die Gross-Schmetterlinge der Erde. Vol. 10. Alfred Kerner Verlag, Stuttgart, 665–728.
- Hirawatari T, Nasu Y, Sakamaki Y, Kishida Y (2013) The standard of moths in Japan III. Gakken Education Publishing, Tokyo, 359 pp. [In Japanese]
- Holloway JD (1990) The Limacodidae of Sumatra. Heterocera Sumatrana 6: 9–77.
- Inoue H (1956) A new species of Heterogeneidae. Kontyû 24(3): 159–160. [In Japanese]
- Inoue H (1982) Limacodidae. In: Inoue H, Sugi S, Kuroko H, Moriuti S, Kawabe A (Eds) Moths of Japan, Vol. 1. Kodansha, Tokyo, 297–301. [In Japanese]
- Irungbam JS, Chib MS, Solovyev AV (2017) Moths of the family Limacodidae Duponchel, 1845 (Lepidoptera: Zygaenoidea) from Bhutan with six new generic and 12 new species records. Journal of Threatened Taxa 9(2): 9795–9813. <https://doi.org/10.11609/jott.2443.9.2.9795-9813>
- Ji SQ (2018) Taxonomic study on the Limacodidae from South-west China (Lepidoptera: Limacodidae). MSc Thesis, South China Agricultural University, Guangzhou. [In Chinese]

- Kawada A (1930) A list of Cochlidionid moths in Japan, with descriptions of two new genera and six new species. *Journal of the Imperial Agricultural experimental Station, Nishigahara* 1(3): 231–262.
- Kononenko VS, Han HL (2007) Atlas Genitalia of Noctuidae in Korea (Lepidoptera). In: Park K-T (Ed.) *Insects of Korea (Series 11)*. Junhaeng-Sa, Seoul, 464 pp.
- Matsumura S (1925) An enumeration of the butterflies and moths from Saghalién, with descriptions of new species and subspecies. *Journal of the College of Agriculture, Hokkaido Imperial University, Sapporo, Japan* 15(3): 83–196.
- Sasaki A (1998) Revision of the genus *Kitanola* Matsumura (Limacodidae) in Japan, with descriptions of two new species. *Japan Heterocerists' Journal* 200: 417–423. [In Japanese]
- Solovyev AV (2008) The limacodid moths (Lepidoptera: Limacodidae) of Russia. *Eversmannia* 15(4): 17–43. [In Russian]
- Solovyev AV (2009) Notes on South-East Asian Limacodidae (Lepidoptera, Zygaenoidea) with one new genus and eleven new species. *Tijdschrift voor Entomologie* 152(1): 167–183. <https://doi.org/10.1163/22119434-900000273>
- Solovyev AV, Witt TJ (2009) The Limacodidae of Vietnam. *Entomofauna (Supplement No. 16)*: 33–229.
- Tshistjakov YA (1995) A review of the Limacodidae (Lepidoptera) of the Russian Far East. *Far Eastern Entomologist = Dal'nevostochnyi Entomolog* 7: 1–12.
- van Nieuwerkerken EJ, Kaila L, Kitching IJ, Kristensen NP, Lees DC, Minet J, Mitter C, Mutanen M, Regier JC, Simonsen TJ, Wahlberg N, Yen SH, Zahiri R, Adamski D, Baixeras J, Bartsch D, Bengtsson BÅ, Brown JW, Bucheli SR, Davis DR, De Prins J, De Prins W, Epstein ME, Gentili-Poole P, Gielis C, Hättenschwiler P, Hausmann A, Holloway JD, Kallies A, Karsholt O, Kawahara AY, Koster SJC, Kozlov MV, Lafontaine JD, Lamas G, Landry JF, Lee S, Nuss M, Park KT, Penz C, Rota J, Schintlmeister A, Schmidt BC, Sohn JC, Solis MA, Tarmann GM, Warren AD, Weller S, Yakovlev RV, Zolotuhin VV, Zwick A (2011) Order Lepidoptera Linnaeus, 1758. In: Zhang ZQ (Ed.) *Animal Biodiversity: An outline of higher-level classification and survey of taxonomic richness*. *Zootaxa* 3148: 212–221. <https://doi.org/10.11646/zootaxa.3148.1.41>
- Wu CS (2010) Analysis on the host plant diversity of slug caterpillar moths in China. *Forest Pest and Disease* 29(2): 1–4. [In Chinese]
- Wu CS (2011) Six new species and twelve newly recorded species of Limacodidae from China (Lepidoptera, Zygaenoidea). *Acta Zootaxonomica Sinica* 36(2): 249–256.
- Wu CS, Fang CL (2008) Discovery of the genus *Kitanola* Matsumura from China, with descriptions of seven new species (Lepidoptera, Limacodidae). *Acta Entomologica Sinica* 51(8): 861–867.
- Wu J, Solovyev AV, Han HL (2022) Two new species and two unrecorded species of Limacodidae (Lepidoptera, Zygaenoidea) from Xizang, China. *ZooKeys* 1100: 71–85. <https://doi.org/10.3897/zookeys.1100.76142>

